



Université
de Lille

THÈSE DE DOCTORAT

Pour obtenir le titre de

DOCTEUR EN CHIMIE

Spécialité Molécules et Matière Condensée

par

Feng NIU

**Development of novel catalysts for selective
amination of alcohols**

**Développement de nouveaux catalyseurs pour
l'amination sélective d'alcools**

soutenue le 17 décembre 2019

<i>Président</i>	Prof. Franck Dumeignil, Université de Lille (France)
<i>Rapporteurs</i>	Prof. Laurent Bonneviot, ENS Lyon (France) Prof. Florence Epron, Université de Poitiers (France)
<i>Examineurs</i>	Prof. Franck Dumeignil, Université de Lille (France) Prof. Karine Vigier, Université de Poitiers (France)
<i>Invité</i>	Dr. Stéphane Streiff, Solvay-E2P2L (Chine)
<i>Directeurs</i>	Prof. Andrei Khodakov, Université de Lille (France) Dr. Vitaly Ordonsky, Université de Lille (France)

Acknowledgements

First, I would like to sincerely acknowledge the grant from Solvay and University of Lille to financially support my PhD research both in Shanghai, China and Lille, France. Thanks to E2P2L director Dr. Stephane Streiff and UCCS director Dr. Franck Dumeignil, who provide me with safe and professional international lab environment and allowing me to perform scientific research in Shanghai and Lille.

My heartiest thank you goes out to Professor Andrei Khodakov and Dr. Vitaly Ordonsky for their constant and excellent supervision over the last three years. Thank you for your patient and professional suggestions and comments with my courses, experiments, patents, publications and thesis. Besides, you are also the life mentors for me, which makes me feel warm and confident when I was in Lille or Shanghai. For all that and more, I would like to express my most sincere gratitude to you!

I am especially honored by the acceptance of Prof. Laurent Bonneviot and Prof. Florence Epron to review my doctoral work. Likewise, I would like to thank Prof. Franck Dumeignil, Dr. Stéphane Streiff and Prof. Karine Vigier for agreeing to take part in the dissertation committee.

I would also like to extend my gratitude to colleagues from UCCS and E2P2L who I was lucky to work with. They gave me lots of advices in terms of my research and daily life, especially Dr. Zhen Yan and Dr. Bright Kusema, who helped me to solve numerous scientific and technical questions when I was in Shanghai. Time from time discussions makes my papers and thesis much more solid.

A big thank you to my family, my parents, my son Chengyi Niu, especially my wife Cong Zhang, thank you for your love, strong support and everything you have done for me. I love you!

Feng NIU

September 2019 in Shanghai

Abstract

Amines are very important intermediates for chemical industry and life science, which can be synthesized through different traditional routes. Metals based catalytic amination of alcohols via the so-called “*hydrogen borrowing*” mechanism is a relative efficient and environmental benign way for synthesis of different primary amines. However, there are still some challenges exist, such as high cost of noble metals, low selectivity of primary amine products, and poor stability and recyclability for industrial applications. To solve these problems, different strategies have been applied in this thesis.

Carbon deposition produced by catalyst pre-treatment with alcohols under the optimized conditions has been employed for major enhancement of the selectivity of alcohol amination to primary amines (from 30-50 to 80-90%), which arises from steric hindrance in hydrogenation of bulky secondary imines as intermediate products over partially carbon-decorated cobalt nanoparticles. An efficient approach to protect cobalt catalyst from catalytic deactivation by liquid bismuth promotion with different loading content was disclosed for selectively amination of 1-octanol. The *N*-alkylation of amines by alcohols over a cheap and efficient heterogeneous catalyst-titanium hydroxide was also proposed. The catalyst with mild Brønsted acidity provides the selectivity higher than 90% to secondary amines for functionalized aromatic and aliphatic alcohols and amines at high catalytic activity and stability.

Keywords: Amination; hydrogen borrowing; carbon deposition; liquid bismuth; titanium hydroxide; acidic sites; alcohol pretreatment

Résumé

Les amines sont des intermédiaires très importants pour l'industrie chimique et la science de la vie, qui peuvent être synthétisés par différentes voies traditionnelles. L'amination catalytique d'alcools à base de métaux via le mécanisme dit "*d'emprunt d'hydrogène*" est un moyen relativement efficace et respectueux de l'environnement pour la synthèse de différentes amines primaires. Toutefois, certains problèmes subsistent, tels que le coût élevé des métaux nobles, la faible sélectivité en amines primaires, ainsi que la faible stabilité et la recyclabilité des catalyseurs. Pour résoudre ce problème, différentes stratégies ont été appliquées.

Les dépôts de carbone produits lors du prétraitement des catalyseurs avec des alcools dans les conditions optimales ont été utilisés pour améliorer de manière importante la sélectivité de l'amination d'alcools en amines primaires (de 30-50 à 80-90%). Cette amélioration provient de l'empêchement stérique de l'hydrogénation des imines secondaires sur des nanoparticules de cobalt partiellement décorées au carbone. Une approche efficace pour protéger le catalyseur au cobalt de la désactivation par la promotion avec du bismuth liquide a été décrite pour l'amination sélective du 1-octanol. La *N*-alkylation d'amines par des alcools sur un catalyseur hétérogène, peu coûteux et efficace, à base d'hydroxyde de titane a également été proposée. Le catalyseur à faible acidité de Brønsted fournit une sélectivité supérieure à 90% en amines secondaires lors la réaction des alcools aromatiques et aliphatiques fonctionnalisés avec les amines

Mots-clés: Amination; emprunt d'hydrogène; dépôt de carbone; bismuth liquide; hydroxyde de titane; sites acides; prétraitement à l'alcool

Contents

Chapter 1. Literature Review	8
1.1 General Introduction	8
1.2 Synthesis Routes of Amines	10
1.2.1 Reductive amination.....	11
1.2.2 Amination of aliphatic acids or esters	15
1.2.3 Amination of alkenes (Hydroamination).....	16
1.2.4 Amination of halides	18
1.2.5 Amination of hydrocarbons.....	19
1.2.6 Amination of ethers	20
1.2.7 Amination of carbon monoxide or carbon dioxide.....	20
1.2.8 Amination of alcohols	21
1.3 Mechanisms of Alcohol Amination	24
1.3.1 Kinetics of amination	27
1.3.2 Reaction conditions.....	28
1.3.3 Side reactions	30
1.3.3.1 Disproportionation of amines	30
1.3.3.2 Aldehyde condensation	30
1.3.3.3 Formation of nitriles.....	31
1.4 Catalysts Used for Amination of Alcohols.....	31
1.4.1 Homogeneous catalysts	31
1.4.2 Heterogeneous catalysts	32
1.4.3 Challenges in amination of alcohols	37
1.5 Strategies for Selectivity Control.....	38
1.6 Objectives and Research Plans of this Thesis.....	42
1.6.1 Catalyst deactivation for primary amine selectivity enhancement.....	43
1.6.2 Creation of highly dispersed Co and Ni nanoparticles by carbon deposition	43
1.6.3 Bi as a promoter for selective amination of 1-octanol	44
1.6.4 Design of non-metal heterogeneous catalyst for amination of alcohol	44
1.7 Outline of this Thesis	45
Chapter 2. Experimental Section.....	47
2.1 Catalyst Preparation.....	47
2.1.1 Chemical reagents	47
2.1.2 Preparation of supported Co, Ni and Bi catalysts	48
2.1.3 Preparation of the alcohols pretreated Co and Ni catalysts	49
2.1.4 Preparation of highly dispersed Co and Ni nanoparticles	50
2.1.5 Preparation of Bi promoted Co catalysts.....	50

2.1.6 Preparation of titanium hydroxide.....	51
2.2 Catalyst Characterization	52
2.2.1 X-ray diffraction (XRD).....	52
2.2.2 Scanning transmission electron microscopy (STEM)	52
2.2.3 Hydrogen temperature-programmed reduction (H ₂ -TPR).....	53
2.2.4 Temperature-programmed reduction-mass spectrometry (TPH-MS).....	54
2.2.5 CO pulse chemisorption.....	54
2.2.6 Temperature-programmed desorption of NH ₃ (NH ₃ -TPD)	55
2.2.7 Surface area and pore size distribution.....	55
2.2.8 Thermogravimetric analysis (TGA)	55
2.2.9 X-ray photoelectron spectrometry (XPS).....	56
2.2.10 Infrared spectroscopy	56
2.2.11 Gas chromatography-mass spectrometer (GC-MS)	57
2.3 Evaluation of Catalytic Performance.....	57
2.3.1 Gas-phase amination of alcohols.....	57
2.3.2 Liquid-phase amination of alcohols	58
2.3.3 <i>N</i> -alkylation of amines with alcohols.....	59
2.3.4 Analysis of reaction products	61
2.3.5 Model reactions.....	62
* Chapter 3. Catalyst Deactivation for Enhancement of Selectivity in Alcohols	
Amination to Primary Amines	63
3.1 Introduction.....	64
3.2 Results and Discussion.....	66
3.2.1 Alcohol amination over cobalt catalysts.....	66
3.2.2 Characterizations of 1-butanol pretreated cobalt.....	73
3.2.3 Characterization of deposited carbon species	76
3.2.4 Carbon deposition and enhancement of the selectivity to primary amines	84
3.3 Conclusion	88
Chapter 4. Disassembly of supported Co and Ni nanoparticles by carbon	
deposition for the synthesis of highly dispersed catalysts	89
4.1 Introduction.....	90
4.2 Results and Discussion.....	91
4.2.1 Catalytic reactions over highly dispersed cobalt and nickel catalysts.....	91
4.2.2 Characterizations and mechanism of decomposition	93
4.3 Conclusion	101
Chapter 5. Bi as Liquid Metal Promoter of Co Catalysts for Highly Efficient	
Amination of Alcohols.....	102

5.1 Introduction.....	103
5.2 Results and Discussion.....	105
5.2.1 Enhancement of catalytic performance on bismuth promotion.....	105
5.2.2 Catalyst characterizations.....	110
5.2.3 Mechanism of bismuth promotion effect	115
5.3 Conclusion	120
Chapter 6. Highly efficient and selective <i>N</i>-alkylation of amines with alcohols catalyzed by <i>in-situ</i> rehydrated titanium hydroxide.....	121
6.1 Introduction.....	122
6.2 Results and Discussion.....	123
6.2.1 Catalysis over oxides and hydroxides	123
6.2.2 Characterizations of material	128
6.2.3 Proposed reaction mechanism.....	135
6.2.4 Substrate scope.....	143
6.3 Conclusion	146
Chapter 7. General Conclusions and Perspectives	147
7.1 General Conclusion.....	147
7.1.1 Modification of supported Co nanoparticles by poisons and promoters for selective amination of alcohols	147
7.1.2 Design of non-metal hydroxide for <i>N</i> -alkylation of alcohols with amines.....	149
7.2 Perspectives	150
8 References	151

Chapter 1. Literature Review

1.1 General Introduction

Amines are compounds which contain a basic nitrogen atom with a lone pair [1,2]. Depending on the numbers of substituent of hydrogen atoms, there are three subcategories of amines: primary amines, secondary amines, and tertiary amines (Shown in **Figure 1.1**). Also, classified by the appearance of aromatic ring, there are aliphatic amines and aromatic amines. The simplest amine is ammonia, NH_3 , in which the central nitrogen atom is bonded to three hydrogen atoms which are all chemically equivalent.

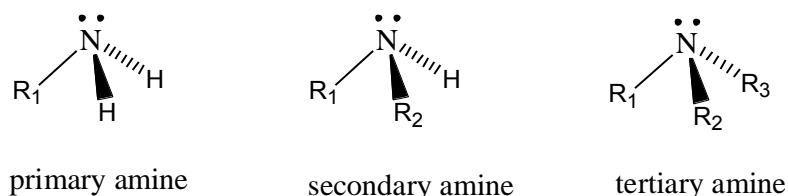


Figure 1.1 Subcategories of amines.

According to the functional properties, there are various types of amines including aliphatic amines (fatty and cyclic amines), aryl amines, heterocyclic amines and inorganic amines (hydrazine, hydroxylamine and amine ligands). Some representative amine molecules are shown in **Figure 1.2**.

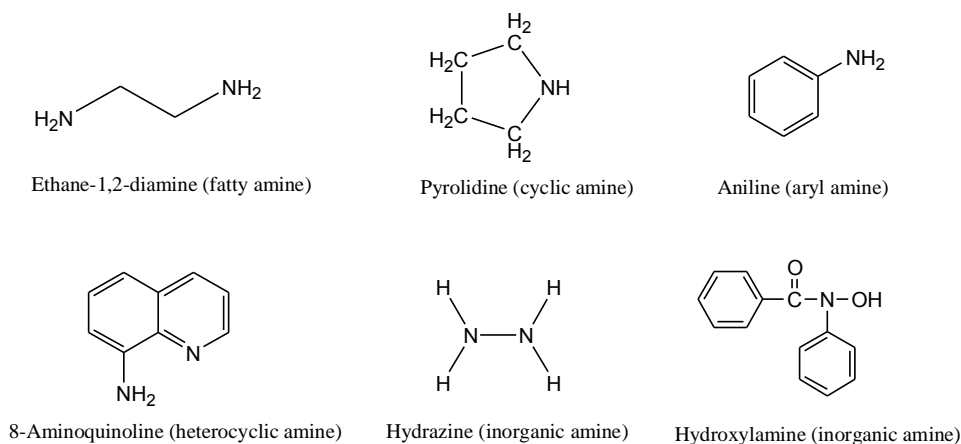


Figure 1.2 Structures of some representative amines.

Due to the high chemical activity, amines are important feedstocks in chemical industry and life science [3]. For instance, most aliphatic amines and their derivatives are essential intermediates in the production of agrochemicals, pharmaceuticals, organic dyes, detergents, fabric softeners, surfactants, corrosion inhibitors, lubricants, polymers and so on [4,5,6,7,8]. **(Figure 1.3)** Furthermore, optically active amines have attracted great attention in asymmetric synthesis such as chiral auxiliaries, catalysts, and resolving agents [9].



Figure 1.3 Applications of amines in chemical industry and life science.

Since the Haber-Bosch process was applied in the early 20th century, ammonia has been available on a large scale and, nowadays, over 100 million tons are synthesized annually, consuming 1-2% of the worldwide produced energy [10]. The percentage of ammonia used in the production of amines is about 3% to 4% of the total worldwide output. There are lots of amines synthesized from ammonia with various functions for industrial applications. An example is fatty amines, which are found use in many applications such as water treatment, agro-chemicals, oilfield chemicals, asphalt additives, anti-caking and others which include mining, personal care, fabric softener, paints & coatings and many more. **(Figure 1.4)** There is a huge growth prospect of the global fatty amines market for the period 2015 to 2020. As is known to all, the world famous chemical industrial companies, like Dow, BASF, Solvay, Amark, Mitsubishi Chemical, whose annual yield of various amines is over hundreds of thousands tons have huge competition in amine market. In terms of

revenue, the global fatty amines market was valued at US\$ 1,721 Mn in 2014, and is estimated to be worth US\$ 2,193 Mn by 2020, whereas, in terms of volume, the global fatty amines market accounted for 615 Kilo Ton in 2014, and is anticipated to reach a volume of 718 Kilo Ton by 2020 [11].

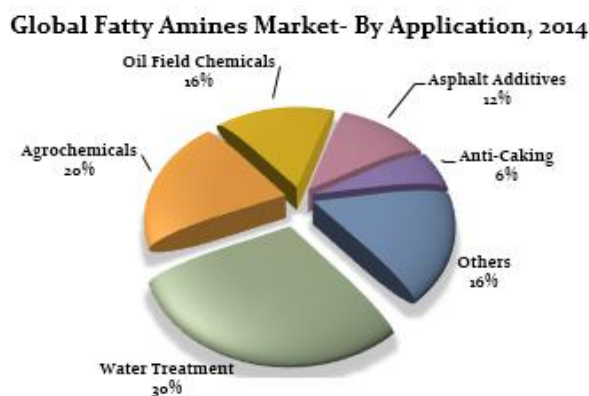


Figure 1.4 Global fatty amines market-by application, 2015 [11].

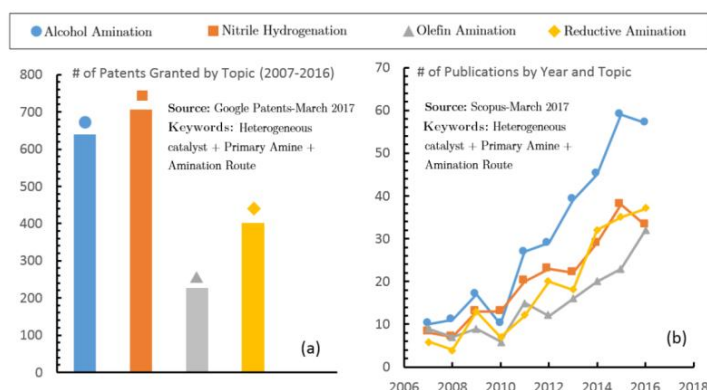


Figure 1.5 Numbers of patents and publications from 2007-2016 regarding different amination routes.

Also, numbers of patents and publications in terms of approaches for amines production focused on this topic has risen exponentially. (Figure 1.5) All in all, investigation on the synthesis of amines is of significant importance for different purposes in the national and global economy.

1.2 Synthesis Routes of Amines

Owing to the importance from the industrial aspects above, a number of routes

for amines synthesis starting from many different types of raw materials have been developed till now, including Hofmann alkylation [12,13], Buchwald-Hartwig [14,15,16,17,18] and Ullmann reactions [19,20,21], hydroamination [22], reduction of nitriles [23], and reductive amination [24]. Here, as functions of the particular amine, raw material availability, plant economics and the ability to sell co-products, the following manufacturing methods are used commercially for synthesis of different amines.

Route 1: Reductive amination. Reaction of an aldehyde or a ketone with ammonia or amines over a metal catalyst or hydrogenation of nitriles over a hydrogenation catalyst.

Route 2: Amination of aliphatic acids or esters. Reaction of aliphatic acids or esters with ammonia over metal or metal oxides catalysts under high temperature and pressure.

Route 3: Hydroamination. Amination of alkenes over a catalyst with acidic sites under high temperature and pressure.

Route 4: Amination of halides. Reaction of ammonia or alkylamine with a halide over a supported metal catalyst.

Route 5: Amination of hydrocarbons. Reaction of ammonia with hydrocarbons over bi-metal oxides.

Route 6: Amination of ethers. Amination of ethers via cleavage of C-O bond by ammonia or amines over acidic catalysts.

Route 7: Amination of carbon monoxide and carbon dioxide. Reaction of CO or CO₂ with hydrogen and ammonia under high temperature.

Route 8: Alcohol amination. Amination of an alcohol over a metal catalyst under hydrogen or over a solid acid catalyst.

Other special routes for synthesis of amines, like *N*-alkylation of sulfonamides and cross-coupling of primary amines.

1.2.1 Reductive amination

Amination of carbonyl compounds (generally regarded as reductive amination) is

considered as a practical and widespread strategy, which provides rapid access to different types of amines, important intermediates for synthesis of natural products and organic compounds, and also production of essential precursors needed for drug development in chemical and biological systems [7]. Generally, direct reductive amination of carbonyl compounds refers to reaction of carbonyl compounds (aldehydes or ketones) with ammonia, primary or secondary amines in the presence of a reductant for providing different kinds of amines (**Figure 1.6**). The initial step of the reaction is the formation of addition product (carbinol amine) which, under controlled appropriate reaction conditions, loses water to offer imine or iminium ion **b**, reduction of **b** produces the amine product.

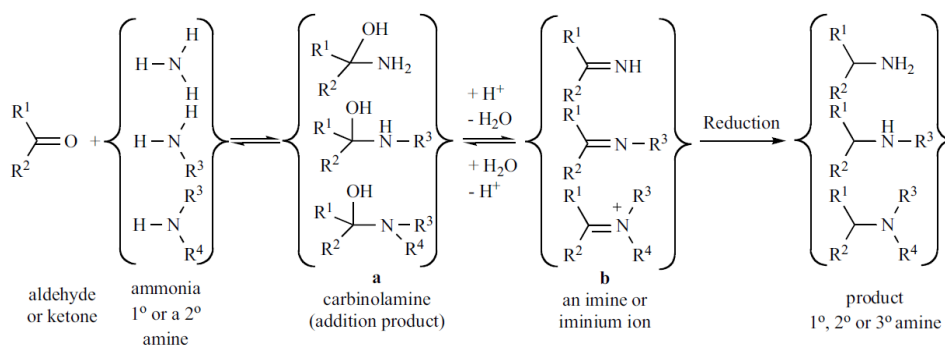


Figure 1.6 Reductive amination process [9].

Reductive amination (RA) was firstly described in the early days of the twentieth century by Mignonac [25]. Since then, it has been widely used for the preparation of different types of amines. A variety of aldehydes or ketones have been effectively converted into the corresponding amines by RA in the presence of homogeneous or heterogeneous catalysts in a continuous-flow reactor or the batch system.

Beller et al. [26] reported the first example of a soluble transition metal Rh complex to catalyze reductive amination of benzyl aldehyde with aqueous ammonia to afford benzylamine. Up to an 86% yield and a 97% selectivity for benzylamines were obtained in the case of various benzaldehydes by using a Rh-catalyst together with water-soluble phosphine and ammonium acetate.

Late on, different homogeneous catalysts like metal based complexes and triflic acids were applied for reductive amination. Enthaler [27] demonstrated the usefulness

of simple zinc(II) triflate catalyst with Lewis acid in the reductive amination of benzyl aldehyde with aniline to access the corresponding secondary amine. This commercial triflate catalyst [Zn(OTf)₂] and PMHS [poly (methylhydrosiloxane)] as a cheap hydride source under non-inert conditions exhibited outstanding yields and a broad functional group tolerance. Werkmeister et al. [28] developed an easily available and inexpensive copper(II) acetate catalyst [Cu(OAc)₂] for reductive amination of acetophenone with aniline to form secondary amine. Advantageously, no complicated ligands or additional acid or base is needed in this system.

As the development of more convenient and operationally simple processes for the synthesis of advanced amines is highly desired, researchers tried to find recoverable and stable heterogeneous catalysts for reductive amination. An unsupported ultra-thin Pt nanowire has been developed by Qi et al. [29] for the synthesis of dibenzylamine through direct reductive amination of benzyl aldehyde with ammonia. This nanowire exhibited excellent stability for reductive amination, which would be an important type of catalyst for the industrial synthesis of amines. Shimizu et al. [30] also reported a highly effective modified supported platinum catalyst (Pt-MoO_x/TiO₂), which shows the highest yield of primary amine for the reductive amination of ketone (2-adamantanone) under ammonia and hydrogen compared with other platinum supported catalysts. It was suggested that Lewis acid sites on the support material plays an important role in this catalytic system.

Among the metal based heterogeneous catalysts, the noble metal Ru-based catalysts are the most active catalysts for the reductive amination of carbonyl compounds to the corresponding primary amines. Bódis and co-workers [31] used carbon supported group VIII noble metals (Pt, Pd, Rh, and Ru) as catalysts for the reductive amination of butyraldehyde with NH₃. It was found that Rh and Ru catalysts were active and selective in the production of primary amine under 50 bar H₂ pressure, while Pt and Pd catalysts favored the secondary amine formation. Liang et al. [32] reported that partially reduced Ru/ZrO₂ was an efficient catalyst for reductive amination of a variety of biomass-derived aldehydes/ketones in aqueous ammonia. The author explained that multivalence Ru association species worked as a

bifunctional catalyst, with RuO₂ as an acidic promoter to facilitate the activation of carbonyl groups and Ru as active sites for the subsequent imine hydrogenation. This is the main reason for high yield of amines.

As the high activity of aldehydes or ketones, selectivity to primary amine is always quite low during reductive amination. Different strategies were applied for primary amine selectivity enhancement. It was found that choosing a suitable support played an important role in determining the catalytic selectivity of primary amine [33,34]. It was reported by Dong et al. [35] that, for the model reaction of amination of heptaldehyde with ammonia, the amphoteric (θ -Al₂O₃ or γ -Al₂O₃)-supported Ru catalysts exhibited high selectivity for primary amine (heptylamine 94% yield) under 100% conversion compared with purely basic (MgO, CaO) and relative acidic (Nb₂O₅, SnO₂, MCM-41, HZSM-5) supports. Komanoya and co-workers [36] found that ruthenium nanoparticles supported on Nb₂O₅ was a highly selective and reusable heterogeneous catalyst for reductive amination of various biomass-based aldehydes with NH₃ and H₂ and prevent the formation of secondary amines and undesired hydrogenated byproducts, which is likely attributable to the weak electron-donating capability of Ru particles on the Nb₂O₅ surface (**Figure 1.7**). Also, some novel catalysts like magnetically separable Fe@Pd/C were used for selective reductive amination [37].

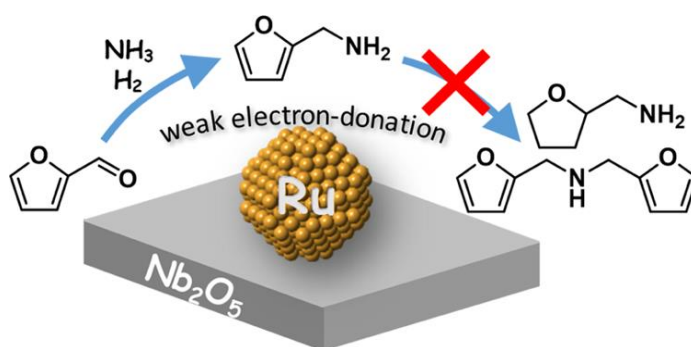


Figure 1.7 Electronic effect of reductive amination [36].

Addition of some additives will also enhance the yield of amines. Zhu et al. [38] described that reductive amination of aldehyde and amine proceeded smoothly with addition of benzothiazoline as an efficient hydrogen donor by means of 20 mol%

trifluoroacetic acid to give the corresponding amines in excellent yields.

Hydrogenation of nitriles is also a desirable approach for synthesis of amines in hydrogen pressure under high temperature. This catalytic method has been studied by several investigators [39,40,41,42] with diverse results. Apparently this reaction is greatly influenced by the nature of the nitrile, the catalyst, the solvent, the conditions of temperature and pressure, etc. Secondary amines are usually formed as well as primary, and the former may frequently constitute the chief reaction products (**Figure 1.8**).

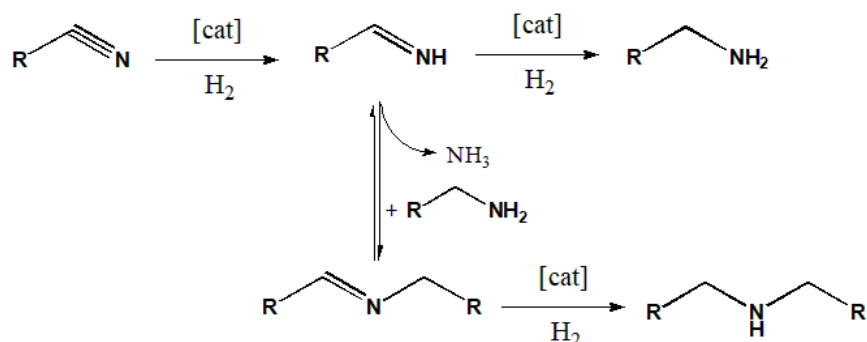


Figure 1.8 Hydrogenation of nitriles to primary amines and secondary reaction with the intermediate imines [39].

1.2.2 Amination of aliphatic acids or esters

The general industrial process for amine synthesis is a three-step reaction starting from natural fats: 1) hydrolysis of fats to acids; 2) amination of acids into nitriles and 3) hydrogenation-condensation of nitriles. An improvement of this process could be the direct conversion of acids or esters into amines.

Amination from aliphatic acids or esters is also one of the most interesting methods in industrial application for the synthesis of fatty amines, which contains two ways: the synthetic route of aliphatic amines from aliphatic acids (or esters) through nitriles, and the direct synthetic route of aliphatic amines from aliphatic acids (or esters).

With the promotion of a good catalyst and high reaction temperature, the aliphatic acids (or esters) can react with ammonia to form the corresponding nitrile, followed

by hydrogenation to produce primary or secondary aliphatic amines. It was reported that under ammonia atmosphere, with the help of hydrogenation catalysts, such as Co or Ni based catalysts, the yield of primary amine could reach 97.8%. To avoid the disadvantage of low yield for one-pot synthesis of nitriles from aliphatic acids, which causes the low yield of aliphatic amines, researchers began to focus on the synthetic route of primary amines from directly reaction of aliphatic acids (or esters), ammonia and hydrogen. The mostly used catalysts in this reaction are zinc oxide, alumina, cobalt or nickel based sulfide. Although the total yield of primary amine is low, the cost is much lower than the two-step route.

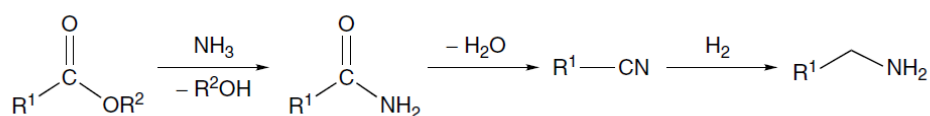


Figure 1.9 Amination of esters.

As shown in **Figure 1.9**, the transformation of ester into primary amine proceeds in three consecutive steps: amide formation; nitrile formation by dehydration; condensation of nitriles. It seems therefore advantageous to prepare multifunctional catalysts with acid-base properties for dehydration and a metallic character for hydrogenation of nitrile. As reported by Barrault [43], 83% of dodecylamine could be obtained in the amination of methyl dodecanoate (ester conversion was generally complete) in a fixed-bed reactor at 50 bar, 250 °C, LHSV 1/3 h⁻¹, ester/NH₃/H₂ 1/10/100 using the multifunctional catalyst Cu_{19.6}-Co_{2.5}-Cr_{1.3}/TiO₂. Also, methyl dodecanoate could be easily converted into *N*-dimethyldodecylamine in the presence of ammonia, hydrogen and methanol over copper-chromite species deposited on alumina or on titania [44]. Adding promoters such as Ca or Mn to CuCr/Al₂O₃ (TiO₂) catalysts demonstrated that selectivity in *N*-dimethyldodecylamine was much enhanced.

1.2.3 Amination of alkenes (Hydroamination)

As most of the lower aliphatic alcohols are manufactured by alkene hydration,

which can be used for alcohol amination, the direct amination of alkenes (also called “hydroamination”) without water production is very valuable due to readily availability of olefins feedstocks and 100% atom efficiency [45,46,47,48,49]. (See **Figure 1.10**) Reaction of alkenes with ammonia is a thermodynamically favorable reaction. But alkenes are really inactive to ammonia. In order to accelerate the reaction, two possible activation approaches can be considered: (a) activating the carbon-carbon multiple bond of alkenes to make it more electrophilic for the nucleophilic attack of nitrogen-hydrogen bond in ammonia; (b) improving the nucleophilicity of ammonia to accelerate the formal addition with alkenes. As the importance of this reaction process, various types of catalysts were developed for the direct amination from alkenes, such as alkali metal catalysts, transition metal catalysts, zeolites, metal hydrides and so on. The direct amination of olefins over zeolites was first reported by Deeba et al. [50]. H-MOR (H-mordenite) and H-OFF (H-offretite) zeolites were shown to be active (~12% ethylene conversion, ~95% ethylamine selectivity) for ethylene amination through Markovnikov addition at 633 K and 52 atm in a fixed-bed reactor (mole ratio of ammonia/ethylene = 4/1). The hydroamination was first used industrially for conversion of isobutene to *tert*-butylamine at temperature and pressure around 573 K and 300 atm commercialized by BASF with 13% yield [51,52]. On the other hand, the anti-Markovnikov hydroamination of simple alkenes provides direct access to linear, aliphatic amines. Through the anti-Markovnikov mechanism, Tillack and co-workers [53] introduced an easily available and stable titanium complex for hydroamination of internal and terminal alkynes with high selectivity. As both ammonia and olefins are nucleophiles, and due to the low reactivity, the thermodynamic equilibrium is reached at relatively high temperature. The base-catalyzed amination of aromatic olefins is described as an environmentally friendly synthesis of various β -arylethylamines. Primary and secondary aliphatic amines as well as aromatic amines react with styrene derivatives to give the corresponding β -arylethylamines with the yield up to 99% [47]. More recently, group of Bell [54] systematically investigated the mechanism of amination of isobutene with NH_3 over Brønsted acidic zeolites at 1 atm and 453-483

K by DFT simulations.

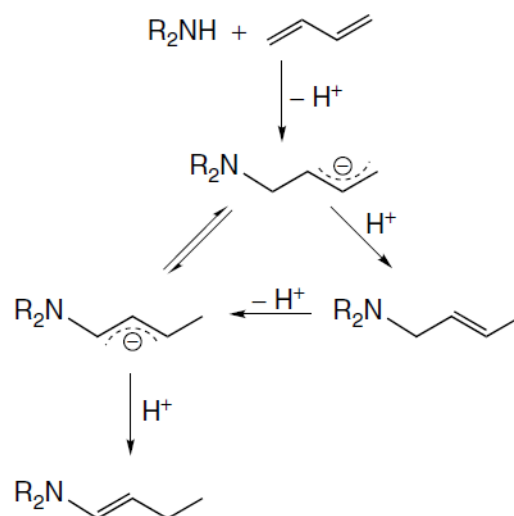


Figure 1.10 Amination of alkenes.

Because of the large activation barrier, the process of catalytic alkenes amination is relatively harsh (high temperature and pressure), which needs a major breakthrough and more investigations upon the development of novel selective catalysts.

1.2.4 Amination of halides

Aminolysis of halides is also a traditional synthetic method of amination. Halides can first react with ammonia to form ammonium, which further contacts with excessive ammonia to produce primary amines. (See **Figure 1.11**) During middle 1900s, researchers developed the method for the liquid-phase amination of aryl halides using palladium based homogeneous catalysts [15,17,55,56,57]. Early literatures in this field are dominated by applications of different homogeneous catalysts. In the following years, several promising heterogeneous based catalysts have been gradually developed. Recently, the copper- and palladium-catalyzed amination of aryl halides has gained increasing attention [13]. The first example of palladium catalyzed amination of aryl halides with ammonia was reported in 2006 by Hartwig et al. [58]. Varieties of different supported ligand-free Pd catalysts were also reported, such as Pd/MgO, Pd/C, Pd/ZrO₂, Pd/TiO₂ and supported zeolite catalysts

[59].

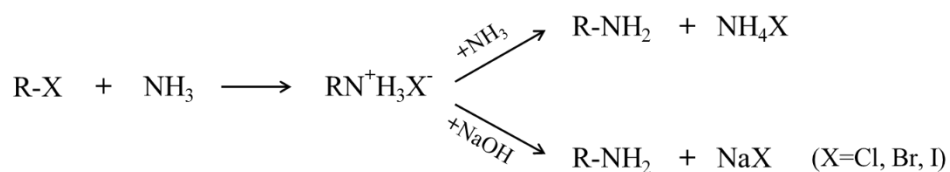


Figure 1.11 The synthetic route of aliphatic amines from halides.

However, using ammonia directly in this reaction is complicated by several issues: first a facile displacement of ancillary ligands from the transition metal by ammonia can occur generating catalytically inactive species, and as this is a consecutive reaction, the produced primary amine can further react with halides to form secondary and tertiary amines. Thus, the final products are always a mixture of primary, secondary and tertiary amines, which largely influences the selectivity to desired amines. Another drawback is the formation of byproduct haloids during reaction, which lowers the atom efficiency. Furthermore, from the industrial point of view, the replacement of traditional expensive noble metal based catalysts by cheaper novel catalysts is urgent and is also of great scientific interest.

1.2.5 Amination of hydrocarbons

The important steps for amination of hydrocarbons are dehydrogenation of hydrocarbons to olefins and reaction with ammonia to form amines. For instance, toluene, toluidines and benzonitrile are formed in similar amounts from methylcyclohexane over the ZnO-TiO₂ catalyst. (See **Figure 1.12**) The distribution of the products is controlled by the nucleophilic attack on an allylic carbenium ion intermediate [60].

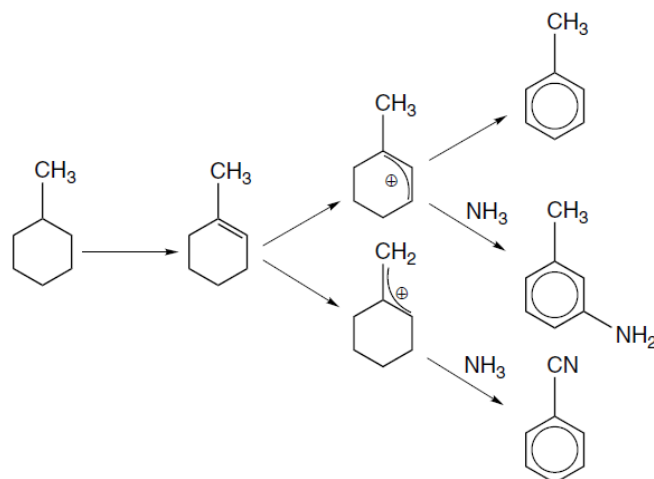


Figure 1.12 The synthetic route of amines from hydrocarbons.

1.2.6 Amination of ethers

Based on the previous studies about selective C-O cleavage reactions [61], it was assumed that amination of ethers with amines might be a promising approach for amine synthesis. (**Figure 1.13**) Cui and co-workers [62] reported an effective approach to produce alkylated amines through catalytic coupling of amines with aromatic ethers or phenols in the presence of a commercial heterogeneous Pd/C catalyst and a co-catalyst with Lewis acid (LA). This protocol provides inspiration for future investigations on the direct transformation of oxygenated compounds to higher valued amines. More recently, Li [63] reported amination of aryl 2-pyridyl ethers via cleavage of the carbon-oxygen bond in the presence of Ni catalyst.

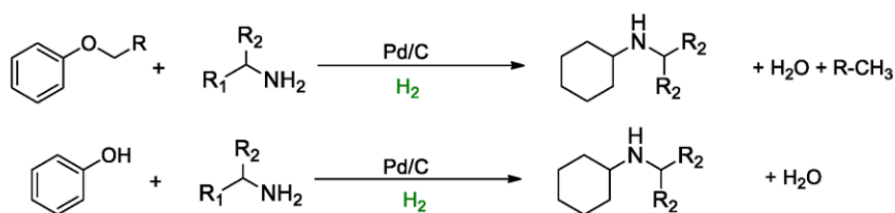


Figure 1.13 Synthesis of alkylated amines from ethers or phenols [62].

1.2.7 Amination of carbon monoxide or carbon dioxide

Several reports showed that synthesis of amines from CO, NH₃ and H₂ is also an important pathway of amination. (See **Figure 1.14**) However, this reaction needs high

temperature and pressure, and the amount of side products are usually higher than that of amines, even at low CO conversion [64,65].

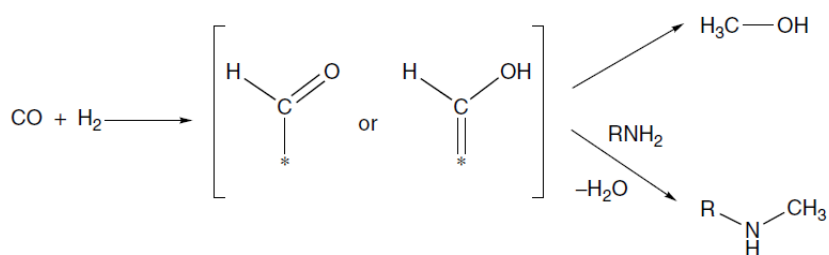


Figure 1.14 The synthetic route of amines from carbon monoxide.

Without addition of hydrogen, direct amination of CO₂ is a typical method for synthesis of methylamines over zeolites, which provides higher conversion and lower selectivity to monomethylamine compared with amination of carbon monoxide.

1.2.8 Amination of alcohols

Among the well-established and important ways for amine synthesis discussed above, by far the most utilized approach is the amination of alcohols, mostly be the reaction of alcohols with ammonia. As we all known, compared with aliphatic acids, esters, alkenes, ethers, and other reactants, alcohols and ammonia are inexpensive and readily starting materials for direct one-pot amination. Alcohols can be produced by different ways: fermentation, hydration of alkenes, reduction of carbonyl compounds, or direct production from synthesis gas. In addition, alcohols with different structures (such as aliphatic alcohols, phenols, amino alcohols and polyalcohols) can also be derived from biomass [61,66]. Another attractive advantage for alcohol amination is that the overall transformation during amination is highly atom-efficient, and water is the only generated side products, which makes this process environmentally benign and safe [4,67,68,69,70,71,72]. Thus, it is becoming more and more essential for the industrial production of various aliphatic amines. For alcohol amination, there exist two types of laboratory reaction systems: liquid phase and gas phase amination, corresponding to discontinuous batch reactors (stirred autoclaves) and continuous flow systems (fixed-bed reactors), respectively [73,74,75]. Continuous fixed-bed

reactors are frequently used as they do not cause high pressure during reaction but provide a good control of residence time of both reactants and products. It is particularly important for obtaining high selectivity to desired amines due to the possibility of consecutive side reactions.

Amines are usually obtained by amination of saturated and unsaturated hydrocarbons, alcohols, halogen-compounds, and carbonyl compounds, by the reduction of a wide variety of nitro-compounds, and by other reactions. Synthesis of amines from alcohols over ThO_2 was first achieved and reported by Sabatier and Mailhe in 1909. From this moment, many investigators were focusing on this reaction. According to the types of catalysts, catalytic alcohol amination can be divided into two categories: amination over dehydration catalysts and amination over dehydrogenation/hydrogenation catalysts in hydrogen atmosphere.

Under elevated temperature and pressure, in the presence of dehydration catalysts, such as Al_2O_3 , SiO_2 , $\text{Al}_2\text{O}_3\text{-SiO}_2$, $\text{Al}_2\text{O}_3\text{-MgO}$, AlPO_4 , and zeolite catalysts (ZSM-5, ZSM-11, ZSM-21), the first stage of amination is the reaction involving the dehydration of gaseous alcohols with formation of olefins, which further react with ammonia, primary, and second amines to form primary, second and tertiary amines, respectively. This reaction process is also named “dehydrative amination” [76]. In the area of industrial application, there is a large demand for ethylamine (Monomethylamine (MMA), dimethylamine (DMA) and trimethylamine (TMA), which are major industrial chemical intermediates) [77]. It was reported in 1884 that methylamines were first synthesized in the batch mode through reaction of methanol and ammonia using zinc chloride as a dehydrating agent at elevated temperature followed by the collection and separation of the desired products, MMA, DMA and TMA [78].

The amination over dehydration catalysts always requires harsh reaction conditions, such as high temperature and pressure. Low yields of amines appears due to a lot of side reactions. This is the reason why another type of catalysts for alcohol amination could be a more attractive approach. With the help of suitable dehydrogenation/hydrogenation catalysts, such as supported Ni, Cu, Pd, Ru, Co, Mo

and metal oxides catalysts, alcohols can react directly with ammonia to form desired amines. This reaction is also regarded as "dehydroamination" process, which has gained increasing attention recently due to its economic advantage. It performs under milder reaction conditions compared with dehydrative alcohols amination [79]. In 1939, Schwegler [80] first proposed the mechanism of alcohol amination where alcohols are initially dehydrogenated to aldehydes or ketones, which will react with ammonia to form imines, followed by hydrogenation to primary amines. Also second and tertiary amines will be produced in the process. Researches showed that, beside the main products, primary, second and tertiary amines, some side products, such as nitriles and olefins occasionally appeared during dehydroamination process and become the main obstacle for achieving high yield and selectivity to desired amines. Thus, numerous works have addressed the exploration of different strategies to obtain high activity and selectivity for alcohol amination. From late 1970s, after major investments by large chemical companies such as Solvay, Dow and BASF, the dehydroamination gradually became mature. This technique mostly uses transitional metals, such as Ni, Cu, Co, Fe, Pt, Ag, et al. as the main active catalysts. Baiker and co-workers started systematic works from 1977 about catalytic alcohols amination, with the goal to establish relationships between active sites of catalysts, activity, selectivity, optimal reaction conditions, formation of metal nitrides, reaction mechanism, kinetics, catalyst deactivation and surface adsorption of reactants [75,81,82,83,84,85,86].

In 1995, Gary and co-workers reported the gas phase amination of ethanol using silica-supported cobalt and nickel catalysts in an atmospheric, continuous fixed bed reactor. They deeply investigated the factors that influenced the reaction: space velocity, hydrogen and ammonia pressure, and reaction temperature [87]. The market also requires the production of bi- and polyfunctional amines. Thus, amination of ethylene glycol to ethylenediamine is meaningful. In an early patent, a Co-oxide catalyst, which provided 70% selectivity to ethylenediamine at 90% glycol conversion, could be achieved under 180 °C and 300 bar pressure [88]. Hammerschmid et al. [89] reported that cyclization of amino-alcohols in a continuous fixed bed reactor at

200-210 °C in the presence of hydrogen is well catalyzed by alumina-supported copper catalyst. The selectivity obtained was higher than 90%.

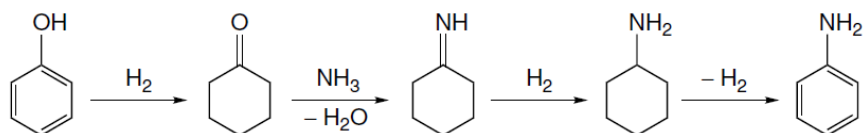


Figure 1.15 Pathway for synthesis of aniline through amination of phenol.

Phenols are considerably less reactive than aliphatic alcohols. In the presence of ammonia and hydrogen, phenols can be converted to aniline. (See **Figure 1.15**) Chang et al. [90] achieved over 90% both of phenol conversion and selectivity of aniline using H-ZSM-5 catalyst at 290 bar and 510 °C.

Except for the above discussed traditional routes for synthesis of amine products, some other special approaches are also developed, like disproportionation of primary amines through thermal method [91,92,93] or photocatalysis [94], and *N*-alkylation of sulfonamides [95].

1.3 Mechanisms of Alcohol Amination

Information about the reaction mechanism is important for description and understanding of reaction kinetics, formation of intermediates and catalyst deactivation. Sabatier et al. [96] firstly reported the mechanism of alcohol amination using ThO₂ as the catalyst. They have found that various alcohols react with ammonia when the vapors are passed over thorium oxide at 350-370 °C. Water is eliminated and the primary amine is formed. So they assumed that the alcohol initially reacts with the catalyst (ThO₂) to form an unstable intermediate ester-alkyl thorate, followed by the rapid reaction with ammonia to produce primary amine. Furthermore, secondary and tertiary amine can be obtained by interaction of alkyl thorate with primary and secondary amine, respectively. During the whole reaction, some side products like olefins might appear. (**Figure 1.16**)

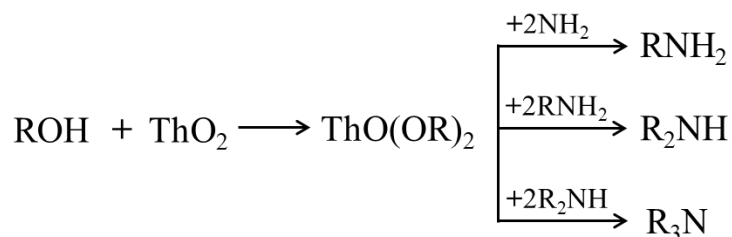


Figure 1.16 Reaction mechanism proposed by Sabatier [96].

Based on the results of alcohol amination over alumina, Baum [97] suggested that ethers formed from alcohols dehydration were intermediates in the synthesis of desired amines. (**Figure 1.17**)

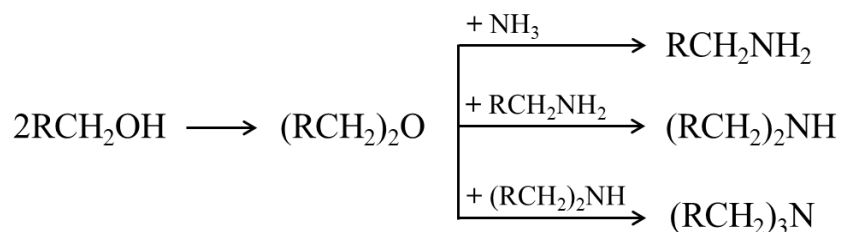


Figure 1.17 Reaction mechanism through ether formation proposed by Baum [97].

Popov [98] thought that in the presence of dehydration catalysts, alcohols were first dehydrated to olefins, which further reacted with ammonia, primary and secondary amines to form primary, secondary and tertiary amines. (**Figure 1.18**)

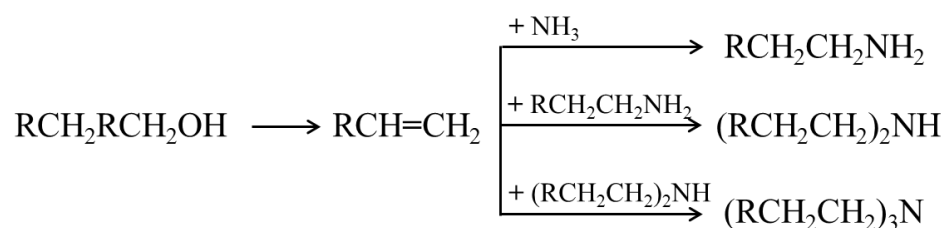


Figure 1.18 Reaction mechanisms through olefin assumed by Popov [98].

In contrast to all the mechanisms reported above, Gruyot and Schwegler [80] speculated that the alcohol was first catalytic dehydrogenated to the corresponding aldehyde or ketone which were stable intermediates of the reaction. The latter would then react with ammonia or an amine to give an imine product which was readily hydrogenated to desired amines. (**Figure 1.19**)

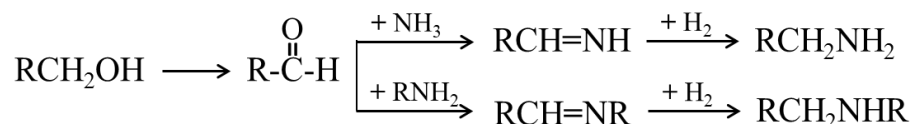


Figure 1.19 The dehydrogenation/hydrogenation mechanism proposed by Gruyot and Schwegler [80].

In addition, Bashkirov and co-workers [99] came to the similar conclusion based on the isotope experiments. In their study, by amination of labeled alcohols with ammonia over dehydrogenation catalysts, they found that dehydrogenation of alcohols take place during amination which indicates that this step may determine the rate of overall reaction. The proposed detailed reaction mechanism is as followed. (**Figure 1.20**)

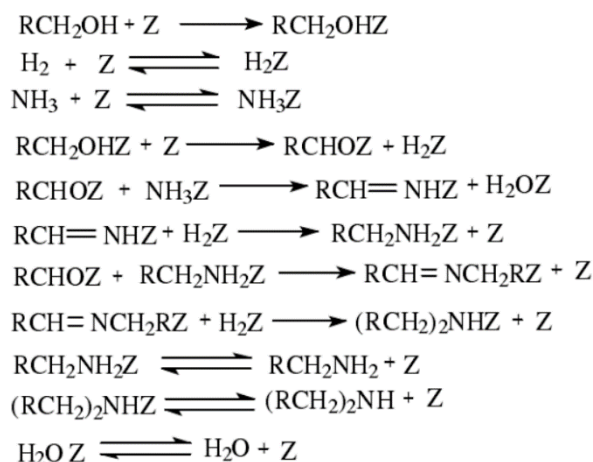


Figure 1.20 Reaction mechanism proposed by Bashkirov and co-workers [99].

It has not been previously identified that an aldehyde (or ketone) is a stable intermediate of alcohols amination. Earlier speculation about mechanism of dehydroamination of alcohols with ammonia was further confirmed until that the aldehyde was first isolated and identified by Baiker [84]. Isotope experiments of the amination of octanol and α,α -dideuterated octanol, $\text{C}_7\text{H}_{15}\text{CD}_2\text{OH}$, with dimethylamine were carried out in the gas phase over alumina-supported copper catalyst at 443 K. The ratio of the reactant conversions was consistent with the kinetic isotope effect found by Miyamoto [100], which supported the view that the rate-determine step involves the abstraction of an α -hydrogen. The most important thing is the consistence

ratio of the product mixture. The absence of the di-substituted product further offered strong support that an aldehyde was the main intermediate during alcohol amination.

In summary, based on the numerous researches, the general mechanism gradually becomes much more clear that the alcohol amination on metal catalysts under hydrogen can be achieved via the so called “Borrowing Hydrogen (BH)” [92, 101, 102, 103, 104, 105, 106, 107, 108, 109, 110] sequence, which consists of dehydrogenation and hydrogenation processes. This mechanism is also known as the hydrogen auto transfer process [69, 111, 112, 113, 114]. The well-known BH mechanism in on-pot alcohol amination generally consists of three consecutive steps: (i) dehydrogenation of an alcohol to a reactive aldehyde (or ketone) (the limiting step); (ii) imine formation from the corresponding aldehyde (or ketone) and the intermediate of amino alcohol; (iii) amine formation via hydrogen transfer from the alcohol to the imine through metal-hydride intermediates. (**Figure 1.21**) During the whole process, water is the only by-product, which means that the route is environmental friendly.

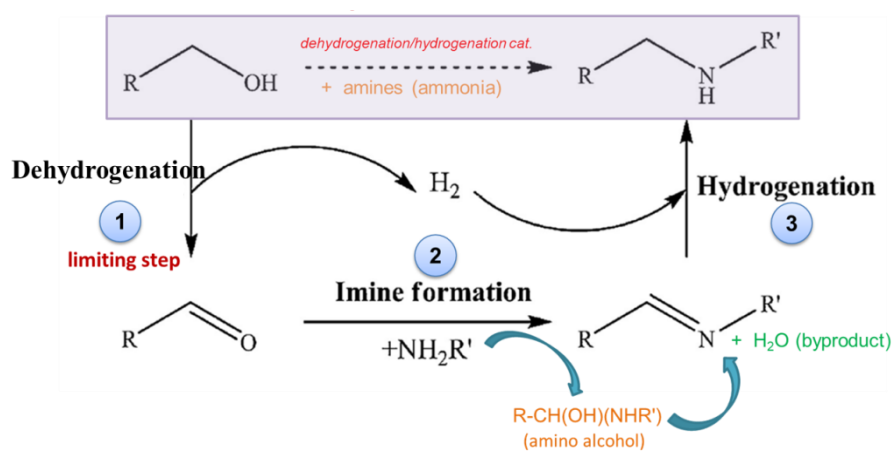


Figure 1.21 A “Borrowing Hydrogen” methodology for directly one-pot amination of alcohol.

1.3.1 Kinetics of amination

The kinetics [84] was investigated in the absence of mass transfer limitations for the dehydroamination of octanol with dimethylamine in both gas and liquid phases using supported copper catalysts. The kinetics in the gas phase was described using the rate equation:

$$r = \frac{k_0 K_{ROH} P_{ROH}}{(1 + \sum K_i P_i)^2} \quad (1-1)$$

where K_i and P_i are the adsorption equilibrium constants and partial pressures for species i , respectively. In order to minimize the correlation between the estimated parameters K_0 and K_i , the parameters were transformed according to the supposition of Himmelblau [115]:

$$k_0 = k_0 (T_m) \exp [(-E_0/R)(1/T - 1/T_m)] \quad (1-2)$$

$$k_i = k_i (T_m) \exp [(-\Delta H_i/R)(1/T - 1/T_m)] \quad (1-3)$$

where $K_0(T_m)$ and $K_i(T_m)$ are the values of K_0 and K_i at the mean reaction temperature, $T_m = 458$ K, and E_0 and ΔH_i are the parameters expressing the temperature dependence of K_0 and K_i .

The liquid-phase reaction of octanol with dimethylamine on alumina-supported copper was found to be first order with respect to the octanol concentration and could be well described by

$$r = k C_{ROH} \quad (1-4)$$

where C_{ROH} (kmol/m^3) is the alcohol concentration in the liquid phase and k ($\text{m}^3/\text{kg} \cdot \text{s}$) is the rate constant.

1.3.2 Reaction conditions

The optimal reaction conditions depend, of course, on the types of reactors used for amination reactions. The parameters for bath reactor and fixed-bed reactor will not be the same for the same model amination reaction. Here, we take amination of ethanol by fixed-bed system as an example to discuss the different reaction parameters which influence the reaction conversion and selectivity. Sewell et al. [87] reported that a silica supported nickel-rhenium catalysts have been shown to be efficient for the amination of ethanol using ammonia. The fixed-bed system is shown in **Figure 1.22**.

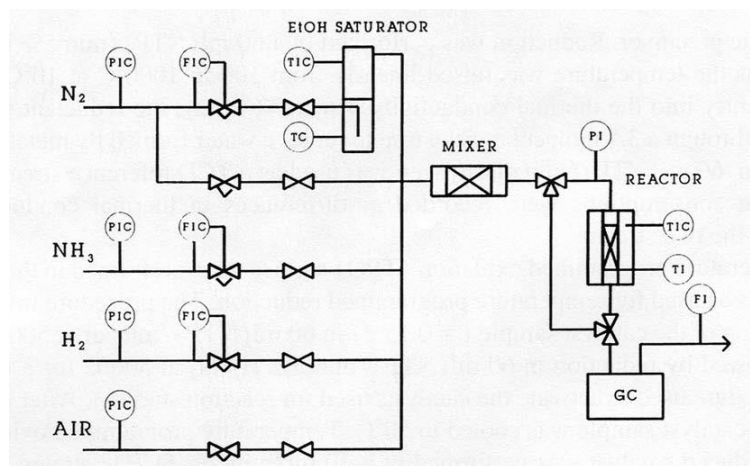


Figure 1.22 Schematic of ethanol amination apparatus designed by Sewell [87].

Several factors influence the reaction: catalyst, space velocity, hydrogen and ammonia pressure, and reaction temperature. Increasing the residence time will result in an increase in ethanol conversion for both the Co/SiO_2 and Ni/SiO_2 catalysts. Decreasing the partial pressure of hydrogen results in a large decrease in ethanol conversion for the Co/SiO_2 which may be ascribed to cobalt nitride formation; whereas the ethanol conversion for the Ni/SiO_2 decreases only slightly which is probably due to the deposition of carbonaceous material. It has been reported that only a small hydrogen pressure is required to prevent nickel nitride formation. Decreasing the hydrogen partial pressure results in a large decrease in the selectivity to the ethylamine product, principally due to the formation of the diethylether $[(\text{C}_2\text{H}_5)_2\text{O}]$ byproduct, which might be due to an acid catalyzed condensation of ethanol by the support silanol groups. Thus, hydrogen plays an important role in alcohol amination, although it has no significant influence on the overall amination reaction rate. Hydrogen improves the selectivity to primary amines by suppressing the simultaneously catalyzed disproportionation of reactant and product amines, and it is crucial to prevent catalyst deactivation caused by metal nitride and/or metal carbide formation occurred by interaction of amines with the metal surface [82,116].

The molar ratio of ammonia to alcohol also affects the whole amination activity and selectivity due to the competitive adsorption of different molecules (reactants and products) on the surface of the catalyst [117]. Increasing the partial pressure of

ammonia resulted in decrease of conversion and increase in MEA selectivity for both Co/SiO₂ and the Ni/SiO₂ catalysts.

1.3.3 Side reactions

1.3.3.1 Disproportionation of amines

Disproportionation of amines plays a decisive role as a major side reaction during the catalytic amination of alcohols, which can strongly decrease the selectivity to the desired amines [75,118]. Braun et al. [119] proposed the following mechanism for the disproportionation of simple amines over hydrogenation /dehydrogenation catalysts (Figure 1.23):

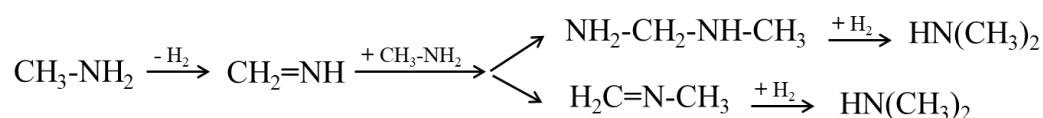
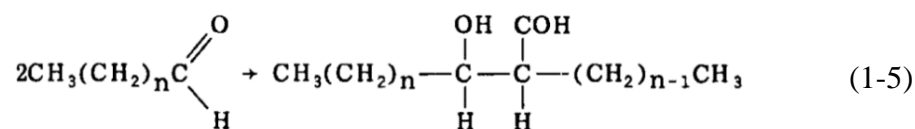


Figure 1.23 Mechanism for the disproportionation of primary amines [119].

Based on the experimental observations, Volf et al. [120] proposed that either addition of amine to imine or decomposition of diamino derivatives is the rate determining step for the disproportionation.

1.3.3.2 Aldehyde condensation

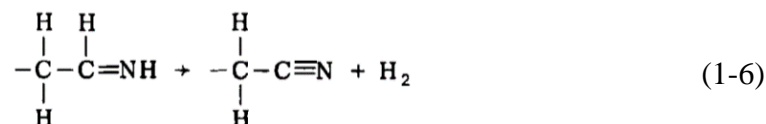
Aldol condensation of intermediate aldehydes may also occur during amination [75,84]:



This reaction can occur unassisted by a metal catalyst. Note that during copper-catalyzed amination, the aldol concentration never exceeded 1 wt% of the total product mixture.

1.3.3.3 Formation of nitriles

Formation of nitriles can also occur as a side reaction during dehydroamination of alcohols with ammonia or primary amines. The nitriles are formed by dehydrogenation of the corresponding imines, which are formed as intermediates during amination:



Generally, nitrile formation is favored at high temperatures (> 570 K) and at low hydrogen partial pressures [121].

1.4 Catalysts Used for Amination of Alcohols

For industrial applications, a suitable catalyst should have high activity, good selectivity, corrosion resistance, thermal stability and mechanical strength. Till now, numbers of homogeneous and heterogeneous catalysts have been applied for investigation of alcohol amination.

1.4.1 Homogeneous catalysts

Most of previous works have addressed development of homogeneous catalysis for alcohol amination reaction. Ru [67,110,122,123], Pd [72], Rh [124], Ir [107,125,126], Fe [127,128,129,130,131], and Mn [132] complexes have shown good activity and selectivity. In addition, Ru and Ir complexes have been shown to catalyze this reaction at relatively low temperatures (90-150 °C). It is suggested that the reaction occurs over a coordinative unsaturated (reactive) metal site and cooperative adjacent acid/base sites. The use of relevant organic ligands is believed to be indispensable for smooth catalyst operation. Also, different metal triflates and triflimides, including the parent triflic acid (HOTf) were active for synthesis of secondary amines through *N*-alkylation of amines with alcohols. Gunanathan et al.

[123] developed a novel air stable ruthenium pincer complex for the selective synthesis of primary amines directly from alcohols and ammonia under mild conditions based on BH mechanism, precluding the need for stoichiometric amounts of toxic reagents, high pressure, and harsh experimental conditions. Payard and co-workers [133] demonstrated that among the best performing homogeneous catalysts for the direct amination of activated secondary alcohols using electron-poor amine derivatives, could be metal triflates, such as aluminum triflate, Al(OTf)₃. Much higher selectivity was achieved when toluene was used as a solvent for amination of benzyl alcohol with aniline based via the S_N2 mechanism predicted from the DFT modelling.

However, these processes have several disadvantages due to use of expensive non-recoverable catalysts, difficulties in catalyst-product separation and indispensable use of additives or co-catalysts such as inorganic or organic bases and stabilizing ligands. All this makes it difficult for industrial application. For these reasons, there is an urgent requirement to develop heterogeneous catalysts for amination of alcohols.

1.4.2 Heterogeneous catalysts

The heterogeneously catalyzed amination of aliphatic alcohols shows several advantages compared to the homogeneous catalysis. First, the heterogeneous catalysts can be easily separated from the reaction mixture. Second, they can be reused for several runs after regeneration in hydrogen without obvious activity and selectivity loss. Till now, different types of catalysts containing supported and non-supported single metals (Ru, Pd, Au, Ag, Cu, Co, Ni, and so on) [117,134,135,136,137,138,139,140], bimetallic [141,142,143,144,145,146,147,148], hydroxides [108,149,150], zeolites [151,152], and some other oxides [73,153] have been applied for alcohol amination.

Different heterogeneous based catalysts for amination of alcohols are summarized in **Table 1.1**.

Table 1.1 Heterogeneous catalysts used for amination of alcohols

Catalysts	Alcohols	Reaction conditions	Yield (%)	Ref.	
Ru/C	Dodecanol	Batch, 4 bar NH ₃ , 2 bar H ₂ , 200 °C	Dodecylamine 68.7%	[135]	
Ru NPs	1-Octanol	Batch, NH ₃ /octanol=17, 2 bar H ₂ , 180 °C, 24 h	1-Octylamine 81%	[134]	
Ru/HAP	BA	Batch, <i>N</i> -methylbenzylamine/BA=1/4, mesitylene, Ar, 130 °C, 6 h	Tertiary amine 74%	[154]	
Pd/C	Dodecanol	Batch, 4 bar NH ₃ , 2 bar H ₂ , 200 °C	Dodecylamine 74.3%	[135]	
Pd/K-OMS-2	BA	Batch, aniline, 1 bar N ₂ or air, 160 °C	Secondary amine 95%	[136]	
Pd/MgO	BA	Batch, BA/aniline=3, N ₂ , n-dodecane, 180 °C	Secondary amine 78.2%	[141]	
PGM	Pd/Al ₂ O ₃	Continuous, phenol/NH ₃ /H ₂ /H ₂ O=1/9.3/9.3/1.1, 250 °C	Aniline 30.9%	[155]	
	Pd/Fe ₂ O ₃	Batch, BA/aniline=1.5, Ar, 140 °C, 12 h	Secondary amine 70.3%	[156]	
	Pd/CeO ₂	Batch, BA/aniline=3, N ₂ , 160 °C, 3 h	Secondary amine 79%	[166]	
	Pt/C	Dodecanol	Batch, 4 bar NH ₃ , 2 bar H ₂ , 200 °C	Dodecylamine 40.9%	[135]
	Pt/MgO	BA	Batch, BA/aniline=3, N ₂ , n-dodecane, 180 °C	Secondary amine 59.8%	[141]
Ir/C	Dodecanol	Batch, 4 bar NH ₃ , 2 bar H ₂ , 200 °C	Dodecylamine 46.1%	[135]	
Os/C	Dodecanol	Batch, 4 bar NH ₃ , 2 bar H ₂ , 200 °C	Dodecylamine 24.7%	[135]	
Au	Au/ZrO ₂	Batch, aniline, 9 bar N ₂ , 180 °C	Secondary amine 59.9%	[140]	
	Au/ZrO ₂	Batch, BA/aniline=1, N ₂ , toluene, 110 °C, 22 h	Secondary amine 93.1%	[157]	
	Au/TiO ₂	Batch, BA/NH ₃ /H ₂ O=1/1/5, o-xylene, 160 °C, 22 h	Secondary amine 42.9%	[139]	
	Au/MgO	Batch, BA/aniline=3, N ₂ , n-dodecane, 180 °C	Secondary amine 35.3%	[141]	
Ni	Ni/γ-Al ₂ O ₃	Batch, 4 bar NH ₃ , 160 °C	2-Octylamine 67.2%	[71]	
	Ni/Al ₂ O ₃ /SiO ₂	Continuous, 60 bar NH ₃ , BA/NH ₃ =1/7, o-xylene, 160 °C	Secondary amine 100%	[139]	
	Ni/CaSiO ₃	Batch, NH ₃ /2-octanol=2.23, o-xylene, 160 °C, 20 h	2-Octylamine 86%	[158]	
	Ni/LaAlSiO	Continuous, total 20 bar, n(NH ₃):n(IPO) = 6:1, WHSV=1 h ⁻¹ , 180 °C	Isopropylamine 94.1%	[159]	
	Ni/HAP	Continuous, propanol/NH ₃ /H ₂ =1/5/95, flow rate at STP = 30 mL min ⁻¹ , 150 °C	Propylamine 9.9%	[137]	
Co	Co/Al ₂ O ₃	Continuous, NH ₃ /alcohol=7, 1 bar,	1-Butylamine 64%	[251]	

			GHSV=20-50 L/g h, 140 °C		
	Co/SiO ₂	Ethanol	Continuous, EtOH/NH ₃ /H ₂ /N ₂ =1/2/8.6/17.1, 180 °C	Ethylamine 32.8%	[160]
	Co/ γ -Al ₂ O ₃	2-Propanol	Continuous, 2-propanol/NH ₃ /H ₂ /N ₂ = 1/4/6/22.8, WHSV=4.29 h ⁻¹ , 210 °C	Isopropylamine 58.4%	[161]
Cu	Cu	BA	Batch, BA/aniline=1.3, KOH, toluene, Ar, 160 °C, 24 h	Secondary amine 99%	[138]
	Cu(OH) _x /Al ₂ O ₃	BA	Batch, mesitylene, 1 bar Ar, 135 °C, 65min	Secondary amine 85%	[150]
	Cu(OH) _x /TiO ₂	BA	Batch, mesitylene, 1 bar Ar, 135 °C, 65min	Secondary amine 80%	[150]
Bimetal	Pt-Sn/ γ -Al ₂ O ₃	BA	Batch, BA/aniline=1, o-xylene, 1 bar N ₂ , 145 °C, 8 h	Secondary amine 97%	[162]
	PdZn/Al ₂ O ₃	BA	Batch, BA/aniline=1, p-xylene, 1 bar Ar, 110 °C, 0.5 h	Secondary amine 99%	[185]
	Cu-Cr	1-Octanol	Continuous, NH ₃ , 200 °C	1-Octylamine 35%	[148]
	CuO-Cr ₂ O ₃ / γ -Al ₂ O ₃	Dodecanol	Continuous, NH ₃ , DMA/DOL = 5.5, 230 °C	Tertiary amine 92.2%	[163]
	PdPt/MgO	BA	Batch, BA/aniline=3, N ₂ , n-dodecane, 180 °C	Secondary amine 80%	[141]
	AuPd/MgO	BA	Batch, BA/aniline=3, N ₂ , n-dodecane, 180 °C	Secondary amine 44.8%	[141]
	AuPt/MgO	BA	Batch, BA/aniline=3, N ₂ , n-dodecane, 180 °C	Secondary amine 31.3%	[141]
	Co-La	1,3-Propanedi ol	Continuous, diol/NH ₃ /H ₂ = 1/60/2, 210 °C	Secondary amine 22.5%	[142]
	Co-Fe	1,3-Propanedi ol	Continuous, diol/NH ₃ /H ₂ = 1/60/2, 210 °C	Secondary amine 32.3%	[142]
	NiCu/ γ -Al ₂ O ₃	BA	Batch, 1 bar argon, alcohol/aniline=5/2, o-xylene, NaOH, CaCl ₂ , 160 °C, 12 h	Secondary amine 90%	[164]
	Rh-In/C	1,2-Propanedi ol	Batch, aqueous NH ₃ , H ₂ , 180 °C, 24 h	1-Amino-2-propanol 5%	[143]
	NiCu/Diatomite	1-Octanol	Batch, NH ₃ /H ₂ (40%/60%, vol/vol), 230 °C	Trioctylamine 97.3%	[165]
CoAl/HT	p-methoxybe nzyl alcohol	Batch, benzylamine, K ₂ CO ₃ , air, 160 °C, 9 h	Secondary amine 92%	[167]	

*BA: benzyl alcohol

Supported metal based dehydrogenation/hydrogenation catalysts for the ammonolysis of alcohols have been extensively studied. Yan and co-workers [166] reported a Pd/CeO₂ catalyst based on high-surface CeO₂ (CeO₂-HS) pre-treated at 500 °C, which had an abnormally high activity and selectivity in the amination of benzyl alcohol with aniline (and ammonia). They proposed that unlike standard Pd supported catalysts, a promoted H₂ transfer on high-surface Pd/CeO₂ via spillover between Pd and ceria can be regarded as a main driver for amination based on the borrowing hydrogen mechanism. **(Figure 1.24)** It opens an avenue for the fine design of H₂ pumps based on ceria for industrially relevant amination reactions.

Ni has been widely used for amination of alcohols due to its high activity and selectivity towards primary amine. Leung et al. [139] investigated that highly selective synthesis of primary amines from alcohols and NH₃ was achieved using a commercially available Ni catalyst (65 wt % Ni-Al₂O₃/SiO₂), without adding H₂. Using a fixed-bed reactor, the amination of aliphatic alcohols can be achieved in good yields and selectivity (51-100% conv., 90-100% sel.), as the accumulation of water byproduct can be removed. Shimizu and co-workers [71] also reported the synthesis of primary amines from alcohols and NH₃ by an Al₂O₃-supported Ni nanoparticle catalyst as a recoverable and noble-metal-free catalytic system

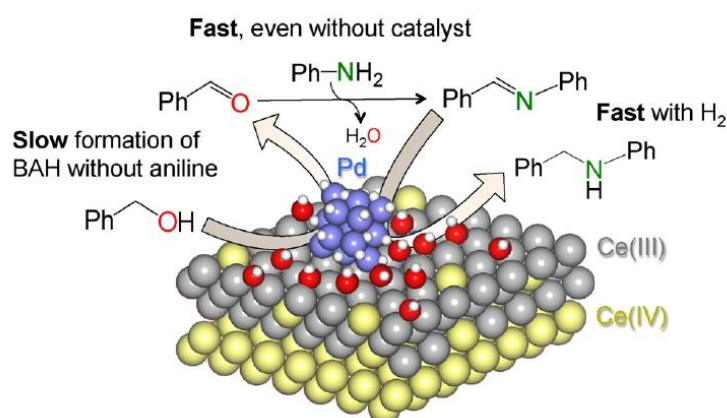


Figure 1.24 Hydrogen transfer pathway over Pd/CeO₂-HS for the amination of benzyl alcohol with aniline (and ammonia) [166].

without additional hydrogen under relatively mild conditions. Various aliphatic alcohols are tolerated, and turnover numbers were higher than those of Ru-based

homogeneous catalysts. It is clarified that the surface metallic Ni sites are the catalytically active species, and the co-presence of acidic and basic sites on the support surface is indispensable for this catalytic system. It is generally accepted that the reaction begins with the dehydrogenation of alcohol by Ni sites to a carbonyl compound, which reacts with ammonia to give an imine. Finally, hydrogen transfer from the Ni-H species to the imine gives the primary amine. It was tentatively assumed that basic sites of the alumina promote the dehydrogenation step, possibly by abstraction of a proton from the alcohol, and the acidic nature of alumina might be relevant to the hydrogen transfer step. Shi [138] proposed a simple self-supported copper powder catalyst for alcohol amination. Notably, the self-supported Cu catalyst showed a significantly better catalytic performance than oxide-supported nano-copper catalysts. In addition, the copper powder catalyst presented stable recyclability and good substrate tolerance. (Figure 1.25)

He et al. [150] reported that easily prepared inexpensive supported copper hydroxides, $\text{Cu}(\text{OH})_x/\text{Al}_2\text{O}_3$ and $\text{Cu}(\text{OH})_x/\text{TiO}_2$, can act as efficient heterogeneous catalysts for the *N*-alkylation of primary amines or ammonia with alcohols. Generally, copper-catalyzed *N*-alkylation performed under high H_2 pressures (≥ 100 atm) and high temperature (≥ 160 °C), and/or stoichiometric amounts of bases (e.g., K_2CO_3) to attain high yields of desired amines [167]. In contrast, *N*-alkylation with supported copper hydroxide catalysts efficiently performed under relatively mild reaction conditions (1 atm of Ar, 135 °C) without any co-catalysts.



Figure 1.25 *N*-alkylation of amines with alcohols over self-supported Cu [138].

Recent years, researchers have found that supports can play an important role in amination of alcohols [168]. Recently, group of Bell [137] reported a Ni-supported hydroxyapatite catalyst (Ni/HAP), which was quite efficient for propanol amination to

propylamine at 423 K. The authors proposed that the superior performance of Ni/HAP is mainly attributed to the high density of basic sites on HAP compared with other oxides, which are responsible for stabilizing alkoxide intermediates and suppressing the disproportionation of primary amines. (**Figure 1.26**)

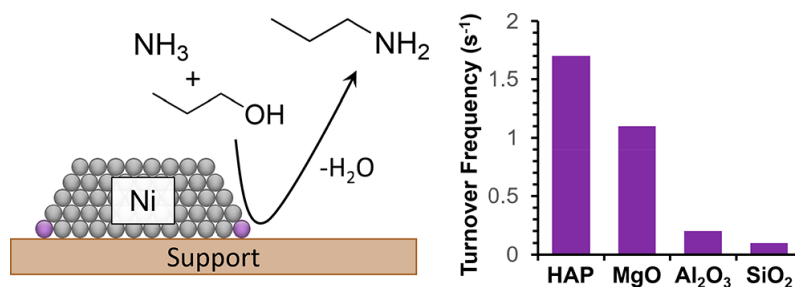


Figure 1.26 Support effects for amination of propanol [137].

1.4.3 Challenges in amination of alcohols

Although heterogeneous catalysts are widely used for amination of alcohols under hydrogen, they still suffer from some drawbacks such as limited substrate scope, the need for high temperature, high pressure of NH₃ and H₂, different undesired side reactions during amination in particular at high conversion, such as disproportionation of amines, aldehyde condensation and formation of nitriles.

i) Difficulties of alcohol dehydrogenation (limiting step);

As we know, the limiting step of alcohol amination was regarded as the dehydrogenation of alcohol to the corresponding aldehyde [111]. Generally, high reaction temperature (150-200 °C) was needed for amination of alcohols (especially aliphatic alcohols) due to the high temperature requirement for oxidant-free alcohol dehydrogenation. During amination reaction, higher temperature is also needed for desorption of surface strongly adsorbed species to accelerate the whole reaction rate.

ii) Catalyst poisoning and leaching problems;

In liquid phase amination, under high temperature, pressure and base environment, active metal sites can be easily poisoned by reactants or amine products. Also, metal particles can be leached from the surface of support in the strong basic

conditions. This problem creates difficulties for industrial application.

iii) Insufficient primary amine selectivity:

The most challenging task for alcohols amination is the selective synthesis of primary amines. As amination of alcohols is a consecutive reaction, disproportionation of the produced primary amine proceeds through self-coupling reaction to produce secondary or tertiary amines, leading to the low selectivity of primary amines [91,94,95].

Thus, it is still challenging to develop catalysts with high activity, selectivity and stability for amination of alcohols.

1.5 Strategies for Selectivity Control

Several strategies can be considered for improvement of the selectivity to primary amines in the alcohols amination. They can be classified into 3 main groups:

- (1) selective catalyst deactivation (“capping”) strategy;
- (2) selectivity control on the basis of structural sensitivity, metal particle size effects;
- (3) catalyst promotion, design of bimetallic catalysts.

The amination selectivity can be also improved by optimizing the reaction conditions such higher ammonium content and conduction of the reaction in supercritical medium.

Catalyst deactivation due to coke formation is an important technological and economic problem of great and continuing concern in the practice of industrial catalytic processes [169,170,171]. Deactivation issues greatly impact research, development, design and operation of commercial processes. The mechanisms of solid catalysts deactivation can be due to poisoning, fouling, thermal degradation and sintering, vapor formation, vapor-solid and solid-solid reactions, and attrition or crushing, which are caused by chemical, mechanical and thermal aspects. Among them, poisoning is the strong chemisorption of species (reactants, products, or impurities) on catalytic sites which block some sites for catalytic reaction

[172,173,174]. Peña et al. [175] reported that during Fischer-Tropsch (FT) synthesis, three types of carbonaceous species (hydrocarbons, strongly adsorbed hydrocarbons and amorphous polymeric carbon) were detected on the surface of used catalysts, which lower the reaction activity. Moodley et al. [176] also investigated the role of carbon deposition in the deactivation of cobalt catalysts exposed to the commercially relevant conditions of FT synthesis.

Although catalyst deactivation is generally undesired, some poisons may be added purposefully to selectively block some active surface sites, thus, ether to moderate the activity and/or to improve the selectivity of fresh catalysts. In addition to other deactivation mechanisms, deposition of carbonaceous species on the surface of the catalyst appears to be one of the main reasons of catalyst deactivation.

Capping agents [177] (organic ligands, polymers, surfactants, etc.) can act as a “poison”, limiting the accessibility of active sites, as well as a “promoter”, producing improved yields and unpredicted selectivity control. Different capping agents have been applied for metal nanoparticles synthesis (**Figure 1.27**):

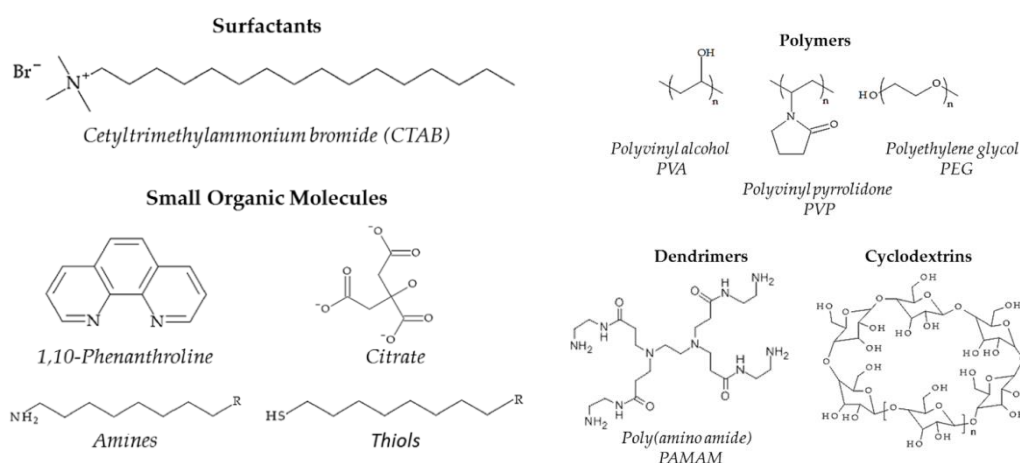


Figure 1.27 Representative capping agents used in metal nanoparticle synthesis [177].

In heterogeneous catalysis, almost all phenomena involved in the catalytic cycle take place at the interphase between the catalyst surface and the reaction medium. Therefore, describing the interface at the nanoscale is necessary for elucidating kinetic mechanisms and the nature of the active sites. The presence of an organic shell generated by capping agents on the nanoparticle surface introduces two different

interfaces: the metal-ligand interface and the ligand-solution interface (**Figure 1.28**).

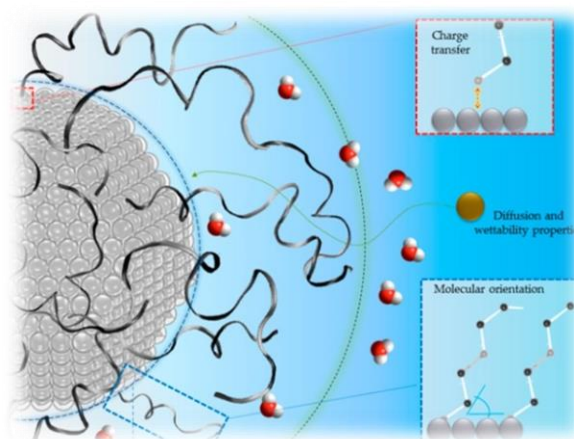


Figure 1.28 The metal-ligand interphase.

The metal ligand interphase can affect the activity and selectivity according to different mechanisms: charge transfer, selective blocking, chiral modification, molecular recognition, adsorption geometry control and steric hindrance [178]. The altered electron density originated by charge transfer process (electron donation) at the metal ligand interphase can promote the activation of the adsorbed reactant, thus enhancing the catalytic activity. Similar effect has been reported by Tsukuda et al. [179]. Electron donation from electron-rich capping agents to the metal surface can be also exploited to control the selectivity of a reaction, by favouring the adsorption of electron deficient substrates. This effect has been proved by Zheng et al. [180]. In other cases the competitive effect between metal-ligand and metal-substrate interactions is on the basis of a modified selectivity of a reaction. Shevchenko and co-workers [181] studied the effect of the capping agent (trioctylphosphine oxide (TOPO) as) on the selectivity in the hydrogenation reaction of alkynes to alkenes. A similar effect has been evidenced by Kaneda et al. [182] in the case of dimethylsulfoxide (DMSO)-protected Pd nanoparticles. By selecting a proper ligand, which strongly adsorbs only on specific active sites (selective blocking), it is possible to suppress undesirable processes without affecting the overall activity of the catalyst. Recently, Campisi et al. [183] ascribed the improved selectivity in benzyl alcohol oxidation to the presence of PVA on Pd NPs.

As shown in **Figure 1.29**, the active site isolation effect has been used for preventing the formation of undesired benzyl benzoate in the Au-catalysed selective oxidation of benzyl alcohol to benzaldehyde [184].

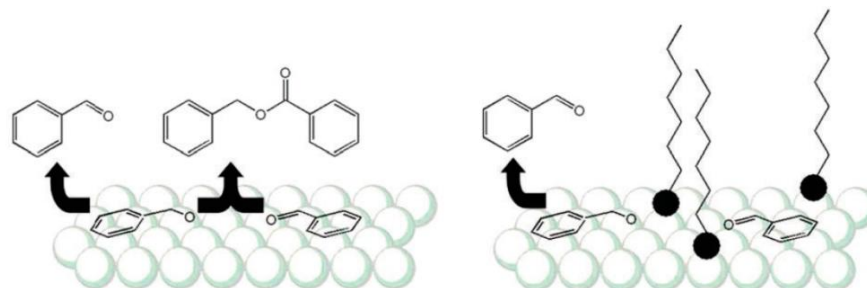


Figure 1.29 Active site isolation effect in benzyl alcohol oxidation [184].

Based on the strategies for selectivity controlling and challenges in amination of alcohols, different attempts have been tried to improve the performance of this reaction. Generally, the reaction rates and selectivity of many metal-catalyzed reactions depend on the size of the metal particles in the nanoscale range. Liang and co-workers [134] developed non-supported ruthenium nanoparticle catalysts (2-9 nm). They found that the smaller Ru nanoparticles has higher primary amine selectivity due to the strong surface negative charge, which could make them less favorable for adsorption over isolated metal domains and activation of the electron-rich secondary imine to form secondary and tertiary amines. (**Figure 1.30**)

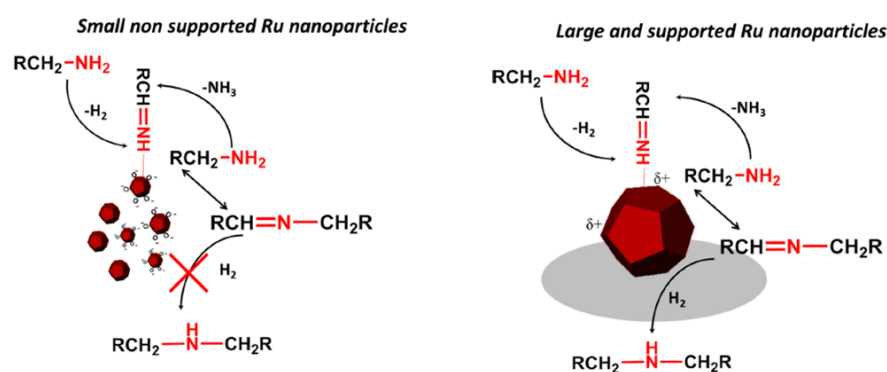


Figure 1.30 Ru nanoparticle size and effect of support on self-coupling of primary amines [134].

An appropriate combination of two metal elements provides not only a substantially modified electronic structure of the active metal component but also a uniform reaction environment. Furukawa et al. [185] developed a bimetallic system by formation of a PdZn intermetallic phase (PdZn/Al₂O₃), which was an efficient catalyst for amination of alcohols. The authors proposed that the unique catalytic performance of PdZn originates from the fundamental change in the C-H activation property and adsorption affinity of the substrates, allowing preferential activation of alcohols over amines (**Figure 1.31**). As we know, the main reason for low selectivity in the synthesis of primary amines is that the product amines are significantly more reactive than the reagent NH₃. Ficher et al. [186] found that the application of supercritical ammonia (scNH₃) as a solvent and reactant provides a remarkable selectivity improvement in the amination of aliphatic diols, compared with the performance of the same catalyst under similar conditions. This selectivity enhancement in the near-critical region may be attributed to elimination of the interfacial mass transfer leading to a higher surface concentration of ammonia.

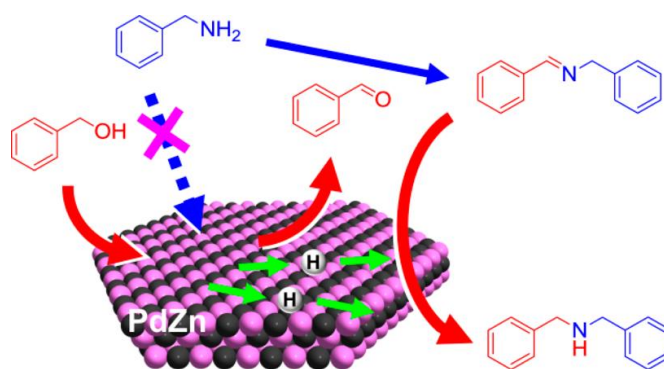


Figure 1.31 Enhancement of amination selectivity in bimetallic system [185].

1.6 Objectives and Research Plans of this Thesis

In summary, amination of alcohols is a relatively environmental benign way compared with other routes for amine synthesis. However, the most challenging problem of alcohols amination is selective synthesis of primary amines, as the reason of easily self-coupling reaction of primary amines, producing secondary or tertiary

amines, leading to the low selectivity of primary amines. So, development of cost saving heterogeneous catalysts for selective amination of alcohols is meaningful and urgent.

Herein, in this thesis, our goal is, to improve the selectivity to primary amines of alcohol amination reactions. This goal will be achieved via, modification on the one hand, of the existing metal based heterogeneous catalysts and elaboration on the other hand, of new efficient non-metal catalysts for selectively synthesis of primary amines by alcohols amination through liquid and gas phase reactions.

1.6.1 Catalyst deactivation for primary amine selectivity enhancement

Generally, catalyst deactivation is an undesired technical issue, which leads to a decline of the catalytic activity and necessity to regenerate, to replace and to recycle the spent catalysts, causing high cost of catalysts for industrial application. However, intentionally blocking some active sites through poisoning, carbon fouling, thermal degradation and sintering may have a positive effect on the catalytic performance, especially on the selectivity to some desired products.

In this thesis, we consider that restraining self-coupling of primary amine through selective blocking active sites by intentional deposition of polymeric carbonaceous species to form some isolated domains on the surface of metals would be possible to improve the selectivity of desired primary amine products.

1.6.2 Creation of highly dispersed Co and Ni nanoparticles by carbon deposition

Co and Ni based catalysts are among the most popular materials used nowadays in industry. Traditional methods of catalyst preparation like impregnation or precipitation lead to formation of large metal nanoparticles (15-30 nm) composed of highly aggregated metal clusters. It results in relatively low metal dispersion and catalytic activity. Hereby we propose an efficient way to significantly increase the dispersion (2-3 times) of metal catalysts by disassembling of metal clusters by in-situ polycondensation of aldehydes produced during dehydrogenation of long chain alcohols. Deposition of bulky polymers at the interface areas decompose metal nanoparticles. Removal of carbon species demonstrates isolated metal nanoparticles

with the sizes about 2-7 nm and 3-6 times higher activity in the reactions of hydrogenation, amination and oxidation.

1.6.3 Bi as a promoter for selective amination of 1-octanol

Except for selective poisoning, catalytic activity and selectivity can be also adjusted by addition of secondary metal promoters over the parent catalysts. The synergetic of bimetals usually have positive effect towards the catalytic performance. Fischer et al. [186] reported the catalytic synthesis of 1,3-diaminopropane from 1,3-propanediol and ammonia in a continuous fixed-bed reactor using unsupported Co-based catalysts. Promotion of the unsupported cobalt catalyst with iron or lanthanum would significantly improve the selectivity of 1,3-diaminopropane. It was suggested that addition of a small amount of iron suppresses the transformation of active metastable β -cobalt phase to the thermodynamically more stable α -cobalt phase under reaction conditions, which was better for catalytic selectivity.

In this thesis, supported cobalt catalyst was modified by addition of metallic bismuth promoter to improve the catalytic activity, primary amine selectivity and stability during liquid phase amination of 1-octanol. The mechanism of bismuth promotion was also uncovered through different characterizations and model reactions.

1.6.4 Design of non-metal heterogeneous catalyst for amination of alcohol

Conventionally, amination of alcohols using different noble metal based homogeneous or heterogeneous catalysts, such as Ru, Ir, Rh, and Pt, has been widely reported. However, disadvantages due to use of expensive non-recoverable catalysts, difficulties in catalyst-product separation and low selectivity to primary amines. Development of easily recoverable and recyclable non-noble metal based heterogeneous catalysts for amination of alcohols is still a challenging topic. In this thesis, we applied the easily available transition metal- and solid acid-based heterogeneous catalyst titanium hydroxide for liquid-phase amination of alcohols. Interestingly, this catalyst exhibits the highest activity and selectivity towards the

desired amine, compared with other hydroxides, metal oxides and zeolites. The mechanism of the reaction using such catalyst involves dehydration of alcohols to ethers with subsequent C-O bond cleavage by amine with formation of secondary amine and recovery of alcohol. The reaction mechanism was investigated in details in chapter 6.

1.7 Outline of this Thesis

This thesis consists of seven chapters:

Chapter 1 summarizes the importance and utilizations of amine products in our daily life and different conventional routes for synthesis of amines. Amination of alcohols is a relatively green route compared with other methods. The basic borrowing hydrogen mechanism for amination of alcohols was illustrated in details. Despite the huge advantages of alcohols amination, it still suffers from the drawback of low selectivity to primary amines caused by some side reactions. Different strategies of catalyst design used for different reactions, such as FT synthesis, hydrogenation and oxidation to optimize the catalytic performance, have been summarized. However, only few studies focus on the primary amine selectivity enhancement by catalyst modifications. Also, few papers reported the non-metal based catalysts for amination of alcohols. The goals of this thesis are summarized in Chapter 1.

Chapter 2 introduces the experimental procedures used for catalyst preparation, methodologies of catalyst characterization and evaluations of catalytic performance.

Chapter 3 explains the strategy of selective carbon deposition over cobalt catalyst, which aims to increase the selectivity to primary amine through suppressing of hydrogenation of secondary imine for both gas-phase and liquid-phase amination of alcohols. This catalytic modification process provides an efficient way for selectivity enhancement even for other reactions.

Chapter 4 is focused on application of carburization of metal catalyst for the synthesis of highly dispersed catalysts to increase catalytic activity of the catalyst in

amination and other catalytic reactions.

Chapter 5 is devoted to application of bismuth as liquid metal promoter to enhance the catalytic performance of cobalt catalyst. The metallic bismuth as a liquid phase during high temperature amination reaction could “wash” the surface of cobalt, which largely increases the activity and stability of amination of 1-octanol. It also has the similar effect as carbon deposition for primary amine selectivity enhancement.

Chapter 6 presents a new cheap non-noble metal based heterogeneous catalyst titanium hydroxide, which provides the selectivity higher than 90% to secondary amines for functionalized aromatic and aliphatic alcohols and amines at high catalytic stability. The mechanism of alcohol amination using such catalyst through ether formation followed by C-O bond cleavage was first proposed in this thesis.

Chapter 7 gives the general conclusion of this thesis and perspectives towards catalyst and process designing for selective amination of alcohols.

Chapter 2. Experimental Section

2.1 Catalyst Preparation

2.1.1 Chemical reagents

All the chemicals used in the experiments were listed in **Table 2.1**. Unless otherwise stated, commercial reagents were used without any purification. Neon, nitrogen, hydrogen, and ammonia used in the catalytic amination test were supplied by Air Liquide.

Table 2.1 Chemical reagents used in the experiments

Chemical	Formula	Purity	Company
Cobalt (II) nitrate hexahydrate	$\text{Co}(\text{NO}_3)_2 \cdot 6\text{H}_2\text{O}$	>99.0%	Sigma-Aldrich
Nickel (II) nitrate hexahydrate	$\text{Ni}(\text{NO}_3)_2 \cdot 6\text{H}_2\text{O}$	>99.0%	Sigma-Aldrich
Bismuth (III) nitrate pentahydrate	$\text{Bi}(\text{NO}_3)_3 \cdot 5\text{H}_2\text{O}$	>98.0%	Sigma-Aldrich
Aluminum oxide	$\gamma\text{-Al}_2\text{O}_3$	/	SASOL
Zeolite Socony Mobil-5	ZSM-5	/	Honeywell
Titanium dioxide	TiO_2	/	Evonik Degussa
1-Butanol	$\text{C}_4\text{H}_{10}\text{O}$	>99.5%	Sinopharm Chemical Reagent Co., Ltd. (China)
1-Hexanol	$\text{C}_6\text{H}_{14}\text{O}$	>99.9%	Sinopharm Chemical Reagent Co., Ltd. (China)
1-Octanol	$\text{C}_8\text{H}_{18}\text{O}$	>99.5%	Sinopharm Chemical Reagent Co., Ltd. (China)
2-Octanol	$\text{C}_8\text{H}_{18}\text{O}$	>99.5%	J&K Chemical Ltd. (China)
2-Octanone	$\text{C}_8\text{H}_{16}\text{O}$	98.0%	J&K Chemical Ltd. (China)
Benzyl alcohol	$\text{C}_7\text{H}_8\text{O}$	99.8%	Shanghai Aladdin Bio-Chem Technology Co., Ltd.
Tert-amyl alcohol	$\text{C}_5\text{H}_{12}\text{O}$	98.0%	Shanghai Aladdin Bio-Chem Technology Co., Ltd.
Butylamine	$\text{C}_4\text{H}_{11}\text{N}$	>99.5%	J&K Chemical Ltd. (China)
Di-butylamine	$\text{C}_8\text{H}_{19}\text{N}$	>99.5%	J&K Chemical Ltd. (China)

Tri-butylamine	C ₁₂ H ₂₇ N	>99.5%	J&K Chemical Ltd. (China)
Octylamine	C ₈ H ₁₉ N	>99.5%	Shanghai Aladdin Bio-Chem Technology Co., Ltd.
Di-octylamine	C ₁₆ H ₃₅ N	>99.5%	Shanghai Aladdin Bio-Chem Technology Co., Ltd.
Tri-octylamine	C ₂₄ H ₅₁ N	>99.5%	Shanghai Aladdin Bio-Chem Technology Co., Ltd.
Benzylamine	C ₇ H ₉ N	>99.0%	J&K Chemical Ltd. (China)
Di-benzylamine	C ₁₄ H ₁₅ N	97.0%	J&K Chemical Ltd. (China)
Tri-benzylamine	C ₂₁ H ₂₁ N	>99.0%	J&K Chemical Ltd. (China)
Octanal	C ₈ H ₁₆ O	99.0%	Alfa Aesar
Tricosan-12-one	C ₂₃ H ₄₆ O	98.0%	Alfa Aesar
<i>N</i> -benzylideneaniline	C ₁₃ H ₁₁ N	99.0%	Alfa Aesar
Biphenyl	C ₁₂ H ₁₀	>99.0%	Sigma-Aldrich
Toluene	C ₇ H ₈	>99.5%	Sinopharm Chemical Reagent Co., Ltd. (China)
Titanium (IV) isopropoxide	C ₁₂ H ₂₈ O ₄ Ti	>97.0%	J&K Chemical Ltd. (China)
Aluminum isopropoxide	C ₉ H ₂₁ AlO ₃	98.0%	J&K Chemical Ltd. (China)
Aluminum tert-butoxide	C ₁₂ H ₂₇ AlO ₃	98.0%	J&K Chemical Ltd. (China)
Zirconium(IV) n-butoxide	C ₁₆ H ₃₆ O ₄ Zr	76-80% in n-butanol	J&K Chemical Ltd. (China)
Zirconium ethoxide	C ₈ H ₂₀ O ₄ Zr	>99.0%	J&K Chemical Ltd. (China)
Pyridine	C ₅ H ₅ N	>99.5%	Sinopharm Chemical Reagent Co., Ltd. (China)
Aniline	C ₆ H ₇ N	>99.5%	Sigma-Aldrich

2.1.2 Preparation of supported Co, Ni and Bi catalysts

Incipient wetness impregnation (IW or IWI), also called capillary impregnation or dry impregnation, is a commonly used technique for the synthesis of heterogeneous catalysts (**Figure 2.1**). This method relies on the use of an impregnation solution with a volume equal to that of the pore volume of the support (e.g., 0.65 mL g⁻¹ for γ -Al₂O₃). The low solution volume favors the dispersion of the active phase driven by capillarity, which is much faster than diffusion. In this thesis, the Co/ γ -Al₂O₃ (14.5 wt% Co) catalyst was prepared by impregnation of γ -Al₂O₃ (SASOL, SIRALOX or

PURALOX SCCa-5/170, D50: 50 μ m-100 μ m) using an aqueous solutions of cobalt nitrate hexahydrate [Co(NO₃)₂ 6H₂O]. The impregnated sample was dried under air at 80 °C overnight and calcined under an air flow [\sim 10 mL (STP)/min] with a heating ramp of 2 °C min⁻¹ from room temperature to 500 °C to get the oxidized catalyst. Before catalytic tests, the catalyst was activated under a pure H₂ flow at 450 °C for 10 h to reduce the cobalt oxide species. The freshly activated Co catalyst is labeled as “CoAl-act”. The general scheme of the synthesis procedure was presented in **Figure 2.1**.

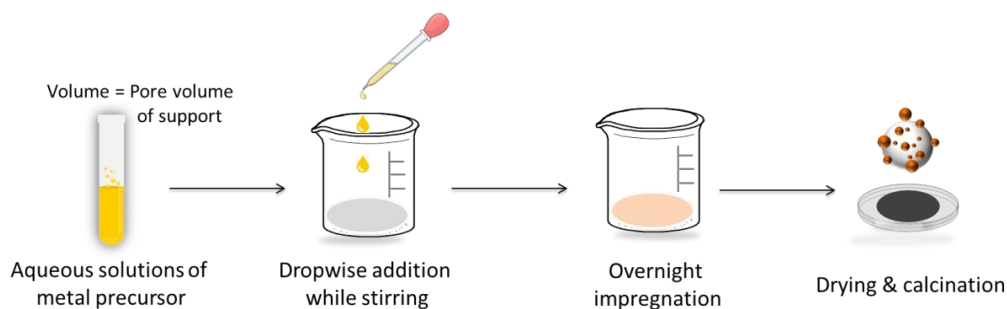


Figure 2.1 Synthesis of supported metallic catalyst through impregnation method.

Ni/ γ -Al₂O₃ (10 wt% Ni) and Bi/ γ -Al₂O₃ (10 wt% Bi) catalysts were prepared by the same method.

2.1.3 Preparation of the alcohols pretreated Co and Ni catalysts

The Co or Ni catalyst was subjected to different alcohols pretreatment under 13 v/v % alcohol/N₂ gas flows (1-butanol, 1-hexanol, 1-octanol) at a flow rate of 1.16 mL (STP)/min at 250 °C and atmospheric pressure in a continuous fixed-bed system for several hours (**Figure 2.2**). The Co/ γ -Al₂O₃ catalysts pre-treated under 1-butanol was denoted as “CoAl-B-250-t” (t = 0.25 h, 0.5 h, 1 h, and 3h), whereas the catalysts pre-treated under 1-hexanol and 1-octanol for 1 h were denoted as “CoAl-H-250-1” and “CoAl-O-250-1”, respectively. To investigate the catalyst reusability of the pretreated catalyst, the CoAl-B-250-1 catalyst was reduced under pure H₂ at 400 °C for 5 h after the amination tests. The regenerated catalyst was denoted as “CoAl-B-250-RG”. Finally, for the liquid-phase amination tests, the *in-situ* pretreated

catalysts were taken out from the fixed-bed reactor and transferred under N₂ protection to the autoclaves for the catalytic tests.

The Ni/ γ -Al₂O₃ catalysts pre-treated under 1-butanol was denoted as “NiAl-B-T-1” (T = 250 °C and 300 °C).

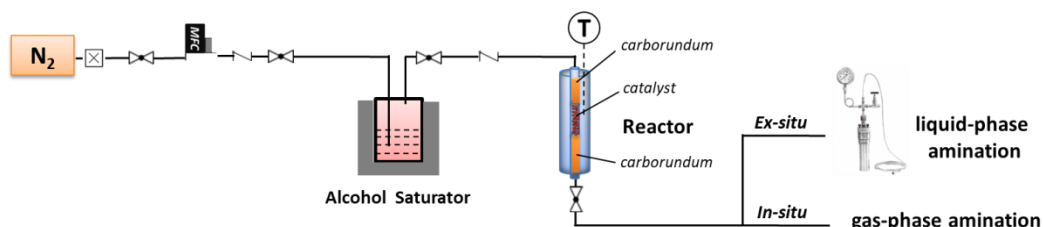


Figure 2.2 Process for *in-situ* alcohols pretreatment on metallic catalysts.

2.1.4 Preparation of highly dispersed Co and Ni nanoparticles

Before 1-octanol pretreatment, the oxidized Co/Al₂O₃ and Ni/Al₂O₃ were reduced at 400 °C for 2 h and then transferred to 30 ml autoclave mixed with 1 g 1-octanol followed by charging 10 bar N₂. The catalyst was treated at 250 °C for 2 h and then washed by ethanol and acetone for several times followed by drying at 80 °C under vacuum for overnight. The catalysts were denoted as “Co-Oct/Al₂O₃” and “Ni-Oct/Al₂O₃”. To remove the surface carbonaceous species after 1-octanol pretreatment, the pretreated catalysts were calcined again at 400 °C for 2 h which was labeled as “Co-Oct-Cal/Al₂O₃” and “Ni-Oct-Cal/Al₂O₃”. Before each catalytic test, the catalysts were activated under a pure H₂ flow at 400 °C for 2 h to reduce the cobalt or nickel oxide species. To trace the formation process of small Co NPs during 1-octanol pretreatment, different pretreatment time (10-120 min) were performed.

2.1.5 Preparation of Bi promoted Co catalysts

The Bi promoted catalysts Co_xBi/Al₂O₃ were prepared through co-impregnation of γ -Al₂O₃ using an aqueous solutions of cobalt nitrate hexahydrate [Co(NO₃)₂·6H₂O] and bismuth(III) nitrate pentahydrate [Bi(NO₃)₃·5H₂O], where *x* represents the weight percentage of Bi (*x* = 0.5, 1.0, 2.0, and 5.0). The weight percentage of Co for all the samples was kept 10 wt%. The impregnated samples were dried in an oven at 80 °C

for overnight and calcined in air with a heating ramp of $2\text{ }^{\circ}\text{C min}^{-1}$ from $25\text{ }^{\circ}\text{C}$ to $500\text{ }^{\circ}\text{C}$ to get the oxidized catalysts. All the catalysts were activated under pure H_2 flow at $450\text{ }^{\circ}\text{C}$ for 2 h before each test. The catalysts $\text{Co}/\text{Al}_2\text{O}_3$ and $\text{Co}1.0\text{Bi}/\text{Al}_2\text{O}_3$ after amination test were labeled as $\text{Co}/\text{Al}_2\text{O}_3\text{-AA}$ and $\text{Co}1.0\text{Bi}/\text{Al}_2\text{O}_3\text{-AA}$, respectively. To evaluate the level of catalytic deactivation resistance for fresh and Bi promoted Co catalysts, $\text{Co}/\text{Al}_2\text{O}_3$ and $\text{Co}1.0\text{Bi}/\text{Al}_2\text{O}_3$ catalysts were poisoned by CO chemisorption using CO pulse on the Micromeritics AutoChem instrument before further amination test.

2.1.6 Preparation of titanium hydroxide

Titanium hydroxide was prepared through the hydrolysis of titanium isopropoxide (99%, supplied by J&K) under neutral condition. 200 ml of distilled water was heated up to $60\text{ }^{\circ}\text{C}$ and 10 mL titanium isopropoxide was added dropwise using a peristaltic pump (0.05 mL/min) under continuous stirring (500 rpm) for almost 10 h. Then the obtained white suspension was centrifuged and washed with ethanol and distilled water for several times followed by drying in vacuum at $80\text{ }^{\circ}\text{C}$ overnight. The obtained sample was denoted as TiOH. The hydrolysis of isopropoxide in hot water is an easy and efficient method to produce amorphous titanium hydroxide with high purity (no NH_3 or Cl^-) and surface area. This sample has been further calcined at $180\text{ }^{\circ}\text{C}$ and $400\text{ }^{\circ}\text{C}$ for 2 h to produce dehydrated samples denoted as TiOH-180 and TiOH-400, respectively.

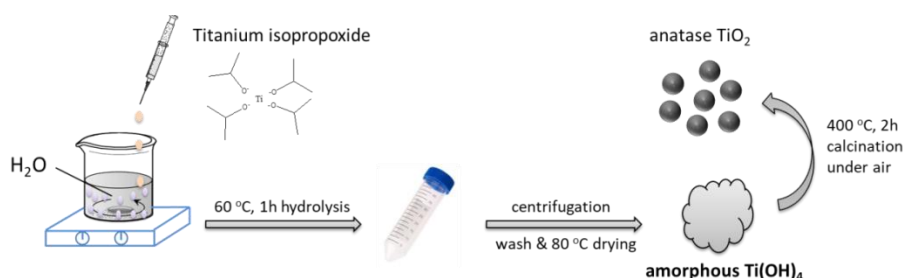


Figure 2.3 Synthesis of titanium hydroxide and corresponding oxides.

The hydroxides of Al (Al-OH) and Zr (Zr-OH) have been prepared in the similar way using alkoxides of aluminium t-butoxide, aluminium isopropoxide, zirconium butoxide and zirconium ethoxide. For comparison, different metal oxides and commercial zeolite ZSM-5 were also used for this reaction as references. The

hydrolyzed AlOH sample was calcined under 180 °C, which was denoted as AlOH-180.

2.2 Catalyst Characterization

2.2.1 X-ray diffraction (XRD)

The *ex situ* Powder X-ray diffraction patterns were measured using an X-ray diffractometer (D5000, Siemens) using Cu K α radiation ($\lambda = 0.15418$ nm). The scans were recorded in the 2θ range between 10° and 80° using a step size of 0.02° and a step time of 5 s. Crystallite phases were determined by comparing the diffraction patterns with those in the standard powder XRD files (JCPDS) published by the International Center for Diffraction Data. The catalysts for measurement were all in oxide state without reduction in hydrogen. The average Co₃O₄ and Bi₂O₃ crystal size were calculated using X-ray line broadening method by Scherrer equation [187] (see Eq. 2-1), which could be used for calculation of metallic cobalt size by the formula: $d(\text{Co}^0) = 0.75 d(\text{Co}_3\text{O}_4)$ [188].

$$\tau = \frac{K\lambda}{\beta \cos \theta} \quad (2-1)$$

where τ is the mean size of the ordered (crystalline) domains, which may be smaller or equal to the grain size; K is a dimensionless shape factor, with a value close to unity. The shape factor has a typical value of about 0.9, but varies with the actual shape of the crystallite; λ is the X-ray wavelength; β is the line broadening at half the maximum intensity (FWHM), after subtracting the instrumental line broadening, in radians. This quantity is also sometimes denoted as $\Delta(2\theta)$; θ is the Bragg angle.

2.2.2 Scanning transmission electron microscopy (STEM)

Scanning transmission electron microscopy (STEM) characterization in the high-angle annular dark-field (HAADF) mode was performed using a Cs-corrected JEOL JEM-2100F microscope operated at 200 keV with an EDX mapping detector from JEOL Silicon Drift Detector (DrySD60GV: sensor size 60 mm²). The EDX analyses were performed far from the carbon membrane and without contamination

effect under acquisition, ensuring that the carbon signal was issued only from the sample. The histograms of metal particle size were obtained using more than 100 detected cobalt particles from the TEM images.

2.2.3 Hydrogen temperature-programmed reduction (H₂-TPR)

Optimum design and efficient utilizations of catalysts require a deep understanding of the surface structure and chemistry of the material. Temperature-programmed reaction techniques can provide much information about the active surface sites in catalysts design and production phases, as well as after a period of use in heterogeneous catalysis [189,190,191]. This technique is usually regarded as relative inexpensive, simple to operate, and fast compared to other techniques. Information from TPR analysis can give insights about phase-support interaction and extent of reduction of the phases at different temperatures for different supported metal based catalysts.

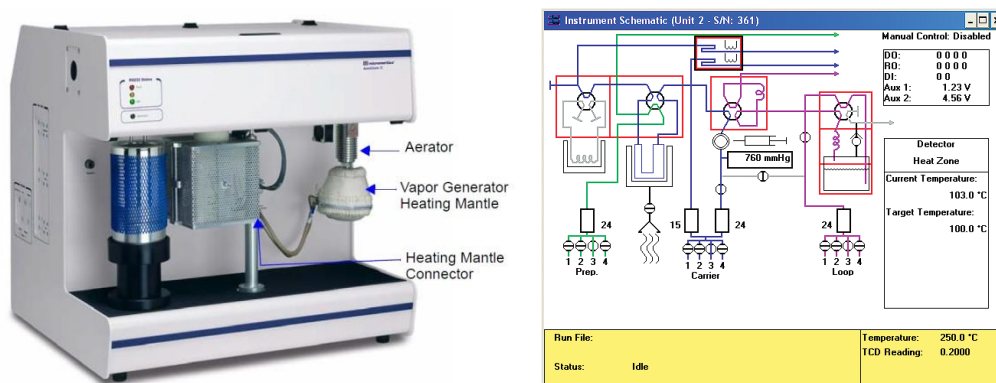


Figure 2.4 Picture of Micromeritics AutoChem II 2920 analyzer and instrument schematic.

The reducibility of all the metallic species in the supported catalysts was characterized by hydrogen temperature-programmed reduction (H₂-TPR), which was performed using a Micromeritics AutoChem II 2920 V3 0.2 apparatus (E2P2L, Solvay Shanghai) equipped with a thermal conductivity detector (TCD) using ~60 mg sample (**Figure 2.4**). The thermal profiles were measured from room temperature to 800 °C with a temperature ramp of 5 °C min⁻¹ under a 5 v/v% H₂/Ar flow [10 mL

(STP)/min]. The total hydrogen consumption was calculated by integration of peaks area based on the calibrated database.

2.2.4 Temperature-programmed reduction-mass spectrometry (TPH-MS)

To investigate the types of deposited carbon species on the surface of metallic catalysts, Micromeritics AutoChem II 2920 V3 0.2 apparatus equipped with a thermal conductivity detector (TCD) and a Balzers Omnistar mass spectrometer (MS) was applied (TPH-MS). In a typical test, the amount of the sample for the test was about 80 mg. The hydrogenation of carbonaceous species: $C_{\text{ads}} + 2H_2 \rightarrow CH_4$ ($m/z = 15$, instead of 16 to avoid interference from ionized oxygen coming from water vapor) was monitored by MS [192].

2.2.5 CO pulse chemisorption

A Pulse Chemisorption analysis determines active surface area, percent metal dispersion, and active metal particle size by applying measured doses of reactant gas to the sample. The techniques of H_2 , O_2 or CO-TPD are efficient methods to evaluate metal dispersion of supported catalysts. It is based on the stoichiometry relationship between gas molecule and metal sites. The ways of CO adsorption on the surface of metals (Pt, Pd, Ru, Ni, Co...) contains linear, bridge and twin, which can be identified through IR analysis (**Figure 2.5**) [193,194,195].

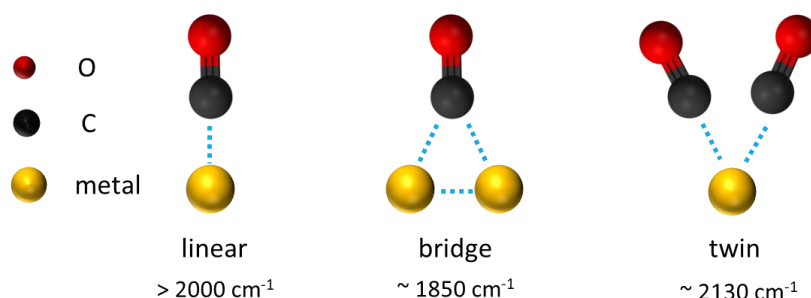


Figure 2.5 Different models for CO adsorption on metal sites.

CO pulse measurements were performed on a Micromeritics AutoChem instrument. Typically, for Co/Al_2O_3 catalyst without alcohol pretreatment or bismuth promotion and Co_xBi/Al_2O_3 catalyst, the calcined samples were firstly placed in

AutoChem for reduction. After reduction with pure H₂ at 400 °C for 4 h, the gas was switched into pure He and the sample was kept in He at 400 °C for 1 h to remove H₂. After cooling down to room temperature, calibrated pulses of CO-He (20 vol% CO) were then added into the continuous He flow until no further adsorption of CO was detected. The cobalt metal surface area and dispersion corresponding to amount of CO adsorption were calculated from the known CO pulse volume, temperature, pressure, and the number of pulses.

For alcohols pretreated Co/Al₂O₃ catalyst, before CO adsorption, the sample was *in-situ* pretreated by dosing of gas-phase 1-butanol at 250 °C for 1 h or 3 h. For H₂ regenerated Co/Al₂O₃ catalyst, the alcohols pretreated sample was kept in H₂ at 400 °C for 2 h to remove the deposited carbon species before CO adsorption. As reported [196], the ratio of adsorbed CO to metallic Co is 1:1.

2.2.6 Temperature-programmed desorption of NH₃ (NH₃-TPD)

NH₃-TPD was carried out on a Micromeritics AutoChem 2920 with a thermal conductivity detector (TCD). In all the experiments, ~50 mg of sample was calcined at 100 °C for 1 h in helium gas flow (20 mL min⁻¹) and then cooled down to 40 °C followed by saturation with 10% ammonia-helium for 1 h. Then the sample was flushed with helium for 1 h to remove the physisorbed ammonia molecule. Finally, desorption profiles were recorded in the temperature range of 40 °C-800 °C with a heating rate of 5 °C min⁻¹.

2.2.7 Surface area and pore size distribution

BET specific surface area and pore size distribution were measured from the N₂ adsorption-desorption isotherms at 77 K on an automated gas sorption analyzer Micromeritics ASAP 2010. The pore size distribution curves were calculated from the desorption branches of the isotherms using Barrett-Joyner-Halenda (BJH) formula [197].

2.2.8 Thermogravimetric analysis (TGA)

Thermogravimetric analysis (TGA) was carried out under air flow [10 mL

(STP)/min] in the temperature range of 20-800 °C using a heating rate of 5 °C min⁻¹ on a Mettler Toledo SMP/PF7458/MET/600W instrument.

2.2.9 X-ray photoelectron spectrometry (XPS)

Ex situ X-ray photoelectron spectrometry (XPS) was carried out using a PHI 5000 Versa Probe X-ray photoelectron spectrometer with Al K α radiation, and C 1s (284.6 eV) was used to calibrate the peak position.

2.2.10 Infrared spectroscopy

Ex situ Fourier transform-infrared (FT-IR) measurement of fresh and used catalysts was carried out on a Nicolet iS50 Spectrometer (**Figure 2.6**) using an Attenuated Total Reflectance (ATR) detector.

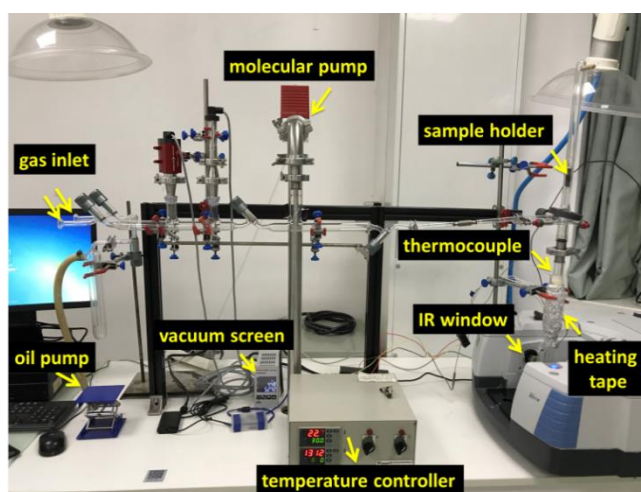


Figure 2.6 Image and details of in-situ IR cell.

In-situ Fourier transform-infrared (FT-IR) experiment for 1-butanol pre-treatment was carried out on the same apparatus as follows: a pellet sample Co/ γ -Al₂O₃ pre-reduced under pure H₂ at 400 °C for 2 h was evacuated to 10⁻⁵ Torr for 1 h, subsequently cooling down to 250 °C, and finally exposing to about 10 Torr gas phase 1-butanol for 0 min to 30 min.

To investigate the nature of acid sites present on the catalyst, the pyridine FTIR technique was employed and the spectra were recorded in the range of 1700-1400

cm⁻¹. The self-supported wafers of all the catalysts were prepared by a pellet press instrument and the samples were degassed at 100 °C for 30 minutes followed by saturation with pyridine as reported elsewhere [198,199,200]. To explain the mechanism of alcohol dehydration over titanium hydroxide, *in-situ* FTIR was performed through heating the pellet from 25 to 180 °C (step 25 °C) in benzyl alcohol vapors (20 Torr).

2.2.11 Gas chromatography-mass spectrometer (GC-MS)

The adsorbed carbon species on the surface of cobalt catalyst after alcohol pretreatment were extracted using an extracting solution of dichloromethane-methanol (CH₂Cl₂:CH₃OH) in a volume ratio of 2:1. Initially, the sample was dissolved in the extracting solution for 10 h employing ultrasound bath. Subsequently, the organic solution was filtered and collected for GC-MS analysis (5977A Series GC/MSD System).

2.3 Evaluation of Catalytic Performance

2.3.1 Gas-phase amination of alcohols

The catalytic activity of the prepared freshly activated and alcohols pretreated Co catalysts was assessed in the gas-phase amination reaction of 1-butanol with NH₃, which was performed in a continuous fixed-bed reactor (down flow mode, D = 3 mm, L = 150 mm) under atmospheric pressure with online gas chromatographic detection of the reaction products (**Figure 2.7**, UCCS, Lille France).

The fixed-bed reactor consists of gas supply, reaction and products analysis systems. To avoid the condensation of reagents and products, the whole gas line was heated at 150 °C. Catalyst loading was typically 30 mg. The bottom and the top parts of the reactor were filled with silicon carbide to have a better heat insulation. A thermocouple was placed in the center of catalytic bed zone to accurately monitor the reaction temperature. The whole gas line was thereafter flushed with H₂ to remove air before catalyst reduction and the amination tests. The Co catalysts were reduced at 450 °C for 10 h under pure H₂ flow before amination test. The amination temperature

was varied between 100 and 180 °C at atmospheric pressure. A N₂ flow (0.5~7 mL (STP)/min) was saturated with 1-butanol at 70 °C, resulting in a gas alcohol feed stream. The variation of the conversion has been performed by change of total flow rate at NH₃/1-butanol molar ratio 7 from 10 to 25 mL (STP)/min with gas composition: 30 v/v % of H₂, 0.8 v/v % of butanol, 5.4 v/v % of NH₃, 4.9 v/v % of N₂ and Ne (rest). The NH₃/1-butanol molar ratio was varied from 7 to 50 by increase of the flow of NH₃ instead of Ne at the same composition of other gases. The reactants and products were analyzed online using a gas chromatography (Shimadzu GC-2014) equipped with an Angilent HP-5 capillary column (length 30 m, diameter 320 μm, film thickness 0.32 μm) and a flame ionization detector (FID).

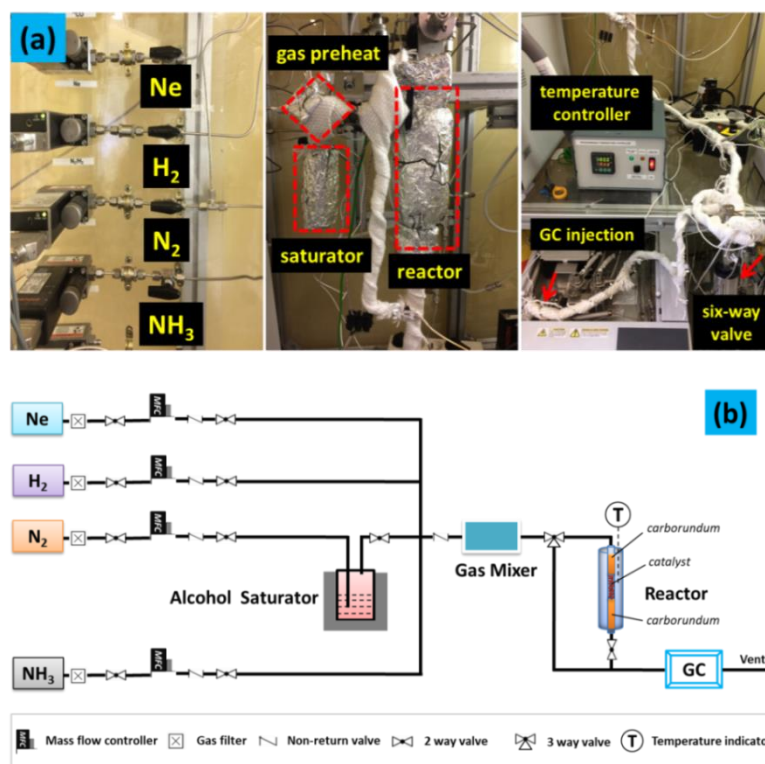


Figure 2.7 (a) Image and details of a fixed-bed reactor; and (b) process flowsheet diagram of the fixed-bed reactor.

2.3.2 Liquid-phase amination of alcohols

The liquid-phase amination of different alcohols with NH₃ or amines were carried out in a 30-mL stainless steel autoclave geared with a pressure gauge and a safety rupture disk (TVS-N2-30, Taiatsu Techno Corporation, Japan, **Figure 2.8**).

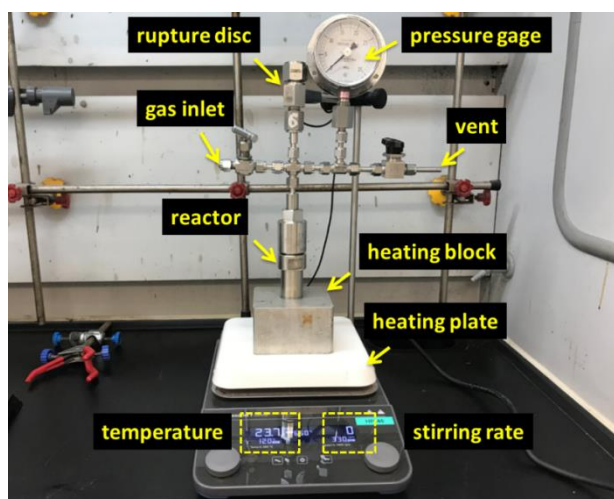


Figure 2.8 Setup for liquid-phase amination of alcohols.

In a typical experiment, the reactor was charged with 1 ml of alcohol and catalyst (~100 mg). No solvent was used in the test. Then, the reactor was sealed and evacuated by applying vacuum followed by charging NH_3 (~7 bar) and H_2 (~3 bar) into the reactor (the exact amount of NH_3 was charged by placing the reactor into ice-water bath to have high solubility). Finally, the reactor was placed on a heating plate equipped with an aluminum heating block and a magnetic stirrer (500 rpm) at 100-180 °C for 5-48 h. At these conditions, the nominal NH_3 /alcohol molar ratio in the reactor was 4-18. After reaction, the reactor was cooled down to room temperature, and the mixture was filtrated and analyzed on a gas chromatography (Agilent 7890B) equipped with a HP-5 capillary column (length 30 m, diameter 320 μm , film thickness 0.32 μm) using biphenyl as the internal standard.

2.3.3 *N*-alkylation of amines with alcohols

Typical procedure for *N*-alkylation of amines with alcohols was carried out in a 30 mL stainless steel autoclave geared with a pressure gauge and a safety rupture disk. In a typical experiment, the reactor was charged with 4.62 mmol benzyl alcohol, 21.5 mmol aniline and 100 mg of catalyst. 2 g xylene, THF or water was used as a solvent. Then, the reactor was purged with N_2 several times to remove the air. Finally, the reactor was placed on a hot plate equipped with a magnetic stirrer (500 rpm) at 50 °C-180 °C for 0.5-48 h. After the reaction, the reactor was cooled down to room

temperature, and the mixture was filtrated and analyzed using an Agilent 7890 GC equipped with a HP-5 capillary column using biphenyl as the internal standard for calculation of alcohol conversion and product yields. After each amination test, the catalyst was washed with ethanol and separated by centrifugation several times and dried at 80 °C for 10 h for further test of the recyclability. The used catalyst after reaction was denoted as TiOH-80-AR. For the rehydration of the dehydrated catalysts TiOH-180, water was added into the reactor before catalytic test. For characterization, the catalyst was suspended in distilled water overnight followed by drying under vacuum at 80 °C before test. The corresponding rehydrated samples were denoted as TiOH-180-Re, TiOH-400-Re, TiO₂-Re and AlOH-180-Re.

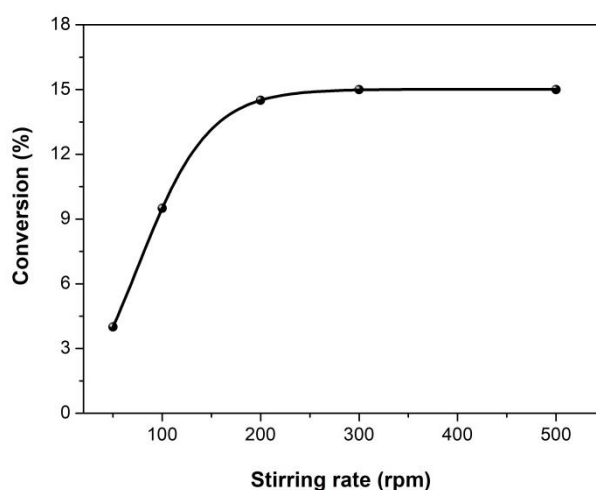


Figure 2.9 Mass transfer effect during amination of 1-octanol over freshly activated cobalt (molar ratio NH₃/alcohol = 18; p_{H₂} = 3 bar; alcohol: 1 ml, catalyst: 50 mg; reaction temperature: 180 °C; 2 h; stirring rate 50-500 rpm; no solvent).

The absence of external and internal mass transfer limitations has been checked both in gas-phase and liquid-phase reaction. The gas phase alcohol amination was conducted with a fixed bed reactor with a plug-flow hydrodynamics. The external diffusion limitation in a batch reactor was excluded by conducting the experiments with different stirring rates (**Figure 2.9**). No effect on the conversion was observed. The internal diffusion limitations were excluded using Weisz-Prater criterion [201,202]:

$$N_{W-P} = \frac{Rr_p^2}{D_{eff}C_s} \leq 0.3$$

where R = observed reaction rate (mol g⁻¹ s⁻¹) 0.017, r_p= catalyst particle radius (m): 30·10⁻⁶, D_{eff} = effective diffusivity (cm² s⁻¹) 2·10⁻², C_s = gas concentration at the external surface of the catalyst (mol cm⁻³) 3.5·10⁻⁷. It results in N_{W-P} equal to 0.002 which is less than 0.3.

For catalytic stability test, after each amination reaction, the used catalyst was washed with ethanol and water and separated by centrifugation for several times and dried at 80 °C under vacuum for 10 h for retest. After 3 cycles, the used Bi promoted Co catalysts were calcined at 400 °C under air to remove surface cokes followed by hydrogenation at 400 °C for further amination test.

2.3.4 Analysis of reaction products

1. Calculation of conversion and selectivity of gas-phase amination of 1-butanol;

$$Conversion (\%) = \frac{f_1A_1 + 2*f_2A_2 + 3*f_3A_3}{f_{BuOH}A_{BuOH} + f_1A_1 + 2*f_2A_2 + 3*f_3A_3} * 100$$

$$Selectivity (\%) = \frac{f_1A_1}{f_1A_1 + 2*f_2A_2 + 3*f_3A_3} * 100$$

A_i refers to the area of peak exported from GC (i = 1, 2, 3 refers to primary, secondary and tertiary amines); f_i are the different response factors;

2. Calculation of conversion and selectivity of liquid-phase amination of alcohols;

$$Conversion (\%) = \left(1 - \frac{n_{ROH}^t}{n_{ROH}^0}\right) * 100$$

$$Selectivity (\%) = \frac{n_i^t}{n_{ROH}^0 - n_{ROH}^t} * 100$$

$$Carbon\ balance (\%) = \frac{mole\ of\ formed\ products + reactants}{mole\ of\ reactants} * 100$$

Where n_{ROH}⁰ and n_{ROH}^t refer to initial and final moles of alcohols, respectively, and I refers to different products.

2.3.5 Model reactions

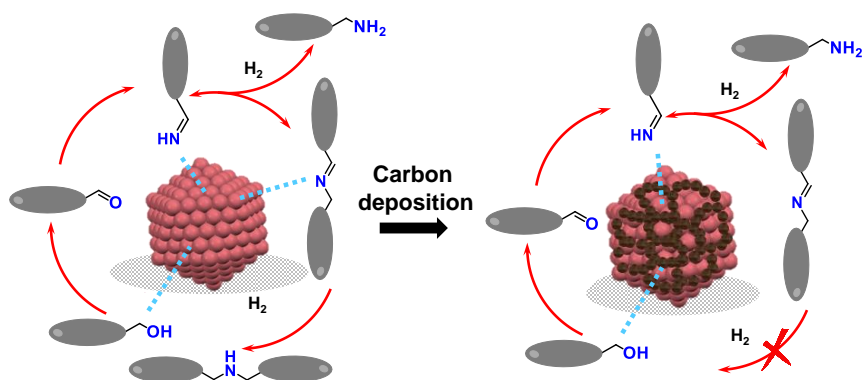
The liquid-phase disproportionation reaction of 1-octylamine over different catalysts was conducted in the same autoclave. In a typical experiment, the reactor was charged with 1 mL 1-octylamine, 20-50 mg of catalyst, NH_3 at a nominal NH_3 /octylamine molar ratio of 18, and H_2 (3 bar). The reaction was performed at 180 °C for 2 h. No solvent was either used during 1-octylamine transformation reaction.

The hydrogenation of carbonyl compounds over fresh and 1-butanol pretreated catalysts was performed in the same autoclave at the following conditions: acetone 0.5 g, octanal 0.5 g, tricosan-12-one 0.1 g, and *N*-benzylideneaniline 1 g together with 3 mL of ethanol under 20 bar H_2 in the presence of fresh or 1-butanol pretreated $\text{Co}/\text{Al}_2\text{O}_3$ (100 mg). The reaction was performed at 120 °C for 6 h.

The catalytic tests for different reactions based on non-pretreated and 1-octanol pretreated highly dispersed Co and Ni catalysts were carried out in a 50 ml stainless steel autoclave. For amination reactions, the reactor was charged with 0.84-1 g of alcohols (1-octanol, 2-octanol and benzyl alcohol) and ~20 mg catalyst followed by charging NH_3 (0.5 g) and H_2 (3 bar) into the reactor. Finally, the reactor was placed on a hot plate equipped with a magnetic stirrer at 180 °C for 2-4.5 h. For hydrogenation reaction, the conditions were as following: tricosan-12-one 0.1 g (or octanal 0.5 g, octanonitrile 0.25 g) together with 5 ml ethanol and 10-20 mg catalyst under H_2 20 bar. The reaction was performed at 120 °C for 10-120 min. For aerobic oxidation reaction, 1 g alcohols (1-octanol, 2-octanol and benzyl alcohol), 2 g toluene mixed with 20 mg catalyst followed by charging 10 bar O_2 was performed at 130 °C for 1-6 h. After each test for all the reactions, the reactor was cooled down to room temperature, and the mixture was filtered and analyzed on an Agilent 7890 GC quipped with a HP-5 capillary column using biphenyl as the internal standard.

The dehydrogenation of 2-octanol over the freshly activated and Bi promoted Co catalysts were conducted in the same autoclave at the following conditions: 2-octanol 50 mg, toluene 1 g in the presence of catalyst 50 mg. The reaction was performed at 140 °C for 15 h.

*Chapter 3. Catalyst Deactivation for Enhancement of Selectivity in Alcohols Amination to Primary Amines



Abstract: Selective synthesis of valuable primary amines is an important target in modern industry. Amination of alcohols with ammonia is an economically efficient and environmental friendly process for primary amine synthesis. This consecutive reaction yields a mixture of primary, secondary and tertiary amines. High selectivity to primary amines is an important challenge of alcohol amination. Carbon deposition on the catalyst surface is conventionally considered as an undesirable process, which leads to poor catalytic performance. In this paper, carbon deposition produced by catalyst pre-treatment with alcohols under the optimized conditions has been employed for major enhancement of the selectivity of alcohol amination to primary amines (from 30-50 to 80-90%). This extremely positive effect of carbon deposition on the amination selectivity arises from steric hindrance in hydrogenation of bulky secondary imines as intermediate products over partially carbon-decorated cobalt nanoparticles.

* This chapter is based on the following publication:

Feng Niu, Shaohua Xie, Mounib Bahri, Ovidiu Ersen, Zhen Yan, Bright T. Kusema, Marc Pera-Titus, Andrei Y. Khodakov and Vitaly V. Ordonsky. *ACS Catal.* **2019**, *9*, 5986-5997.

3.1 Introduction

Catalyst deactivation is an important technological hurdle in industrial processes [170,171,203]. Catalyst deactivation leads to a decline of the catalytic activity and necessity to regenerate, to replace and to recycle the spent catalysts. Deactivation can be induced by several phenomena: poisoning, carbon fouling, thermal degradation, sintering, and undesirable reactions involving active phase (**Table 3.1**). Poisoning occurs by reversible or irreversible adsorption of reactants, products, or impurities on the active sites [172,180,204,205]. Both coke and carbon species can be generated on the surface of the catalyst during catalytic reactions. Carbon species may vary from high molecular hydrocarbons or oxygenates to primary carbons (*e.g.*, graphite) depending on the catalyst type and operation conditions. These species can alter the catalyst reactivity towards hydrogen, water, NH₃ or oxygen. In the particular case of amination reactions, carbonaceous deposits and metal carbides are known to generate over Ni and Co during the reaction, resulting in an irreversible deactivation of the metal surface [85].

Table 3.1 Mechanisms of catalyst deactivation

Mechanism	Type	Description
Poisoning	Chemical	Strong chemisorption of species on catalytic sites which block sites for catalytic reaction
Fouling	Mechanical	Physical deposition of species from fluid phase onto the catalytic surface and in catalyst pores
Thermal degradation & sintering	Thermal	Thermally induced loss of catalytic surface area, support area, and active phase-support reactions
Vapor formation	Chemical	Reaction of gas with catalyst phase to produce volatile compound
Vapor-solid & solid-solid reactions	Chemical	Reaction of vapor, support, or promoter with catalytic phase to produce inactive phase
Attrition/crushing	Mechanical	Loss of catalytic material and surface area due to abrasion and mechanical-induced crushing

The influence of carbon and coke on the catalytic performance depends on their

chemical composition, structure and localization within the catalysts. Menon [206] broadly classified catalytic reactions into two major classes: coke-sensitive or coke-insensitive. In the coke-sensitive reactions, coke precursors selectively form on the active sites and the catalytic activity rapidly declines. In contrast, in the coke-insensitive reactions, the catalyst can tolerate up to 6-10 wt. % of coke, which is principally deposited on the support, while the reactive coke precursors are readily removed from the active sites under the reaction conditions. At least three types of carbonaceous species (i.e. hydrocarbons, strongly adsorbed hydrocarbons and amorphous polymeric carbon) were reported by Peña et al. [175] and Moodley et al. [176] on Co catalysts after conducting Fischer-Tropsch synthesis.

Although catalyst deactivation is generally undesired, blocking some active surface sites may exert a positive effect on the catalytic performance [207]. Indeed, deactivation can moderate the overall activity and/or improve the selectivity to the desired products. Baiker et al. [208] reported selective blocking of active sites on supported Au nanoparticles by 1-octadecanethiol and mercaptoacetic acid for benzyl alcohol oxidation and ketopantolactone hydrogenation, respectively. More recently, McKenna et al. [209] reported diphenyl sulfide and its sulfur residue as an appropriate poisoner for Pd/TiO₂ catalysts leading to an enhanced selectivity in acetylene hydrogenation in the presence of ethylene.

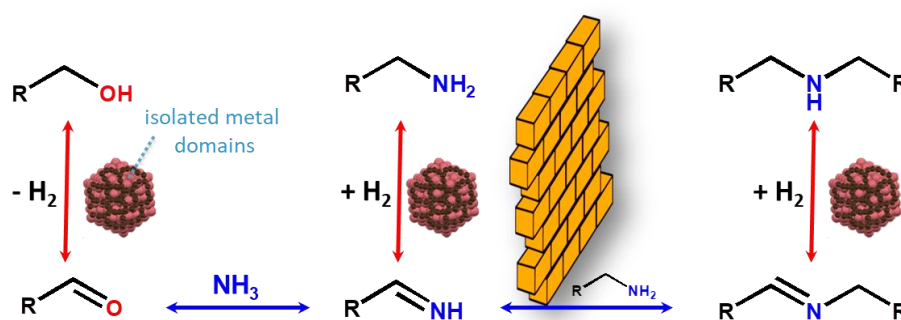


Figure 3.1 A proposed strategy for selectivity enhancement of primary amine.

Based on the above mechanism and strategies, we consider that restraining the self-coupling of primary amine through selectively blocking active sites to form some isolated domains on the surface of metals would be possible to improve the selectivity

of desired primary amine products (**Figure 3.1**).

In the present work, intentional deposition of polymeric carbonaceous species on the surface of Co/Al₂O₃ catalysts was used to considerably improve the selectivity of alcohol amination to primary amines in the reaction of aliphatic alcohols with NH₃ both in gas and liquid-phase processes. The catalysts were pretreated with alcohols at the temperature of the amination reaction. The effect was attributed to the suppression of hydrogenation of intermediate bulky secondary imines over Co domains isolated by carbon species. The selectivity enhancement to primary amines after the pretreatment of the catalysts with alcohols was observed for the 1-butanol, 1-octanol and benzyl alcohol amination.

3.2 Results and Discussion

3.2.1 Alcohol amination over cobalt catalysts

The heterogeneous catalyst, 14.5 wt% Co/ γ -Al₂O₃ was used for selective synthesis of primary 1-butylamine directly from 1-butanol and ammonia in the presence of hydrogen in a continuous fixed-bed reactor and in a batch reactor. No 1-butanol conversion was observed in the blank experiments without catalyst addition.

The catalytic performances at different reaction temperatures and NH₃/1-butanol molar ratios in a fixed bed reactor are investigated. As shown in **Figure 3.2a**, the conversion increases with temperature and reaches 100% at 140 °C. As the NH₃/1-butanol molar ratio increases from 7 to 50, the conversion drops to nearly 0, which might be due to the competitive adsorption between ammonia and 1-butanol over cobalt metal sites (**Figure 3.2b**). Importantly, no decrease in the catalytic activity with time on stream was observed at 120 °C in presence of hydrogen with the NH₃/1-butanol ratio = 7. This observation suggests almost negligible catalyst deactivation under these conditions. These conditions are considered in this work as standard for the 1-butanol gas-phase amination in a continuous fixed bed reactor.

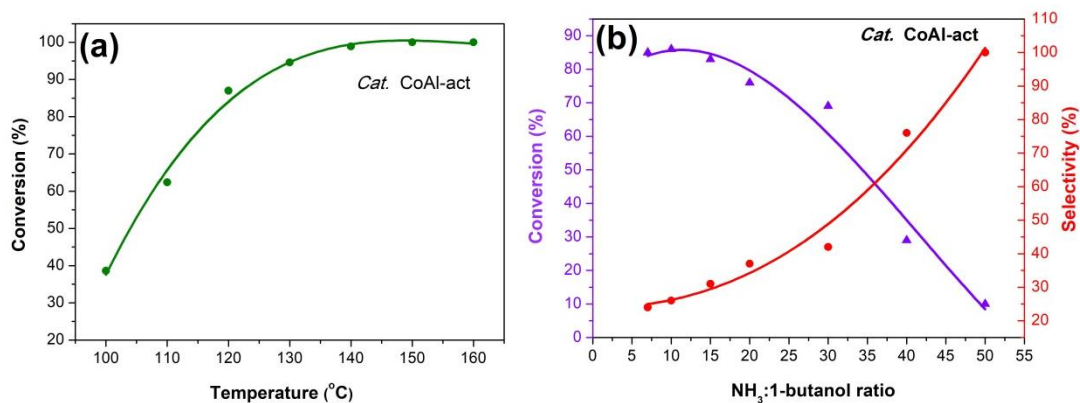


Figure 3.2 Effect of reaction temperature (a) (molar ratio NH₃/alcohol = 7; P = 1 bar; gas composition: 30 v/v % of H₂, 0.8 v/v % of butanol, 5.4 v/v % of NH₃, 4.9 v/v % of N₂ and Ne (rest), T= 100 to 160 °C) and ammonia to 1-butanol molar ratio at 140 °C (b) (molar ratio NH₃/alcohol = 7 to 50; P = 1 bar; gas composition: 30 v/v % of H₂, 0.8 v/v % of butanol, 5.4-38 v/v % of NH₃, 4.9 v/v % of N₂ and Ne (rest)) on amination of 1-butanol over catalyst “CoAl-act”.

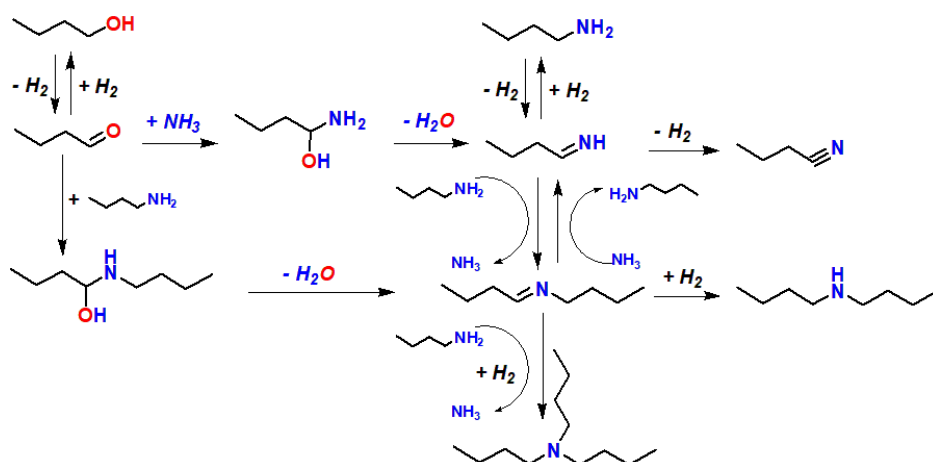


Figure 3.3 Reaction paths in amination of 1-butanol over cobalt catalysts.

The rate determining step for 1-butanol amination on metal catalysts is shown in **Figure 3.3**. The kinetically relevant step in the amination of 1-butanol appears to be its dehydrogenation to aldehyde [210]. Afterwards, the aldehyde might non-catalytically react with ammonia or 1-butylamine resulting in the formation of the primary or secondary hemiaminal, followed by dehydration into the primary or secondary imines, respectively [140]. Subsequent hydrogenation results in the synthesis of primary and secondary amines.

As shown in **Figure 3.4**, at higher conversion, the selectivity to primary

1-butylamine decreases because of the side self-coupling reaction of imines and primary amines to secondary and then to tertiary amines [211]. This leads to the decrease in the primary amine selectivity. Likewise, the increase in the 1-butylamine selectivity at higher NH_3 /1-butanol ratios can be due to the competitive interaction of the aldehyde (or 1-butylimine) with NH_3 and 1-butylamine. The presence of larger amounts of NH_3 hinders the condensation of the aldehyde with 1-butylamine and self-coupling of 1-butylamine to dibutylamine or tributylamine.

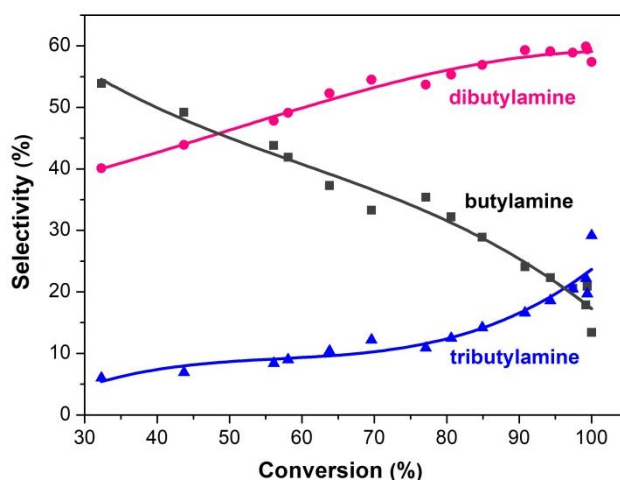


Figure 3.4 Selectivity-conversion curves for amination of 1-butanol over “CoAl-act” catalyst (GHSV = 20~50 L/g h; molar ratio NH_3 /alcohol = 7; P = 1 bar; gas composition: 30 v/v % of H_2 , 0.8 v/v % of butanol, 5.4 v/v % of NH_3 , 4.9 v/v % of N_2 and Ne (rest); catalyst: 30 mg; reaction temperature: 140 °C).

The curves showing 1-butanol conversions as function of gas space velocity for the freshly activated cobalt catalyst and catalysts exposed to 1-butanol pre-treatments are displayed in **Figure 3.5a**. Pre-treatment of the catalyst in the gas-phase 1-butanol flow at high temperature (250 °C) for different times (0-3 h) leads to lower catalytic activity. This is indicative of the catalyst deactivation. Only a slight decrease in the 1-butanol conversion was observed after catalyst pre-treatment with 1-butanol for 15 min, while very significant catalyst deactivation was observed after 3 h of the pre-treatment. As expected, for a given catalyst, the 1-butanol conversion gradually decreases at higher GHSV, which is due to the lower contact time between the catalyst and reagents. At the same GHSV, lower 1-butanol conversion was observed for the

catalysts pretreated with 1-butanol for longer time. This is consistent with a catalyst deactivation process.

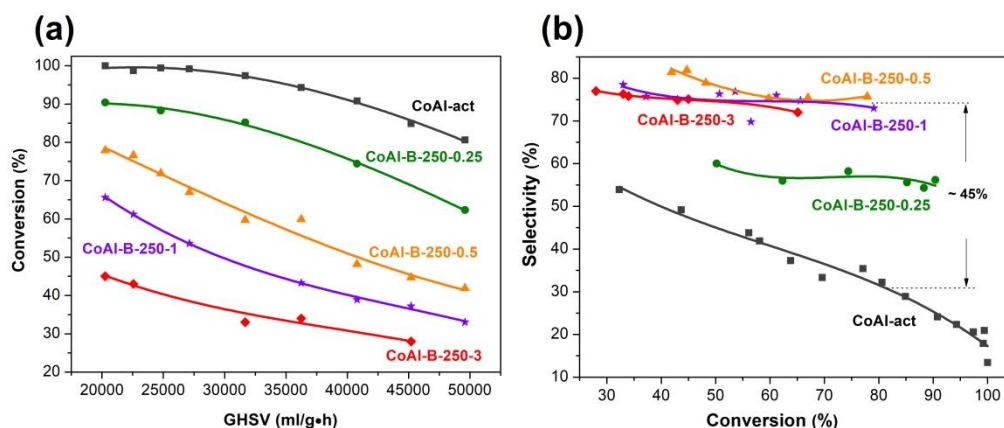


Figure 3.5 Conversion influenced by catalyst deactivation (a) and butylamine selectivity modification (b) for amination of 1-butanol over fresh and 1-butanol pre-treated cobalt catalyst for different time. (GHSV = 20~50 L/g h; molar ratio $\text{NH}_3/\text{alcohol} = 7$; $P = 1$ bar; gas composition: 30 v/v % of H_2 , 0.8 v/v % of butanol, 5.4 v/v % of NH_3 , 4.9 v/v % of N_2 and Ne (rest); catalyst: 30 mg; reaction temperature: 140 °C).

Surprisingly, catalyst pre-treatment with 1-butanol produces a very strong impact on the 1-butylamine selectivity (**Figure 3.5b**). The selectivity to the primary amine significantly increases over the catalysts pretreated with 1-butanol. Even a relatively short time pre-treatment of the cobalt catalyst (for 0.25 h) results in a noticeable increase in the 1-butylamine selectivity. The selectivity to 1-butylamine (at the 80 % 1-butanol conversion) increases from 30 % for the freshly activated catalyst to almost 80 % over the cobalt catalyst pretreated with 1-butanol for 1 h. The effect of 1-butanol pretreatment on the 1-butylamine selectivity is particularly pronounced at high 1-butanol conversion.

Alcohol amination was also conducted in liquid phase in a batch reactor. 1-Octanol and benzyl alcohol were used as substrates. No 1-octanol or benzyl alcohol conversion was observed in blank experiments without catalyst. Catalytic deactivation phenomenon was observed as well in the liquid phase amination of 1-octanol over catalysts exposed to 1-butanol pre-treatments at different times (**Figure 3.6**). However,

in comparison with gas-phase amination, the activity decrease was less significant, which could be explained by a stronger contact of carbon with the cobalt surface in gas phase in comparison with liquid phase.

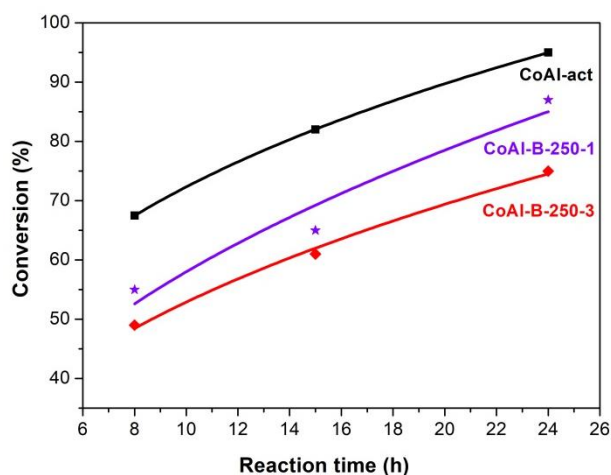


Figure 3.6 Conversion-time curves for amination of 1-octanol over fresh and 1-butanol pre-treated cobalt catalyst at different times (molar ratio $\text{NH}_3/\text{alcohol} = 18$; $p\text{H}_2 = 3$ bar; amount of alcohol: 1 ml, catalyst: 100 mg; reaction temperature: 180°C ; time: 5-24 h; no solvent).

The pretreatment of the freshly activated cobalt catalyst with 1-butanol also produces a strong effect on the selectivity to primary amines in the liquid phase. **Figure 3.7** shows the selectivity-conversion curves for liquid-phase amination of 1-octanol and benzyl alcohol measured on the cobalt catalyst before and after the 1-butanol pre-treatment. Similar to 1-butanol amination in the gaseous phase, the selectivity to primary amines in the amination of 1-octanol and benzyl alcohol decreases with an increase in the alcohol conversion due to the self-coupling reactions of primary amines to di- and tertiary amines. On the freshly activated catalyst, the selectivities to primary amines were only about 60 % at the 80 % conversion of 1-octanol or benzyl alcohol. This is similar to the selectivities observed in the gas-phase amination of 1-butanol. The catalyst pre-treatment with 1-butanol leads to a noticeable increase in the selectivities towards the primary octylamine or benzylamine. Over the cobalt catalyst after the 1-butanol pre-treatment, the selectivity to primary amines increases from 60 to more than 80 % at the 80 % conversions of 1-octanol and

benzyl alcohol. Moreover, the selectivity to primary amines can be controlled by adjusting the pre-treatment time. Clearly, the pre-treatment of cobalt catalysts with 1-butanol results in the enhancement of the selectivity to primary amines in the amination of 1-butanol, 1-octanol and benzyl alcohol both in the gas and liquid phases. The enhancement in primary amine selectivity is particularly pronounced at high alcohol conversion.

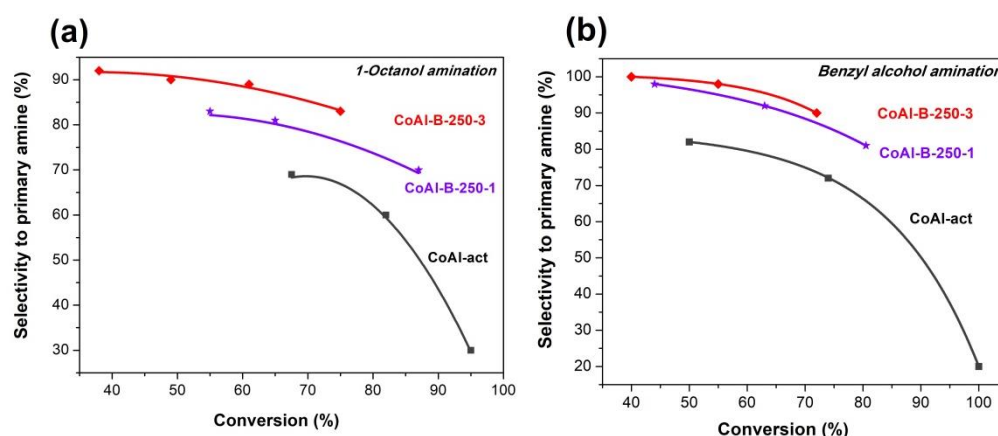


Figure 3.7 Selectivity-conversion curves for different alcohols amination before and after 1-butanol pre-treatment: (a) 1-octanol; (b) benzyl alcohol; (molar ratio $\text{NH}_3/\text{alcohol} = 18$; $p_{\text{H}_2} = 3$ bar; amount of alcohol: 1 ml, catalyst: 100 mg; reaction temperature: 180 °C; time: 5-24 h; no solvent).

The pre-treatment of the freshly activated cobalt catalysts with 1-octanol and 1-hexanol (instead of 1-butanol) also affects the selectivity of 1-octanol amination in liquid phase. **Figure 3.8** shows the selectivity-conversion curves for 1-octanol liquid-phase amination before and after 1-octanol or 1-hexanol pre-treatments of the cobalt catalyst. Similar to 1-butanol, the catalyst pre-treatment with 1-octanol and 1-hexanol leads to a significant enhancement of the selectivity to primary 1-octylamine in the 1-octanol amination. The most significant effect in the 1-octylamine selectivity is observed at the 1-octanol conversion higher than 70-80 %. The selectivity to primary 1-octylamine increases from 60 to 80 %. Indeed, the effect by alcohol pre-treatment on the selectivity to primary amines over cobalt catalysts does not depend on the used alcohol and seems to be rather general. The selectivity to primary amines is then affected in the amination reactions involving different

alcohols.

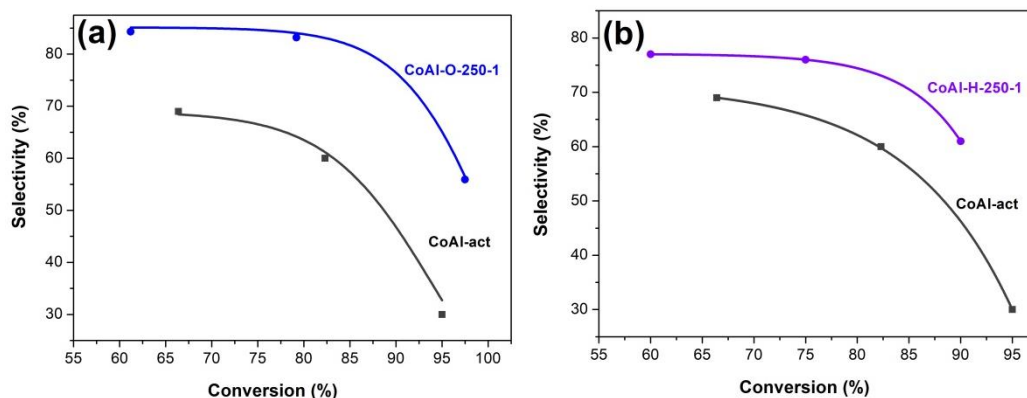


Figure 3.8 Selectivity-conversion curves for 1-octanol amination before and after pre-treatment by: (a) 1-octanol; (b) 1-hexanol. (Molar ratio $\text{NH}_3/\text{alcohol} = 18$; $\text{pH}_2 = 3$ bar; amount of alcohol: 1 ml, catalyst: 100 mg; reaction temperature: 180°C ; time: 5-24 h, no solvent).

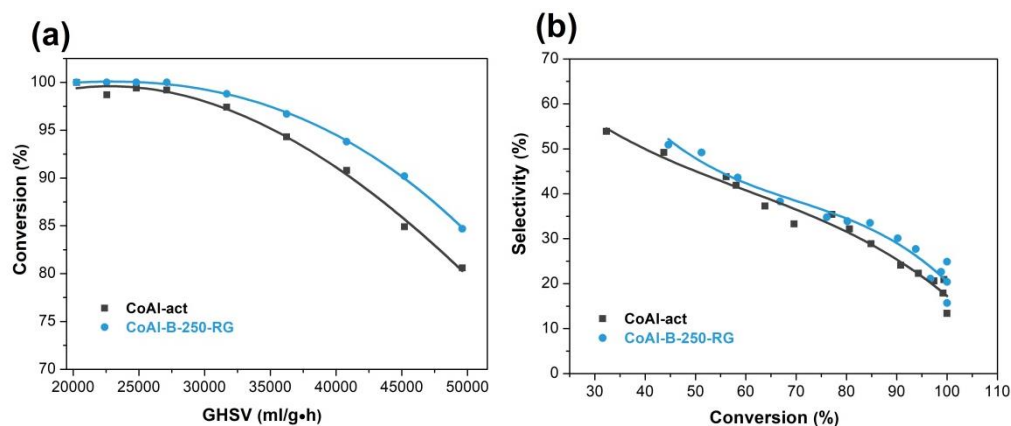


Figure 3.9 Amination activity (a) and butylamine selectivity (b) recovery after regeneration under hydrogen at 400°C for 5 h for the 1-butanol pre-treated cobalt catalyst ($\text{GHSV} = 20\sim 50$ L/g h; molar ratio $\text{NH}_3/\text{alcohol} = 7$; $P = 1$ bar; gas composition: 30 v/v % of H_2 , 0.8 v/v % of butanol, 5.4 v/v % of NH_3 , 4.9 v/v % of N_2 and Ne (rest); catalyst: 30 mg; reaction temperature: 140°C).

The pre-treatment of cobalt catalyst with alcohols can lead to the formation of carbon species over the catalyst surface. These carbon species might affect the concentration, density, intrinsic activity and localization of active sites and thus the catalyst performance in alcohol amination. In order to confirm this hypothesis, the cobalt catalysts after the pre-treatment with 1-butanol were exposed to H_2 at 450°C .

The results are shown in **Figure 3.9**. After catalyst regeneration in hydrogen, the amination activity totally recovers back to the initial state. This indicates that the carbon surface species formed from 1-butanol have been removed from the catalyst under hydrogen. Meanwhile, the selectivity enhancement caused by the 1-butanol pre-treatment also disappears. The selectivity-conversion curve recovers their initial shape observed for the freshly activated catalyst.

3.2.2 Characterizations of 1-butanol pretreated cobalt

The XRD patterns of all samples are shown in **Figure 3.10**. The unreduced fresh Co/ γ -Al₂O₃ catalyst shows the patterns characteristic of the Co₃O₄ phase and γ -Al₂O₃ support. The XRD profiles of all samples after their reduction in hydrogen at 450 °C indicate the presence of metallic cobalt fcc phase. Note that the XRD patterns of the reduced catalyst and pretreated with 1-butanol exhibit only very small modification of the XRD patterns. The shape and width of the XRD peaks are also identical before and after alcohol pre-treatment. XRD implies that cobalt species are present as a metallic phase after the catalyst activation and during the amination reaction with and without 1-butanol pre-treatment.

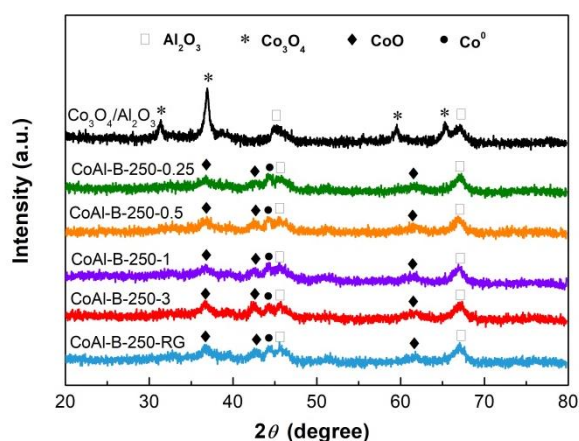


Figure 3.10 XRD patterns of all the samples with and without pre-treatment.

The TEM images and histograms (**Figure 3.11**) suggest average cobalt metal particle sizes of ~10 nm for freshly activated CoAl-act and 1-butanol pretreated cobalt catalysts. This indicates that no noticeable particle size modification occurs under the reaction conditions. In the spent catalysts, however, CoO was the major phase. The

presence of cobalt oxide can be caused by partial re-oxidation of the spent catalysts exposed to air during their transfer from the reactor for XRD measurements. No cobalt carbide was detected in all the spent catalysts.

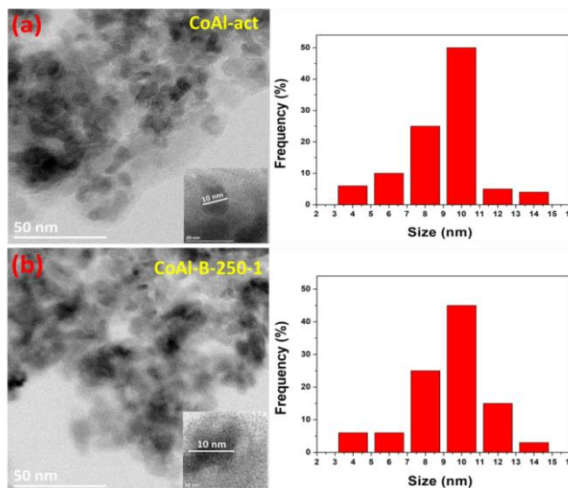


Figure 3.11 TEM images and histograms of cobalt particle size in (a) freshly activated and (b) 1-butanol pretreated cobalt catalyst.

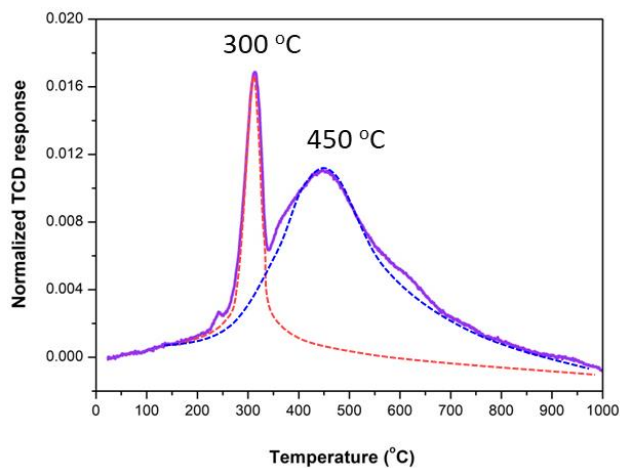


Figure 3.12 Temperature-programmed reduction of $\text{Co}_3\text{O}_4/\gamma\text{-Al}_2\text{O}_3$ catalyst precursor.

Figure 3.12 shows that the TPR profiles for the cobalt catalyst are constituted by several overlapping peaks, which are due to the reduction of supported cobalt species. Previous reports [212,213,214] suggest that the narrow TPR peak at 300 °C can be assigned to the reduction of Co_3O_4 to metallic cobalt with formation of intermediate CoO , while the broad peak at 450 °C is usually attributed to strong interaction of

cobalt oxide species with alumina [190]. The TPR analysis suggests that a considerable fraction of cobalt is present as metallic species after catalyst activation in hydrogen at 450 °C.

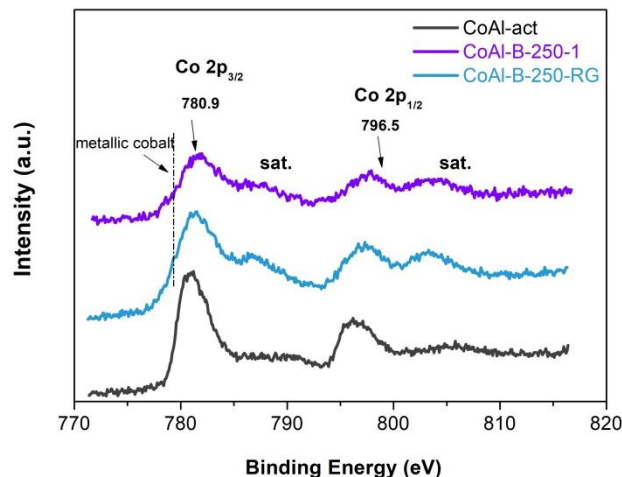


Figure 3.13 XPS of 2p Co before, after pre-treatment and after regeneration of the catalyst.

XPS experiments provided additional information about cobalt species in the catalysts. The Co2p XPS spectrum of the calcined cobalt catalyst is very similar to the spectrum of the reference Co_3O_4 sample (**Figure 3.13**). The Co_3O_4 $\text{Co}2p_{3/2}$ binding energies are about 780 eV; the spin-orbital splittings being 15.1 eV [215,216,217,218,219]. The XPS spectra of the activated catalyst, catalyst after 1-butanol pretreatment and the regenerated counterpart exhibit an intense satellite structure centered at 797 and 804 eV characteristic of the Co^{2+} ions [220,221]; the spin orbital splitting being 15.7 eV. The main $\text{Co}2p_{3/2}$ peak shifts to higher binding energies (782-782.4 eV) relative to the spectrum of Co_3O_4 . Cobalt metal phase in the reduced catalysts was identified in the XPS spectra by $\text{Co}2p_{3/2}$ binding energies ($\text{Co}2p_{3/2}=778$ eV), spin-orbital splitting (15.0 eV) and line shape. The shape and intensity of the spectra is only slightly affected by the pre-treatment with 1-butanol and subsequent catalyst regeneration in hydrogen.

Characterization by STEM confirms the assumption about small influence of the pretreatment with 1-butanol on cobalt dispersion (**Figure 3.14**). The initial $\text{Co}/\text{Al}_2\text{O}_3$ catalyst demonstrates a broad distribution of metal nanoparticles on the surface of

alumina from 4 to 14 nm and Co nanoparticle aggregation. The treatment of the catalyst in 1-butanol or in 1-octanol flows does not lead to any significant changes in the distribution of Co species on the surface. Thus, the enhancement of the alcohol amination selectivity to primary amines cannot be explained by a modification of the cobalt dispersion and could be possibly due to other phenomena such as carbon deposition.

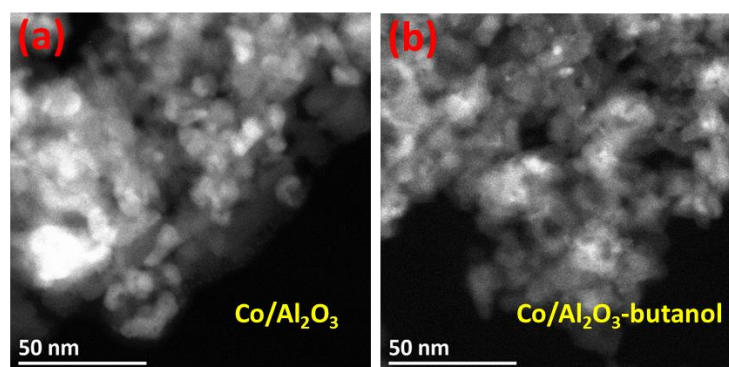


Figure 3.14 TEM images of alumina supported cobalt catalysts after activation in hydrogen (a) and exposure to 1-butanol (b).

3.2.3 Characterization of deposited carbon species

The catalytic data are indicative of carbon deposition over the cobalt catalysts after their exposure to 1-butanol. TGA under oxygen atmosphere was performed in order to determine the weight loss related to the decomposition and oxidation of carbon species on the cobalt catalyst after its pretreatment with 1-butanol. As shown in **Figure 3.15**, the TG profile of the catalyst after 1-butanol pre-treatment for 3 h exhibits a total weight loss of about 3.5 %. The first weight loss of about 2 % can be ascribed to the removal of chemisorbed water from the catalyst. The second weight loss of about 3 % at around 200 °C can be due to desorption of the organic compounds [222]. Finally, the third weight loss of about 0.5 % at above 300 °C can be attributed to the oxidation of amorphous polymeric or graphene/graphite-like carbons. Longer pre-treatment time with 1-butanol results in a more significant weight loss. This suggests that the amount of carbon species on the surface of the catalyst can be a function of the alcohol pre-treatment time.

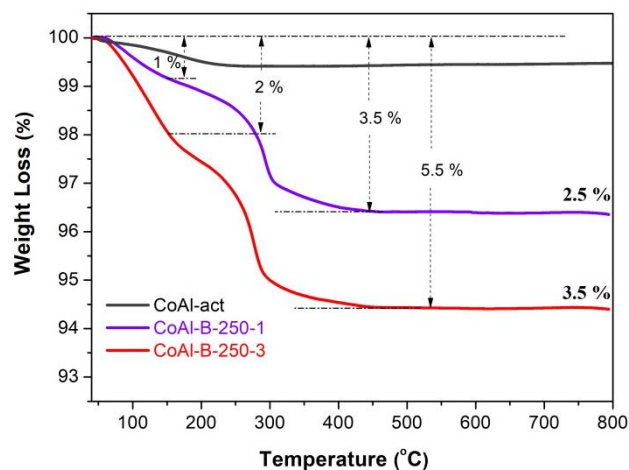


Figure 3.15 TGA profiles of the 1-butanol pre-treated cobalt catalysts for different time.

The BET surface area and metal dispersion of fresh and pre-treated catalysts are shown in **Table 3.2**. The BET surface area of cobalt catalysts pre-treated with 1-butanol decreases with an increase in the pre-treatment time. This could be due to the slight increase in the weight of the catalyst due to deposited carbon species and partial pore blockage. Both these phenomena can lower the apparent BET surface area [223].

Table 3.2 Main Properties and Catalytic Activity of the Fresh and 1-Butanol Pretreated Catalysts

Catalyst	Surface area (m ² /g) ^a	Metallic surface area (m ² /g) ^b	Co _(CO) /Co (%) ^b	TOF for 1-octanol amination (h ⁻¹) ^c	TOF for octylamine coupling (h ⁻¹) ^d
CoAl-act	146.2	9.07	0.92	104.8	158.3
CoAl-B-250-1	140.0	6.62	0.67	104.6	33.4
CoAl-B-250-3	138.6	4.23	0.43	101.9	27.5
CoAl-B-250-RG	145.2	9.15	0.93	-	-

^a BET surface area.

^b Obtained from CO chemisorption measurement (assuming CO/Co = 1).

^c Conditions: molar ratio NH₃/alcohol = 18; p_{H₂} = 3 bar; amount of alcohol: 1 ml, catalyst: 100 mg; reaction temperature: 180 °C; time: 3 h. no solvent used. TOF evaluated at low conversion (~10%).

^d Conditions: catalysts 50 mg; octylamine 1 ml, molar ratio NH₃/octylamine = 18; p_{H₂} = 3 bar; reaction temperature: 180 °C; time 2 h. no solvent used. TOF evaluated at low conversion (~10%).

The Co metal surface area was evaluated using CO adsorption in a pulse mode. The metallic surface area of cobalt catalysts decreases as the pre-treatment time with 1-butanol prolongs from 1 h to 3 h (**Table 3.2**). This suggests that carbon deposition during the alcohol pre-treatment on the surface of cobalt metallic particles can possibly block the sites for alcohol amination. It also explains the observed decrease in the catalytic activity.

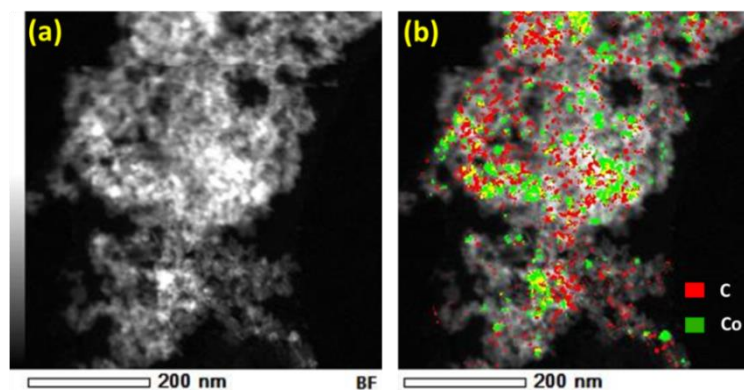


Figure 3.16 (a) STEM-HAADF image of 1-butanol pretreated catalyst, (b) Corresponding STEM-EDX mapping of Co (in green) and C (in red).

The localization of carbon species on the surface of the catalysts was further investigated using scanning transmission electron microscopy (STEM) combined with Energy dispersive X-ray analysis (EDX) (**Figure 3.16**). **Figure 3.16b** shows the EDX cobalt and carbon maps on the catalyst. Interestingly, cobalt and carbon mapping overlap in the catalyst pretreated with 1-butanol. This confirms the presence of carbon species produced during the 1-butanol pre-treatment on the surface of Co nanoparticles. The pre-treatment with 1-butanol results in a noticeable drop in the catalytic activity. Localization of carbon species over the surface of cobalt active phase and a significant drop in the overall activity after the 1-butanol pre-treatment are indicative of carbon sensitivity of the amination reaction according to the classification of Menon [206]. No graphitic layers were observed by high resolution STEM on the support around Co nanoparticles.

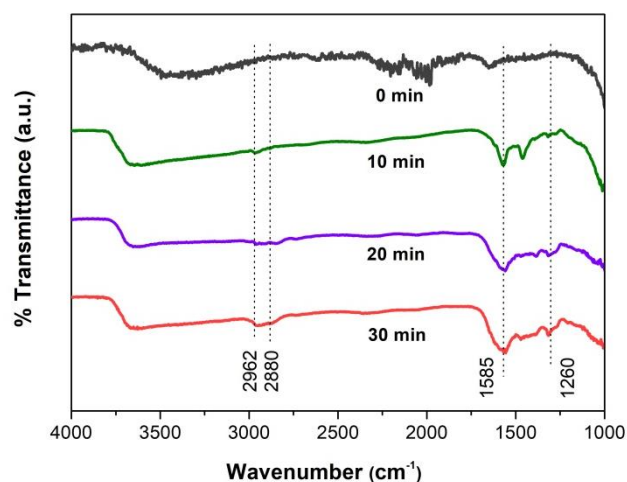


Figure 3.17 In-situ FTIR spectroscopy of 1-butanol pre-treated cobalt catalyst.

The mechanism of carbon deposition on the cobalt catalyst has been further studied by in-situ FTIR spectroscopy (**Figure 3.17**). The fresh catalyst CoAl-act (0 min) does not exhibit any IR bands ascribed to carbon species. After the catalyst exposure to 1-butanol for 10 min, new IR bands appear at 2962 cm^{-1} and 2880 cm^{-1} ascribed to the C-H stretching vibrations in the $-\text{CH}_3$ and $-\text{CH}_2$ groups, respectively, with a higher intensity of the $-\text{CH}_3$ mode. In addition, two intensive bands were observed at 1585 cm^{-1} , which might be assigned to the C=C stretching vibrations of conjugated olefins [224]. The sharp band at 1420 cm^{-1} might be assigned to OH bending vibration of hydroxyl group of adsorbed 1-butanol. The band at 1420 cm^{-1} is accompanied by a broad IR band at 3600 cm^{-1} attributed to the hydrogen-bonded hydroxyl groups and water molecules. As the pre-treatment time with 1-butanol increases, the intensity of the $-\text{CH}_2$ signal becomes stronger. Besides, as the pre-treatment time prolongs from 10 min to 30 min, the intensity of the signals at 1585 cm^{-1} and 1260 cm^{-1} ascribed respectively to the C-H bending vibrations of $=\text{C-H}$ groups also increases. The IR spectra suggest therefore the presence of hydrocarbon fragments on the surface of cobalt catalyst after its pre-treatment with 1-butanol. These fragments also contain unsaturated C=C bonds.

The methane TPH-MS profiles ($m/z = 15$, **Figure 3.18**) resulting from the decomposition of different types of carbonaceous species provided further information about the nature of carbon deposited on the surface of the catalysts. The

analysis of these peaks was performed in a similar way as reported by Moodley et al. [176]. In the TPH-MS profiles of freshly activated catalysts, no obvious methane signal was detected. This suggests that no carbon species are present. After pre-treatment with 1-butanol, two main peaks corresponding to methane signal are identified at 230 and 425 °C, indicating two major types of carbon species deposited on the active surface sites of the pre-treated catalyst. The shoulder-like peak at ~230 °C might be attributed to the deposited carbon species containing long chain hydrocarbons. The sharp peak at ~425 °C can be assigned to graphene/graphite-like highly condensed carbons. The temperature and methane peak shapes referring to different types of carbonaceous species are in good agreement with previous reports [180].

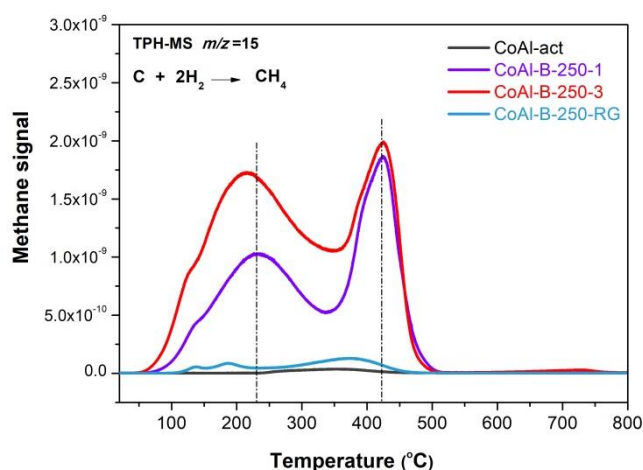


Figure 3.18 TPH-MS profiles ($m/z = 15$) measured on the fresh and 1-butanol pre-treated cobalt catalysts.

The intensity of the TPH-MS peaks for the regenerated catalyst was close to those of the freshly activated catalyst, indicating that after regeneration of the spent catalyst under hydrogen atmosphere, the surface deposited carbon species could be almost removed to the initial extremely low level.

Further information about deposited carbon species was obtained using X-ray photoelectron spectroscopy (XPS) (**Figure 3.19**). The C 1 s spectra of the 1-butanol pre-treated catalyst shows the presence of a peak at 284.8 eV, which could be assigned to the surface $-CH_2-$ species adsorbed on the surface of metallic Co [225]. The $-CH_2-$

species may probably come from long-chain hydrocarbon fragments, which seem to be the main carbon species in the 1-butanol pretreated catalysts. The peaks at 286.2 eV and 288.3 eV are attributed to the C-O and C=O groups in the polymeric carbons. Note that a very low-intense C 1s peak at 284.5 eV could be attributed to carbon contamination inside the XPS chamber for the fresh and regenerated catalysts.

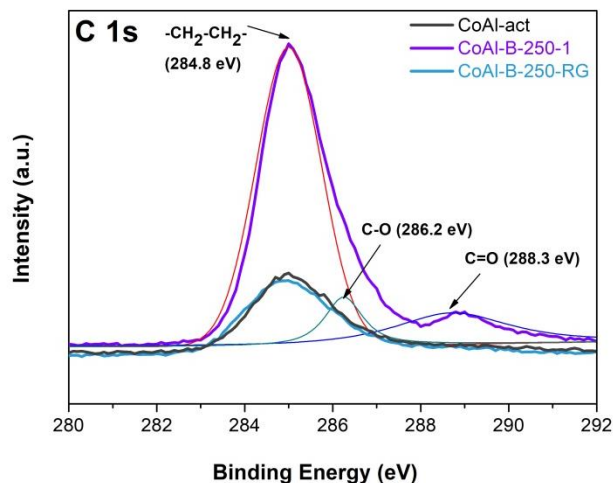
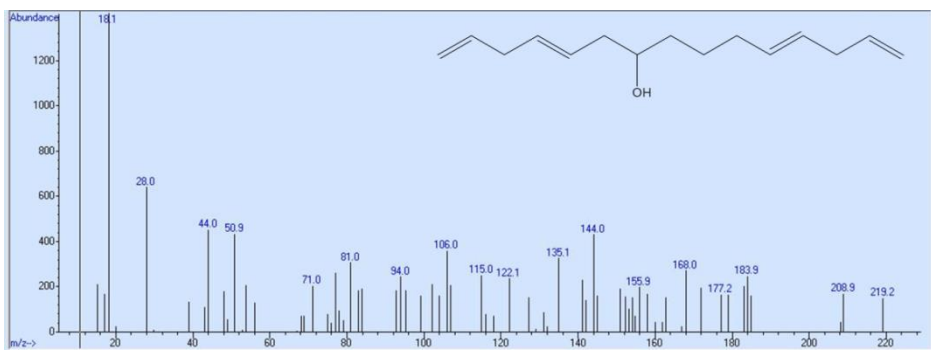
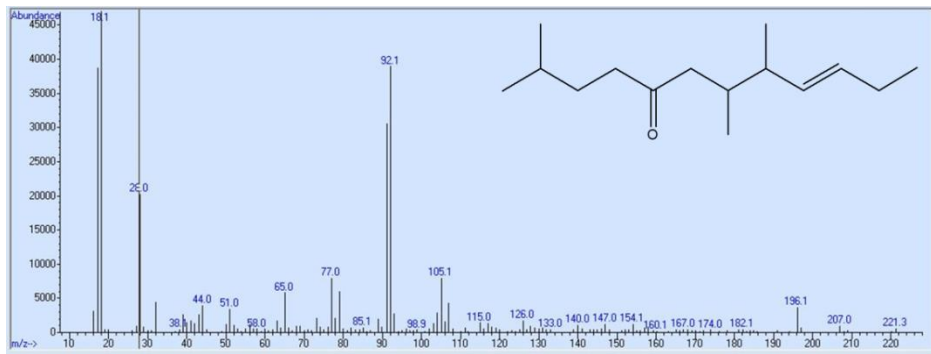
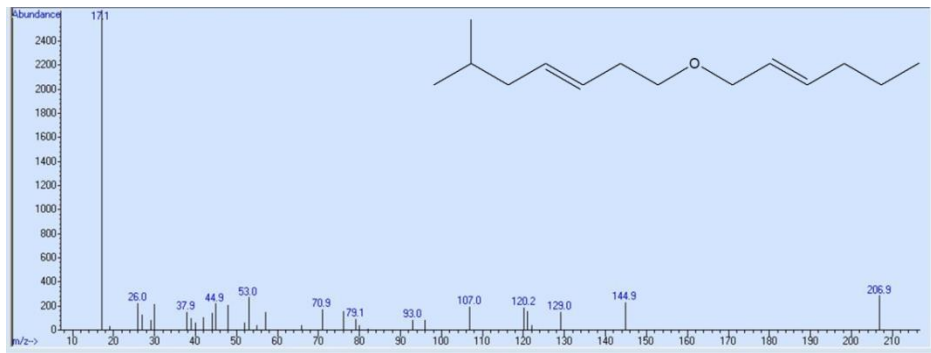
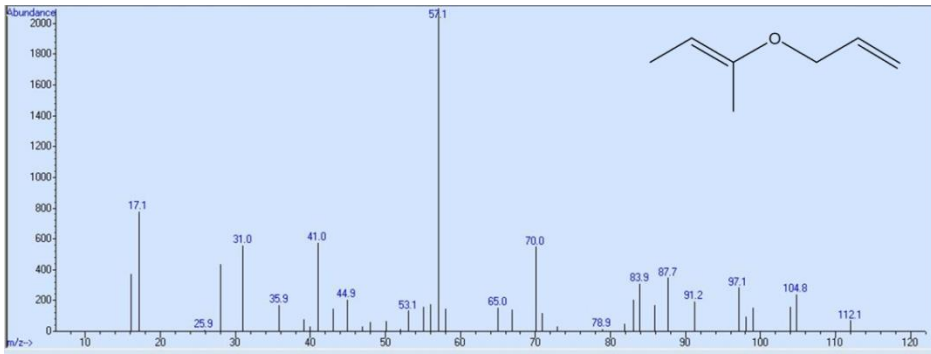
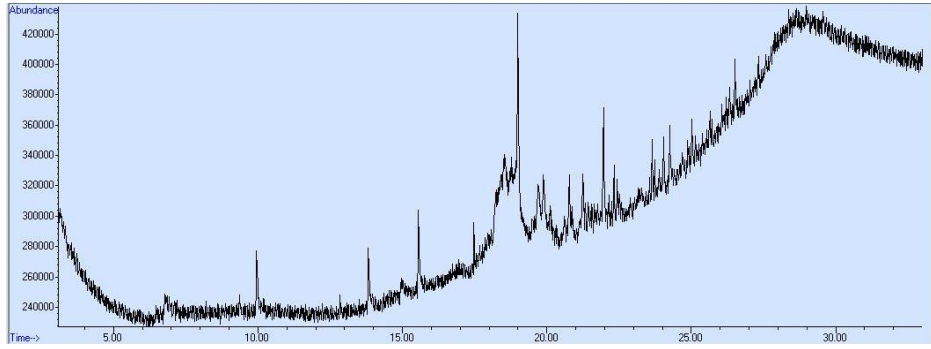


Figure 3.19 XPS spectra of C 1s for cobalt catalyst with and without 1-butanol pre-treatment.

Overall, the characterization results indicate the formation of unsaturated polymeric species constituted by long hydrocarbon chains on the surface of the cobalt catalysts after the pre-treatment with 1-butanol. The intensity of the IR broad band at 3600 cm^{-1} suggests the production of water during this pre-treatment, which might arise from dehydration of oxygenates. To provide a more accurate identification of carbon species formed over cobalt catalysts after pre-treatment with 1-butanol, the catalysts were subjected to extraction with a mixture of dichloromethane and methanol. The extract was then analyzed using GC-MS. The relevant chromatograms are displayed in **Figure 3.20**. The GC-MS results are consistent with other characterization methods. They indicate the presence of polymeric compounds containing the C=C double bonds and ketone C=O groups. This clearly indicates aldol type condensation of aldehydes produced via alcohol dehydrogenation over cobalt metal sites.



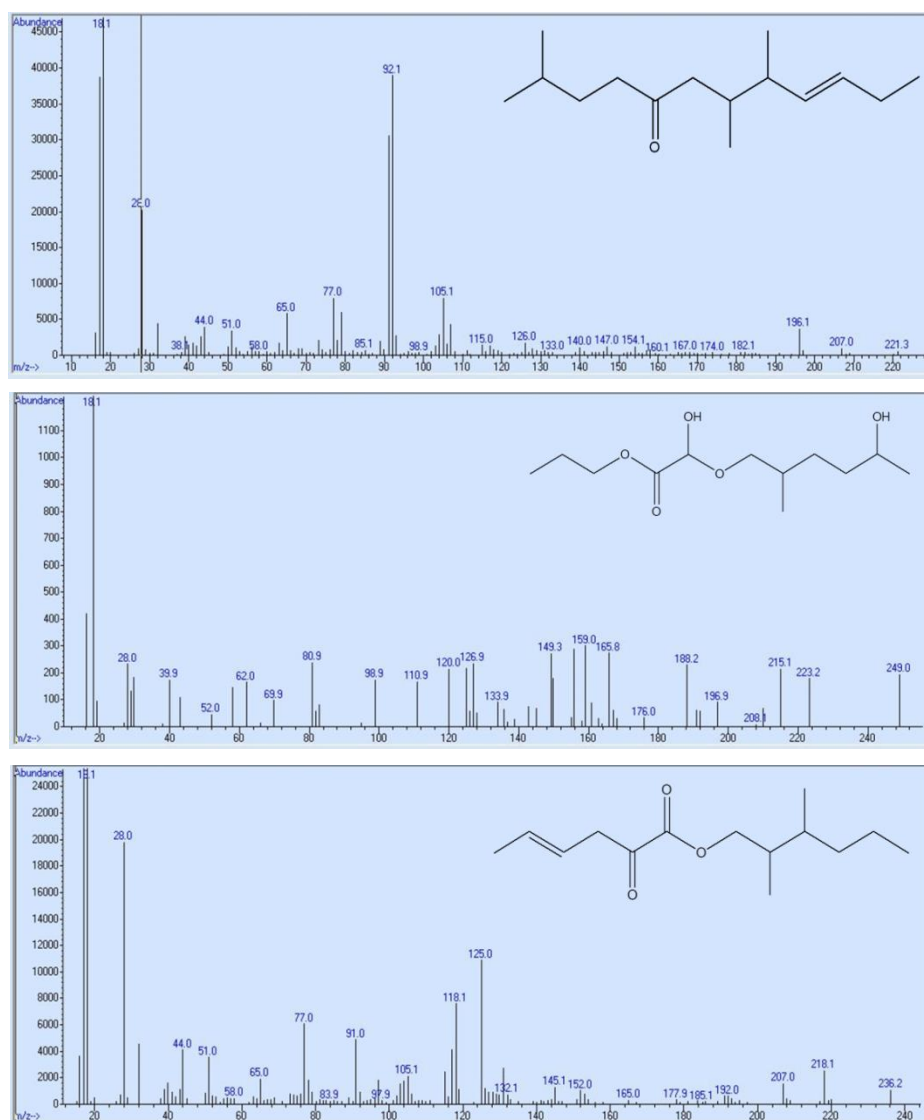


Figure 3.20 GC-MS results for carbon species from carbon extraction.

The combination of characterization results suggest that carbon deposition on the surface of the cobalt catalyst during its pre-treatment with alcohols proceeds according to the following sequence:

- i) dehydrogenation of the alcohol to aldehyde over Co sites,
- ii) subsequent fast aldol condensation between an aldehyde molecule and an adjacent alcohol molecule to an α,β -unsaturated carbonyl adduct,
- iii) dehydration with formation of unsaturated polymeric hydrocarbons observed by FTIR,
- iv) in the presence of hydrogen in the fixed bed reactor the C-C double bonds are hydrogenated to saturated polymeric hydrocarbons:

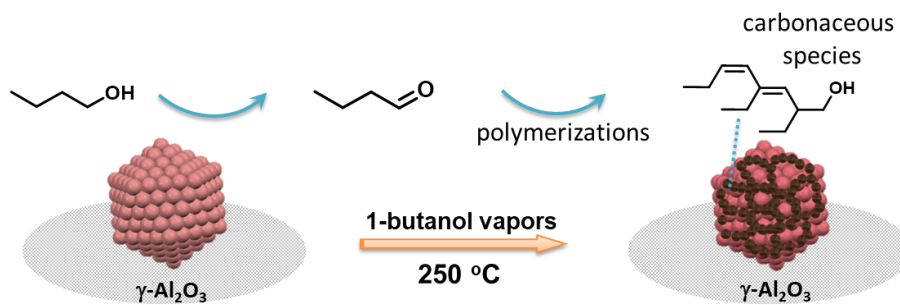


Figure 3.21 Processes for carbon deposition on the surface of cobalt during alcohol pretreatment.

This scheme also explains localization of carbon species on the surface of Co nanoparticles (**Figure 3.21**). Indeed, the first step in carbon deposition is alcohol dehydrogenation with formation of the aldehyde. It could be expected that the highly reactive aldehydes would react with alcohol forming polymeric hydrocarbon fragments in a close proximity with the site where they were produced.

3.2.4 Carbon deposition and enhancement of the selectivity to primary amines

It is generally accepted that the secondary amines are produced by self-coupling reaction of primary amine at high conversions. In alcohol amination (**Figure 3.3**), the primary amine is first dehydrogenated to the corresponding imine, which reacts with another primary amine to form secondary imine. This reaction step coincides with the release of NH_3 . Additionally, the secondary imine could be formed by nucleophilic attack of the aldehyde by the primary amine. However, at high alcohol conversion in liquid-phase amination, this route is expected not to play a significant role in the decrease of selectivity to the primary amine (**Figure 3.5, 3.7**). In particular, the shape of the conversion-selectivity curves for gas-phase amination of 1-butanol is flatter in comparison with the sharper decrease for liquid-phase amination, which suggests a higher contribution of this route for gas-phase amination.

Once formed, the secondary amine is produced by hydrogenation of the secondary imine. Alternatively, the secondary imine might interact with another amine molecule with formation of tertiary amine by the same mechanism. **Figure 3.22** shows the distribution of the 1-octylamine conversion products on the freshly

activated and 1-butanol pretreated cobalt catalysts at the same conversion level (\approx 10%). It is interesting to note that the selectivity to secondary imine was relatively higher in the primary amine conversion over the 1-butanol pretreated cobalt catalysts compared to the freshly activated counterpart. The main product of 1-octylamine coupling over the cobalt catalyst pretreated with 1-butanol was the corresponding secondary imine, which is produced by a reversible coupling reaction of the primary 1-octylamine and primary 1-octylimine. The selectivity to secondary amine was relatively low for the 1-butanol pretreated catalysts. An increase of the 1-butanol pre-treatment time from 0.25 h to 3 h leads to a gradual decrease in the selectivity to dioctylamine. Thus, carbon deposition seems to slow hydrogenation of secondary imines to amines.

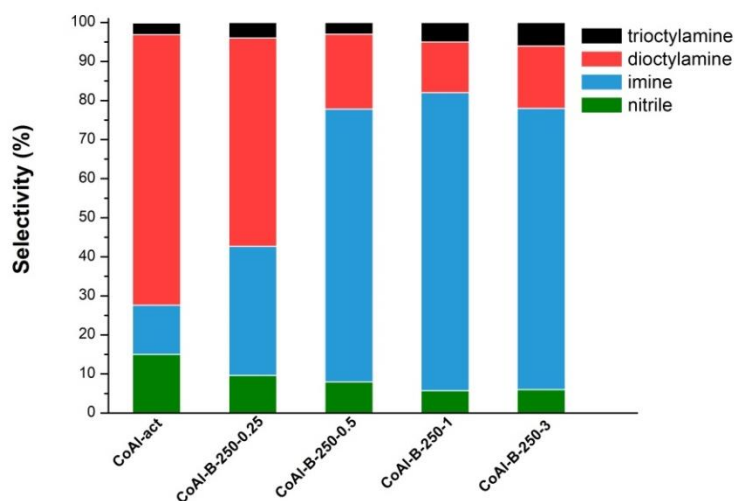


Figure 3.22 Model reaction of 1-octylamine transformation over freshly activated and 1-butanol pretreated cobalt catalyst at the conversion of \sim 10% (Conditions: catalysts 50 mg; 1-octylamine 1 ml, molar ratio NH_3 /1-octylamine = 18; P_{H_2} = 3 bar; reaction temperature: 180 °C; time 2 h; no solvent).

The TOF values calculated for the 1-octylamine self-coupling reaction to secondary amine significantly varied as a function of carbon deposition (**Table 3.2**, **Table 3.3**). They were respectively 158, 33 and 27 h^{-1} for the fresh catalyst and after 1-butanol pretreatment for 1 and 3 h, respectively. This observation points out a significantly lower intrinsic activity for 1-octylamine coupling to dioctylamine over partially deactivated catalysts compared to the parent catalyst. At the same time, the

TOF numbers for the different catalysts before and after deactivation in 1-octanol amination at low conversion are about 100 h^{-1} (**Table 3.2**). Thus, the ratio of TOF (1-octylamine coupling)/TOF (1-octanol amination) is almost 6 times higher for the parent catalyst compared to the pretreated catalysts. This observation suggests that the 1-octylamine self-coupling rate over the surface Co sites in the presence of carbon species is much slower compared to that of 1-octanol amination to 1-octylamine. The similar effect of strong structure sensitivity in coupling of amines in comparison with insensitive 1-octanol amination has been discovered earlier for Ru nanoparticles [134]. The rate of alcohol amination was independent on Ru nanoparticle size, while the rate of alcohol self-coupling decreases with the decrease in the size of Ru nanoparticles. Alcohol pretreatment of cobalt catalysts induces similar effect on the rate of alcohol amination and self-coupling as variation of Ru nanoparticle size.

Table 3.3 TOF values calculated for 1-octanol amination and 1-octylamine self-coupling reaction for the catalysts with and without pretreatment

Catalyst	Conversion for 1-octanol amination (%) ^a	Yield for octylamine coupling (%) ^a	TOF for 1-octanol amination (h^{-1}) ^b	TOF for octylamine coupling (h^{-1}) ^b	Ratio of TOF (octylamine coupling)/TOF (octanol amination)
CoAl-act	11	10	104.8	158.3	1.51
CoAl-B-250-1	8	7	104.6	33.4	0.32
CoAl-B-250-3	5	3	101.9	27.5	0.27
CoAl-B-250-RG	-	-	-	-	-

^a Reaction time for 1-octanol amination and 1-octylamine coupling are 3 h and 2 h, respectively.

^b The TOF value is defined as $\text{mol}_{\text{reactant}} / \text{mol}_{\text{Co}_{\text{surf}}}^{-1} \text{ h}^{-1}$ at low conversion (~10%).

Deposition of polymeric species over cobalt nanoparticles should lead to the growth of the carbon polymeric walls around domains of active metal sites and could result in formation of isolated cobalt domains. A possible explanation of the slow hydrogenation of secondary imines over the catalysts pretreated with alcohols could be steric hindrance effect, which inhibits the planar mode adsorption of bulky

secondary imines in comparison with easier vertical adsorption of primary imines. Recent report [226] assigned selective hydrogenation of cinnamaldehyde to cinnamyl alcohol over metal catalysts in the presence of alcohol to a steric effect induced by adsorbed alcohols on the catalyst surface. DFT modeling explained it by planary adsorption of internal C=C over the metal surface in comparison with vertical geometry for primary hydroxyl and carbonyl groups [227,228]. Similar phenomena seem to occur for alcohol amination. The formation of carbon deposits seems to affect differently the rates of hydrogenation of primary and secondary imines.

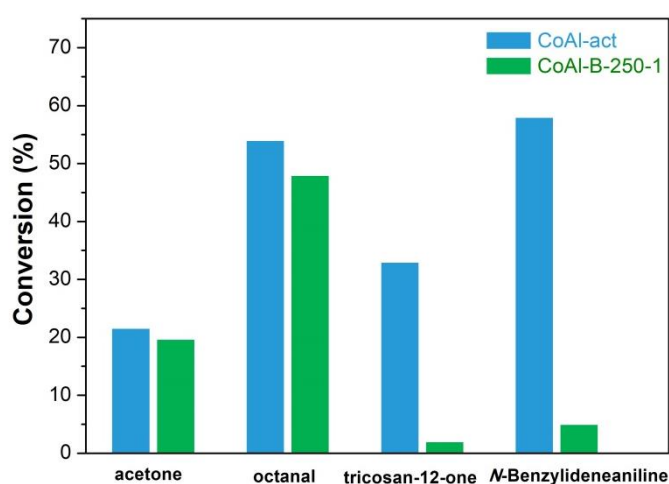


Figure 3.23 Model hydrogenation reactions illustrating the steric hindrance effect on the hydrogenation of bulky secondary imines after carbon deposition. (Conditions: tricosan-12-one 0.1 g, octanal 0.5 g, acetone 0.5 g, N-benzylideneaniline 0.5 g, H₂ 20 bar, ethanol 3 ml, tert-amyl alcohol 2 g, fresh and 1-butanol pretreated Co/Al₂O₃ 20-100 mg, 120 °C, 1-6 h).

In order to confirm the strong influence of steric hindrances on the hydrogenation of bulky molecules, which might be created by carbon deposition, we have performed hydrogenation of model carbonyl compounds (tricosan-12-one, octanal, acetone) and secondary imine (*N*-benzylideneaniline) over the freshly activated catalyst and its counterparts pretreated with 1-butanol (**Figure 3.23**). Hydrogenation of the long chain secondary carbonyl compound (tricosan-12-one) was largely constrained over the 1-butanol pretreated cobalt catalyst. However, hydrogenation of primary carbonyl compounds (octanal) occurred with only 20 % lower rate over pretreated catalyst compared to the freshly activated counterpart. The activity difference for

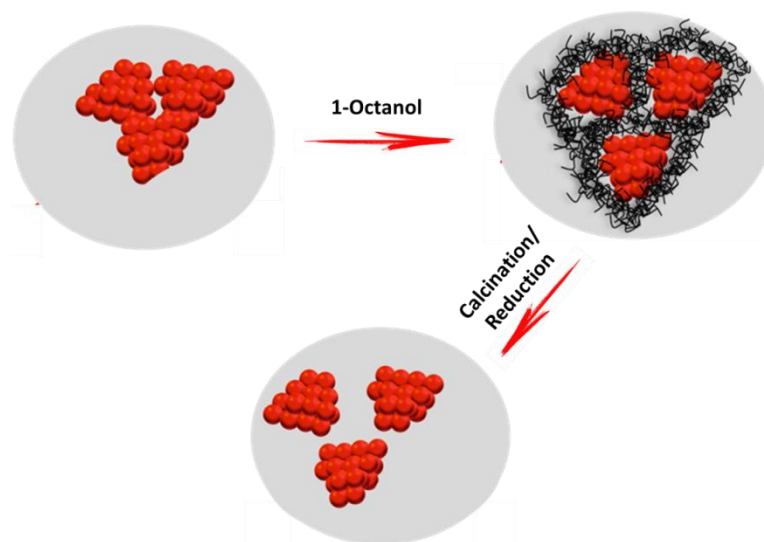
hydrogenation of short chain ketone (acetone) was only slightly affected by the catalyst pretreatment with 1-butanol. These model reactions suggest steric effects caused by carbon deposition over cobalt catalyst for the hydrogenation of bulky molecules such as tricosan-12-one. Interestingly, hydrogenation of secondary imine *N*-benzylideneaniline was also strongly constrained after carbon deposition over cobalt catalyst. It can explain suppression of self-coupling reaction of primary amine over cobalt catalysts after carbon deposition. These results confirm importance of steric effects on the selectivity of alcohol amination over metallic catalysts.

3.3 Conclusion

Pre-treatment of cobalt catalysts with alcohols leads to a decrease in the rate of alcohol amination with ammonia, but coincides with considerable enhancement of the selectivity to primary amines. The enhancement of primary amine selectivity is particularly pronounced at higher alcohol conversions.

Extensive characterizations have provided important information about the carbon species, which form, on the catalyst during their pre-treatment with alcohols. During the pre-treatment, alcohols are dehydrogenated over cobalt nanoparticles to aldehydes, which then polymerize via the aldol type condensation into unsaturated long chain hydrocarbon species. The polymeric carbon species can be removed via treatment in hydrogen. The increase in the selectivity to primary amines occurs because of slowing down primary amine self-coupling and in particular because of hindering of secondary imine hydrogenation. The effect is attributed to the steric constraints for hydrogenation of bulky secondary imines occurring over isolated cobalt domains in the cobalt nanoparticles with deposited carbon species.

Chapter 4. Disassembly of supported Co and Ni nanoparticles by carbon deposition for the synthesis of highly dispersed catalysts



Abstract: Co and Ni based catalysts are among the most popular materials used nowadays in industry. Traditional methods of catalyst preparation like impregnation or precipitation lead to formation of large metal nanoparticles (15-30 nm) composed of highly aggregated metal clusters. It results in relatively low metal dispersion and catalytic activity. Hereby we propose an efficient way to significantly increase the dispersion (2-3 times) of metal catalysts by disassembling of metal clusters by in-situ polycondensation of aldehydes produced during dehydrogenation of long chain alcohols. Deposition of bulky polymers at the interface areas decompose metal nanoparticles. Removal of carbon species demonstrates isolated metal nanoparticles with the sizes about 2-7 nm and 3-6 times higher activity in the reactions of hydrogenation, amination and oxidation.

4.1 Introduction

The cobalt and nickel based catalysts are among the most popular and important materials for modern chemical industry, which have been widely used in the reactions of methanation [229], Fischer-Tropsch synthesis [230], hydrogenation and dehydrogenation [231], oxidation [232] and hydrogenolysis [233]. Generally, Co and Ni based catalysts are prepared based on impregnation (or precipitation process) of Co and Ni salts precursors over silica (SiO_2), alumina (Al_2O_3) or active carbon with subsequent calcination followed by reduction in hydrogen to form active metallic catalyst [234]. Nevertheless, the metal NPs synthesized by this way often shows a broad particle size distribution (20-200 nm) with relatively low metal dispersion and catalytic activity [235]. The reasons of large metal particle sizes is aggregation of metal oxide in the course of nucleation, calcination and sintering during the catalyst reduction and catalytic reaction [236].

There are several different ways to prepare highly dispersed metal NPs proposed in the literature such as: (i) creation of high amount of nucleation sites and nanoconfinement in porous supports such as SBA-15, ZSM-5, MCM-48 or carbon materials [237]; (ii) use organic agents such as polyvinylpyrrolidone (PVP) to facilitate nanoparticle nucleation and anchoring onto the support [238] and (iii) plasma treatment [239], (iv) mild decomposition of metal salts in the presence of NO [240]. The main drawbacks of these routes are application of complicated organic ligands and procedures as well as expensive equipment, which are difficult for large-scale catalysts preparation. It would be of great importance development of simple and efficient method for the synthesis of highly dispersed Co and Ni catalysts for industrial applications.

The possible route to increase dispersion of the metal nanoparticles could be disassembling of metal nanoparticles in already prepared catalysts. Recently we have discovered that treatment of $\text{Co}/\text{Al}_2\text{O}_3$ catalyst by light alcohols results in selective carbon deposition over metal surface through fast polycondensation of in-situ formed aldehyde [251]. Hereby we propose the method to increase dispersion of Co and Ni

supported catalysts by formation of bulky polymers from long chain alcohols with subsequent removal of carbon species (**Figure 4.1**). It significantly increases the dispersion of Co and Ni metal catalysts and catalytic activity.

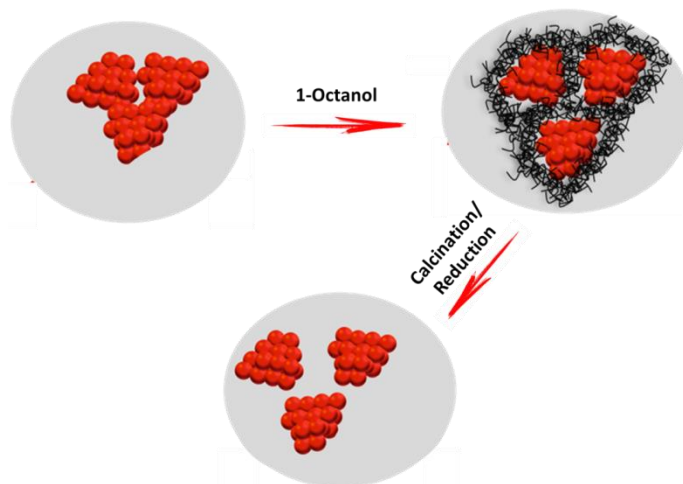


Figure 4.1 Scheme of disassembly of metal aggregates by carbon deposition

4.2 Results and Discussion

4.2.1 Catalytic reactions over highly dispersed cobalt and nickel catalysts

The catalytic performance of non-pretreated and 1-octanol pretreated cobalt and nickel catalysts was evaluated in the reactions of amination of 1-octanol, hydrogenation of tricosan-12-one and aerobic oxidation of benzyl alcohol (**Figure 4.2, Table 4.1**). The selectivity to the target products for all the reactions was 85-100% for different catalysts with conversion lower than 15 % to define the reaction rate. The activity of the Co catalyst after pretreatment in alcohol and calcination results in significant (3-6 times) increase of the catalytic activity, which totally correlates with increase of accessible active sites for the reaction mostly due to higher dispersion. The catalytic activity can be to a lesser extent affected by slightly better cobalt reducibility in the catalysts pretreated by 1-octanol. The effect was less significant for amination reaction and stronger for hydrogenation and oxidation reactions. The catalytic tests over Ni catalysts show less significant effect with only 2-3 times higher catalytic activity after pretreatment, which correlates with characterization results and effect of

1-octanol pretreatment on the dispersion of Ni catalyst.

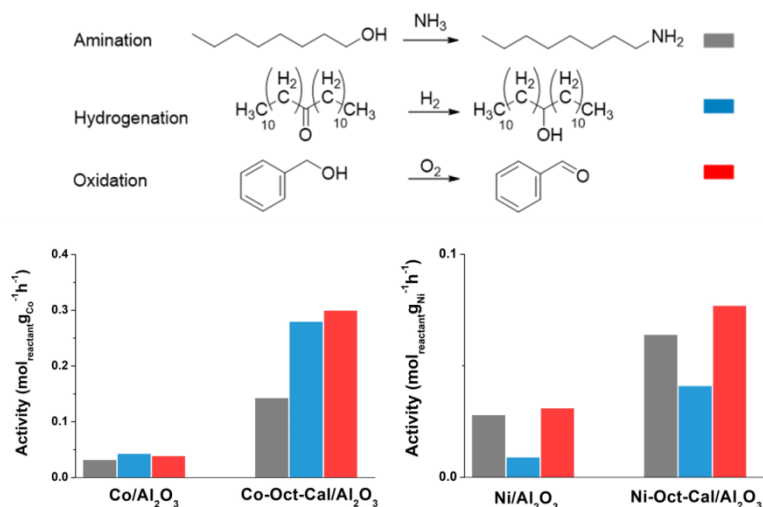


Figure 4.2 Catalytic results of in amination, hydrogenation and oxidation reactions over Co and Ni catalysts before and after pretreatment (amination: 1-octanol/ $\text{NH}_3/\text{H}_2 = 1/4.5/0.85$; $P_{\text{H}_2} = 3$ bar; alcohol, 1 mL; 20 mg catalyst; 180 °C; hydrogenation: tricosan-12-one 0.1 g with 5 ml ethanol, 20 mg catalyst, 20 bar H_2 , 120 °C; oxidation: 1 g benzyl alcohol with 2 g toluene mixed, 20 mg catalyst, 10 bar O_2 ; 130 °C)

Table 4.1 Catalytic performance of Co and Ni catalysts in different reactions

Reactions	Catalyst	Catalyst amount (mg)	Reactants (g)	T (°C)	t (h)	Conv.% (%)	Selec.% (%)	Activity ($\text{mol}_{\text{reactant}} \text{g}_{\text{Co}}^{-1} \text{h}^{-1}$)	TOF (h^{-1})
Amination	Co/ Al_2O_3	25	0.84	180	4.5	5.5	100	0.032	166
	Co-Oct-Cal/ Al_2O_3				2	11.1	100	0.143	403
Hydrogenation	Co/ Al_2O_3	10	0.1	120	0.75	10.8	100	0.043	220
	Co-Oct-Cal/ Al_2O_3				0.17	15.8	100	0.28	873
Oxidation	Co/ Al_2O_3	20	1	130	5.9	5	90	0.039	200
	Co-Oct-Cal/ Al_2O_3				1.26	8	85	0.3	828
Amination	Ni/ Al_2O_3	20	0.84	180	4	3.5	100	0.028	-
	Ni-Oct-Cal/ Al_2O_3				4	8	100	0.064	-
Hydrogenation	Ni/ Al_2O_3	20	0.1	120	1	6	100	0.009	-
	Ni-Oct-Cal/ Al_2O_3				0.5	14	100	0.041	-
Oxidation	Ni/ Al_2O_3	20	1	130	6	4	95	0.031	-
	Ni-Oct-Cal/ Al_2O_3				6	10	80	0.077	-

To check the stability of the highly dispersed cobalt NPs, the catalytic performance in amination of 1-octanol was performed for 3 cycles (**Figure 4.3**). The catalyst “Co-Oct-Cal/Al₂O₃” demonstrates comparable conversion with slight deactivation, which was attributed to small cobalt metal leaching and poisoning of ammonia. The high stability of the highly dispersed cobalt NPs is consistent with earlier mentioned study by Llorca et al. that the smallest cobalt particles seemed more stable towards coking as compared to larger ones [241].

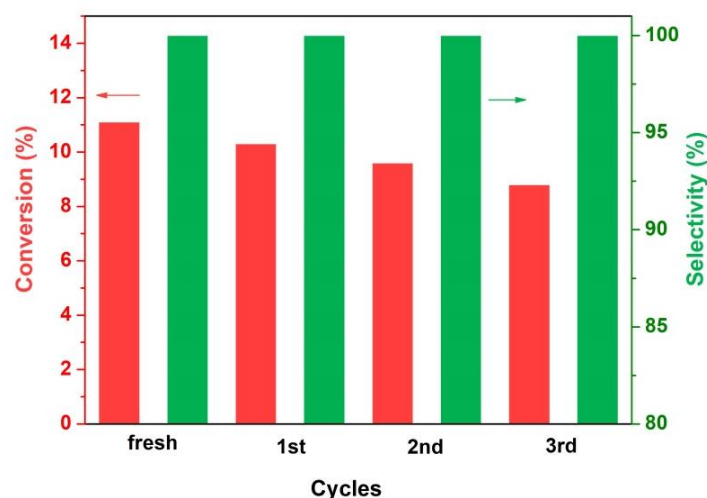


Figure 4.3 Catalytic stability of Co-Oct-Cal/Al₂O₃ in amination of 1-octanol (Reaction conditions: octanol: 0.84 g, molar ratio NH₃/alcohol = 4.5, P_{H₂} = 3 bar, catalyst: 25 mg, reaction temperature: 180 °C, time: 2 h).

4.2.2 Characterizations and mechanism of decomposition

The catalysts Co/Al₂O₃ and Ni/Al₂O₃ containing 10 wt. % of metal have been prepared by incipient wetness impregnation of γ -Al₂O₃ using an aqueous solutions of cobalt and nickel nitrates. The samples have been calcined at 400 °C and reduced at 400 °C before reaction or subsequent pretreatment. For alcohol pretreatment the catalyst after reduction has been transferred to 30 ml autoclave mixed with 1 g 1-octanol followed by charging 10 bar N₂. The catalyst was treated at 250 °C for 2 h and then washed by ethanol and acetone for several times followed by drying at 80 °C under vacuum for overnight. The catalysts were denoted as “Co-Oct/Al₂O₃” and “Ni-Oct/Al₂O₃”. To remove the surface carbonaceous species after 1-octanol

pretreatment, the pretreated catalysts were calcined again at 400 °C for 2 h, which was labeled as “Co-Oct-Cal/Al₂O₃” and “Ni-Oct-Cal/Al₂O₃”.

The characterization results of the catalysts before and after pretreatment are demonstrated in the **Table 4.2**. The amount of surface carbon species for the catalysts after 1-octanol pretreatment and calcination were analyzed by TGA technique (**Figure 4.4**). There is no obvious weight loss for the fresh Co/Al₂O₃, which indicates carbon-free clean surface for the original catalyst. After 1-octanol pretreatment the catalyst Co-Oct/Al₂O₃ exhibits a total weight loss of about 6 % at 200-400 °C due to oxidation of amorphous polymeric carbon species. After calcination for the 1-octanol pretreated catalyst at 400 °C, the degree of the weight loss is similar to the initial Co/Al₂O₃ catalyst indicating the total removal of the surface deposited carbon species over Co-Oct-Cal/Al₂O₃.

Table 4.2 Characterization of the catalysts Co/Al₂O₃ and Ni/Al₂O₃ before and after pretreatment

Catalyst	Weight loss, %	Particle size (nm)			TPR H ₂ consumption (mmol/g)	CO consumption (mmol/g)	Co/Al ^a
		$D_{\text{MeOx}}^{\text{XRD}}$	$d_{\text{Me}}^{\text{XRD}}$	$d_{\text{MeOx}}^{\text{TEM}}$			
Co/Al ₂ O ₃	2	12.2	9.2	20.5	0.9	0.019	0.52
Co-Oct/Al ₂ O ₃	6	-	3.0	6.6	2.9	0.01	-
Co-Oct-Cal/Al ₂ O ₃	2	4.8	3.6	5.2	0.9	0.036	1.0
Ni/Al ₂ O ₃	2	10.2	7.7	10.5	2.1	0.039	-
Ni-Oct/Al ₂ O ₃	4.5	-	7.1	5.6	4.5	-	-
Ni-Oct-Cal/Al ₂ O ₃	1.5	6.6	5.0	5.2	2.1	0.06	-

^a The ratio of areas of Co to Al peak in XPS spectrum

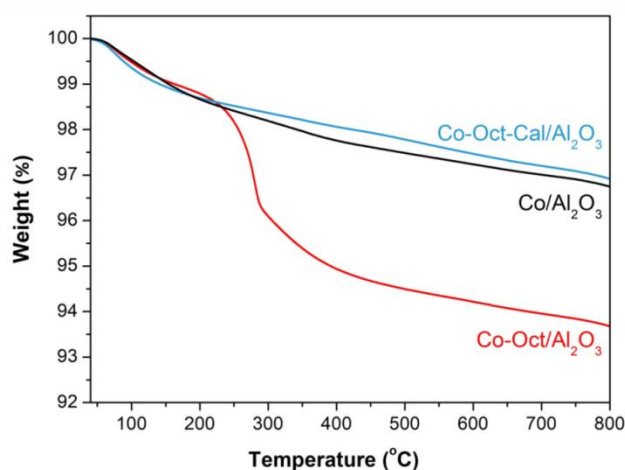


Figure 4.4 TG analysis of Co catalysts before (Co/Al₂O₃), after pretreatment (Co-Oct/Al₂O₃) and calcination (Co-Oct-Cal/Al₂O₃)

The nature of carbon species has been studied using FTIR spectroscopy (**Figure 4.5**). The peak at 1560 cm⁻¹ corresponds to stretching vibrations of olefins and the peaks at 1410 and 1250 cm⁻¹ can be attributed to -CH₂- bending frequencies [224]. Thus, FTIR spectroscopy indicates on the presence of unsaturated aliphatic polymer.

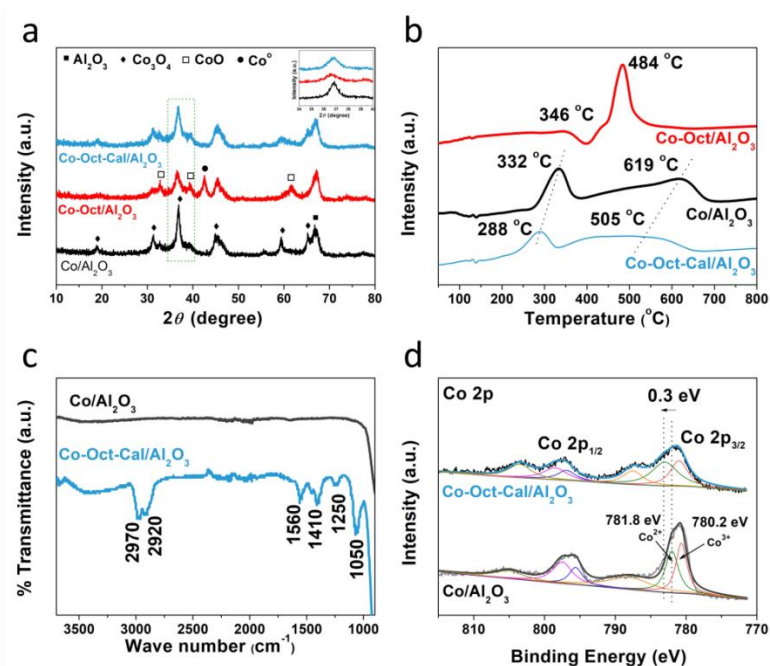
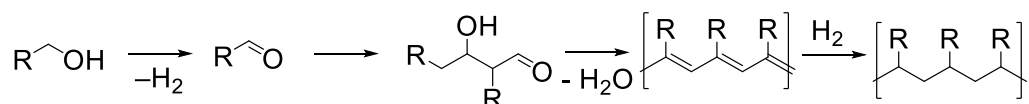


Figure 4.5 XRD, TPR H₂, FTIR and XPS analysis of the catalysts before (Co/Al₂O₃), after pretreatment (Co-Oct/Al₂O₃) and calcination (Co-Oct-Cal/Al₂O₃)

A combination of characterization results suggest that carbon deposition on the surface of the cobalt catalyst during its pre-treatment with alcohols proceeds according to the following sequence: dehydrogenation of alcohol, fast aldol condensation, dehydrogenation with formation of unsaturated polymer and partial hydrogenation of polymer:



The state of the catalyst and average particle size were analyzed by *ex situ* X-ray diffraction technique (**Figure 4.5**). The unreduced fresh Co/Al₂O₃ catalyst exhibits the patterns characteristic of the Co₃O₄ phase. After 1-octanol pretreatment, the peaks

corresponding to CoO and metallic Co appear, which is mainly because that the surface Co_3O_4 can be partially and gradually reduced to CoO and Co^0 by 1-octanol at high temperature and pressure. It is interesting to note that, the main diffraction peak at $2\theta = 36.8^\circ$ corresponding to Co_3O_4 becomes broader after calcination in comparison with the fresh $\text{Co}/\text{Al}_2\text{O}_3$ catalyst. The average particle size of Co_3O_4 is calculated by Scherrer equation using X-ray line broadening method. The calculated size of Co_3O_4 for $\text{Co}/\text{Al}_2\text{O}_3$ and $\text{Co-Oct-Cal}/\text{Al}_2\text{O}_3$ are 12.2 nm and 4.8 nm, respectively (**Table 4.2**). This indicates that the cobalt particle size significantly decrease after pretreatment in 1-octanol.

Additional information about the state and dispersion of Co in the catalysts before and after 1-octanol pretreatment could be obtained by XPS analysis (**Figure 4.5d**). Each spectrum has two major peaks corresponding to Co $2p_{3/2}$ and Co $2p_{1/2}$ and satellite peaks. The parent catalyst contains peaks in Co $2p_{3/2}$ assigned to Co^{3+} and Co^{2+} at 780.2 and 781.8, respectively [242]. The peaks for $\text{Co-Oct-Cal}/\text{Al}_2\text{O}_3$ catalyst is broader and shifts (~ 0.3 eV) to higher BE in comparison with the fresh $\text{Co}/\text{Al}_2\text{O}_3$. This shift could be caused by presence of small size highly defected oxide nanoparticles, which should lead to higher positive charge of metal in oxide [243]. Increase of the dispersion of metal catalyst can be measured by analysis of the area of metal to the area of oxide peak in XPS spectrum [244]. Hereby, we have compared the ratio of the areas of Co to Al before and after pretreatment in 1-octanol (**Table 4.2**, **Figure 4.6**). The ratio in initial catalyst was 0.52 and increased to 1 in $\text{Co-Oct-Cal}/\text{Al}_2\text{O}_3$ indicating on significantly higher dispersion of Co in the catalyst after pretreatment.

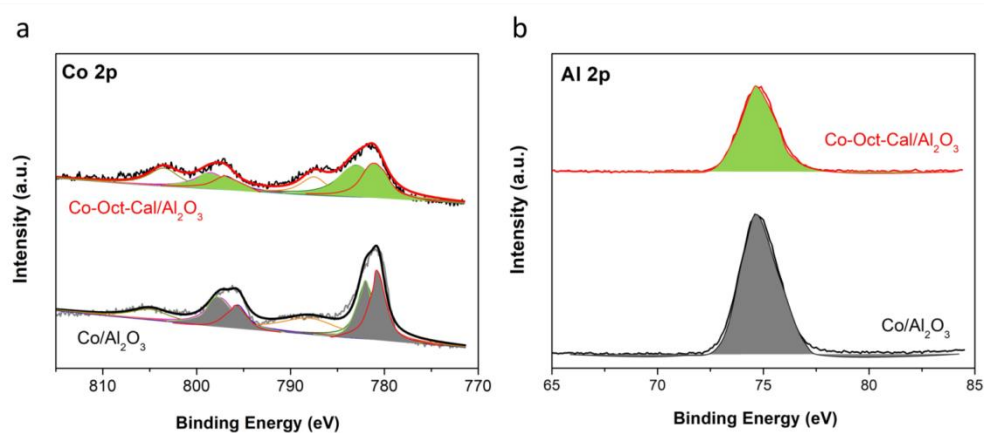


Figure 4.6 XPS spectra of Co 2p and Al 2p for $\text{Co}/\text{Al}_2\text{O}_3$ and $\text{Co-Oct-Cal}/\text{Al}_2\text{O}_3$

The particle size, dispersion and morphology were also studied by HAADF-STEM and EDX technique. As displayed in **Figure 4.7**, the fresh $\text{Co}/\text{Al}_2\text{O}_3$ demonstrates large aggregated nanoparticles with sizes in the range 15-30 nm (**Figure 4.8**). After 1-octanol pretreatment metal particles have been covered by polymeric carbon species (**Figure 4.9**). It is interesting to note that carbon deposits also in the intersection of aggregates with separation of nanoparticles from each other. Removal of carbon species shows highly dispersed isolated Co_3O_4 nanoparticles with sizes 2-7 nm (**Figure 4.7**).

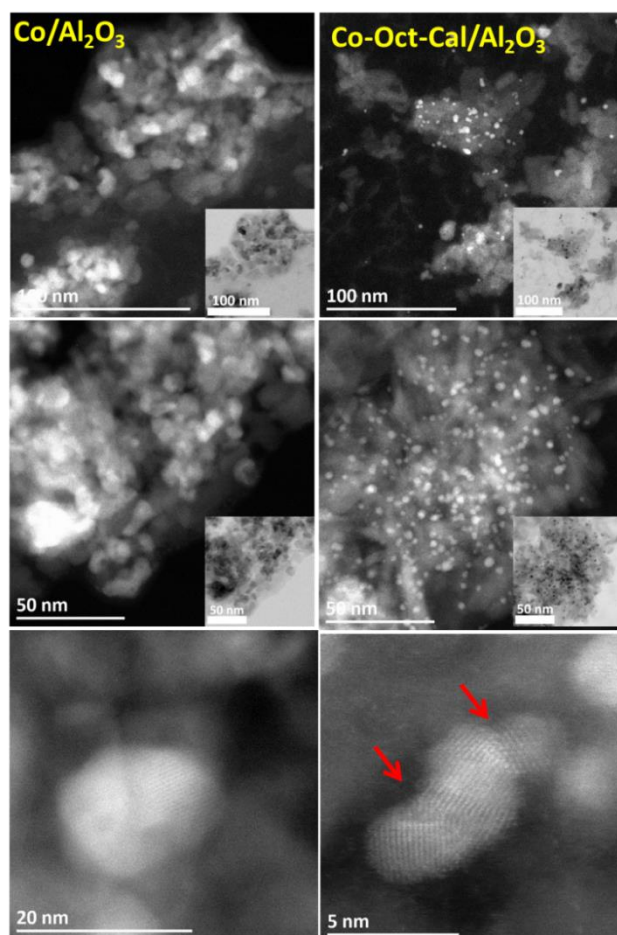


Figure 4.7 HAADF-TEM analysis of $\text{Co}/\text{Al}_2\text{O}_3$ and $\text{Co-Oct-Cal}/\text{Al}_2\text{O}_3$

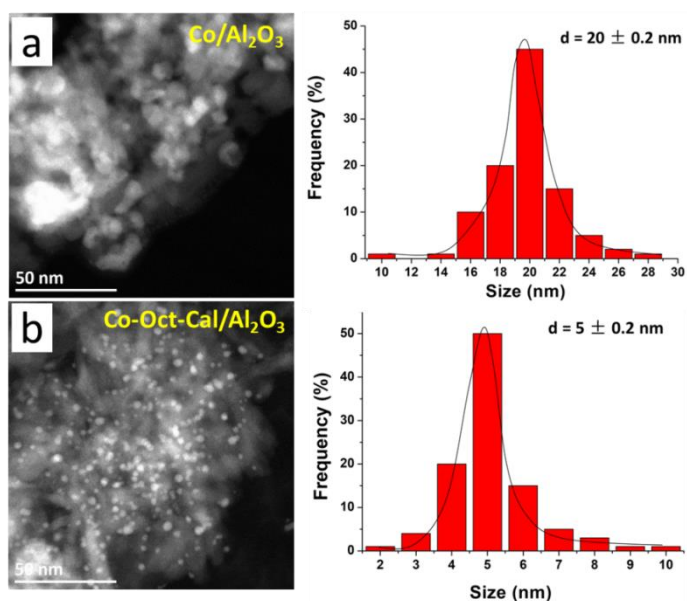


Figure 4.8 TEM images and cobalt particle size distribution in (a) Co/Al₂O₃ and (b) Co-Oct-Cal/Al₂O₃

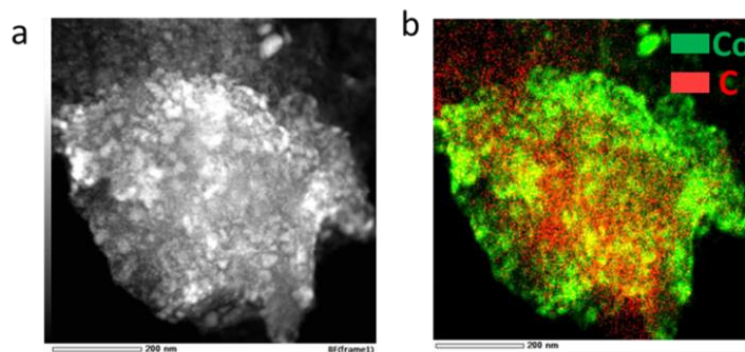


Figure 4.9 HAADF-TEM analysis (a) and TEM-EDX analysis (b) of Co-Oct/Al₂O₃

The reducibility of cobalt catalysts before and after 1-octanol pretreatment and calcination was studied by H₂-TPR method. As shown in **Figure 4.5**, the TPR profile of fresh Co/Al₂O₃ depicts hydrogen consumption peaks at about 330, which corresponds to the two-step reduction of Co₃O₄ to metallic cobalt with formation of intermediate CoO [245]. The broad second reduction peak at 620 °C is usually attributed to strong interaction of cobalt oxide species with alumina [190]. The pretreated catalyst Co-Oct/Al₂O₃ shows single peak at 450 °C with higher hydrogen consumption (2.9 mmol/g) in comparison with the parent catalyst, which is due to

reduction of both cobalt oxides and carbon deposited on the surface. Removal of carbon for Co-Oct-Cal/ Al_2O_3 shifts both reduction peaks to lower temperature especially for high temperature peak in comparison with the parent Co/ Al_2O_3 . This effect could be explained by easier reduction of small size Co oxide nanoparticles and weaker interaction with alumina support.

The Co metal dispersion and surface area after reduction were evaluated using CO adsorption in a pulse mode. CO adsorption is not totally quantitative method to evaluate amount of surface Co sites due to different ratio depending on the surface coverage, however, should correlate with amount of surface active sites [246]. The CO adsorption over Co-Oct-Cal/ Al_2O_3 (0.036 mmol/g) is nearly two times higher than that of the fresh Co/ Al_2O_3 catalyst (0.019 mmol/g) [247].

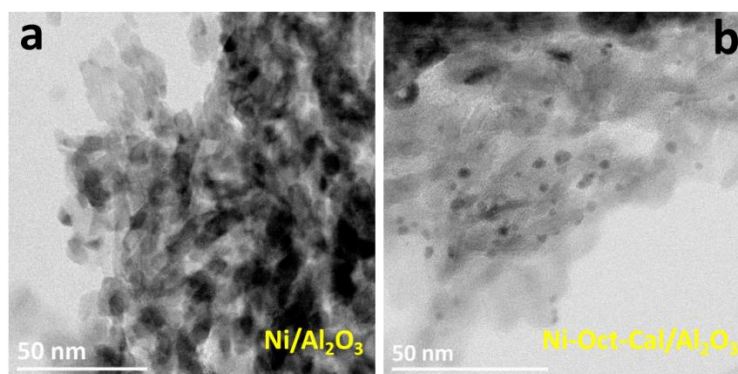


Figure 4.10 TEM analysis of Ni/ Al_2O_3 and Ni-Oct-Cal/ Al_2O_3

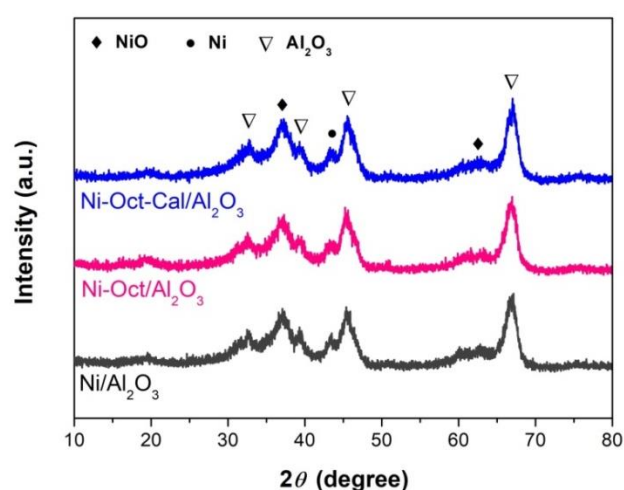


Figure 4.11 XRD pattern of Ni catalysts before (Ni/ Al_2O_3), after pretreatment (Ni-Oct/ Al_2O_3) and calcination (Ni-Oct-Cal/ Al_2O_3)

Similar effects have been observed for Ni catalyst (**Table 4.2**). Thus, the size of metal nanoparticles according to TEM (**Figure 4.10**) and XRD (**Figure 4.11**) results decreases twice from about 10 to 5 nm. CO adsorption over reduced catalyst shows 1.5 times higher dispersion in comparison with the parent catalyst. The lower effect of 1-octanol pretreatment for Ni based catalyst could be explained by higher hydrogenolysis activity of Ni catalysts during alcohol pretreatment leading to methanation of deposited carbon species. It results in lower content of carbon in the Ni catalyst (**Figure 4.12**).

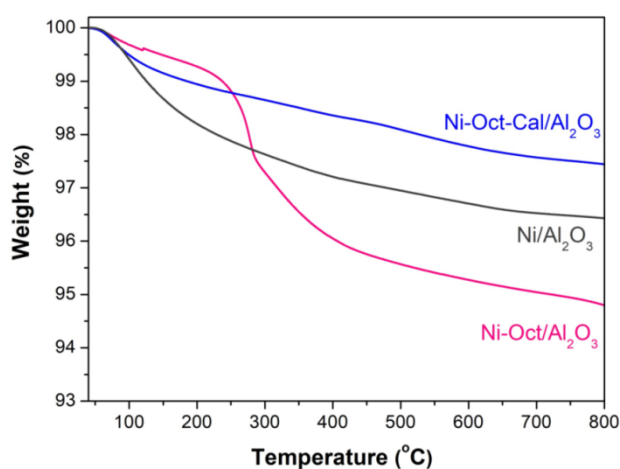


Figure 4.12 TG analysis of Ni catalysts before (Ni/Al₂O₃), after pretreatment (Ni-Oct/Al₂O₃) and calcination (Ni-Oct-Cal/Al₂O₃)

Based on the results above, we can conclude about significant increase of the dispersion of Co and Ni catalysts after 1-octanol pretreatment. Treatment of Co and Ni catalysts in 1-octanol leads to intensive growing of the bulky polymer mainly on the metal surface due to fast polymerization process. Note that no cobalt dispersion enhancement was observed after the catalyst pretreatment with lighter alcohols [251]. Low temperature N₂ adsorption shows fast increase of BET surface area from 110 to 150 m²/g after 2 h of treatment due to highly porous structure of the polymer (**Figure 4.13**). HRTEM analysis shows presence of high agglomerated metal clusters on the surface of alumina support (**Figure 4.7**). The dehydrogenation of 1-octanol should be especially intensive over edges or corners at the interface of Co clusters. Immediate polymerization at these zones should significantly increase the tension with finally decomposition of agglomerates into individual nanoparticles. Finally, after calcination in air under high temperature, the surface carbon layer will be totally removed,

leaving the highly dispersed and small size cobalt and nickel NPs with more exposed surface active atoms.

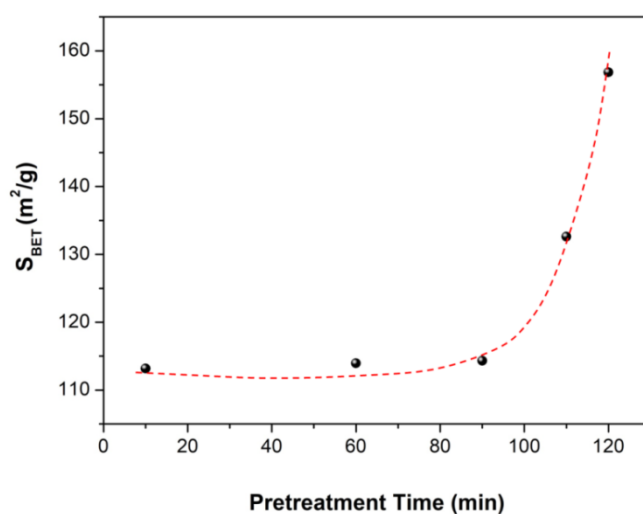
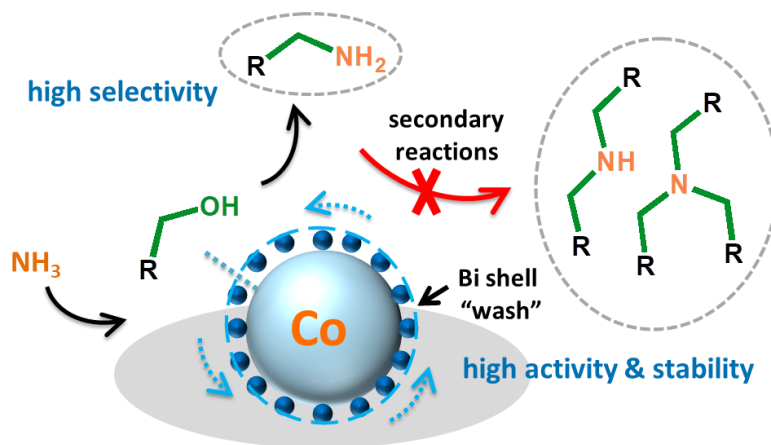


Figure 4.13 BET surface area of Co/Al₂O₃ pretreatment in 1-octanol for different time (0-2 h)

4.3 Conclusion

To conclude, 1-octanol pretreatment followed by calcination of Co and Ni catalysts leads to significant decrease of the sizes of metal NPs with increase of dispersion 1.5-2 times. It arises from the decomposition of large Co and Ni agglomerates by gradually deposited surface carbon layer in the process of dehydrogenation of alcohol to aldehyde and immediate polymerization over metal surface. The catalytic results show a significant (2-6 times) increase of activity of the pretreated cobalt and nickel catalysts for amination, hydrogenation and oxidation reactions.

Chapter 5. Bi as Liquid Metal Promoter of Co Catalysts for Highly Efficient Amination of Alcohols



Abstract: Supported cobalt catalysts are generally used for selective synthesis of primary amines in amination of alcohols with ammonia, which is an economically efficient and environmental friendly process. However, low selectivity to primary amines and cobalt catalyst deactivation due to surface coking and oxidation of metallic cobalt during reactions are still big issues. In this work, we disclosed an efficient approach to protect cobalt catalysts from deactivation by bismuth promotion. Characterizations identify the metallic bismuth on the interface between cobalt nanoparticles and support for bismuth modified cobalt catalyst. Amination activity and selectivity to 1-octylamine was obviously enhanced particularly at higher 1-octanol conversion (> 90 %). The observed phenomena are due to dehydrogenation promotion and selective poisoning by metallic bismuth. Moreover, catalyst recycling test uncovers the extremely high stability for bismuth promoted cobalt catalyst, which might be attributed to the coke resistance and ability for protecting from re-oxidation of metallic cobalt to cobalt oxides.

5.1 Introduction

Due to the high chemical activity, amines are important materials in chemical industry and life science [5]. For instance, most aliphatic amines and their derivatives are essential intermediates for organic synthesis, which are widely used in productions of agrochemicals, pharmaceuticals, organic dyes, detergents, fabric softeners, surfactants, corrosion inhibitors, lubricants, polymers and so on [248]. In particular, primary amines have attracted great attention in different derivatization reactions.

Owing to their importance, a number of routes for amines synthesis have been developed till now, including Hofmann alkylation, Buchwald-Hartwig and Ullmann reactions, hydroamination, reduction of nitriles, and reductive amination [13,23,49,249]. Among the well-established and important synthesis ways above, by far the most utilized approach is the direct one-pot amination of alcohols with ammonia.

The alcohol amination on different supported metallic catalysts, such as Ru [134], Ni [250] and Co [251], under hydrogen can be achieved via the so called “Borrowing Hydrogen” or hydrogen auto transfer methodology [92,107,109,110], which consists dehydrogenation and hydrogenation processes. The one-pot alcohol amination generally consists of three consecutive steps: (i) dehydrogenation of an alcohol to a reactive aldehyde (or ketone); (ii) imine formation by dehydration of hemiaminal from the corresponding aldehyde (or ketone); (iii) amine formation via hydrogen transfer from the alcohol to the imine through metal-hydride intermediates. During the whole process, water is the only by-product, which emphasizes the advantage of environmental friendly. Generally, the catalysts usually suffer from the main drawback of low selectivity to primary amines in particular at high conversion [6]. Recently, liquid phase amination of 1-octanol with ammonia over unsupported Ru nanoparticles was reported to be a structure insensitive reaction and the selectivity to primary amines could be adjusted by tuning the Ru particle size [134].

Generally, catalytic activity and selectivity can be adjusted by different approaches, such as capping agents' modification [207], carbon deposition [251] and

promotion [252,253,254,255]. Baiker et al. [208] reported selective blocking of active sites on supported Au nanoparticles by 1-octadecanethiol and mercaptoacetic acid for benzyl alcohol oxidation and ketopantolactone hydrogenation, respectively. More recently, McKenna et al. [209] reported diphenyl sulfide and its sulfur residue as an appropriate poison for Pd/TiO₂ catalysts leading to an enhanced selectivity in acetylene hydrogenation in the presence of ethylene. In our previous work [251], intentional deposition of polymeric carbonaceous species on the surface of Co/Al₂O₃ catalysts was used to considerably improve the selectivity of primary amines in gas and liquid-phase amination of aliphatic alcohols with NH₃. The selectivity enhancement was attributed to the slowing down of primary amine self-coupling and in particular because of hindering of secondary imine hydrogenation.

Addition of secondary metals over the parent catalyst is also an efficient way to enhance the reaction activity and selectivity. Fischer et al. [142] reported the catalytic synthesis of 1,3-diaminopropane from 1,3-propanediol and ammonia in a continuous fixed-bed reactor using unsupported Co-based catalysts. Promotion of the unsupported cobalt catalyst with iron or lanthanum would significantly improve the selectivity of 1,3-diaminopropane. It was suggested that addition of a small amount of iron suppressed the transformation of active metastable β -cobalt phase to the thermodynamically more stable α -cobalt phase under reaction conditions, which was better for catalytic selectivity. Cherkasov et al. [252] reported that bismuth-poisoned Pd/SiO₂ catalyst had a strong effect for hydrogenation of furfural. Compared to the initial Pd catalyst, the Bi-poisoned catalyst suppressed oligomerisation of furfural and increased the formation of cyclopentanol at a higher reaction temperature. It can be explained in terms of active site isolation.

Supported cobalt nanoparticles have been widely used for Fischer-Tropsch synthesis [230], dehydrogenation reactions [70] and amination reactions [142]. However, it is generally accepted that cobalt catalysts will always suffer from catalytic deactivation due to coking, chemical residuals and re-oxidation of metallic cobalt to cobalt oxides after catalytic reactions. Recently, it was reported [256] that the promotion of iron catalysts with metals used for soldering (Bi and Pb) results in a

remarkable increase in the light olefin production rate with a possibility to conduct Fischer-Tropsch synthesis at low reaction pressure.

Among the poisoning agents, metallic bismuth is particularly interesting because Bi atoms predominantly block the step sites of the cobalt nanoparticle leaving the flat terraces. Also, the high mobility of bismuth due to its low melting point makes it a flexible promoter during high temperature reaction [256]. There were few reports about the effect of Bi promotion of supported cobalt catalysts on selective amination of alcohols. In the present work, supported cobalt catalyst was modified by addition of metallic bismuth promoter to improve the catalytic activity, primary amine selectivity and stability during liquid phase amination of 1-octanol. The mechanism of bismuth promotion was also uncovered through different characterizations and model reactions.

5.2 Results and Discussion

5.2.1 Enhancement of catalytic performance on bismuth promotion

Direct liquid phase amination of 1-octanol with ammonia over supported cobalt catalyst based on the “Borrowing Hydrogen” methodology comprises several consecutive reactions. The possible reaction pathway is shown in **Figure 5.1**.

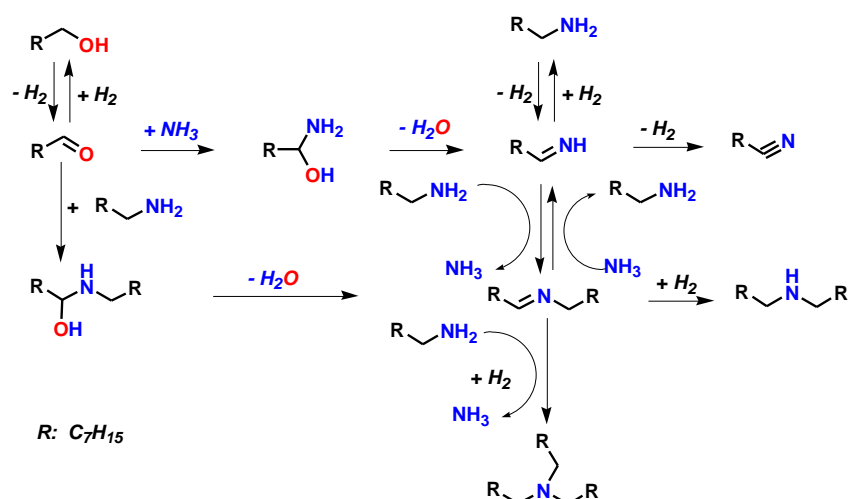


Figure 5.1 Reaction paths in amination of 1-octanol over cobalt catalyst.

Generally, the rate determining step in amination of 1-octanol appears to be its

catalytic dehydrogenation to corresponding aldehyde [67]. Then, condensation of octanal with ammonia or octylamine results in the formation of primary or secondary hemiaminal, followed by elimination of water to produce primary or secondary imines, which is a fast and non-catalytic process [135]. Finally, hydrogenation of imines leads to the formation of primary or secondary amines. Obviously, at higher 1-octanol conversion, the selectivity to 1-octylamine sharply decreases because of the self-coupling reaction of imine with 1-octylamine to secondary and to tertiary amines.

The Co/Al₂O₃ catalysts with and without Bi promotion were used for selective synthesis of primary 1-octylamine directly from 1-octanol and ammonia in the presence of hydrogen in a batch reactor. Note that no 1-octanol conversion was observed in a blank experiment without catalyst addition.

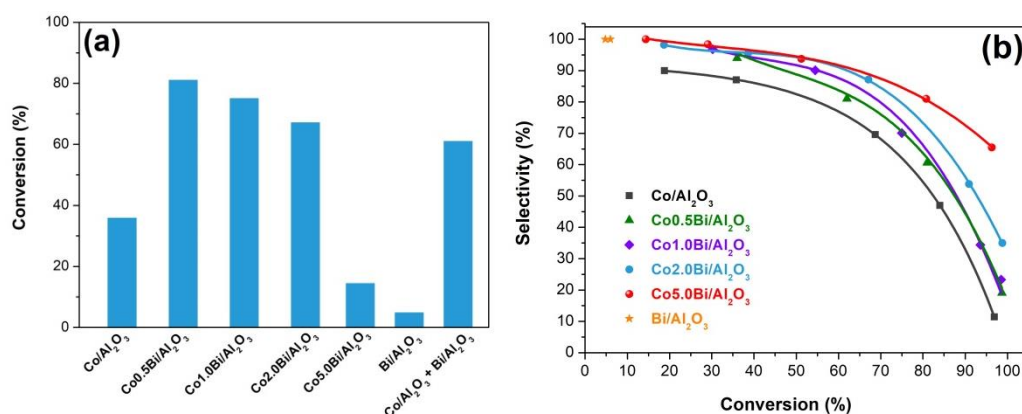


Figure 5.2 Catalytic conversion modification by Bi promotion (a) and selectivity-conversion curves (b) for liquid phase amination of 1-octanol over activated Co/Al₂O₃ and bimetallic Co_xBi/Al₂O₃ catalysts (1-octanol, 0.84 g; molar ratio of 1-octanol/NH₃/H₂ = 1/4.5/0.85; P_{H₂} = 3 bar; catalyst amount, 100 mg; reaction temperature, 180 °C; time, 0-48 h; no solvent used).

The catalytic activity for liquid phase amination of 1-octanol over the catalysts before and after Bi addition on Co is displayed in **Figure 5.2a**. The catalytic conversion and reaction rate for Co0.5Bi/Al₂O₃ catalyst (conv.% = 81 %, 0.105 mol_{octanol} g_{Co}⁻¹ h⁻¹) were ~2.3 times higher than that of fresh catalyst without Bi promotion (conv.% = 35.8 %, 0.046 mol_{octanol} g_{Co}⁻¹ h⁻¹), which indicates that metallic Bi addition on Co would largely increase the amination activity. As the Bi loading

content increased from 0.5 wt% to 5 wt%, 1-octanol conversion gradually decreased from 81 % to 14.4 %. The corresponding reaction rate also decreased from 0.105 $\text{mol}_{\text{octanol}} \text{g}_{\text{Co}}^{-1} \text{h}^{-1}$ to 0.019 $\text{mol}_{\text{1-octanol}} \text{g}_{\text{Co}}^{-1} \text{h}^{-1}$ (**Figure 5.3**).

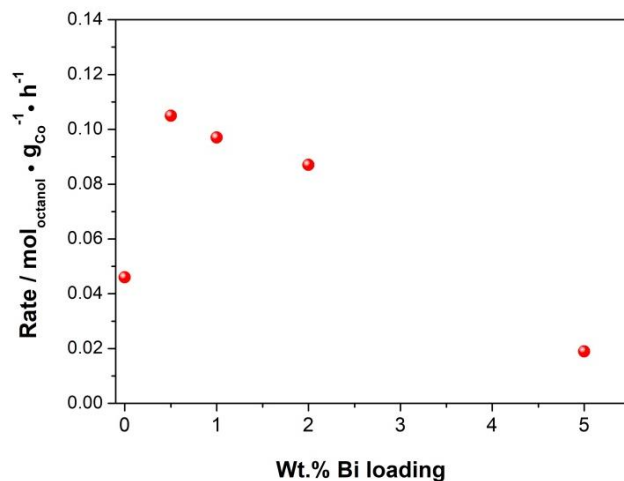


Figure 5.3 Catalytic reaction rate for liquid phase amination of 1-octanol over cobalt catalysts with different Bi loading content (1-octanol, 0.84 g; molar ratio of 1-octanol/ $\text{NH}_3/\text{H}_2 = 1/4.5/0.85$; $P_{\text{H}_2} = 3$ bar; catalyst amount, 100 mg; reaction temperature, 180 °C; time, 0-48 h; no solvent used).

Cobalt dispersion is not much affected, while cobalt reducibility is even enhanced by the Bi promotion (see below). The possible explanation of the enhancement of catalytic activity in the presence of Bi could be continuous regeneration of the surface of Co by removal of adsorbed amines, alcohols and aldehydes due to high mobility of Bi on the surface of Co. In order to prove this assumption, amination of 1-octanol was performed in the presence of CO poisoned catalysts. The activity of freshly activated Co sharply decreased after CO poisoning while there was no big difference of 1-octanol conversion for Bi promoted Co catalyst (**Figure 5.4**). Thus, indeed, increase of activity could be explained by Co surface “cleaning” by mobile Bi promoter. The higher Bi loading leads to deactivation of the catalytic activity due to decrease of the amount of accessible Co atoms for the catalytic reaction. The poisoning of active sites by Bi overloading is consistent with the decreased CO adsorption on Co (**Table 5.1**). For comparison, pure $\text{Bi}/\text{Al}_2\text{O}_3$ catalyst was also tested with a low conversion of 4.5 %, which reveals that Co metal is the main active phase for 1-octanol amination

before and after Bi promotion. Mechanical mixture of Co/Al₂O₃ and Bi/Al₂O₃ exhibited 61% conversion, which further proves the easy mobility of metallic Bi on the catalyst surface under high reaction temperature resulting the high amination activity.

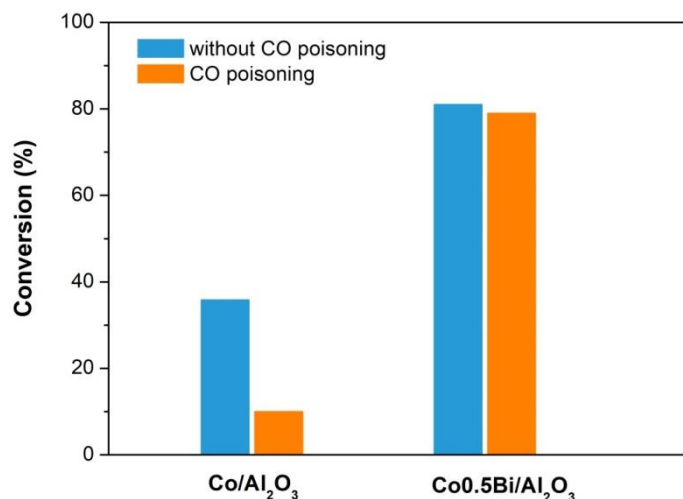


Figure 5.4 Catalytic amination of 1-octanol over Co/Al₂O₃ and Co_{0.5}Bi/Al₂O₃ catalysts with and without CO poisoning. (1-octanol, 0.84 g; molar ratio of 1-octanol/NH₃/H₂ = 1/4.5/0.85; P_{H₂} = 3 bar; catalyst amount, 100 mg; reaction temperature, 180 °C; time, 0-48 h; no solvent used).

The selectivity-conversion curves for amination of 1-octanol investigated for Co catalysts before and after Bi promotion with different loading content are shown in **Figure 5.2b**. Different 1-octanol conversions were obtained by varying the reaction time from 0 h to 48 h. The freshly activated sample Co/Al₂O₃ displays 90 % selectivity to 1-octylamine at the conversion of 20 %. As the conversion increases to nearly 100 %, the selectivity to 1-octylamine dramatically decreases to 11 %, which is similar to the reported results in both gas phase and liquid phase amination of alcohols due to the self-coupling of primary amines to secondary and tertiary amines [92]. Surprisingly, Co catalysts with Bi promotion have shown the selectivity enhancement especially at high 1-octanol conversion. The selectivity to 1-octylamine gradually increases (at the same 1-octanol conversion) as Bi loading content increases. The optimal selectivity (at 1-octanol conversion of 97 %) over Co_{5.0}Bi/Al₂O₃ catalyst even increases from 11 % to 66 %, which is 6 times higher than that of freshly

activated $\text{Co}/\text{Al}_2\text{O}_3$. Clearly, the selectivity to primary 1-octylamine during liquid phase amination of 1-octanol can be controlled by adjusting the loading content of the promoting Bi metal.

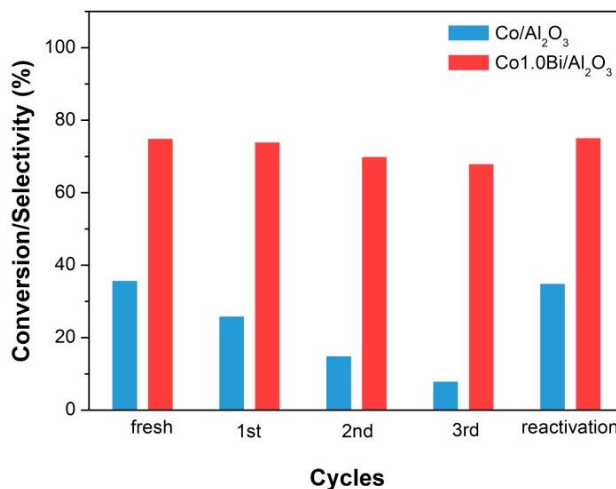


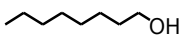
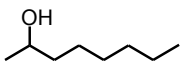
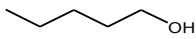
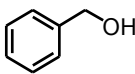
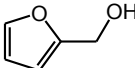
Figure 5.5 Catalytic reusability and stability for liquid phase amination of 1-octanol over activated $\text{Co}/\text{Al}_2\text{O}_3$ and $\text{Co}1.0\text{Bi}/\text{Al}_2\text{O}_3$ catalysts (1-octanol, 0.84 g; molar ratio of 1-octanol/ $\text{NH}_3/\text{H}_2 = 1/4.5/0.85$; $P_{\text{H}_2} = 3$ bar; catalyst amount, 100 mg; reaction temperature, 180 °C; time, 5 h; no solvent used; reactivation condition: 400 °C calcination under air followed by H_2 activation at 450 °C).

The catalytic stability for liquid phase amination of 1-octanol over freshly activated $\text{Co}/\text{Al}_2\text{O}_3$ and Bi promoted $\text{Co}1.0\text{Bi}/\text{Al}_2\text{O}_3$ is shown in **Figure 5.5**. After 3 catalytic amination cycles, for the freshly activated $\text{Co}/\text{Al}_2\text{O}_3$ catalyst, 1-octanol conversion gradually decreases from 35.8 % to 8 %, which is mainly due to the catalyst coking by residual amines, alcohol and aldehydes as well as partially oxidation of metallic Co to Co oxides when exposure to air during catalytic cycles. Interestingly, for the Bi promoted Co catalyst, there is nearly no conversion loss after 3 cycles, which indicates higher stability and reusability of the Bi promoted Co catalysts. After hydrogen reactivation process for both catalysts, the 1-octanol conversion both recovers to the initial state, which further proves the high effect of coke and oxidation resistance after Bi promotion.

To determine the generality of Bi promotion effect, we extend the substrate scope to other aliphatic and aromatic alcohols. 2-Octanol, 1-pentanol, benzyl alcohol, and

furfuryl alcohol were aminated in the presence of NH_3 over $\text{Co}/\text{Al}_2\text{O}_3$ and $\text{Co1.0Bi}/\text{Al}_2\text{O}_3$ catalysts. As shown in **Table 5.1**, under the same amination reaction conditions, there were also some activity and selectivity enhancement for amination of different alcohols over Bi promoted Co.

Table 5.1 Comparison of catalytic performance in amination of different alcohols over supported fresh and Bi promoted cobalt catalysts ^a

Substrate	Catalyst	Conversion (%)	Selectivity (%)		
			Primary amine	Secondary amine	Tertiary amine
	$\text{Co}/\text{Al}_2\text{O}_3$	36	94	6	0
	$\text{Co1.0Bi}/\text{Al}_2\text{O}_3$	75	70	27	3
	$\text{Co}/\text{Al}_2\text{O}_3$	49	80	16	4
	$\text{Co1.0Bi}/\text{Al}_2\text{O}_3$	68	88	12	0
	$\text{Co}/\text{Al}_2\text{O}_3$	21	95	5	0
	$\text{Co1.0Bi}/\text{Al}_2\text{O}_3$	40	90	8	2
	$\text{Co}/\text{Al}_2\text{O}_3$	^b 76	69	20	11
	$\text{Co1.0Bi}/\text{Al}_2\text{O}_3$	^b 88	78	13	9
	$\text{Co}/\text{Al}_2\text{O}_3$	^b 80	91	6	3
	$\text{Co1.0Bi}/\text{Al}_2\text{O}_3$	^b 100	92	5	0

a: alcohol, 1 mmol; molar ratio of alcohol/ NH_3 / H_2 = 1/4.5/0.85; P_{H_2} = 3 bar; catalyst amount, 100 mg; reaction temperature, 180 °C; time, 5 h; no solvent used. *b*: 160 °C, 15 h; toluene 2 g.

5.2.2 Catalyst characterizations

N_2 adsorption-desorption and BET results shows similar surface area and pore size for fresh $\text{Co}/\text{Al}_2\text{O}_3$ and $\text{Co}_x\text{Bi}/\text{Al}_2\text{O}_3$ catalysts (**Table 5.2**). **Figure 5.6** shows the XRD patterns of all samples. The calcined fresh $\text{Co}/\text{Al}_2\text{O}_3$ and $\text{Bi}/\text{Al}_2\text{O}_3$ catalysts show the presence of Co_3O_4 and Bi_2O_3 phases, respectively. For Bi promoted Co catalysts, 2 θ peaks corresponding to Bi_2O_3 phase gradually appear as the loading content of Bi increased from 0.5 wt% to 5.0 wt% and reached to the highest intensity for $\text{Co5.0Bi}/\text{Al}_2\text{O}_3$.

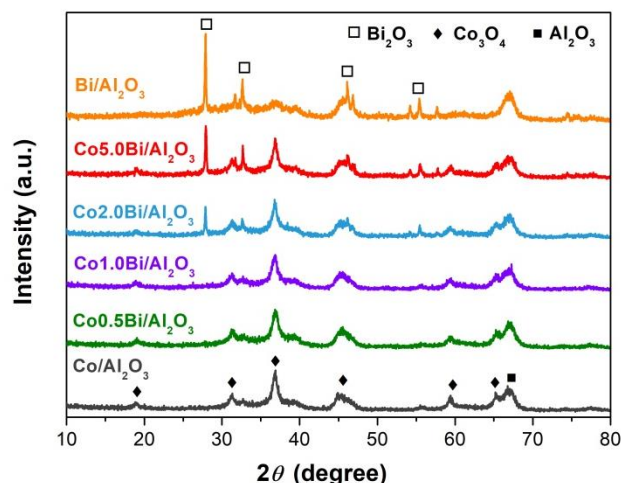


Figure 5.6 XRD patterns of oxidized Co/Al₂O₃, Bi/Al₂O₃ and bimetallic Co_xBi/Al₂O₃ catalysts.

The average particle size of Co₃O₄ calculated by Scherrer equation using X-ray line broadening method was around 10 nm for fresh and Bi promoted Co catalysts as well as the one after amination reaction (**Table 5.2**), which was consistent with STEM results calculated from size distribution (**Figure 5.7**). Therefore, it indicates no obvious modification of Co particle size and distribution after Bi promotion.

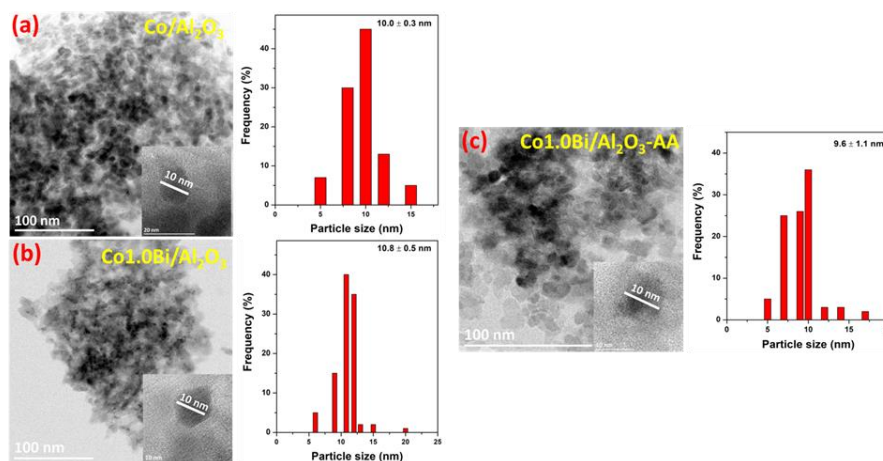


Figure 5.7 STEM images and histograms of Co particle size distribution of catalysts (a) Co/Al₂O₃, (b) Co1.0Bi/Al₂O₃, and (c) Co1.0Bi/Al₂O₃-AA.

The localization of Bi promoter for catalyst Co1.0Bi/Al₂O₃ was further investigated using HAADF-STEM and corresponding EDX mapping technique. As shown in **Figure 5.8**, Bi promoted Co catalyst exhibits a broad particle size

distribution of agglomerated Co nanoparticles in the range of 5 to 20 nm (**Figure 5.7**). The EDX mapping graph in **Figure 5.8c** clearly shows that Bi was uniformly located closely to alumina supported Co nanoparticles. As the HRTEM image shown in **Figure 5.8d**, the measured crystal interplanar spacing of the particle was 0.33 nm, which could be identified as (012) of metallic Bi. This result disclosed high affinity between Bi and Co for promotion.

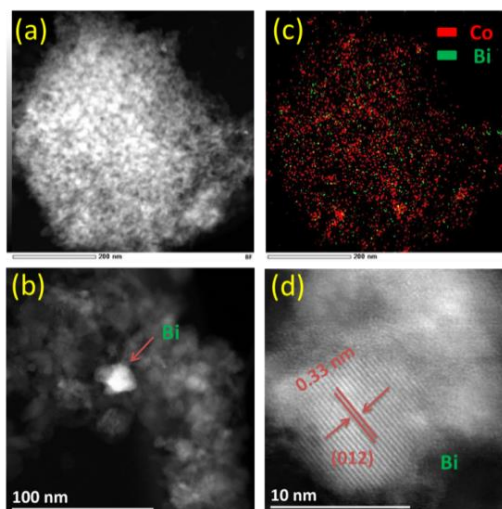


Figure 5.8 (a), (b) and (d) HAADF-STEM images of activated $\text{Co}_{1.0}\text{Bi}/\text{Al}_2\text{O}_3$ catalyst and (c) corresponding EDX mapping of Co (in red) and Bi (in green).

The reducibility of Co before and after Bi promotion was investigated by H_2 -TPR technique. As shown in **Figure 5.9**, the TPR profile of fresh oxidized $\text{Co}/\text{Al}_2\text{O}_3$ depicts two hydrogen consumption peaks at 335 °C and 622 °C. The first peak at 335 °C corresponds to the reduction process of $\text{Co}_3\text{O}_4 \rightarrow \text{CoO} \rightarrow \text{Co}$, while the broad reduction peak at 622 °C mostly due to the formation of Co-Al mixed oxide phases [190]. After Bi promotion, the catalysts $\text{Co}_x\text{Bi}/\text{Al}_2\text{O}_3$ exhibit extra hydrogen consumption peaks at 270 °C-310 °C, which corresponds to the reduction of $\alpha\text{-Bi}_2\text{O}_3$ phase. This was consistent with the increased total H_2 consumption calculated by integration from TPR for Bi promoted catalysts (**Table 5.2**). Interestingly, the broad reduction peak at 622 °C corresponding to strong interaction between Co and Al disappeared for all $\text{Co}_x\text{Bi}/\text{Al}_2\text{O}_3$ catalysts, which indicates better cobalt reducibility after Bi promotion. The H_2 -TPR analysis suggests that all the samples were mostly

present as metallic Co for catalytic amination reaction after catalysts activation in hydrogen at 450 °C.

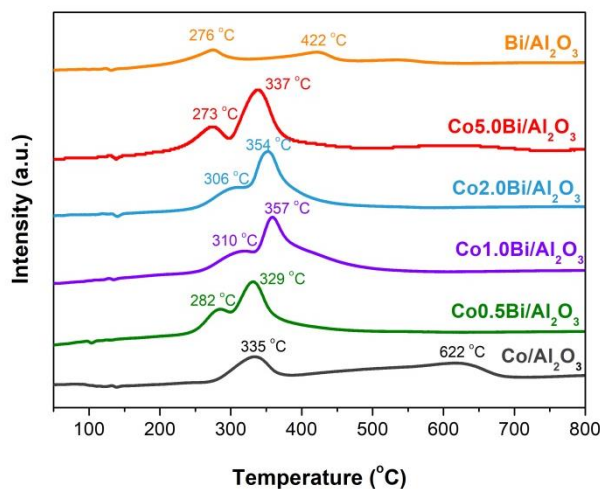


Figure 5.9 H₂-TPR profiles of calcined Co/Al₂O₃, Bi/Al₂O₃ and bimetallic Co_xBi/Al₂O₃ catalysts.

Cobalt metal dispersion and surface area were evaluated using CO adsorption in a pulse mode after *in-situ* reduction for all samples. The adsorption molar ratio of CO to Co was suggested to be 1:1 as reported [196]. Note that there was no CO adsorption on activated Bi/Al₂O₃. Fresh Co/Al₂O₃ catalyst shows relatively low dispersion (1.14%). The dispersion of Co gradually decreased from 1.14% to 0.18% caused by increasing content of Bi loading, which was consistent with H₂-TPR results (**Figure 5.9, Table 5.2**). This would be explained by partial coating of Co nanoparticles with Bi metal illustrated in EDX mapping graph (**Figure 5.8c**).

Table 5.2 Physical properties of supported fresh and Bi promoted cobalt catalysts

Catalyst	S_{BET}^a (m ² /g)	V_{tot}^b (cm ³ /g)	D_{meso}^c (nm)	Particle size (nm)			Total H ₂ consumption (mmol/g) ^g	Metallic surface area (m ² /g) ^h	Co _(CO) /Co (%) ^h
				$d_{\text{Co}_3\text{O}_4}^d$	d_{Co}^e	$d_{\text{Co}}^{\text{TEM}f}$			
Co/Al ₂ O ₃	120.72	0.39	10.55	13.2	9.9	10.0	0.87	7.73	1.14
Co0.5Bi/Al ₂ O ₃	121.32	0.40	10.61	13.9	10.4	10.2	1.43	5.6	0.83
Co1.0Bi/Al ₂ O ₃	122.23	0.42	10.82	12.8	9.6	10.8	1.5	4.5	0.67
Co2.0Bi/Al ₂ O ₃	119.04	0.39	10.85	13.0	9.8	10.3	1.3	3.1	0.46
Co5.0Bi/Al ₂ O ₃	120.66	0.38	10.28	14.1	10.6	10.5	1.52	1.2	0.18
Bi/Al ₂ O ₃	124.06	0.41	10.45	-	-	-	0.67	-	-

a BET surface area measured by N₂ adsorption-desorption;

b Pore volume of pores;

c Pore diameter in mesoporous region;

d The average particle size of Co₃O₄ is calculated by Scherrer equation using X-ray line broadening method;

e Determined from the molar volume correction of size using $d(\text{Co}) = 0.75 d(\text{Co}_3\text{O}_4)$;

f Determined from randomly selected particles in HAADF-STEM;

g The total H₂ consumption from H₂-TPR analysis;

h Obtained from CO chemisorption measurement (assuming CO/Co = 1).

5.2.3 Mechanism of bismuth promotion effect

To investigate the amination activity enhancement after Bi promotion over Co catalyst, liquid phase dehydrogenation of 2-octanol to 2-octanone was tested over activated Co/Al₂O₃ and bimetallic Co_xBi/Al₂O₃ catalysts.

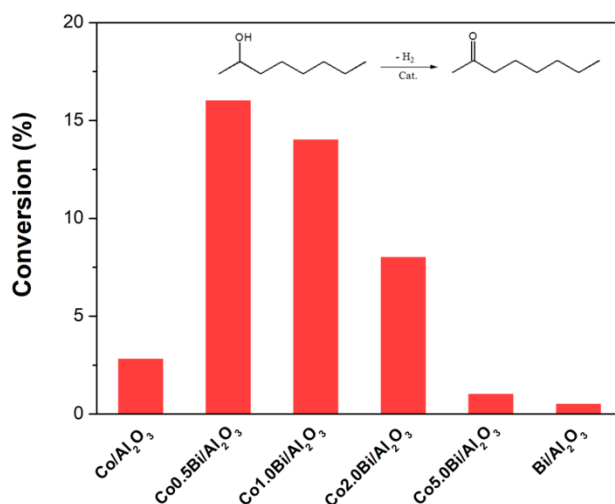


Figure 5.10 Comparison of catalytic conversion for liquid phase dehydrogenation of 2-octanol over Co/Al₂O₃ and bimetallic Co_xBi/Al₂O₃ catalysts (2-octanol, 50 mg; toluene, 1 g; catalyst amount, 50 mg; reaction temperature, 140 °C; time, 15 h).

As shown in **Figure 5.10**, the dehydrogenation conversion was only 2.8 % for fresh Co catalyst after overnight reaction [257]. After Bi addition, 2-octanol conversion increased to 16 %, which indicates that Bi addition on Co would increase the activity of dehydrogenation of 2-octanol. Then the conversion gradually decreased from 16 % to 1 % when Bi loading content increased from 0.5 wt% to 5 wt%. The variation of the activity in dehydrogenation of 2-octanol with Bi content is consistent with the activity enhancement effect for 1-octanol amination. It can be therefore suggested that the amination activity promotion effect mainly comes from the enhancement of the limiting step of alcohol dehydrogenation during liquid phase amination of 1-octanol over Bi promoted Co catalysts. Higher amount of Bi would slow down the dehydrogenation reaction possibly by blocking the active sites of metallic Co.

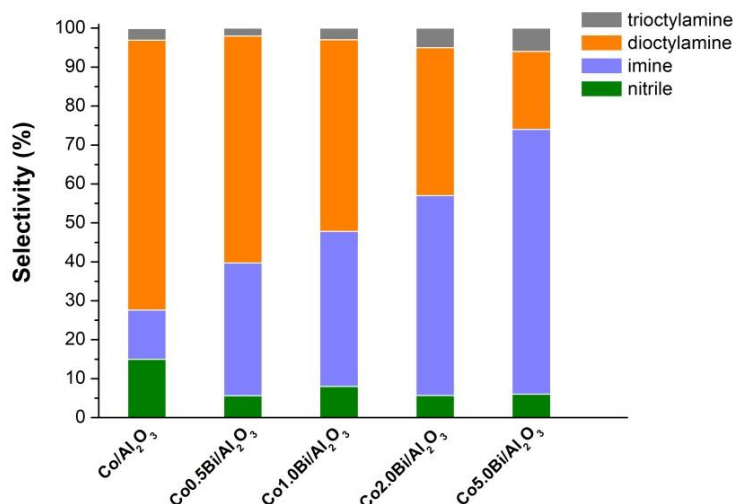


Figure 5.11 Model reaction of 1-octylamine transformation over activated Co/Al₂O₃ and bimetallic Co_xBi/Al₂O₃ catalysts at a conversion of < 10% (1-octylamine, 1 mL; catalyst amount, 20 mg; molar ratio of 1-octanol/NH₃/H₂ = 1/4.5/0.85; P_{H₂} = 3 bar; reaction temperature, 180 °C; time, 0-4 h; no solvent used).

It is widely accepted that secondary and tertiary amines can form according to two mechanisms: amination of remaining 1-octanol with 1-octylamine or self-coupling reaction of 1-octylamine through condensation of primary amines with corresponding imines. 1-Octylamine self-coupling reaction seems to be the main reason for the selectivity loss at higher 1-octanol conversion. To investigate the relationship between Bi promoter and the 1-octylamine selectivity enhancement during liquid phase amination of 1-octanol, transformation of 1-octylamine to dioctylamine was conducted at a relatively low 1-octylamine conversion (< 10%). **Figure 5.11** shows the distribution of 1-octylamine converted products over freshly activated Co/Al₂O₃ and Bi promoted catalysts at a similar conversion. The main products of 1-octylamine coupling were secondary imine and amines. The selectivity to secondary imine is relatively higher for the Bi promoted Co catalysts than that of fresh Co/Al₂O₃, while the selectivity to secondary amine is lower.

The calculated TOF values for 1-octylamine self-coupling reaction gradually decreased after Bi promotion (**Table 5.3**). They were respectively 364.5, 290.4, 217.1, 196.1 and 148.4 h⁻¹ for freshly activated Co and promoted Co with different Bi loading content, which indicates a significant lower intrinsic activity for

1-octylamine coupling to secondary amine over Bi promoted catalysts compared to the freshly activated Co catalyst. The corresponding TOF numbers for 1-octanol amination gradually increased as the Bi loading content increased. Thus, the ratio of TOF (1-octylamine coupling)/TOF (1-octanol amination) is about 10 times higher for fresh Co compared to Co_{5.0}Bi/Al₂O₃ catalyst. This result demonstrates that the reaction rate of 1-octylamine self-coupling over Bi promoted surface Co sites was much lower than that of 1-octanol amination to 1-octylamine, which could be the reason of 1-octylamine selectivity enhancement after Bi promotion. A possible explanation for the selectivity enhancement effect would be the slow rate for hydrogenation of secondary imine caused by steric hindrance effect of metallic Bi on the surface of Co, which inhibits the planar mode adsorption of bulky secondary imine compared with easier vertical adsorption of primary imine. Similar effect has been disclosed in our previous work [251].

Table 5.3 TOF values for 1-octanol amination and 1-octylamine self-coupling reactions for supported fresh and Bi promoted cobalt catalysts

Catalyst	Conversion for 1-octanol amination (%)	Yield for 1-octylamine coupling (%)	TOF for 1-octanol amination (h ⁻¹) ^a	TOF for octylamine coupling (h ⁻¹) ^a	Ratio of TOF (octylamine coupling)/TOF (octanol amination)
Co/Al ₂ O ₃	5	7	66.9	364.5	5.45
Co _{0.5} Bi/Al ₂ O ₃	7	4	214.3	290.4	1.36
Co _{1.0} Bi/Al ₂ O ₃	7	2.5	199.2	217.1	1.09
Co _{2.0} Bi/Al ₂ O ₃	6	1.5	226.1	196.1	0.87
Co _{5.0} Bi/Al ₂ O ₃	4	0.6	282.4	148.4	0.53
Bi/Al ₂ O ₃	-	-	-	-	-

^a The TOF value is defined as $\text{mol}_{\text{reactant}} / \text{mol}_{\text{Co}_{\text{surf}}}^{-1} \text{h}^{-1}$ at low conversion (< 10%).

Generally, Co based catalysts were easily to be deactivated by carbon deposition as well as oxidation of metallic Co to Co oxides after catalytic test, which would largely influence the catalytic performance. In this work, Bi promoted Co catalyst showed better catalytic stability for liquid phase amination of 1-octanol, in order to

uncover the reasons, TGA (Figure 5.12) and FTIR (Figure 5.13) techniques were used to investigate the ability of catalytic deactivation resistance for both fresh and Bi promoted Co catalysts before and after amination test.

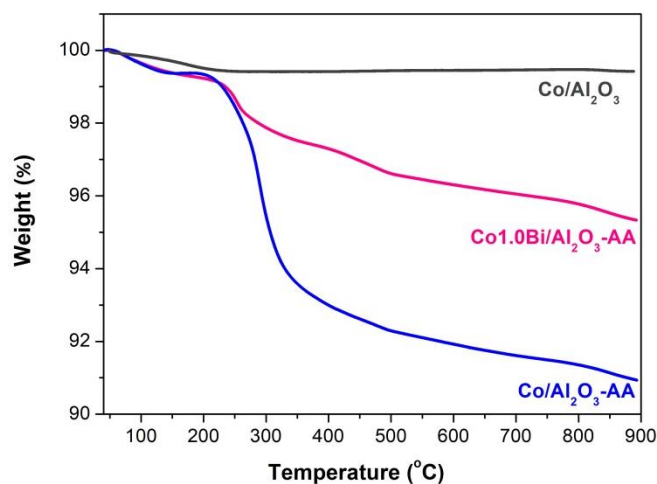


Figure 5.12 TGA profiles of fresh Co/Al₂O₃ and used catalysts Co/Al₂O₃-AA and Co1.0Bi/Al₂O₃-AA.

As Figure 5.12 shows, the TG profile of freshly activated Co/Al₂O₃ after amination exhibits a total weight loss of about 8 %, which was nearly half of that of the Bi promoted Co catalyst (~4 %). It was obvious that after Bi promotion, Co catalysts exhibit less significant carbon deposition.

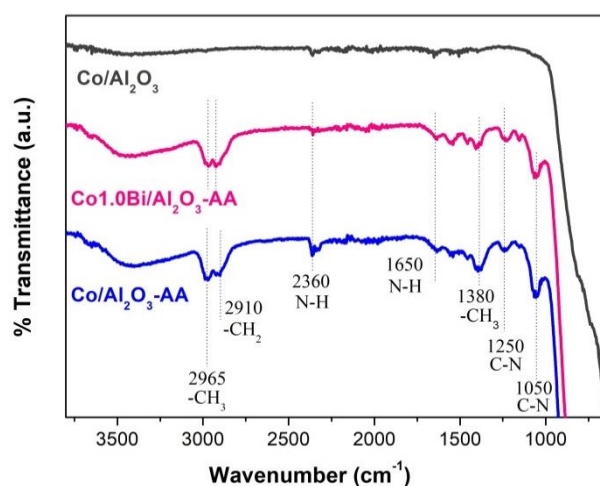


Figure 5.13 Ex situ FTIR spectroscopy of fresh Co/Al₂O₃ and used catalysts Co/Al₂O₃-AA and Co1.0Bi/Al₂O₃-AA.

The identification of deposited carbon species over the surface of Co catalysts after amination test has been further studied by *ex situ* FTIR spectroscopy (**Figure 5.13**). The freshly activated Co catalyst does not exhibit any IR bands ascribed to any carbon species. After amination test, both Co/Al₂O₃ and Co1.0Bi/Al₂O₃ exhibit IR bands corresponding to carbon deposits. IR bands appeared at 2965 cm⁻¹ and 2910 cm⁻¹ were ascribed to C-H stretching vibration in -CH₃ and -CH₂ groups, respectively. The small band at 2360 cm⁻¹ and 1650 cm⁻¹ might be assigned to N-H stretching vibration in aliphatic amines. The vibration at 1250 cm⁻¹ and 1050 cm⁻¹ also shows the presence of amine-like compounds, which would deactivate the surface of Co catalyst after amination test.

H₂-TPR profiles of the re-oxidized fresh and Bi promoted Co catalysts were measured to provide further insights into the stability enhancement after the Bi promotion (**Figure 5.14**). After exposure of reduced Co/Al₂O₃ to air for a short time, the broad reduction peak at 622 °C corresponding to Co-Al mixed oxide phases appeared, which indicates partial cobalt reduction in the activated catalyst. After exposure of reduced Co1.0Bi/Al₂O₃ to air, no hydrogen consumption peak was observed. This suggests that in the Bi-promoted catalyst, cobalt remains in metallic state even after exposure to air.

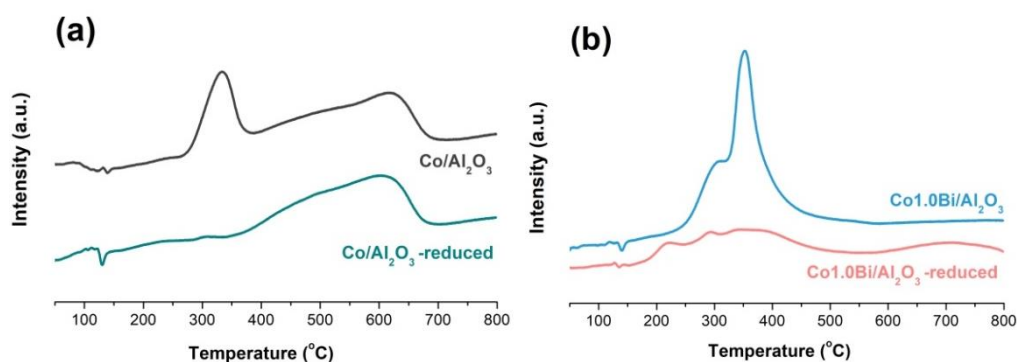


Figure 5.14 Comparison of H₂-TPR profiles of (a) reduced Co/Al₂O₃ and (b) reduced Co1.0Bi/Al₂O₃ catalysts.

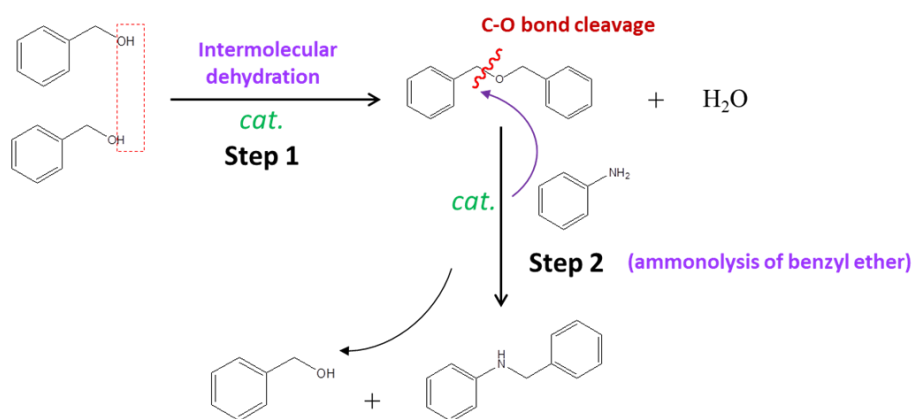
To summarize, metallic Bi promoter really strongly improves the stability of supported cobalt catalysts and can protect metallic Co from the re-oxidation to Co oxides.

5.3 Conclusion

We have disclosed a novel versatile bimetallic $\text{Co}_x\text{Bi}/\text{Al}_2\text{O}_3$ catalyst with high activity, selectivity and stability for liquid phase amination of alcohols with ammonia. Different characterizations have provided detailed information about the chemical state and localization of metallic Bi on the surface of Co.

After the Bi addition, the amination activity largely increases due to the enhancement of the limiting step of alcohol amination, alcohol dehydrogenation. The effect has been proven by the model reaction of dehydrogenation of 2-octanol. The increase in the selectivity to 1-octylamine occurs after Bi addition possibly because of slowing down of 1-octylamine self-coupling caused by hindering of bulky secondary imine hydrogenation over isolated Co domains in Co nanoparticles with metallic Bi. Furthermore, the high stability of Bi promoted Co catalyst is attributed to less significant carbon deposition and ability for protecting metallic Co from the re-oxidation to Co oxides..

Chapter 6. Highly efficient and selective *N*-alkylation of amines with alcohols catalyzed by *in-situ* rehydrated titanium hydroxide



Abstract: Catalytic *N*-alkylation of amines by alcohols to produce desired amines is an important catalytic reaction in industry. Various noble metal-based homogeneous and heterogeneous catalysts have been reported for this process. Development of cheap non-noble metal heterogeneous catalysts for *N*-alkylation reaction would be highly desirable. Hereby, we propose the *N*-alkylation of amines by alcohols over a cheap and efficient heterogeneous catalyst - titanium hydroxide. The catalyst provides the selectivity higher than 90% to secondary amines for functionalized aromatic, aliphatic alcohols and amines at high catalytic activity and stability. Mild Brønsted acidity formed by continuous rehydration of Lewis acidity excludes side reactions and deactivation by adsorbed species. The mechanism of the reaction involves dehydration of alcohols to ethers with subsequent C-O bond cleavage by amine with formation of secondary amine and recovery of alcohol.

6.1 Introduction

Complex amines are very important intermediates in chemical industry and life science. They are widely used in the production of agrochemicals, pharmaceuticals, organic dyes, detergents, fabric softeners, surfactants, corrosion inhibitors, lubricants, polymers and so on [4]. Due to the widespread use of these products, a number of synthesis routes have been developed based on classic nucleophilic substitution, like Buchwald-Hartwig [5], Ullmann reactions [20], and hydroamination [22,49,51]. Conventionally, *N*-alkyl amines are synthesized using alkylating agents, such as alkyl halides, which is environmentally unfriendly due to the toxic nature of halides and production of large amount of inorganic salts as waste. The selectivity to desired amines is generally low due to further over-alkylation [17,18,258].

In the last few decades, three main strategies have been applied for amination of alcohols: (i) “Borrowing Hydrogen” methodology using either noble metal based Ru- [110], Ir- [259], Rh- [260], and Pt- [261] complexes, and more recently non-noble metal Ag- [262], Co- [263] and Fe- [130] complexes. Also various of heterogeneous catalysts [128,138,141,149,157,166, 264] have been used. (ii) Tsuji-Trost type reactions for allylic alcohols using Pd [265] or Ni [266] complexes. (iii) Lewis-acid catalyzed reactions using a variety of salts and ligands [68,267]. Among the best performing catalysts, different metal triflates and triflimides, including the parent triflic acid (HOTf) were found active for synthesis of secondary amines through *N*-alkylation of amines with alcohols based on S_N1 or S_N2 mechanisms [133]. However, these processes have several disadvantages due to use of expensive non-recoverable catalysts, difficulties in catalyst-product separation and indispensable use of additives or co-catalysts such as inorganic or organic bases and stabilizing ligands [164]. Thus, development of easily recoverable and recyclable non-noble metal based heterogeneous catalysts for *N*-alkylation system is still a challenging topic.

Herein, we firstly report the selective *N*-alkylation of amines by alcohols in the absence of hydrogen, bases and organic ligands under ambient pressure of N_2 by an

easily prepared transition metal- and solid acid-based heterogeneous catalyst such as titanium hydroxide. For comparison, a number of metal oxides and hydroxides have been tested in the *N*-alkylation process. Interestingly, titanium hydroxide exhibits the highest activity and selectivity towards the desired amine. In addition, the titanium hydroxide catalyst provides high catalyst stability and good substrate tolerance for amination of different alcohols and substituted amines under optimized conditions. To the best of our knowledge, this new efficient heterogeneous catalyst provides a green route for selective synthesis of amines.

In terms of catalytic mechanism, it is generally accepted that substitution of OH-groups with N nucleophiles proceeds via a S_N1 or S_N2 type mechanism, in the presence of hard Lewis or Brønsted acids [268]. In this work, we show that *N*-alkylation process of alcohols involves intermediate formation of ethers, which could be a kinetic relevant step of the whole reaction. The high yield of secondary amine can be attributed to the easier C-O bond cleavage in the ether by amines based on effect of mild Brønsted acidity formed by adsorbed water over Lewis acid sites.

6.2 Results and Discussion

6.2.1 Catalysis over oxides and hydroxides

The additive-free *N*-alkylation reaction of benzyl alcohol (**1**) with aniline (**2**) to give corresponding secondary amine *N*-phenylbenzylamine (**3**) has been used as a model reaction over different non-noble metal hydroxide, oxide and zeolite catalysts (**Table 6.1**). The product has been identified by GC-MS, ¹H-NMR and ¹³C-NMR analysis (**Figure 6.1, 6.2, 6.3**). The blank test without catalyst did not show formation of desired amine (entry 1). The titanium hydroxide obtained by hydrolysis of titanium isopropoxide showed the highest catalytic activity and gave the desired secondary amine *N*-phenylbenzylamine (**3**) with the 99.6% yield (entry 2) without formation of secondary imine. Only traces of dibenzyl ether have been detected as byproduct. The product yield was slightly lower for the reaction performed without solvent due to easier formation of tertiary amine through condensation reaction

(entry 3). It is interesting to note that the reaction can be performed in aqueous phase (entry 5), however, organic solvents provide the highest yield of the product (entry 4). The reaction in air atmosphere provides a bit lower yield than that under N₂ mainly due to the partial oxidation of benzyl alcohol to benzoic acid (entry 6). Hydroxides of Al and Zr prepared by hydrolysis of different types of alkoxides could afford the maximum yield of *N*-phenylbenzylamine of only 16.9% (entry 7-10). Additionally, different metal oxides were also tested for *N*-alkylation reaction. The yield was lower than 2% for TiO₂, CeO₂, ZrO₂, MgO, SiO₂ and Al₂O₃ (entry 11-16). The alkylation yield for commercial zeolite ZSM-5 was only 25% (entry 17).

Table 6.1 Amine synthesis from benzyl alcohol and aniline over various non-noble metal oxides and hydroxides (benzyl alcohol (4.62 mmol), aniline (21.5 mmol), xylene 2 g, catalyst 0.1 g, reaction temperature 180 °C, 15 h, atmospheric N₂)

Reaction scheme: Benzyl alcohol (1) + Aniline (2) $\xrightarrow[\text{xylene (2 g)}]{180\text{ }^\circ\text{C, 15 h cat.}}$ *N*-Phenylbenzylamine (3) + H₂O

Entry	Catalyst	Yield of 3 (%)	Entry	Catalyst	Yield of 3 (%)
<i>Hydroxides</i>			<i>Oxides</i>		
1	—	0	11	TiO ₂	1.4
2	Ti-OH	99.6	12	MgO	<1
3	^a Ti-OH	92.4	13	SiO ₂	<1
4	^b Ti-OH	99.2	14	Al ₂ O ₃	<1
5	^c Ti-OH	97	15	CeO ₂	0
6	^d Ti-OH	89.8	16	ZrO ₂	<1
7	^e Al-OH	16.9	<i>Zeolites</i>		
8	^f Al-OH	10	17	ZSM-5	25
9	^g Zr-OH	8.1			
10	^h Zr-OH	12			

^aNo solvent used; ^bunder solvent THF; ^cunder water; ^dunder air; ^ehydrolysis from aluminium *t*-butoxide; ^fhydrolysis from aluminium isopropoxide; ^ghydrolysis from zirconium butoxide; ^hhydrolysis from zirconium ethoxide.

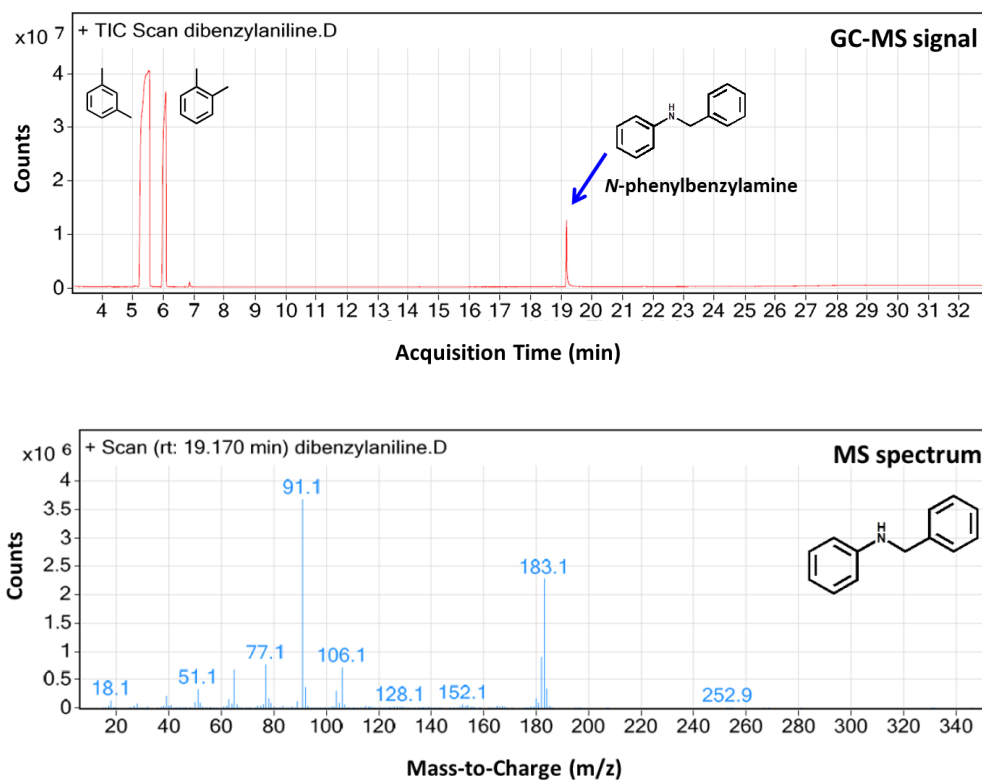


Figure 6.1 GC-MS analysis of product **3**, *N*-phenylbenzylamine.

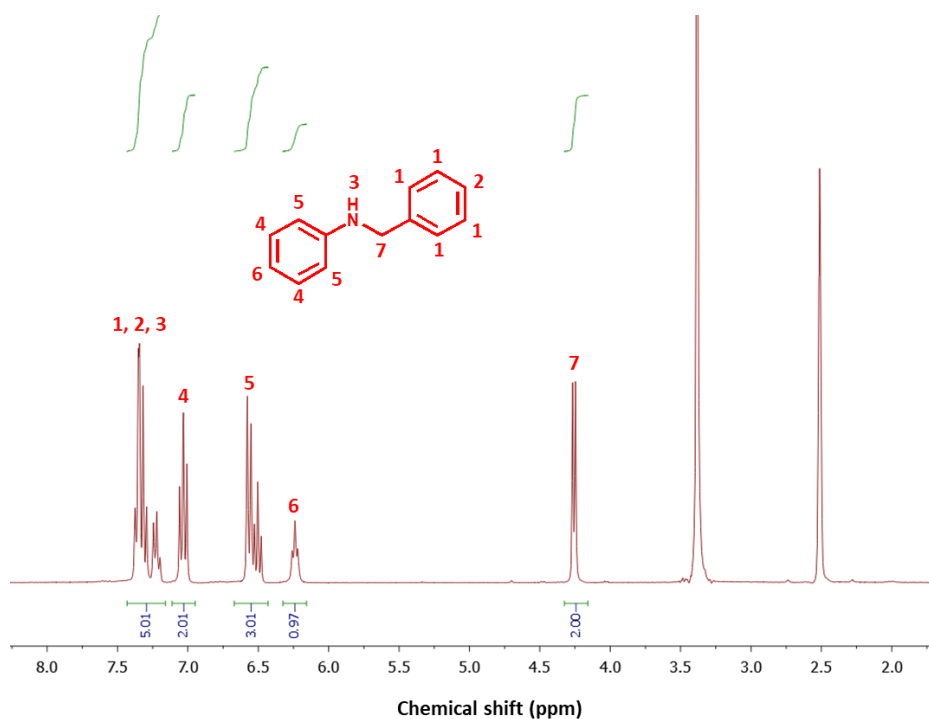


Figure 6.2 ¹H NMR spectrum of product **3**, *N*-phenylbenzylamine.

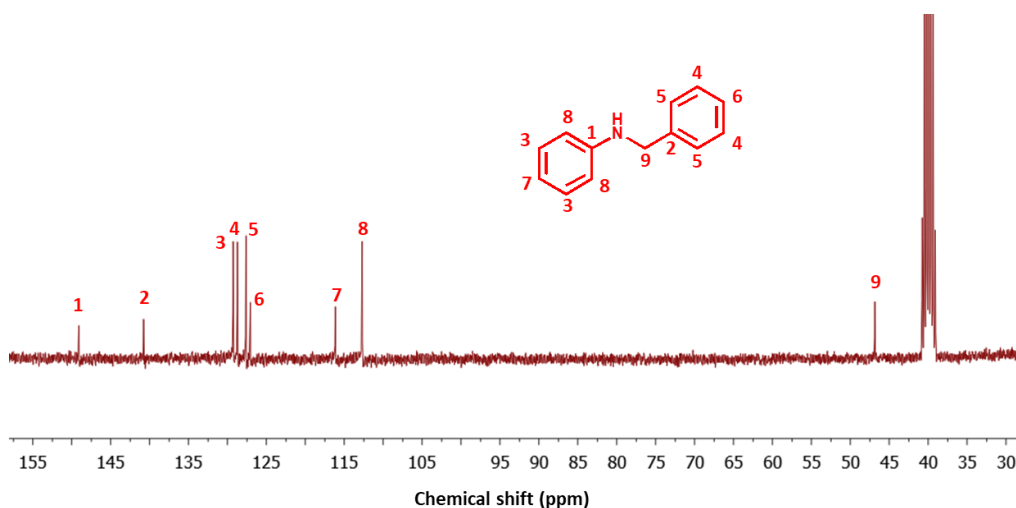


Figure 6.3 ^{13}C NMR spectrum of product **3**, *N*-phenylbenzylamine.

Titanium hydroxide (TiOH-80) was the most active catalyst. The reaction temperature dependence of the secondary amine yield in the *N*-alkylation of benzyl alcohol with aniline on this catalyst was further investigated (**Figure 6.4**).

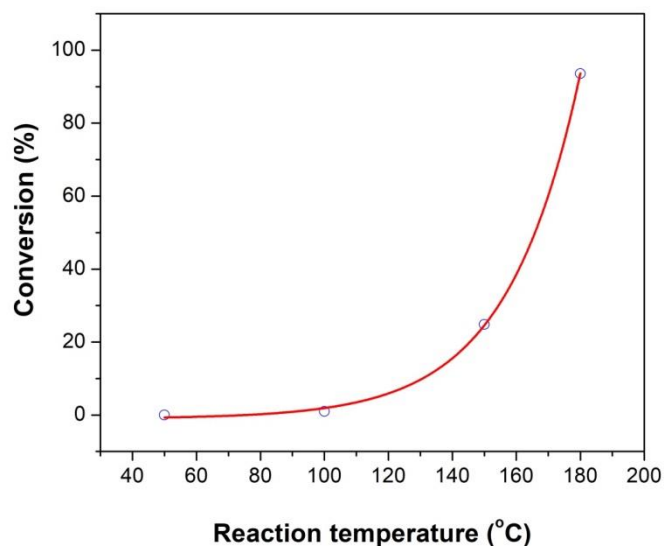


Figure 6.4 Reaction temperature dependence on conversion for secondary amine formation from benzyl alcohol and aniline over titanium hydroxide. (Benzyl alcohol 4.62 mmol, aniline 21.5 mmol, xylene 2 g, catalyst TiOH-80, 100 mg, 15 h, atmospheric N_2 .)

Below 100 °C, there was nearly no activity in this reaction. The conversion gradually increases as the temperature increases from 100 to 180 °C reaching full

conversion. The apparent activation energy of the reaction corresponds to 66.4 kJ/mol (Figure 6.5).

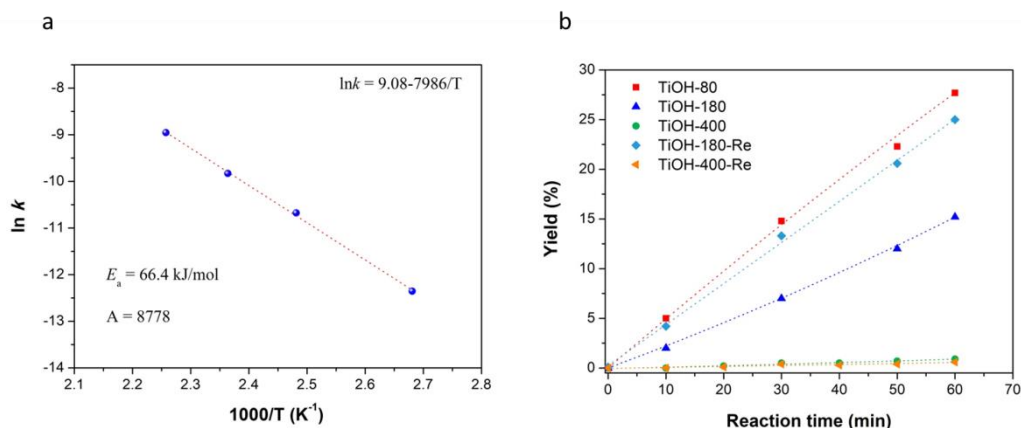


Figure 6.5 The Arrhenius plot of secondary amine yield for *N*-alkylation from benzyl alcohol and aniline over titanium hydroxide TiOH-80 (a) and time dependence for *N*-alkylation with catalysts before and after dehydration (b).

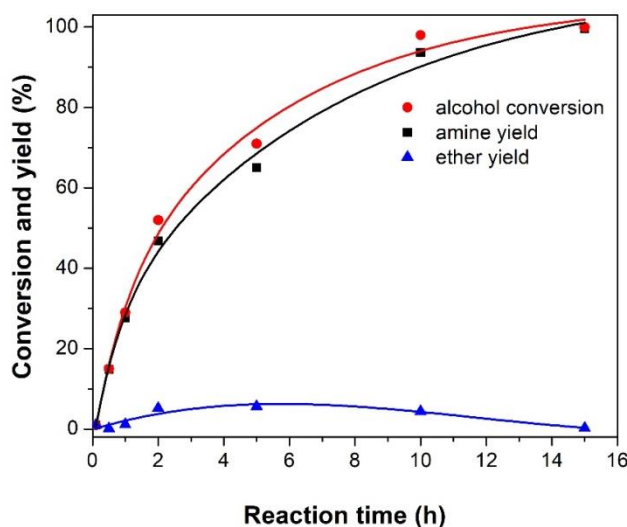


Figure 6.6 Time dependence on amine yield for *N*-alkylation from benzyl alcohol and aniline over titanium hydroxide. (Benzyl alcohol 4.62 mmol, aniline 21.5 mmol, xylene 2 g, catalyst 100 mg, 180 °C, atmospheric N_2 .)

The time course of the secondary amine synthesis over titanium hydroxide (TiOH-80) at 180 °C was investigated (Figure 6.6). The reaction proceeded smoothly to afford the corresponding secondary amine with 99% yield in 15 h. Dibenzyl ether was observed at the initial stage and its yield slowly decreased with time, suggesting the dibenzyl ether could be an intermediate. The reaction seems to

proceed in two consecutive steps: 1) transformation of benzyl alcohol to dibenzyl ether and 2) secondary amine formation from dibenzyl ether with aniline.

6.2.2 Characterizations of material

To identify, whether the high performance of secondary amine synthesis comes from the suitable acidic sites formed from surface hydroxyl group of the catalyst, titanium hydroxide obtained by hydrolysis was calcined at different temperatures. The TGA analysis (**Figure 6.7a**) shows that titanium hydroxide exhibited weight loss in two main steps. The initial weight loss below 250 °C can be assigned to desorption of surface water. The weight loss between 250 °C and 450 °C could be due to the removal of surface hydroxyl groups through dehydroxylation process [269]. No obvious weight loss was detected for TiOH-400 sample. This indicates that high crystalline TiO₂ phase was formed after calcination at 400 °C. The catalyst TiOH-80-AR after reaction showed similar weight loss compared to the fresh catalyst. This indicates similar content of hydroxyl groups and rehydration of the catalyst during reaction.

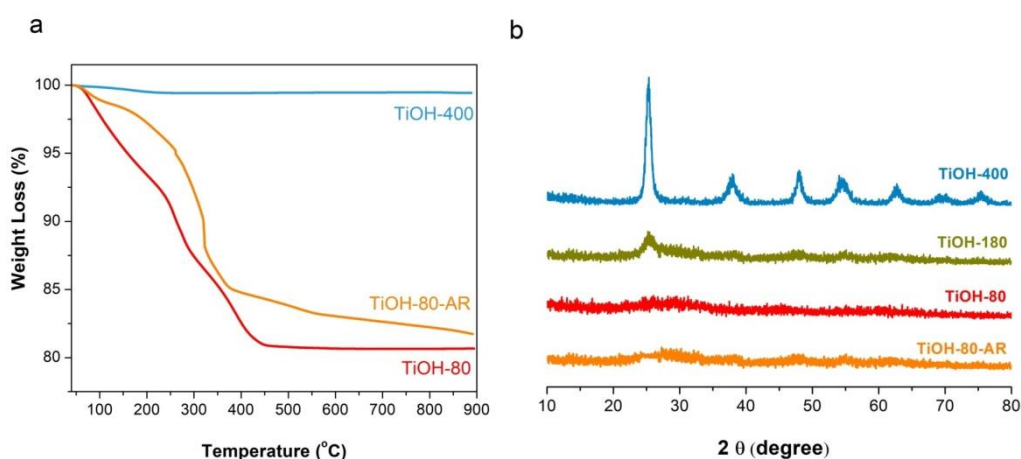


Figure 6.7 Characterization of titanium hydroxide catalysts using TG analysis (a) and XRD (b)

The state of the material during calcination at different temperatures has been studied by XRD. The parent sample and sample after calcination at 180 °C are

amorphous, the presence of anatase was detected after calcination at 400 °C [270]. XRD showed that the catalyst was still amorphous after reaction (**Figure 6.7b**).

FTIR has provided further information about the concentration and acidity of surface hydroxyl groups in titanium hydroxide. As shown in **Figure 6.8a**, the titanium hydroxide without calcination exhibited a broad peak at 3600 cm^{-1} and a peak at 1626 cm^{-1} due to the stretching vibration of hydroxyl groups interacting with adsorbed water and bending vibration of hydroxyl groups of adsorbed water, respectively [271]. As the calcination temperature increased, the intensity of the peak at 1626 cm^{-1} decreased and finally disappeared at 400 °C with significant narrowing of the peak at 3600 cm^{-1} . It indicates desorption of water and significant decrease in the amount of hydroxyl groups during dehydration of hydroxide and its transformation to anatase phase.

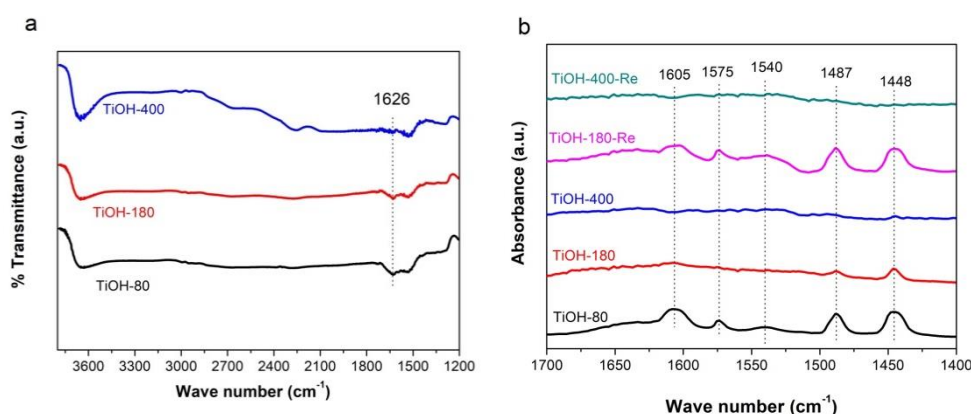


Figure 6.8 FTIR spectra of titanium hydroxide catalysts (a) and Py adsorption over titanium hydroxide catalysts (b)

To identify the acidic properties of the surface hydroxyl groups of the catalyst, FTIR spectra of pyridine adsorbed on titanium hydroxide calcined at different temperatures were recorded (**Figure 6.8b**). The interaction of pyridine with Lewis acid sites gives rise to the specific bending vibration bands of pyridine ring at 1448 cm^{-1} , 1575 cm^{-1} and 1605 cm^{-1} [224]. The peak located at 1540 cm^{-1} can be assigned to the interaction of pyridine with Brønsted acid sites. It can be observed that an increase in the calcination temperature of titanium hydroxide to 180 °C leads to decrease in the intensity of all the peaks related to Lewis acid sites and nearly

disappearance of Brönsted acid sites [269]. Further increase in the calcination temperature to 400 °C results in disappearance of all adsorbed pyridine species over the catalyst, which means nearly no acidic sites left on the catalyst. It is interesting to note that the process of dehydration is reversible and treatment of TiOH-180 in water leads to recovery of adsorbed pyridine species corresponding to Brönsted and Lewis acid sites (**Figure 6.8b**). However, rehydration process did not lead to acidity generation over the crystalline sample TiOH-400, which could be explained by high stability of anatase structure. Thus, defected labile nature of titanium hydroxide provides both Brönsted and Lewis acid sites, which disappear during dehydration procedure due to the process of healing of defected sites (**Figure 6.9**). Indeed, the formation of Brönsted and Lewis acid sites can be proposed as reaction of protonation of hydroxyl groups with subsequent dehydration. The easy rehydration process provide constant presence of both types of acid sites in the catalyst during reaction (**Figure 6.9**).

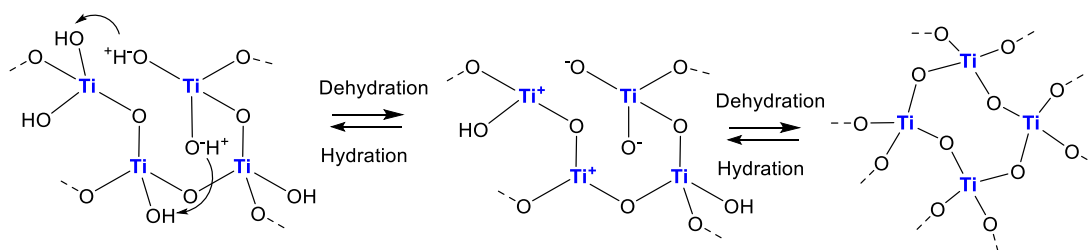


Figure 6.9 Proposed process of dehydration and rehydration for titanium hydroxide

To further identify the amount and strength of the acid sites, temperature programmed desorption of ammonia (NH_3 -TPD) has been measured as shown in **Figure 6.10**. The highest amount of acid sites is observed over pristine titanium hydroxide TiOH-80 with the broad desorption peak at 168 °C and narrow intensive peak at 312 °C corresponding to weak and intermediate acid sites, respectively [272]. Calcination of titanium hydroxide at 180 °C leads to nearly disappearance of intermediate acidity with the weak acidity peak shift to lower temperatures (100 °C). Combined with the results of Py-FTIR, it indicates that high temperature peak (intermediate acidity) can be assigned to desorption of pyridine from Brönsted acidic sites and low temperature peak (weak acidity) to desorption of pyridine from Lewis

acidic sites. The sample further calcined at 400 °C did not show any obvious NH₃ desorption.

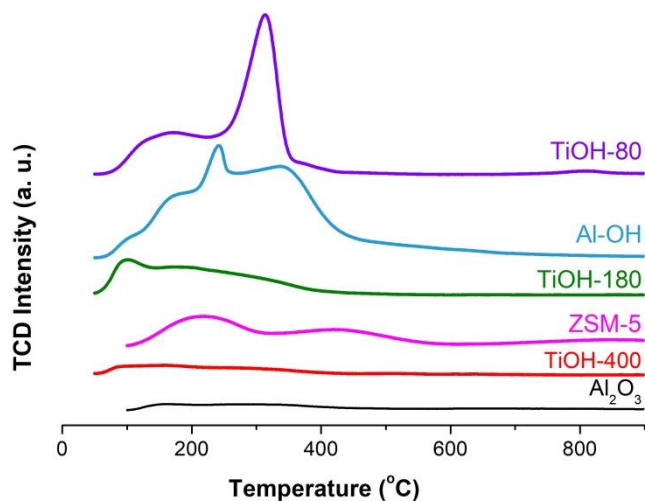


Figure 6.10 NH₃-TPD profiles of different samples.

The NH₃-TPD results for titanium hydroxide were compared with those obtained for aluminum hydroxide and zeolites. Aluminum hydroxide also shows the presence of weak and intermediate acid sites. The broad desorption peaks at 220 °C and 420 °C for ZSM-5 can be respectively assigned to intermediate and strong acidities. The amount of acid sites for all the samples calculated through integration and calibration is listed in **Table 6.2**.

Table 6.2 Acidity of the catalysts

Catalyst	Total acidity (mmol/g)	Partial acidities (mmol/g) ^a			Reaction rate (mmol/g h)
		w	i	s	
TiOH-80	5.576	1.731	3.845	-	116.2
TiOH-180	2.286	0.679	1.607	-	64.7
TiOH-400	0.217	0.08	0.137	-	2
TiOH-180-Re	4.026	1.314	2.712	-	106.1
TiOH-400-Re	0.201	0.101	0.100	-	1
Al-OH	6.487	1.786	4.701	-	19.4
Al ₂ O ₃	0.384	0.132	0.252	-	1.5
ZSM-5	1.255	-	0.739	0.516	30

^a w: weak (50-200 °C); i: intermediate (200-400 °C); s: strong (400-600 °C)

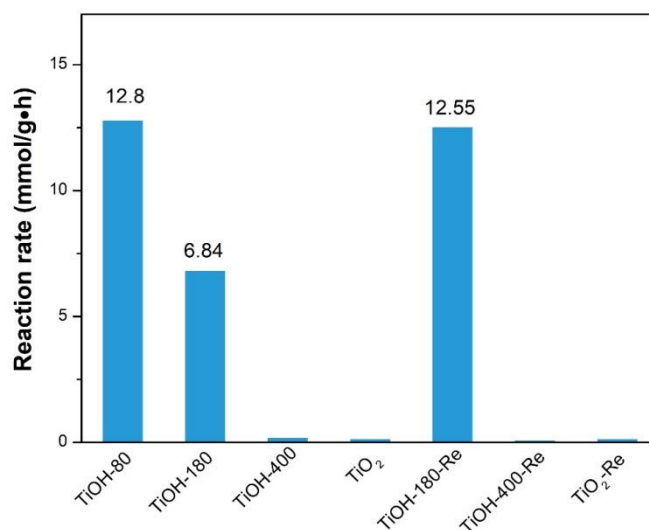


Figure 6.11 Comparison of the initial reaction rate for titanium hydroxide and calcined samples at different temperature (Benzyl alcohol 4.62 mmol, aniline 21.5 mmol, xylene 2 g, catalyst 100 mg, 15 h, atmospheric N₂).

The samples pre-treated at different temperatures have been additionally tested in the *N*-alkylation reaction. The initial reaction rate for different samples is shown in **Figure 6.11**. The initial reaction rate for the sample TiOH-80 (**Figure 6.5b**, **Figure 6.11**) was 12.8 mmol/g h, which was nearly twice higher than that of dehydrated sample TiOH-180 (6.84 mmol/g h). Calcination at 400 °C almost totally deactivates the TiOH catalyst in *N*-alkylation reaction. It means that anatase structure of TiO₂ without any significant amount of acid sites is not active in *N*-alkylation of benzyl alcohol with aniline. The catalytic test over commercial TiO₂ catalyst further confirms this conclusion (**Table 6.1**). It is interesting to note that the sample calcined at 180 °C with low content of acid sites (**Table 6.2**) still provides significant activity in amination reaction. This result can be explained by rehydration of amorphous titanium oxide by water, which produces new acid sites for the reaction. Indeed, the structure of amorphous oxide is very labile and interaction of Lewis acid sites with water formed during reaction should result in regeneration of Brønsted acidity.

Crystalline anatase TiO₂ cannot be rehydrated to form acidity during reaction. This suggestion has been further proven by addition of extra water before amination test

with the dehydrated catalysts (**Figure 6.11**). The reaction rate (12.55 mmol/g h) for amorphous titanium hydroxide (TiOH-180) was almost recovered to the initial state after addition of water. We could propose reversible process of dehydration and rehydration for titanium hydroxide during reaction, which provides permanent acidity for amination reaction [273,274] (**Figure 6.9**).

Table 6.3 BET surface area of all samples

Catalyst	S_{BET} (m ² /g) ^a	V_{tot} (cm ³ /g) ^b	D_{meso} (nm) ^c
TiOH-80	279.15	0.58	7.85
TiOH-180	165.03	0.32	7.58
TiOH-400	114.43	0.23	7.32
AlOH	332.19	0.84	5.37
ZrOH	163.78	0.15	2.51
TiO ₂	43.4	0.097	8
MgO	10.8	0.03	9.3
SiO ₂	333.3	0.7	8.8
Al ₂ O ₃	249.7	0.68	10.4
CeO ₂	207	-	-
ZrO ₂	25	0.04	8.7
ZSM-5	291.38	0.03	1.74

a BET surface area measured by N₂ adsorption-desorption;

b Pore volume of pores;

c Pore diameter in mesoporous region;

To investigate the structure-performance correlation, BET analysis of all catalysts has been performed. There is no obvious relationship between reaction activity and surface area or pore structure of the catalysts (**Table 6.3**). Indeed, high surface area of

hydroxides AlOH and ZrOH or oxides Al₂O₃ and SiO₂ does not provide high activity of these catalysts in amination.

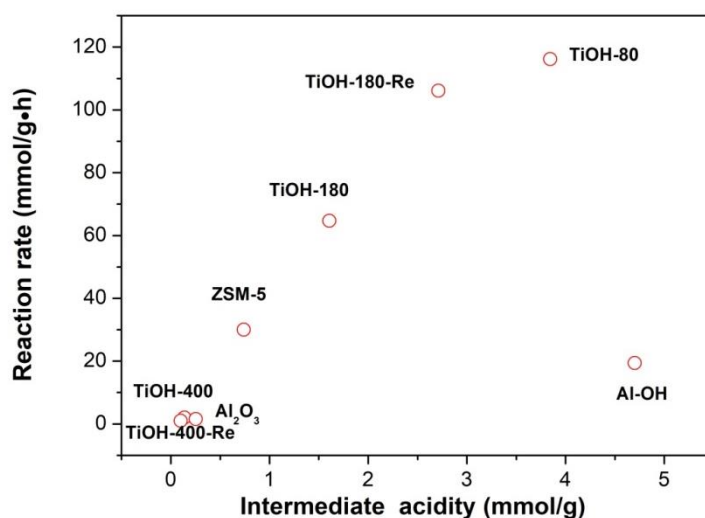


Figure 6.12 Relationship between reaction rate and intermediate acidity.

Analysis of the structure-catalytic performance relationship shows good correlation between intermediate acidity measured by NH₃ desorption in the range 200-400 °C and reaction rate in amination over different catalysts (**Figure 6.12**). It is obvious that the reaction rate increases with increase in the intermediate acidity. However, high content of intermediate acid sites over Al-OH does not lead to high activity in amination. The possible explanation of this effect could be low rehydration of Al-OH at the reaction conditions. Dehydration of Al-OH at 180 °C leads to significantly lower activity in comparison with the parent catalyst Al-OH (**Figure 6.13**). Rehydration of AlOH-180 does not show significant increase of the activity in comparison with the rehydration of TiOH-180. This fact could be explained by less labile structure of Al hydroxide in terms of reversible hydration-dehydration process. The activity recovery for the rehydrated sample TiOH-180 was mainly attributed to the continuous regeneration of intermediate Brønsted and Lewis acidic sites, (**Figure 6.9**). The lower activity for ZSM-5 was partially because of quasi-irreversible adsorption of aniline on the zeolite strong acid sites under the reaction conditions. Consequently, we could assume that weak and strong acidities would not play a determining role in amination reaction. Titanium hydroxide with optimum

intermediate acidity and able to be rehydrated shows an exceptional catalytic performance for the *N*-alkylation reactions.

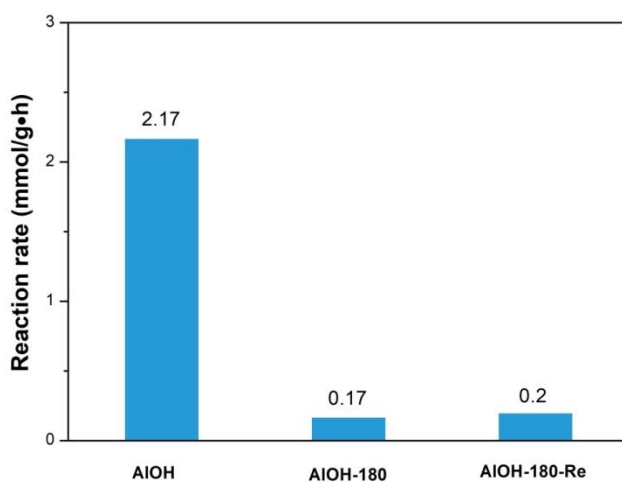


Figure 6.13 Comparison of reaction rate for dehydrated and rehydrated aluminum hydroxide

6.2.3 Proposed reaction mechanism

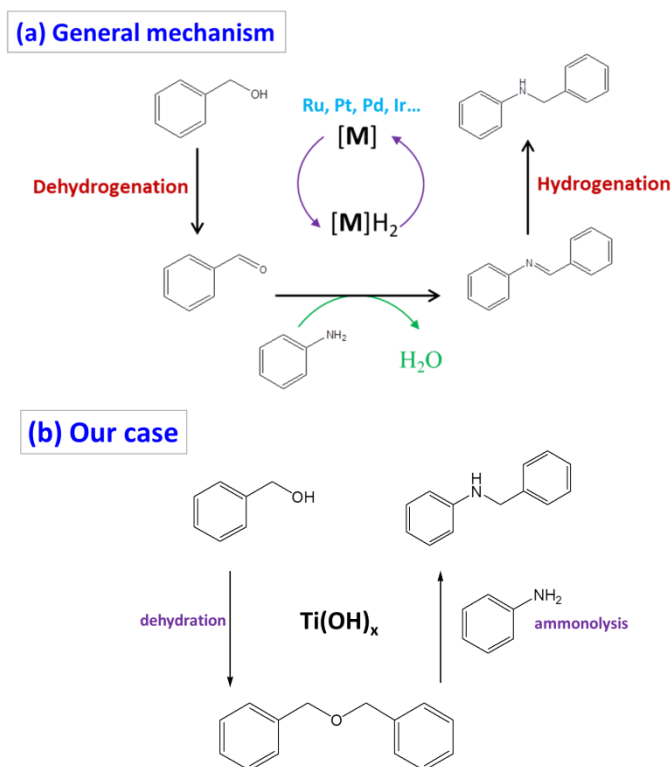


Figure 6.14 (a) General hydrogen borrowing mechanism and (b) proposed non-metallic mechanism through ether formation.

Among various strategies for amines synthesis, amination of alcohols using a borrowing hydrogen methodology (or hydrogen auto-transfer process) has been regarded as a highly atom-efficiency choice [102,105,134]. In this approach (**Figure 6.14a**) alcohol was first dehydrogenated to the corresponding aldehyde with assistance of noble metals like Ru, Pt, Pd, Ir [84,117,275,276]. Then the aldehyde was nucleophilically attacked by an amine to form secondary imine with the eliminating of water as the only byproduct. Finally, imine was hydrogenated to the desired secondary amine. During the whole process, additional hydrogen is usually added for inhibition of the catalyst deactivation and fast hydrogenation step to suppress secondary processes.

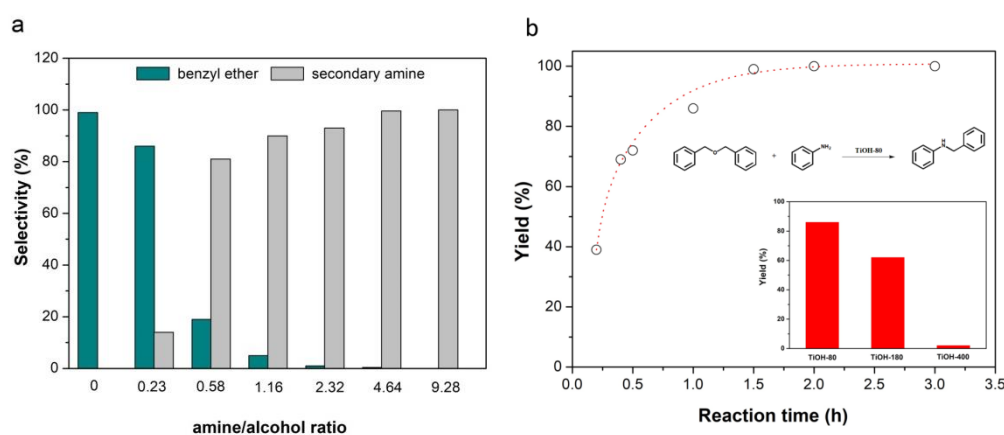


Figure 6.15 (a) Products distribution under different amine/alcohol molar ratio. Condition: benzyl alcohol 4.62 mmol, aniline/benzyl alcohol molar ratio 0-9.28, xylene 2 g, catalyst 100 mg, 15 h, atmospheric N₂. (b) Time dependence for amine formation directly from dibenzyl ether. Condition: dibenzyl ether 5 mmol, aniline 20 mmol, xylene 2 g, catalyst 100 mg, atmospheric N₂ (inset: reaction performed with different catalysts for 1 h).

In our case, the non-metallic acidic heterogeneous catalyst such as titanium hydroxide without dehydrogenation/ hydrogenation functions was found to be very efficient for the direct *N*-alkylation of benzyl alcohol with aniline to give desired secondary amine. A possible reaction mechanism in this case can be based on S_N2 mechanism of direct nucleophilic attack of α -carbon atom by N of aniline [133,277,278]. The effect of the ratio of aniline to benzyl alcohol from 0 to 10 on the reaction selectivity is displayed in **Figure 6.15**. It is interesting and obvious to note the presence of dibenzyl ether, which might be produced by dehydration of benzyl alcohol. The intermolecular dehydration of benzyl alcohol catalyzed by acid sites of metal oxides like alumina has been observed earlier [279,280,281]. Surprisingly, in

the presence of larger amounts of aniline (amine to alcohol ratio >1), the dehydration of benzyl alcohol is completely suppressed. There are two possible explanations of this effect:

- 1) acid sites of titanium hydroxide are responsible for dehydration of alcohol and amination of alcohol. The presence of excess of aniline suppresses the first reaction;
- 2) ether is the primary product of the reaction. The ammonolysis of the ether by aniline proceeds much faster than that of the relevant alcohol.

To provide experimental evidence for the second hypothesis, the catalytic reaction of dibenzyl ether with aniline over titanium hydroxide was investigated (**Figure 6.15b**). No product was formed without catalyst. TiOH-80 clearly catalyzed the ammonolysis reaction of dibenzyl ether with high initial reaction rate (80 mmol/g h), which was about 6 times higher than that of the whole *N*-alkylation reaction (12.8 mmol/g h) (**Figure 6.5b**, **Figure 6.10**). It demonstrates that the ammonolysis of dibenzyl ether through C-O bond cleavage [62,63,282,283] to the desired secondary amine proceeds much faster than the relevant reaction of benzyl alcohol. This indicates that dehydration of alcohol could be the limiting step of the whole *N*-alkylation reaction (**Figure 6.14**). Water was the only byproduct during the whole reaction process. The product yield for the ammonolysis reaction dramatically decreased from 86 % to nearly 0 as the pretreatment temperature increased from 180 to 400 °C (inset of **Figure 6.15b**). It indicates that the ammonolysis of dibenzyl ether requires acid sites as well, which is consistent with the previous report [95]. However, the reaction is less sensitive to amount of acid sites in comparison with dehydration of alcohol to ether.

To investigate the alcohol dehydration process on the acid sites of titanium hydroxide, in-situ FTIR experiments were performed (**Figure 6.16**). Adsorption of benzyl alcohol leads to appearance of the bands at 1230, 1380, 1360, 1447, 1470 and 1494 cm⁻¹. The bands at 1447 and 1494 cm⁻¹ can be assigned to the in-plane C-O-H bending modes [284]. The bands at 1230 and 1470 cm⁻¹ are associated usually with methylene group. The bands at 1360 and 1380 cm⁻¹ can be assigned to aromatic skeletal vibrations [285].

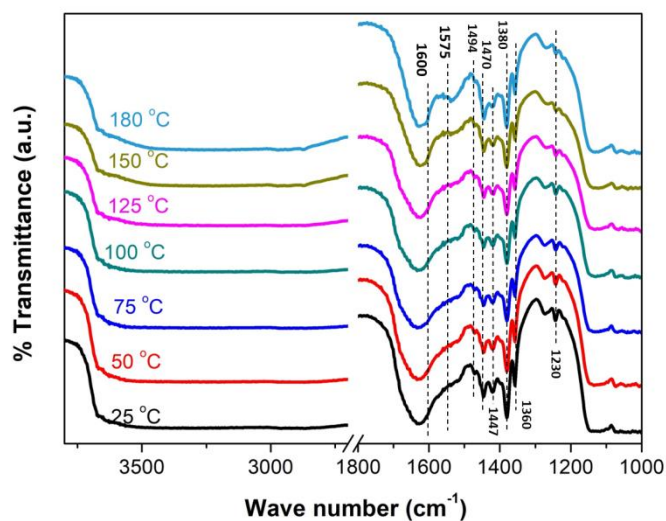


Figure 6.16 In-situ FTIR spectra of titanium hydroxide exposed to benzyl alcohol vapor calcined under different temperature.

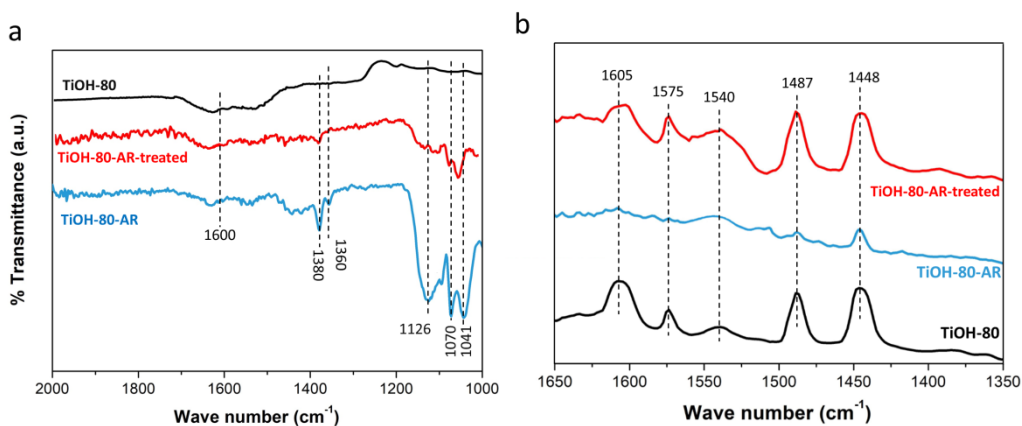


Figure 6.17 FTIR spectra of titanium hydroxide (a) and Py adsorption (b) before reaction (TiOH-80), after reaction (TiOH-80-AR) and treatment in xylene (TiOH-80-AR-treated)

As the temperature increased from room temperature to N-alkylation temperature, the additional bands appears at 1600 cm^{-1} and 1575 cm^{-1} (**Figure 6.16**). These bands can be assigned to bending vibrations of strongly adsorbed water over Lewis acid sites and C=C stretching vibrations in benzyl ether [286]. This indicates dehydration of alcohol with formation of water and ether.

The FTIR spectrum of the catalyst after reaction and intensive washing in xylene shows the peaks at 1380 and 1360 cm^{-1} similar to FTIR spectra after benzyl alcohol adsorption (**Figure 6.17**). In order to verify if these species could be intermediates during catalytic reaction, the catalyst after reaction has been treated at the reaction conditions in pure xylene. The liquid phase after reaction contained 0.33 mmol (3.3 mmol ether/gcat.) of dibenzyl ether which was the only product of the reaction (**Figure 6.18**).

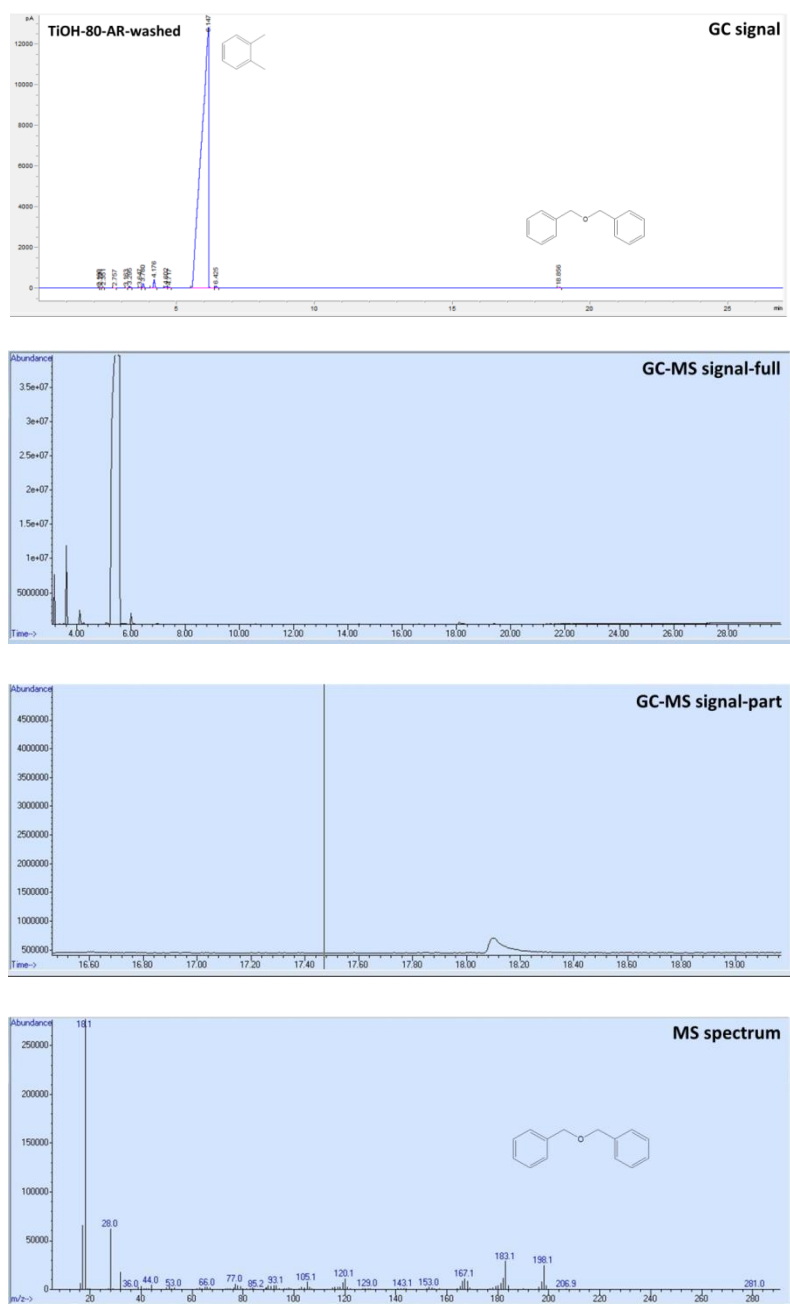
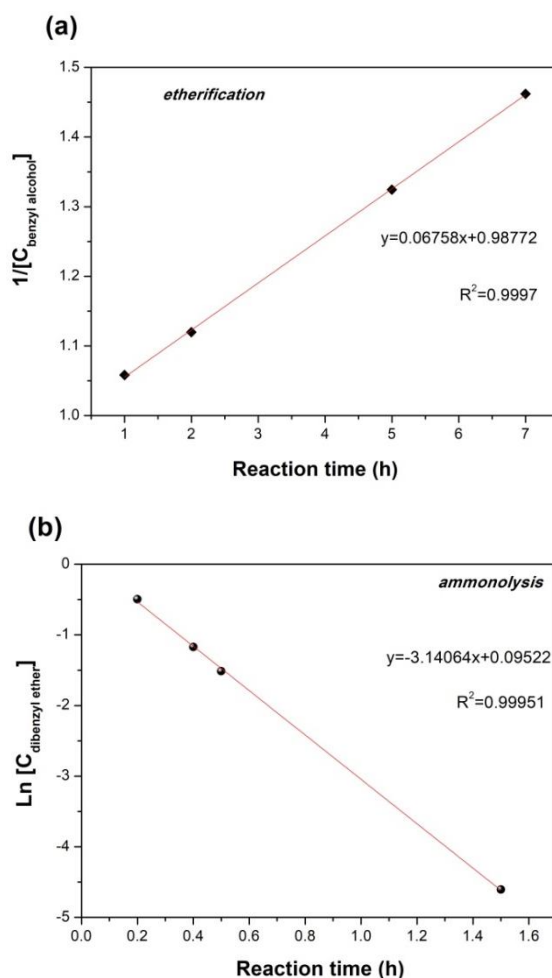


Figure 6.18 GC-MS analysis of the surface species of titanium hydroxide after washing in xylene.

The amount of the product corresponds well to the amount of acidic active sites determined by TPD of NH_3 (Table 6.2). FTIR analysis shows that surface species have disappeared after reaction (Figure 6.17). In order to identify the localization of these species, Py has been adsorbed over the catalyst before and after treatment in solvent (Figure 6.17). It is interesting to note that the peak attributed to adsorption of Py over Lewis acid sites decreased significantly after reaction but has been totally recovered after treatment in xylene. The possible explanation of this effect could be formation of surface alkoxide species by interaction of alcohol with Lewis acid sites (Figure 6.17). The presence of intermediate surface alkoxides have been observed earlier over alumina [287]. FTIR analysis of low wavenumber region (Figure 6.17) of the catalyst after reaction (TiOH-80-AR) shows intensive bands at 1126, 1070 and 1041 cm^{-1} , which has been earlier assigned to vibration modes of Ti-O-C species in alkoxides [288].



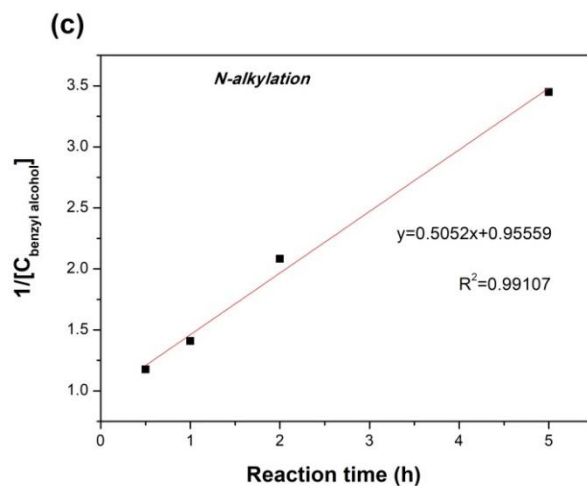


Figure 6.19 Kinetic analysis of (a) etherification, (b) ammonolysis, and (c) *N*-alkylation reactions. (Benzyl alcohol 4.62 mmol, aniline 21.5 mmol, xylene 2 g, catalyst 100 mg, 180 °C, N₂.)

The kinetic analysis of the reaction of benzyl alcohol dehydration to benzyl ether shows that it corresponds to the second order similar to the whole *N*-alkylation reaction (**Figure 6.19**).

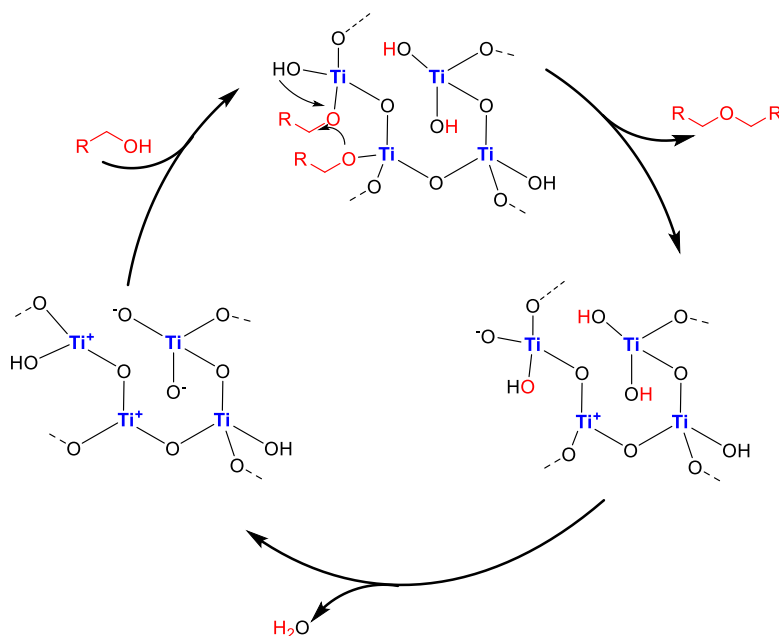


Figure 6.20 Scheme of the reaction mechanism of alcohol dehydration over TiOH.

Based on the catalytic and characterization results discussed above, a possible reaction mechanism of ether formation on acidic titanium hydroxide as key intermediate for further ammonolysis to *N*-alkylation product was proposed in **Figure**

6.20. The alcohol reacts with Lewis acid sites over the TiOH catalyst with formation of surface alkoxides. Protonation of oxygen of alkoxide species by hydroxyl group with S_N2 attack of α -carbon by oxygen of another alkoxide results in formation of ether and partial hydration of the catalyst. Subsequent dehydration leads to regeneration of the active sites. Thus, synergetic effect of mild Brønsted and Lewis acid sites over titanium hydroxide for activation of alcohol able to transform it to ether by dehydration is necessary. These properties make titanium hydroxide unique for this reaction.

To investigate the stability and reusability of titanium hydroxide, the used catalyst was washed with ethanol and separated from the liquid phase by centrifugation for several cycles and dried at 80 °C for 10 h. As shown in **Figure 6.21**, the titanium hydroxide could be used for at least three catalytic cycles without obvious change in reaction rate and amine yield, indicating good stability and recyclability for titanium hydroxide.

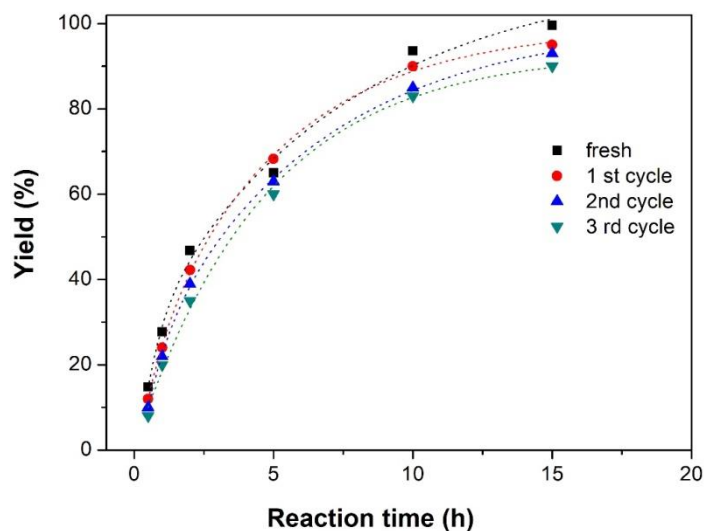


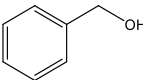
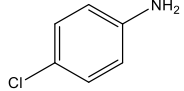
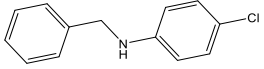
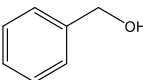
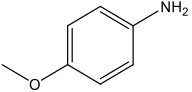
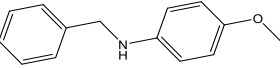
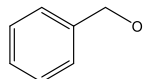
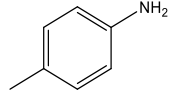
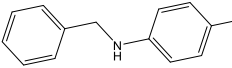
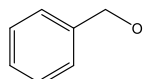
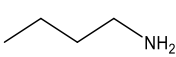
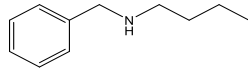
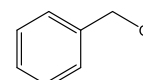
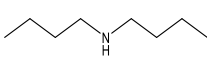
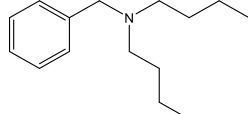
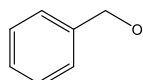
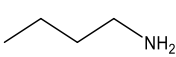
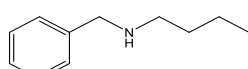
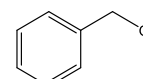
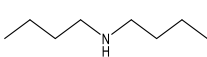
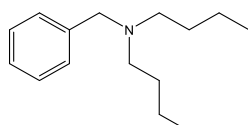

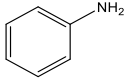
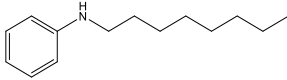
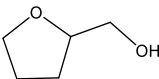
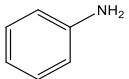
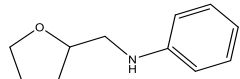
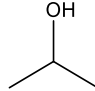
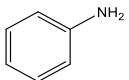
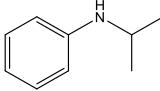

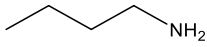

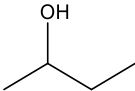
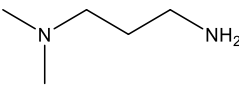
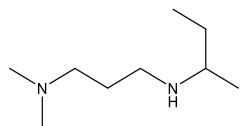
Figure 6.21 Reusability test of *N*-alkylation of benzyl alcohol with aniline using titanium hydroxide. Reaction conditions: alcohols (4.62 mmol), amines (21.5 mmol), xylene 2 g, catalyst 100 mg, reaction temperature 180 °C, 15 h, atmospheric N_2 .

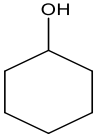
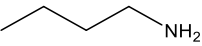
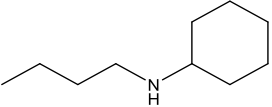
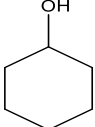
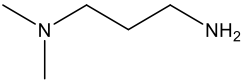
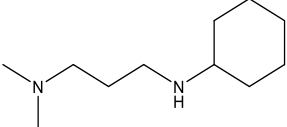
6.2.4 Substrate scope

The scope of the present titanium hydroxide system with regard to alkylation of various amines and alcohols was also examined. **Table 6.4** shows that the catalyst can be used for selective conversion with aniline of structurally diverse aromatic and biomass based alcohols to the secondary amines (entry 1-5). The *o*-methyl benzyl alcohol (entry 4) was less reactive, which could be due to the steric hindrance effect of the methyl group at the *o*-position [138]. Aniline derivatives bearing an electron-donating or electron-withdrawing group also reacted with benzyl alcohol to afford the corresponding secondary amines with the yields higher than 90 % (entry 6-9).

Table 6.4 Scope of alcohols and amines for amine synthesis^a

Entry	Alcohols	Amines	Products	Conv.%	Sele.%	Ethers (%)
1				99.4	100	0
2				99	100	0
3				97	98	0
^b 4				90	91	2
5				100	98	0
^b 6				99	95	0

7				99	97	0
8				100	99	0
9				100	99	0
^e10				78	62	30
^e11				69	40	54
^d12				93	96	3
^d13				91	92	4
^e14				65	76	21
^e15				62	68	24
^e16				74	70	25
^f17				55	64	31
^f18				60	61	34

f_{19}				67	66	29
f_{20}				64	71	26

^aReaction conditions: alcohols (4.62 mmol), amines (21.5 mmol), xylene 2 g, catalyst 100 mg, reaction temperature 180 °C, 15 h, atmospheric N₂; ^b24 h; ^c48 h; ^d48 h (alcohols 0.5 mmol, amines 2.3 mmol, xylene 2 g, catalyst 200 mg); ^e72 h; ^f96 h.

Aliphatic amines (butylamine and dibutylamine) can be also used for the synthesis of secondary and tertiary amines by reaction with benzyl alcohol, respectively (entry 10 and 11). However, the yield of the product in this case is lower than in the case of aromatic amines (<50 %) with significant contribution of ethers in the products due to the lower reactivity of aliphatic amine. The reaction conditions have been modified: the time of the test, amount of the catalyst were increased, while the loading of reagents were decreased (entry 12 and 13). Higher yield of the products comparable to the aromatic amines ($\approx 90\%$) was obtained.

Titanium hydroxide provides high selectivity at reasonable conversions for the reaction of octanol, tetrahydrofurfuryl alcohol and isopropanol with aniline (entry 14-16). There is still a significant contribution of ether but the yield of the target product can be easily improved by increase of the contact time as it has been demonstrated earlier (entry 12 and 13).

Titanium hydroxide also provides reasonable yield of secondary aliphatic amine through *N*-alkylation of aliphatic alcohols (primary and secondary) with aliphatic amines (entry 17-20). The main difference in comparison with aromatic alcohols and amines is higher contribution of ether in the case of aliphatic amines and alcohols (**Table 6.4**). Note that variation of the product yields with time of aliphatic amine remains consistent with the hypothesis about the role of ether as an intermediate of alcohol ammonolysis. Indeed, *N*-alkylation of isopropanol with aniline demonstrate continuous increase of the yield of the product and a volcano curve for the

di-isopropyl ether as a function of time (**Figure 6.22**). Thus, unique structure of titanium hydroxide provides efficient amination of aromatic and aliphatic alcohols by aromatic and aliphatic amines toward secondary and tertiary amines.

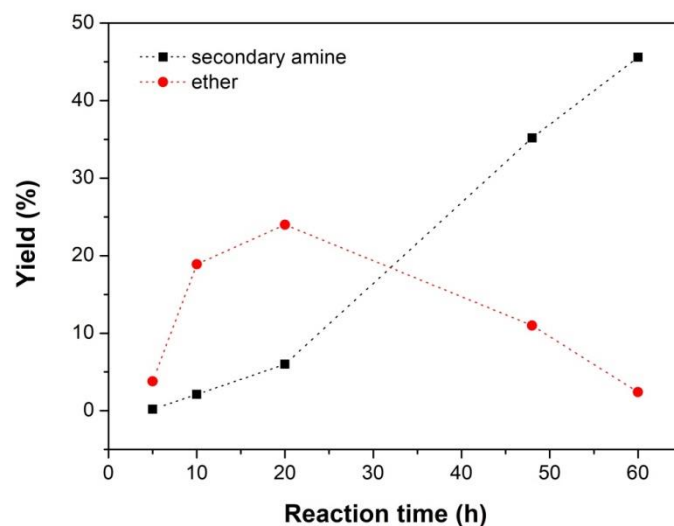


Figure 6.22 Reaction time dependence on secondary amine and ether yield for *N*-alkylation of isopropanol with aniline.

6.3 Conclusion

In summary, we have demonstrate that a non-noble metal solid titanium hydroxide acts as a stable, reusable and efficient heterogeneous catalyst for *N*-alkylation of amines with alcohols to secondary amines without hydrogen, bases or organic ligands promotion. The conversion and selectivity of titanium hydroxide were much higher than other hydroxides, metal oxides and zeolite due to the availability of mild intermediate Brønsted and Lewis acidities formed by rehydration-dehydration processes. The high yield for direct secondary amine synthesis can be attributed to the acidic catalytic intermolecular dehydration of alcohol to form corresponding ether followed by easier ether ammonolysis.

Chapter 7. General Conclusions and Perspectives

Amines are very important platform molecules for the chemical industry and life sciences. Various ways of amine synthesis are discussed in the literature review. Amination of alcohols seems to be the most sustainable approach to amine synthesis. Different homogeneous and heterogeneous based catalysts have been applied for selective amination of alcohols. The most challenging thing for alcohols amination is the selective synthesis of primary amines. As amination of alcohols is a consecutive reaction, disproportionation of the produced primary amine will easily happen through its self-coupling reaction to produce secondary or tertiary amines, reducing the selectivity to primary amines. Also, the alcohol dehydrogenation to aldehyde is a rate limiting step in the amination; this step requires high temperature to perform this reaction. Besides, metal leaching or poisoning problems often occur during liquid phase amination at high pH. Thus, in this thesis, several strategies in order to increase the selectivity to primary amines and to improve catalyst stability are evaluated. More specifically, we try to modify the supported cobalt catalyst by carbon deposition through different alcohol pretreatment procedures, addition of secondary metal and development of a highly stable heterogeneous based titanium hydroxide for selective amination of alcohols.

This thesis was performed at “Unité de Catalyse et de Chimie du Solide” (UCCS), Lille, France, and Solvay’s “Eco-Efficient Products and Processes Laboratory” (E2P2L), Shanghai, China.

7.1 General Conclusion

7.1.1 Modification of supported Co nanoparticles by poisons and promoters for selective amination of alcohols

Intentional introduction of poisons or promoters could modify the catalyst structure, which will influence the amination reactions. In the conclusion of this thesis, we would like to summarize different approaches which were used to enhance

the activity, selectivity and stability of cobalt catalysts in amination of alcohols. (Figure 7.1)

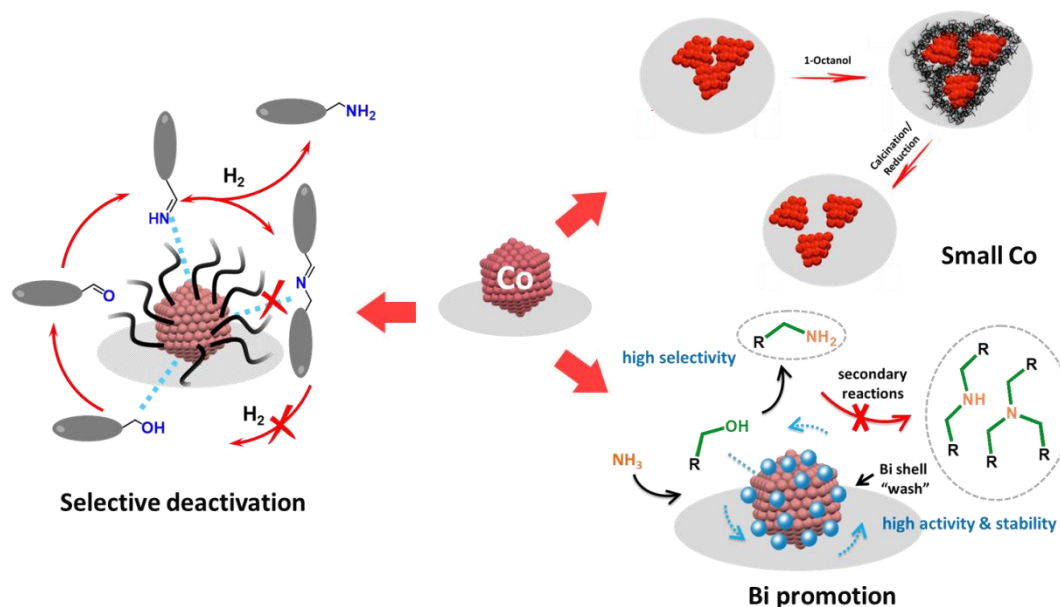


Figure 7.1 Modification of cobalt catalyst for selective amination of alcohols

1. Pre-treatment of cobalt catalysts with alcohols leads to a decrease in the rate of alcohol amination with ammonia, but coincides with considerable enhancement of the selectivity to primary amines. The enhancement of primary amine selectivity is particularly pronounced at higher alcohol conversions. Extensive characterizations have provided important information about the carbon species, which form, on the catalyst during their pre-treatment with alcohols. During the pre-treatment, alcohols are dehydrogenated over cobalt nanoparticles to aldehydes, which then polymerize via the aldol type condensation into unsaturated long chain hydrocarbon species. The increase in the selectivity to primary amines occurs because of slowing down primary amine self-coupling and in particular because of hindering of secondary imine hydrogenation. The effect is attributed to the steric constraints for hydrogenation of bulky secondary imines occurring over isolated cobalt domains in the cobalt nanoparticles with deposited carbon species. The polymeric carbon species deposited on the catalyst surface by the pretreatment with alcohols can be removed via catalyst exposure to hydrogen at high temperatures.

2. The pretreatment of cobalt and nickel catalysts with 1-octanol followed by

calcination results in another important phenomenon. When we tried to remove the surface carbons (formed through pretreatment of long chain alcohol 1-octanol) by calcination, highly dispersed and smaller cobalt and nickel nanoparticles were formed. The resulting catalysts exhibited enhanced activity of amination, hydrogenation and oxidation reactions.

3. In this thesis, we developed a novel bimetallic $\text{Co}_x\text{Bi}/\text{Al}_2\text{O}_3$ catalyst, which showed high activity, selectivity and stability for liquid phase amination of 1-octanol with ammonia. Different characterizations have provided detailed information about the chemical state and localization of metallic Bi on the surface of Co. After Bi promotion, the amination activity significantly increases. The Bi promotion facilitates alcohol hydrogenation, which is the rate limiting step in amination. The increase in the selectivity to 1-octylamine occurs after the Bi addition because of slowing down of 1-octylamine self-coupling caused by hindering of bulky secondary imine hydrogenation over isolated Co domains in Co nanoparticles with metallic Bi. Furthermore, the high stability of Bi promoted Co catalyst is attributed to less significant carbon deposition and protection of metallic Co from the re-oxidation to Co oxides,

7.1.2 Design of non-metal hydroxide for *N*-alkylation of alcohols with amines

We have demonstrated that a non-metal solid titanium hydroxide acts as a stable, reusable and efficient heterogeneous catalyst for selective *N*-alkylation of amines with alcohols to give desired secondary amines without hydrogen, bases or organic ligands. The conversion and selectivity for titanium hydroxide were much higher than other hydroxides, metal oxides and zeolites due to mild intermediate Brønsted acidity formed by rehydration process of condensed structure. The high yield for direct secondary amine synthesis can be attributed to the acidic catalytic intermolecular dehydration of alcohol to form corresponding ether followed by easier ether ammonolysis.

7.2 Perspectives

Controlling the primary amine selectivity by modifying the catalyst through alcohol pretreatment is a very useful way for selective amination of alcohol. Inspired by this strategy, in the future research, several work can be done in terms of catalyst modification or process optimizing:

- (1) Our result suggest that selective synthesis of primary amines is a sterically constraint reaction and requires small surface zone (domain) over cobalt nanoparticles. Selective poisoning of the metal catalyst surface by some gases, like CO, H₂S and SO₂ could improve the primary amine selectivity through creation of these small surface zones .
- (2) The addition of an ammonium salt (NH₄Cl, CH₃COONH₄, etc.) can also lead to improved yield of primary amines by protonating the primary amine to yield less nucleophilic alkylammonium ion.
- (3) For future industrial application, it is promising to separate the produced primary amine immediately during reaction to improve the selectivity.
- (4) Facilitate the alcohol dehydrogenation by addition of hydrogen scavenges to facilitate the whole amination process under low temperature.
- (5) The uncovered method of redispersion of cobalt in supported catalysts by consecutive pretreatment with alcohols and calcination can be extended to other metal catalysts and can be used for enhancement of catalytic performance in numerous catalytic reactions.

All in all, with the fast development of material science, more techniques can be elaborated to design more selective catalysts or explore new processes to enhance the primary amine selectivity in the alcohol amination.

8 References

- [1] *The American Heritage Dictionary of the English Language*. (5th edition, Houghton Mifflin Harcourt, Boston, USA, **2011**).
- [2] <https://en.wikipedia.org/wiki/Amine>.
- [3] Standen, A. *Kirk-Othmer Encyclopedia of Chemical Technology*. (2nd edition, Wiley, New York, **1963**, 116-138).
- [4] Lawrence, S. A. *Amines: Synthesis, Properties and Applications*. (Cambridge University Press, Cambridge, UK, **2004**).
- [5] Magano, J. & Dunetz, J. R. Large-scale applications of transition metal-catalyzed couplings for the synthesis of pharmaceuticals. *Chem. Rev.* **2011**, *111*, 2177-2250.
- [6] Froidevaux, V., Negrell, C., Caillol, S., Pascault, J.-P. & Boutevin, B. Biobased amines: from synthesis to polymers; present and future. *Chem. Rev.* **2016**, *116*, 14181-14224.
- [7] Nador, F., Moglie, Y., Ciolino, A., Pierini, A., Dorn, V., Yus, M., Alonso, F. & Radivoy, G. Direct reductive amination of aldehydes using lithium-arene (cat.) as reducing system. A simple one-pot procedure for the synthesis of secondary amines. *Tetrahedron Lett.* **2012**, *53*, 3156-3160.
- [8] Gallezot, P. Conversion of biomass to selected chemical products. *Chem. Soc. Rev.* **2012**, *41*, 1538-1558.
- [9] Alinezhad, H., Yavari, H. & Salehian, F. Recent advances in reductive amination catalysis and its applications. *Curr. Org. Chem.* **2015**, *19*, 1021-1049.
- [10] Vlught, J. I. Advances in selective activation and application of ammonia in homogeneous catalysis. *Chem. Soc. Rev.* **2010**, *39*, 2302-2322.
- [11] Fatty amines market: global industry analysis and opportunity assessment 2015-2020. *Future Market Insights* **2015**.
- [12] Hofmann, A. W. Beiträge zur Kenntniss der flüchtigen organischen Basen. *Justus Liebigs Ann. Chem.* **1851**, *78*, 253-286.
- [13] Xu, Q., Xie, H. M., Zhang, E.-L., Ma, X. T., Chen, J. H., Yu, X.-C. & Li, H. Selective catalytic Hofmann *N*-alkylation of poor nucleophilic amines and amides with catalytic amounts of alkyl halides. *Green Chem.* **2016**, *18*, 3940-3944.
- [14] Magano, J. & Dunetz, J. R. Large-scale applications of transition metal -catalyzed couplings for the synthesis of pharmaceuticals. *Chem. Rev.* **2011**, *111*, 2177-2250.
- [15] Aubin, Y., Fischmeister, C., Thomas, C. M. & Renaud, J. L. Direct amination of aryl halides with ammonia. *Chem. Soc. Rev.* **2010**, *39*, 4130-4145.
- [16] Kienle, M. S., Dubbaka, R., Brade, K. & Knochel, P. Modern amination reactions. *Eur. J. Org. Chem.* **2007**, *2007*, 4166-4176.

- [17] Buchwald, S. L., Mauger, C., Mignani, G. & Scholz, U. Industrial-scale palladium-catalyzed coupling of aryl halides and amines—a personal account. *Adv. Synth. Catal.* **2006**, *348*, 23-39.
- [18] Navarro, O., Marion, N., Mei, J. & Nolan, S. P. Rapid room temperature Buchwald-Hartwig and Suzuki-Miyaura couplings of heteroaromatic compounds employing low catalyst loadings. *Chem. Eur. J.* **2006**, *12*, 5142-5148.
- [19] Sperotto, E. G., Klink, P. M., Koten, G. & Vries, J. G. The mechanism of the modified Ullmann reaction. *Dalton Trans.* **2010**, *39*, 10338-10351.
- [20] Monnier, F. & Taillefer, M. Catalytic C-C, C-N, and C-O Ullmann-type coupling reactions: copper makes a difference. *Angew. Chem. Int. Ed.* **2008**, *47*, 3096-3099.
- [21] Jiang, D., Fu, H., Jiang, Y. & Zhao, Y. CuBr/*rac*-BINOL-catalyzed *N*-Arylations of aliphatic amines at room temperature. *J. Org. Chem.* **2007**, *72*, 672-674.
- [22] Yadav, J. S., Antony, A., Rao, T. S. & Reddy, B. V. S. Recent progress in transition metal catalyzed hydrofunctionalisation of less activated olefins. *J. Organomet. Chem.* **2011**, *696*, 16-36.
- [23] Reguillo, R., Grellier, M., Vautravers, N., Vendier, L. & Sabo-Etienne, S. Ruthenium-catalyzed hydrogenation of nitriles: insights into the mechanism. *J. Am. Chem. Soc.* **2010**, *132*, 7854-7855.
- [24] Natte, K., Neumann, H., Jagadeesh, R. V. & Beller, M. Convenient iron-catalyzed reductive aminations without hydrogen for selective synthesis of *N*-methyamines. *Nat. Commun.* **2017**, *8*, 1-9.
- [25] Mignonac, G. New general method for preparation of amines from aldehydes or ketones. *Compt. Rend.* **1921**, *172*, 223.
- [26] Gross, T., Seayad, A. M., Ahmad, M. & Beller, M. Synthesis of primary amines: first homogeneously catalyzed reductive amination with ammonia. *Org. Lett.* **2002**, *4*, 2055-2058.
- [27] Enthaler, S. Practical one-pot synthesis of secondary amines by zinc-catalyzed reductive amination. *Catal. Lett.* **2011**, *141*, 55-61.
- [28] Werkmeister, S., Junge, K. & Beller, M. Copper-catalyzed reductive amination of aromatic and aliphatic ketones with anilines using environmental-friendly molecular hydrogen. *Green Chem.* **2012**, *14*, 2371-2374.
- [29] Qi, F. Q., Hu, L., Lu, S. L., Cao, X. Q. & Gu, H. W. Selective synthesis of secondary amines by Pt nanowire catalyzed reductive amination of aldehydes and ketones with ammonia. *Chem. Commun.* **2012**, *48*, 9631-9633.
- [30] Nakamura, Y., Kon, K., Touchy, A. S., Shimizu, K.-I. & Ueda, W. Selective synthesis of primary amines by reductive amination of ketones with ammonia over supported Pt catalysts, *ChemCatChem* **2015**, *7*, 921-924.

- [31] Bódis, J., Lefferts, L., Müller, T. E., Pestman, R. & Lercher, J. A. Activity and selectivity control in reductive amination of butyraldehyde over noble metal catalysts. *Catal. Lett.* **2005**, *104*, 23-28.
- [32] Liang, G. F., Wang, A. Q., Li, L., Xu, G., Yan, N. & Zhang, T. Production of primary amines by reductive amination of biomass-derived aldehydes/ketones. *Angew. Chem. Int. Ed.* **2017**, *56*, 3050-3054.
- [33] Merger, F., Otterbach, A., Witzel, T. & Renz, H. 2,2-dialkylpentane 1,5-diisocyanates, 2,2-dialkylpentane 1,5-diurethanes and 2,2-dialkylpentane 1,5-dicarbamoyl chlorides, and their preparation and use. *U.S. Patent* 5554,787 A1, 1996.
- [34] Tamura, M., Shimizu, K.-I. & Satsuma, A. Comprehensive Ir study on acid/base properties of metal oxides. *Appl. Catal. A* **2012**, *433*, 135-145.
- [35] Dong, B., Guo, X. C., Zhang, B., Chen, X. F., Guan, J., Qi, Y. F., Han, S. & Mu, X. D. Heterogeneous Ru-based catalysts for one-pot synthesis of primary amines from aldehydes and ammonia. *Catalysts* **2015**, *5*, 2258-2270.
- [36] Komanoya, T., Kinemura, T., Kita, Y., Kamata, K. & Hara, M. Electronic effect of ruthenium nanoparticles on efficient reductive amination of carbonyl compounds. *J. Am. Chem. Soc.* **2017**, *139*, 11493-11499.
- [37] Patil, N. M. & Bhanage, B. M. Fe@Pd/C: an efficient magnetically separable catalyst for direct reductive amination of carbonyl compounds using environment friendly molecular hydrogen in aqueous reaction medium. *Cataly. Today* **2015**, *247*, 182-189.
- [38] Zhu, C. & Akiyama, T. Brønsted acid catalyzed reductive amination with benzothiazoline as a highly efficient hydrogen donor. *Synlett.* **2011**, *9*, 1251-1254.
- [39] Reguillo, R., Grellier, M., Vautravers, N., Vendier, L. & Sabo-Etienne, S. Ruthenium-catalyzed hydrogenation of nitriles: insights into the mechanism. *J. Am. Chem. Soc.* **2010**, *132*, 7854-7855.
- [40] Carothers, W. H. & Jones, G. A. The preparation of some primary amines by the catalytic reduction of nitriles. *J. Am. Chem. Soc.* **1925**, *47*, 3051-3057.
- [41] Gomez, S., Peters, J. A. & Maschmeyer, T. The reductive amination of aldehydes and ketones and the hydrogenation of nitriles: mechanistic aspects and selectivity control. *Adv. Synth. Catal.* **2002**, *344*, 1037-1057.
- [42] Bagal, D. B. & Bhanage, B. M. Recent advances in transition metal-catalyzed hydrogenation of nitriles. *Adv. Synth. Catal.* **2015**, *357*, 883-900.
- [43] Barrault, J., Seffen, M., Forquy, C. & Brouard, R. *Heterogeneous Catalysis and Fine Chemicals*, Guisnet, M., Barrault, J., Bouchoule, C., Duprez, D., Montassier, C. & Perot, G. (Editors) *Studies in Surface Science and Catalysis*, Elsevier, Amsterdam, **1988**.

- [44] Barrault, J. & Pouilloux, Y. Synthesis of fatty amines. Selectivity control in presence of multifunctional catalysts. *Catal. Today* **1997**, *37*, 137-153.
- [45] Tillack, A., Trauthwein, H., Hartung, C. G., Eichberger, M., Pitter, S., Jansen, A. & Beller, M. Rhodium-catalyzed amination of aromatic olefins. *Monatsh. Chem.* **2000**, *131*, 1327-1334.
- [46] Beller, M., Thiel, O. R., Trauthwein, H. & Hartung, C. G. Amination of aromatic olefins with anilines: a new domino synthesis of quinolines. *Chem. Eur. J.* **2000**, *6*, 2513-2522.
- [47] Beller, M. & Breindl, C. Base-catalyzed amination of olefins: an example of an environmentally friendly synthesis of amines. *Chemosphere* **2001**, *43*, 21-26.
- [48] Fleischer, S., Werkmeister, S., Zhou, S. L., Junge, K. & Beller, M. Consecutive intermolecular reductive hydroamination: cooperative transition-metal and chiral Brønsted acid catalysis. *Chem. Eur. J.* **2012**, *18*, 9005-9010.
- [49] Pirnot, M. T., Wang, Y.-M. & Buchwald, S. L. Copper hydride catalyzed hydroamination of alkenes and alkynes. *Angew. Chem. Int. Ed.* **2016**, *55*, 48-57.
- [50] Deeba, M., Ford, M. E. & Johnson, T. A. Direct amination of ethylene by zeolite catalysis. *J. Chem. Soc., Chem. Commun.* **1987**, *8*, 562-563.
- [51] Lequitte, M., Figueras, F., Moreau, C. & Hub, S. Amination of butenes over protonic zeolites. *J. Catal.* **1996**, *163*, 255-261.
- [52] Hölderich, W. F. & Heitmann, G. Synthesis of intermediate and fine chemicals on heterogeneous catalysts with respect to environmental protection. *Catal. Today* **1997**, *38*, 227-233.
- [53] Tillack, A., Castro, I. G., Hartung, C. G. & Beller, M. Anti-markovnikov hydroamination of terminal alkynes. *Angew. Chem. Int. Ed.* **2002**, *41*, 2541-2543.
- [54] Ho, C. R., Bettinson, L. A., Choi, J., Head-Gordon, M. & Bell, A. T. Zeolite-catalyzed isobutene amination: mechanism and kinetics. *ACS Catal.* **2019**, *9*, 7012-7022.
- [55] Guram, A. S., Rennels, R. A. & Buchwald, S. L. A simple catalytic method for the conversion of aryl bromides to arylamines. *Angew. Chem. Int. Ed.* **1995**, *34*, 1348-1350.
- [56] Louie, J. & Hartwig, J. F. Palladium-catalyzed synthesis of arylamines from aryl halides. Mechanistic studies lead to coupling in the absence of tin reagents. *Tetrahedron Lett.* **1995**, *36*, 3609-3612.
- [57] Hartwig, J. F. Palladium-catalyzed amination of aryl halides: mechanism and rational catalyst design. *Synlett.* **1997**, *4*, 329-340.
- [58] Shen, Q. L. & Hartwig, J. F. Palladium-catalyzed coupling of ammonia and lithium amide with aryl halides. *J. Am. Chem. Soc.* **2006**, *128*, 10028-10029.

- [59] Djakovitch, L., Wagner, M. & Köhler, K. Amination of aryl bromides catalysed by supported palladium. *J. Organomet. Chem.* **1999**, *592*, 225-234.
- [60] Weigert, F. J. & Del Pesco, T. W. Substitutive aromatization. *J. Catal.* **1981**, *68*, 218-219.
- [61] Corma, A., Iborra, S. & Velty, A. Chemical routes for the transformation of biomass into chemicals. *Chem. Rev.* **2007**, *107*, 2411-2502.
- [62] Cui, X. J., Junge, K. & Beller, M. Palladium-catalyzed synthesis of alkylated amines from aryl ethers or phenols. *ACS Catal.* **2016**, *6*, 7834-7838.
- [63] Li, J. & Wang, Z.-X. Nickel-catalyzed amination of aryl 2-pyridyl ethers via cleavage of the carbon-oxygen bond. *Org. Lett.* **2017**, *19*, 3723-3726.
- [64] Vedage, G. A., Herman, R. G. & Klier, K. *Catalysis of Organic Reactions*. Rylander, P. N., Greenfield, H. & Augustine, R. L. (Editors) Dekker, New York, **1988**, Chapter 9.
- [65] Vedage, G. A., Herman, R. G. & Klier, K. Chemical trapping of surface intermediates in methanol synthesis by amines. *J. Catal.* **1985**, *95*, 423-434.
- [66] Straathof, A. J. J. Transformation of biomass into commodity chemicals using enzymes or cells. *Chem. Rev.* **2014**, *114*, 1871-1908.
- [67] Imm, S., Böhn, S., Neubert, L., Neumann, H. & Beller, M. An efficient and general synthesis of primary amines by ruthenium-catalyzed amination of secondary alcohols with ammonia. *Angew. Chem. Int. Ed.* **2010**, *49*, 8126-8129.
- [68] Böhn, S., Imm, S., Neubert, L., Zhang, M., Neumann, H. & Beller, M. The catalytic amination of alcohols. *ChemCatChem* **2011**, *3*, 185-1864.
- [69] Guillena, G., Ramón, D. J. & Yus, M. Hydrogen autotransfer in the *N*-alkylation of amines and related compounds using alcohols and amines as electrophiles. *Chem. Rev.* **2010**, *110*, 1611-1641.
- [70] Gunanathan, C. & Milstein, D. Applications of acceptorless dehydrogenation and related transformations in chemical synthesis. *Science* **2013**, *341*, 1229712.
- [71] Shimizu, K.-I., Kon, K., Onodera, W., Yamazaki, H. & Kondo, J. N. Heterogeneous Ni catalyst for direct synthesis of primary amines from alcohols and ammonia. *ACS Catal.* **2013**, *3*, 112-117.
- [72] Dang, T. T., Ramalingam, B., Shan, S. P. & Seayad, A. M. An efficient palladium-catalyzed *N*-alkylation of amines using primary and secondary alcohols. *ACS Catal.* **2013**, *3*, 2536-2540.
- [73] Baiker, A. & Richarz, W. Activity, Selectivity, decay and long-term behaviour of amination catalysts. *Helv. Chim. Acta* **1978**, *61*, 1169-1174.
- [74] Baiker, A. & Richarz, W. Synthesis of long chain aliphatic amines from the corresponding alcohols. *Tetrahedron Lett.* **1977**, *22*, 1937-1938.

- [75] Baiker, A. & Richarz, W. Catalytic amination of long chain aliphatic alcohols. *Ind. Eng. Chem. Prod. Res. Dev.* **1977**, *16*, 261-266.
- [76] Pandya, R., Mane, R. & Rode, C. V. Cascade dehydrative amination of glycerol to oxazoline, *Catal. Sci. Technol.* **2018**, *8*, 2954-2965.
- [77] Corbin, D. R., Schwarz, S. & Sonnichsen, G. C. Methylamines synthesis: a review. *Catal. Today* **1997**, *37*, 71-102.
- [78] Turner, W. D. & Howald, A. M. Methyl amines from methyl alcohol and ammonium chloride. *J. Am. Chem. Soc.* **1920**, *42*, 2663-2665.
- [79] Baiker, A. & Kijenski, J. Catalytic synthesis of higher aliphatic amines from the corresponding alcohols. *Catal. Rev. Sci. Eng.* **1985**, *27*, 653-697.
- [80] Schwegler, E. D. & Adkins, H. Preparation of certain amines. *J. Am. Chem. Soc.* **1939**, *61*, 3499-3502.
- [81] Baiker, A. & Richarz, W. Some aspects of catalytic amination of fatty alcohols. *Proc. 5th Can., Symp. Catal., Chem. Inst. Can.* **1977**, 289-300.
- [82] Baiker, A. Catalytic amination of aliphatic alcohols. The role of hydrogen as inhibitor for catalyst deactivation. *Ind. Eng. Chem. Prod. Res. Dev.* **1981**, *20*, 615-618.
- [83] Baiker, A., & Monti, D. Interaction of ammonia with metallic copper, nickel and cobalt studied by temperature programmed desorption. *Ber. Bunsenges. Phys. Chem.* **1983**, *87*, 602-605.
- [84] Baiker, A., Caprez, W. & Holstein, W. L. Catalytic amination of aliphatic alcohols in the gas and liquid phases. kinetics and reaction pathway. *Ind. Eng. Chem. Prod. Res. Dev.* **1983**, *22*, 217-225.
- [85] Baiker, A., Monti, D. & Fan, Y. S. Deactivation of copper, nickel, and cobalt catalysts by interaction with aliphatic amines. *J. Catal.* **1984**, *88*, 81-88.
- [86] Baiker, A. & Kijenski, J. Catalytic synthesis of higher aliphatic amines from the corresponding alcohols. *Catal. Rev. Sci. Eng.* **1985**, *27*, 653-697.
- [87] Sewell, G., O'Connor, C. Steen, E. Reductive amination of ethanol with silica supported cobalt and nickel catalysts. *Appl. Catal. A* **1995**, *125*, 99-112.
- [88] S. Winderl, E. Haarer, H. Corr, P. Hornberger, US Patent 3 270 059 (**1966**).
- [89] Hammerschmidt, W., Baiker, A., Wokaun, A. & Fluhr, W. Copper catalyzed synthesis of cyclic amines from amino-alcohols. *Appl. Catal.* **1986**, *20*, 305-312.
- [90] Chang, C. D. & Perkins, P. D. 2-methylpyridine from benzamine. a novel rearrangement catalysed by zeolite. *Zeolites* **1983**, *3*, 298-299.
- [91] Hollmann, D., Böhn, S., Tillack, A. & Beller, M. A general ruthenium-catalyzed synthesis of aromatic amines. *Angew. Chem. Int. Ed.* **2007**, *46*, 8291-8294.

- [92] Saidi, O., Blacker, A. J., Farah, M. M., Marsden, S. P. & Williams, J. M. J. Selective amine cross-coupling using iridium-catalyzed “borrowing hydrogen” methodology. *Angew. Chem. Int. Ed.* **2009**, *48*, 7375-7378.
- [93] Kim, I., Itagaki, S., Jin, X. J., Yamaguchi, K. & Mizuno, N. Heterogeneously catalyzed self-condensation of primary amines to secondary amines by supported copper catalysts. *Catal. Sci. Technol.* **2013**, *3*, 2397-2403.
- [94] Wang, L.-M., Kobayashi, K., Arisawa, M., Saito, S. & Naka, H. Pd/TiO₂-photocatalyzed self-condensation of primary amines to afford secondary amines at ambient temperature. *Org. Lett.* **2019**, *21*, 341-344.
- [95] Fu, W. Q., Shen, R. S., Bai, E. H., Zhang, L., Chen, Q., Fang, Z. X., Li, G. C., Yi, X. F., Zheng, A. M. & Tang, T. D. Reaction route and mechanism of the direct *N*-alkylation of sulfonamides on acidic mesoporous zeolite β -catalyst. *ACS Catal.* **2018**, *8*, 9043-9055.
- [96] Sabatier, P. & Mailhe, A. *Compt. Rend.* **1909**, *148*, 898.
- [97] Baum, G. Über der Katalytische Alkylierung von Ammoniak. Zürich, **1945**.
- [98] Popov, M. A. Candidate's Thesis, Institute of General Chemistry of the USSR Academy of Sciences, Moscow, **1952**.
- [99] Kliger, G. A., Lazutina, L. F., Kryukov, Y. B., Fridman, R. A., Bashkurov, A. N. & Snagovskii, Y. S. *Neftekhimiya* **1975**, *16*, 665.
- [100] Miyamoto, A. & Ogino, Y. Studies on the catalysis by the molten metal: VIII. Kinetic isotope effects measured by using a pulse reaction technique. *J. Catal.* **1975**, *37*, 133-141.
- [101] Hamid, M. H. S. A., Slatford, P. A. & Williams, J. M. J. Borrowing Hydrogen in the activation of alcohols. *Adv. Synth. Catal.* **2007**, *349*, 1555-1575.
- [102] Winans, C. F. & Adkins, H. The alkylation of amines as catalyzed by nickel. *J. Am. Chem. Soc.* **1932**, *54*, 306-312.
- [103] Roundhill, D. M. Transition metal and enzyme catalyzed reactions involving reactions with ammonia and amines. *Chem. Rev.* **1992**, *92*, 1-27.
- [104] Tsuji, Y., Takeuchi, R., Ogawa, H. & Watanabe, Y. Platinum complex catalyzed transformation of amine. *N*-alkylation and *N*-allylation using primary alcohols. *Chem. Lett.* **1986**, *15*, 293-294.
- [105] Dobereiner, G. E. & Crabtree, R. H. Dehydrogenation as a substrate-activating strategy in homogeneous transition-metal catalysis. *Chem. Rev.* **2010**, *110*, 681-703.
- [106] Nixon, T. D., Whittlesey, M. K. & Williams, J. M. J. Transition metal catalysed reactions of alcohols using borrowing hydrogen methodology. *Dalton Trans.* **2009**, 753-762.

- [107] Zhang, Y., Lim, C.-S., Sim, D. S. B., Pan, H.-J. & Zhao, Y. Catalytic enantioselective amination of alcohols by the use of borrowing hydrogen methodology: cooperative catalysis by iridium and a chiral phosphoric acid. *Angew. Chem. Int. Ed.* **2014**, *53*, 1399-1403.
- [108] Yamaguchi, K., He, J. L., Oishi, T. & Mizuno, N. The “Borrowing Hydrogen Strategy” by supported ruthenium hydroxide catalysts: synthetic scope of symmetrically and unsymmetrically substituted amines. *Chem. Eur. J.* **2010**, *16*, 7199-7207.
- [109] Corma, A., Navas, J. & Sabater, M. J. Advances in one-pot synthesis through borrowing hydrogen catalysis. *Chem. Rev.* **2018**, *118*, 1410-1459.
- [110] Marichev, K. O. & Takacs, J. M. Ruthenium-catalyzed amination of secondary alcohols using borrowing hydrogen methodology. *ACS Catal.* **2016**, *6*, 2205-2210.
- [111] Guillena, G., Ramón, D. J. & Yus, M. Alcohols as electrophiles in C-C bond-forming reactions: the hydrogen autotransfer process. *Angew. Chem. Int. Ed.* **2007**, *46*, 2358-2364.
- [112] Xiao, M., Yue, X., Xu, R. R., Tang, W. J., Xue, D., Li, C. Q., Lei, M., Xiao, J. L. & Wang, C. Transition-metal-free hydrogen autotransfer: diastereoselective *N*-alkylation of amines with racemic alcohols. *Angew. Chem. Int. Ed.* **2019**, *58*, 10528-10536.
- [113] Martínez, R., Ramón, D. J. & Yus, M. Selective *N*-monoalkylation of aromatic amines with benzylic alcohols by a hydrogen autotransfer process catalyzed by unmodified magnetite. *Org. Biomol. Chem.* **2009**, *7*, 2176-2181.
- [114] Peñá-López, M., Piehl, P., Elangovan, S., Neumann, H. & Beller, M. Manganese-catalyzed hydrogen-autotransfer C-C bond formation: α -alkylation of ketones with primary alcohols. *Angew. Chem. Int. Ed.* **2016**, *55*, 14967-14971.
- [115] Himmelblau, D. M. *Process Analysis by Statistical Methods* Wiley, New York, **1970**, p. 194.
- [116] Baiker, A. The role of hydrogen in the catalytic amination of alcohols and the disproportionation of amines. *Stud. Surf. Sci. Catal.* **1988**, *41*, 283-290.
- [117] Rausch, A. K., Steen, E. & Roessner, F. New aspects for heterogeneous cobalt-catalyzed hydroamination of ethanol. *J. Catal.* **2008**, *253*, 111-118.
- [118] Anderson, J. R. & Clark, N. J. Reactions of aliphatic amines over evaporated metal films. *J. Catal.* **1966**, *5*, 250-263.
- [119] Braun, J., Blessing, G. & Zobel, F. *Berichte* **1923**, *3*, 1988.
- [120] Volf, J., Pasek, J. & Duraj, M. Disproportionation of diethylamine in the presence of cobalt and copper. *Collect. Czech. Chem. Commun.* **1973**, *38*, 1038-1048.

- [121] Card, R. J. & Schmitt, J. L. Gas-phase synthesis of nitriles. *J. Org. Chem.* **1981**, *46*, 754-757.
- [122] Pinggen, D., Lutz, M. & Vogt, D. Mechanistic study on the ruthenium catalyzed direct amination of alcohols. *Organometallics* **2014**, *33*, 1623-1629.
- [123] Gunanathan, C. & Milstein, D. Selective synthesis of primary amines directly from alcohols and ammonia. *Angew. Chem. Int. Ed.* **2008**, *47*, 8661-8664.
- [124] Wu, Z. S., Laffoon, D. & Hull, K. L. Asymmetric synthesis of γ -branched amines via rhodium-catalyzed reductive amination. *Nat. Commun.* **2018**, *9*, 1185.
- [125] Blank, B., Madalska, M. & Kempe, R. An efficient method for the selective iridium-catalyzed monoalkylation of (hetero)aromatic amines with primary alcohols. *Adv. Synth. Catal.* **2008**, *350*, 749-758.
- [126] Kawahara, R., Fujita, K.-I. & Yamaguchi, R. Multialkylation of aqueous ammonia with alcohols catalyzed by water-soluble Cp*Ir-ammine complexes. *J. Am. Chem. Soc.* **2010**, *132*, 15108-15111.
- [127] Pan, H.-J., Ng, T. W. & Zhao, Y. Iron-catalyzed amination of alcohols assisted by Lewis acid. *Chem. Commun.* **2015**, *51*, 11907-11910.
- [128] Yan, T., Feringa, B. L., & Barta, K. Benzylamines via iron-catalyzed direct amination of benzyl alcohols. *ACS Catal.* **2016**, *6*, 381-388.
- [129] Cui, X. J., Shi, F., Zhang, Y. & Deng, Y. Q. Fe(II)-catalyzed *N*-alkylation of sulfonamides with benzylic alcohols. *Tetrahedron Lett.* **2010**, *51*, 2048-2051.
- [130] Zhao, Y. S., Foo, S. W. & Saito, S. Iron/amino acid catalyzed direct *N*-alkylation of amines with alcohols. *Angew. Chem. Int. Ed.* **2011**, *50*, 3006-3009.
- [131] Yan, T., Feringa, B. L. & Barta, K. Iron catalysed direct alkylation of amines with alcohols. *Nat. Commun.* **2014**, *5*, 5602.
- [132] Elangovan, S., Neumann, J., Sortais, J.-B., Junge, K., Darcel, C. & Beller, M. Efficient and selective *N*-alkylation of amines with alcohols catalyzed by manganese pincer complexes. *Nat. Commun.* **2016**, *7*, 12641.
- [133] Payard, P.-A., Gu, Q. Y., Guo, W. P., Wang, Q. R., Corbet, M., Michel, C., Sautet, P., Grimaud, L., Wischert, R. & Pera-Titus, M. Direct amination of alcohols catalyzed by aluminum triflate: an experimental and computational study. *Chem. Eur. J.* **2018**, *24*, 14146-14153.
- [134] Liang, G. F., Zhou, Y. G., Zhao, J. P., Khodakov, A. Y. & Ordonsky, V. V. Structure-sensitive and insensitive reactions in alcohol amination over nonsupported Ru nanoparticles. *ACS Catal.* **2018**, *8*, 11226-11234.
- [135] Ruiz, D., Aho, A., Saloranta, Eränen, K., Wärnå J., Leino, R. & Murzin, D. Y. Direct amination of dodecanol with NH₃ over heterogeneous catalysts. Catalyst screening and kinetic modelling. *Chem. Eng. J.* **2017**, *307*, 739-749.

- [136] Ousmane, M., Perrussel, G., Yan, Z., Clacens, J. M., Campo, F. & Pera-Titus, M. Highly selective direct amination of primary alcohols over a Pd/K-OMS-2 catalyst. *J. Catal.* **2014**, *309*, 439-452.
- [137] Ho, C. R., Defalque, V., Zheng, S. & Bell, A. T. Propanol amination over supported nickel catalysts: reaction mechanism and role of the support. *ACS Catal.* **2019**, *9*, 2931-2939.
- [138] Wu, Y. J., Huuqang, Y. J., Dai, X. C. & Shi, F. Alcohol amination catalyzed by copper powder as a self-supported catalyst. *ChemSusChem* **2019**, *12*, 3185-3191.
- [139] Leung, A. Y. K., Hellgardt, K. & Hii, K. K. Catalysis in flow: nickel-catalyzed synthesis of primary amines from alcohols and NH₃. *ACS Sustainable Chem. Eng.* **2018**, *6*, 5479-5484.
- [140] Demidova, Y. S., Simakova, I. L., Estrada, M., Beloshapkin, S., Suslov, E. V., Korchagina, D. V., Volcho, K. P., Salakhutdinov, N. F., Simakov, A. V. & Murzin, D. Y. One-pot myrtenol amination over Au nanoparticles supported on different metal oxides. *Appl. Catal. A* **2013**, *464-465*, 348-356.
- [141] Corma, A., Ródenas, T. & Sabater, M. J. A bifunctional Pd/MgO solid catalyst for the one-pot selective *N*-monoalkylation of amines with alcohols. *Chem. Eur. J.* **2010**, *16*, 254-260.
- [142] Fischer, A., Maciejewski, M., Bürgi, T., Mallat, T. & Baiker, A. Cobalt-catalyzed amination of 1,3-propanediol: effects of catalyst promotion and use of supercritical ammonia as solvent and reactant. *J. Catal.* **1999**, *183*, 373-383.
- [143] Takanashi, T., Nakagawa, Y. & Tomishige, K. Amination of alcohols with ammonia in water over Rh-In catalyst. *Chem. Lett.* **2014**, *43*, 822-824.
- [144] Sankar, M., He, Q., Dawson, S., Nowicka, E., Lu, L., Bruijninx, P. C. A., Beale, A. M., Kiely, C. J. & Weckhuysen, B. M. Supported bimetallic nano-alloys as highly active catalysts for the one-pot tandem synthesis of imines and secondary amines from nitrobenzene and alcohols. *Catal. Sci. Technol.* **2016**, *6*, 5473-5482.
- [145] Ball, M. R., Wesley, T. S., Rivera-Dones, K. R., Huber, G. W. & Dumesic, J. A. Amination of 1-hexanol on bimetallic AuPd/TiO₂ catalysts. *Green Chem.* **2018**, *20*, 4695-4709.
- [146] Adamska, K., Okal, J. & Tylus, W. Stable bimetallic Ru-Mo/Al₂O₃ catalysts for the light alkane combustion: effect of the Mo addition. *Appl. Catal. B* **2019**, *246*, 180-194.
- [147] Chung, H., Han, S., Chung, Y. K. & Park, J. H. Conversion of primary amines to symmetrical secondary and tertiary amines using a Co-Rh heterobimetallic nanocatalyst. *Adv. Synth. Catal.* **2018**, *360*, 1267-1272.
- [148] Tlustý, T., Pasek, J. & Vonka, P. Gas phase amination of 1-octanol over a Cu-Cr catalyst. *React. Kinet. Catal. Lett.* **2006**, *88*, 371-379.

- [149] Kim, J. W., Yamaguchi, K. & Mizuno, N. Heterogeneously catalyzed selective *N*-alkylation of aromatic and heteroaromatic amines with alcohols by a supported ruthenium hydroxide. *J. Catal.* **2009**, *263*, 205-208.
- [150] He, J. L., Yamaguchi, K. & Mizuno, N. Selective synthesis of secondary amines via *N*-alkylation of primary amines and ammonia with alcohols by supported copper hydroxide catalysts. *Chem. Lett.* **2010**, *39*, 1182-1183.
- [151] Veefkind, V. A. & Lercher, J. A. Zeolite catalysts for the selective synthesis of mono- and diethylamines. *J. Catal.* **1998**, *180*, 258-269.
- [152] Veefkind, V. A. & Lercher, J. A. On the elementary steps of acid zeolite catalyzed amination of light alcohols. *Appl. Catal. A* **1999**, *181*, 245-255.
- [153] Gonzalez-Arellano, C., Yoshida, K., Luque, R. & Gaib, P. L. Highly active and selective supported iron oxide nanoparticles in microwave-assisted *N*-alkylations of amines with alcohols. *Green Chem.* **2010**, *12*, 1281-1287.
- [154] Peeters, A., Claes, L., Geukens, I., Stassen, I. & Vos, D. D. Alcohol amination with heterogeneous ruthenium hydroxyapatite catalysts. *Appl. Catal. A* **2014**, *469*, 191-197.
- [155] Ono, Y. & Ishida, H. Amination of phenols with ammonia over palladium supported on alumina. *J. Catal.* **1981**, *72*, 121-128.
- [156] Zhang, Y. Qi, X. J., Cui, X. J., Shi, F. & Deng, Y. Q. Palladium catalyzed *N*-alkylation of amines with alcohols. *Tetrahedron Lett.* **2011**, *52*, 1334-1338.
- [157] Ishida, T., Takamura, R., Takei, T., Akita, T. & Haruta, M. Support effects of metal oxides on gold-catalyzed one-pot *N*-alkylation of amine with alcohol. *Applied Catalysis A* **2012**, *413-414*, 261-266.
- [158] Shimizu, K.-I., Kanno, S., Kon, K., Siddiki, S. M. A. H., Tanaka, H. & Sakata, Y. *N*-alkylation of ammonia and amines with alcohols catalyzed by Ni-loaded CaSiO₃. *Catal. Today* **2014**, *232*, 134-138.
- [159] Li, S. Z., Wen, M., Chen, H., Ni, Z. L., Xu, J. & Shen, J. Y. Amination of isopropanol to isopropylamine over a highly basic and active Ni/LaAlSiO catalyst. *J. Catal.* **2017**, *350*, 141-148.
- [160] Sewell, G., O'Connor, C. Steen, E. Effect of activation procedure and support on the reductive amination of ethanol using supported cobalt catalysts. *J. Catal.* **1997**, *167*, 513-521.
- [161] Cho, J. H., Park, J. H., Chang, T.-S., Seo, G. & Shin, C.-H. Reductive amination of 2-propanol to monoisopropylamine over Co/ γ -Al₂O₃ catalysts. *Appl. Catal. A* **2012**, *417-418*, 313-319.
- [162] He, W., Wang, L. D., Sun, C. L., Wu, K. K., He, S. B., Chen, J. P., Wu, P. & Yu, Z. K. Pt-Sn/ γ -Al₂O₃-catalyzed highly efficient direct synthesis of secondary and tertiary amines and imines. *Chem. Eur. J.* **2011**, *17*, 13308-13317.

- [163] Baiker, A. & Richan, W. Activity, Selectivity, decay and long-term behaviour of amination catalysts. *Helvetica Chimica Acta* **1978**, *61*, Nr. 112.
- [164] Sun, J., Jin, X. D., Zhang, F. W., Hu, W. Q., Liu, J. T. & Li, R. Ni-Cu/ γ -Al₂O₃ catalyzed *N*-alkylation of amines with alcohols. *Catal. Commun.* **2012**, *24*, 30-33.
- [165] Li, Y. L., Li, Q. X., Zhi, L. F. & Zhang, M. H. Catalytic amination of octanol for synthesis of trioctylamine and catalyst characterization. *Catal. Lett.* **2011**, *141*, 1635-1642.
- [166] Yan, Z., Tomer, A., Perrussel, G., Ousmane, M., Katryniok, B., Dumeignil, F., Ponchel, A., Liebens, A. & Pera-Titus, M. A Pd/CeO₂ “H₂ Pump” for the direct amination of alcohols. *ChemCatChem* **2016**, *8*, 3347-3352.
- [167] Likhar, P. R., Arundhathi, R., Kantam, M. L. & Prathima, P. S. Amination of alcohols catalyzed by copper-aluminium hydrotalcite: a green synthesis of amines. *Org. Chem.* **2009**, *2009*, 5383-5389.
- [168] Lif, J., Odenbrand, I. & Skoglundh, M. Sintering of alumina-supported nickel particles under amination conditions: support effects. *Appl. Catal. A* **2007**, *317*, 62-69.
- [169] Bartholomew, C. H. Catalyst deactivation. *Chem. Eng.* **1984**, *91*, 96-112.
- [170] Argyle, M. D. & Bartholomew, C. H. Heterogeneous catalyst deactivation and regeneration: a review. *Catalysts* **2015**, *5*, 145-269.
- [171] Moulijn, J. A. Catalyst deactivation. *Appl. Catal. A* **2001**, *212*, 1-255.
- [172] Maxted, E. B. The poisoning of metallic catalysts. *Adv. Catal.* **1951**, *3*, 129-177.
- [173] Hegedus, L. L., & McCabe, R.W. Catalyst poisoning. Marcel Dekker: New York, NY, USA, **1984**.
- [174] Bartholomew, C. H. Mechanisms of nickel catalyst poisoning. In catalyst deactivation. *Studies in Surface Science and Catalysis*. Delmon, B., Froment, G.F., Eds.; Elsevier: Amsterdam, The Netherlands, **1987**, *34*, 81-104.
- [175] Peña, D., Griboval-Constant, A., Lecocq, V., Diehl, F. & Khodakov, A. Y. Influence of operating conditions in a continuously stirred tank reactor on the formation of carbon species on alumina supported cobalt Fischer-Tropsch catalysts. *Catal. Today* **2013**, *215*, 43-51.
- [176] Moodley, D. J., Loosdrecht, J., Saib, A. M., Overett, M. J., Datye, A. K. & Niemantsverdriet, J. W. Carbon deposition as a deactivation mechanism of cobalt-based Fischer-Tropsch synthesis catalysts under realistic conditions. *Appl. Catal. A* **2009**, *354*, 102-110.
- [177] Campisi, S., Schiavoni, M., Chan-Thaw, C. E. & Villa, A. Untangling the role of the capping agent in nanocatalysis: recent advances and perspectives. *Catalysts* **2016**, *6*, 185.

- [178] Boudart, M. *Principles of Heterogeneous Catalysis*. In *Handbook of Heterogeneous Catalysis*. Wiley-VCH: Weinheim, Germany, **1997**.
- [179] Tsunoyama, H., Ichikuni, N., Sakurai, H. & Tsukuda, T. Effect of electronic structures of Au clusters stabilized by poly (N-vinyl-2-pyrrolidone) on aerobic oxidation catalysis. *J. Am. Chem. Soc.* **2009**, *131*, 7086-7093.
- [180] Chen, G. X., Xu, C. F., Huang, X. Q., Ye, J. Y., Gu, L., Li, G., Tang, Z. C., Wu, B. H., Yang, H. Y., Zhao, Z. P., Zhou, Z. Y., Fu, G. & Zheng, N. F. Interfacial electronic effects control the reaction selectivity of platinum catalysts. *Nat. Mater.* **2016**, *15*, 564-569.
- [181] Kwon, S. G., Krylova, G., Sumer, A., Schwartz, M. M., Bunel, E. E., Marshall, C. L., Chattopadhyay, S., Lee, B., Jellinek, J. & Shevchenko, E. V. Capping ligands as selectivity switchers in hydrogenation reactions. *Nano Lett.* **2012**, *12*, 5382-538.
- [182] Mitsudome, T. & Kaneda, K. Advanced core-shell nanoparticle catalysts for efficient organic transformations. *ChemCatChem* **2013**, *5*, 1681-1691.
- [183] Campisi, S., Ferri, D., Villa, A., Wang, W., Wang, D., Kröcher, O. & Prati, L. Selectivity control in palladium-catalyzed alcohol oxidation through selective blocking of active sites. *J. Phys. Chem. C* **2016**, *120*, 14027-14033.
- [184] Chen, K., Wu, H., Hua, Q., Chang, S. & Huang, W. Enhancing catalytic selectivity of supported metal nanoparticles with capping ligands. *Phys. Chem. Chem. Phys.* **2013**, *15*, 2273-2277.
- [185] Furukawa, S., Suzuki, R. & Komatsu, T. Selective activation of alcohols in the presence of reactive amines over intermetallic PdZn: efficient catalysis for alcohol-based *N*-alkylation of various amines. *ACS Catal.* **2016**, *6*, 5946-5953.
- [186] Fischer, A., Maciejewski, M., Bürgi, T., Mallat, T. & Baiker, A. Cobalt catalyzed amination of 1,3-propanediol: effects of catalyst promotion and use of supercritical ammonia as solvent and reactant. *J. Catal.* **1999**, *183*, 373-383.
- [187] Holzwarth, U. & Gibson, N. The Scherrer equation versus the 'Debye-Scherrer equation'. *Nature Nanotech.* **2011**, *6*, 534.
- [188] Schanke, D., Vada, S., Blekkan, E. A., Hilmen, A. M., Hoff, A. & Holmen, A. Study of Pt-promoted cobalt CO hydrogenation catalysts. *J. Catal.*, **1995**, *156*, 85-95.
- [189] Monti, D. A. M. & Baiker, A. Temperature-programmed reduction. Parametric sensitivity and estimation of kinetic parameters. *J. Catal.* **1983**, *83*, 323-335.
- [190] James, O. O. & Maity, S. Temperature programme reduction (TPR) studies of cobalt phases in γ -alumina supported cobalt catalysts. *J. Pet. Technol. Altern. Fuels.* **2016**, *7*, 1-12.
- [191] Huizinga, T., Grondelle, van, J. & Prins, R. A temperature programmed reduction study of Pt on Al₂O₃ and TiO₂. *Appl. Catal.* **1984**, *10*, 199-213.

- [192] Cheng, K., Subramanian, V., Carvalho, A., Ordonsky, V. V., Wang, Y. & Khodakov, A. Y. The role of carbon pre-coating for the synthesis of highly efficient cobalt catalysts for Fischer-Tropsch synthesis. *J. Catal.* **2016**, *337*, 260-271.
- [193] Sheu, L.-L., Karpinski, Z. & Sachtler, W. H. Effects of palladium particle size and palladium silicide formation on fourier transform infrared spectra of CO adsorbed on Pd/SiO₂ catalysts. *J. Phys. Chem.* **1989**, *93*, 4890-4894.
- [194] Stavitski, E. & Weckhuysen, B. M. Infrared and Raman imaging of heterogeneous catalysts. *Chem. Soc. Rev.* **2010**, *39*, 4615-4625.
- [195] Dulaurent, O., Courtois, X., Perrichon, V. & Bianchi, D. Heats of adsorption of CO on a Cu/Al₂O₃ catalyst sing FTIR spectroscopy at high temperatures and under adsorption equilibrium conditions. *J. Phys. Chem. B* **2000**, *104*, 6001-6011.
- [196] Khassin, A. A., Yurieva, T. M., Kaichev, V. V., Bukhtiyarov, V. L., Budneva, A. A., Paukshtis, E. A. & Parmon, V. N. Metal-support interactions in cobalt-aluminum co-precipitated catalysts: XPS and CO adsorption studies. *J. Mol. Catal. A: Chem.* **2001**, *175*, 189-204.
- [197] Dollimore, D., Spooner, P. & Turner, A. The BET method of analysis of gas adsorption data and its relevance to the calculation of surface areas. *Surf. Tech.* **1976**, *4*, 121-160.
- [198] Zhao, X. S., Lu, G. Q., Whittaker, A. K., Millar, G. J. & Zhu, H. Y. Comprehensive study of surface chemistry of MCM-41 using ²⁹Si CP/MAS NMR, FTIR, pyridine-TPD, and TGA. *J. Phys. Chem. B* **1997**, *101*, 6525-6531.
- [199] Barzetti, T., Selli, E., Moscotti, D. & Forni, L. Pyridine and ammonia as probes for FTIR analysis of solid acid catalysts. *J. Chem. Soc. Faraday Trans.* **1996**, *92*, 1401-1407.
- [200] Jin, F. & Li, Y. D. A FTIR and TPD examination of the distributive properties of acid sites on ZSM-5 zeolite with pyridine as a probe molecule. *Catal. Today* **2009**, *145*, 101-107.
- [201] Mears, D. E. Tests for transport limitations in experimental catalytic reactors. *Ind. Eng. Chem. Process Des. Dev.* **1971**, *10*, 541-547.
- [202] Weisz, P. B. & Prater, C. D. Interpretation of measurements in experimental catalysis. *Adv. Catal.* **1954**, *6*, 143-196.
- [203] Engel, J., Smit, W., Foscatto, M., Occhipinti, G., Törnroos, K. W. & Jensen, V. R. Loss and reformation of ruthenium alkylidene: connecting olefin metathesis, catalyst deactivation, regeneration, and isomerization. *J. Am. Chem. Soc.* **2017**, *139*, 16609-16619.
- [204] Barbier, J. Effect of poisons on the activity and selectivity of metallic catalysts. In deactivation and poisoning of catalysts; Oudar, J., Wise, H., Eds. Marcel Dekker: New York, NY, USA, **1985**, 109-150.

- [205] Kahsar, K. R., Schwartz, D. K., & Medlin, J. W. Control of metal catalyst selectivity through specific noncovalent molecular interactions. *J. Am. Chem. Soc.* **2014**, *134*, 520-526.
- [206] Menon, P. G. Coke on catalysts-harmful, harmless, invisible and beneficial types. *J. Molec. Catal.* **1990**, *59*, 207-220.
- [207] Marshall, S. T., O'Brien, M., Oetter, B., Corpuz, A., Richards, R. M., Schwartz, D. K. & Medlin, J. W. Controlled selectivity for palladium catalysts using self-assembled monolayers. *Nat. Mater.* **2010**, *9*, 853-858.
- [208] Haider, P., Urakawa, A., Schmidt, E. & Baiker, A. Selective blocking of active sites on supported gold catalysts by adsorbed thiols and its effect on the catalytic behavior: A combined experimental and theoretical study. *J. Mol. Catal. A Chem.* **2009**, *305*, 161-169.
- [209] McKenna, F. M. & Anderson, J. A. Selectivity enhancement in acetylene hydrogenation over diphenyl sulphide-modified Pd/TiO₂ catalysts. *J. Catal.* **2011**, *281*, 231-240.
- [210] Jaiswal, G., Landge, V. G., Jagadeesan, D. & Balaraman, E. Iron-based nanocatalyst for the acceptorless dehydrogenation reactions. *Nat. Commun.* **2017**, *8*, 2147.
- [211] Ji, L., Lin, J. & Zeng, H. C. Metal-support interactions in Co/Al₂O₃ catalysts: a comparative study on reactivity of support. *J. Phys. Chem. B* **2000**, *104*, 1783-1790.
- [212] Khodakov, A. Y., Griboval-Constant, A., Bechara, R. & Villain, F. Pore-size control of cobalt dispersion and reducibility in mesoporous silicas. *J. Phys. Chem. B* **2011**, *105*, 9805-9811.
- [213] Hong, J. P., Marceau, E., Khodakov, A. Y., Griboval-Constant, A., Fontaine, C., Villain, F., Briois, V. & Chernavskii, P. A. Impact of sorbitol addition on the structure and performance of silica-supported cobalt catalysts for Fischer-Tropsch synthesis, *Catal. Today* **2011**, *175*, 528-533.
- [214] Shafer, W. D., Jacobs, G. & Davis, B. H. Fischer-Tropsch synthesis: investigation of the partitioning of dissociated H₂ and D₂ on activated cobalt catalysts. *ACS Catal.* **2012**, *2*, 1452-1456.
- [215] Fernández-García, M., Martínez-Arias, A., Hanson, J. C. & Rodríguez, J. A. Nanostructured oxides in chemistry: characterization and properties. *Chem. Rev.* **2004**, *104*, 4063-4104.
- [216] Oku, M. & Sato, Y. In-situ X-ray photoelectron spectroscopic study of the reversible phase transition between CoO and Co₃O₄ in oxygen of 10⁻³ Pa. *Appl. Surf. Sci.* **1992**, *55*, 37-41.

- [217] Kim, J.-G., Pugmire, D. L., Battaglia, D. & Langell, M. A. Analysis of the NiCo₂O₄ spinel surface with Auger and X-ray photoelectron spectroscopy. *Appl. Surf. Sci.* **2000**, *165*, 70-84.
- [218] Herbet, J. J., Senecal, P., Martin, D. J., Bras, W., Beaumont, S. k. & Beale, A. M. X-ray spectroscopic and scattering methods applied to the characterisation of cobalt-based Fischer-Tropsch synthesis catalysts. *Catal. Sci. Technol.* **2016**, *6*, 5773-5791.
- [219] Castner, D. G., Watson, P. R. & Chan, I. Y. X-ray absorption spectroscopy, x-ray photoelectron spectroscopy, and analytical electron microscopy studies of cobalt catalysts. 1. Characterization of calcined catalysts. *J. Phys. Chem.* **1989**, *93*, 3188-3194.
- [220] Haber, J., Stoch, J. & Ungier, L. X-ray photoelectron spectra of oxygen in oxides of Co, Ni, Fe and Zn. *J. Electron Spectrosc.* **1976**, *9*, 459-467.
- [221] Ho, S. W., Horiolla, M. & Hercules, D. M. Effect of particle size on carbon monoxide hydrogenation activity of silica supported cobalt catalysts. *J. Phys. Chem.* **1990**, *94*, 6396-6399.
- [222] Moradi, G. R., Basir, M. M., Taeb, A. & Kiennemann, A. Promotion of Co/SiO₂ Fischer-Tropsch catalysts with zirconium. *Catal. Commun.* **2003**, *4*, 27-32.
- [223] Berteau, P. & Delmon, B. Modified aluminas: relationship between activity in 1-butanol dehydration and acidity measured by NH₃ TPD. *Catal. Today* **1989**, *5*, 121-137.
- [224] Vimont, A., Thibault-Starzyk, F. & Daturi, M. Analysing and understanding the active site by IR spectroscopy. *Chem. Soc. Rev.* **2010**, *39*, 4928-4950.
- [225] Swiatowska, J., Lair, V., Pereira-Nabais, C., Cote, G., Marcus, P. & Chagnes, A. XPS, XRD and SEM characterization of a thin ceria layer deposited onto graphite electrode for application in lithium-ion batteries. *Appl. Surf. Sci.* **2011**, *257*, 9110-9119.
- [226] Breen, J. P., Burch, R., Gomez-Lopez, J. & Hayes, M. Steric effects in the selective hydrogenation of cinnamaldehyde to cinnamyl alcohol using an Ir/C catalyst. *Appl. Catal. A* **2004**, *268*, 267-274.
- [227] Delbecq, F. & Sautet, P. Competitive C=C and C=O adsorption of α - β -unsaturated aldehydes on Pt and Pd surfaces in relation with the selectivity of hydrogenation reactions: a theoretical approach. *J. Catal.* **1995**, *152*, 217-236.
- [228] Delbecq, F. & Sautet, P. A density functional study of adsorption structures of unsaturated aldehydes on Pt (111): a key factor for hydrogenation selectivity. *J. Catal.* **2002**, *211*, 398-406.
- [229] Chen, S. L., Abdel-Mageed, A. M., Li, D., Bansmann, J., Cisneros, S., Biskupek, J., Huang, W. X. & Behm, R. J. Morphology-engineered highly active and

- stable Ru/TiO₂ catalysts for selective CO methanation. *Angew. Chem. Int. Ed.* **2019**, *58*, 10732-10736.
- [230] Khodakov, A.Y., Chu, W. & Fongarland, P. Advances in the development of novel cobalt Fischer-Tropsch catalysts for synthesis of long-chain hydrocarbons and clean fuels. *Chem. Rev.* **2007**, *107*, 1692-1744.
- [231] Zhang, G. Q., Vasudevan, K. V., Scott, B. L. & Hanson, S. K. Understanding the mechanisms of cobalt-catalyzed hydrogenation and dehydrogenation reactions. *J. Am. Chem. Soc.* **2013**, *135*, 8668-8681.
- [232] Zhu, J. J., Kailasam, K., Fischer, A. & Thomas, A. Supported cobalt oxide nanoparticles as catalyst for aerobic oxidation of alcohols in liquid phase. *ACS Catal.* **2011**, *1*, 342-347.
- [233] Guo, X. H., Li, Y., Shi, R. J., Liu, Q. Y., Zhan, E. S. & Shen, W. J. Co/MgO catalysts for hydrogenolysis of glycerol to 1, 2-propanediol. *Appl. Catal. A* **2009**, *371*, 108-113.
- [234] Larmier, K., Chizallet, C. & Raybaud, P. Tuning the metal-support interaction by structural recognition of cobalt-based catalyst precursors. *Angew. Chem. Int. Ed.* **2015**, *54*, 6824-6827.
- [235] Munnik, P., Jongh, P. E. & Jong, K. P. Recent developments in the synthesis of supported catalysts. *Chem. Rev.* **2015**, *115*, 6687-6718.
- [236] F. Fischer and H. Koch, *Brennstoff-Chemie* **1932**, *13*, 61.
- [237] Wan, Y. & Zhao, D. Y. On the controllable soft-templating approach to mesoporous silicates. *Chem. Rev.* **2007**, *107*, 2821-2860.
- [238] Prati, L. & Villa, A. Gold colloids: from quasi-homogeneous to heterogeneous catalytic systems. *Acc. Chem. Res.* **2014**, *47*, 855-863.
- [239] Chu, W., Wang, L.-N., Chernavskii, P. A. & Khodakov, A. Y. Glow-discharge plasma-assisted design of cobalt catalysts for Fischer-Tropsch synthesis. *Angew. Chem. Int. Ed.* **2008**, *47*, 5052-5055.
- [240] Zhou, Y. G., Baaziz, W., Ersen, O., Kots, P. A., Vovk, E. I., Zhou, X. H., Yang, Y. & Ordonsky, V. V. Decomposition of supported Pd hydride nanoparticles for the synthesis of highly dispersed metallic catalyst. *Chem. Mater.* **2018**, *30*, 8116-8120.
- [241] Llorca, J., Homs, N., Sales, J. & Piscina, P. R. Efficient production of hydrogen over supported cobalt catalysts from ethanol steam reforming. *J. Catal.* **2002**, *209*, 306-317.
- [242] Kang, M., Song, M. W. & Lee, C. H. Catalytic carbon monoxide oxidation over CoO_x/CeO₂ composite catalysts. *Appl. Catal. A. Gen.* **2003**, *251*, 143-156.

- [243] Yu, W. T., Porosoff, M. D. & Chen, J. G. Review of Pt-based bimetallic catalysis: from model surfaces to supported catalysts. *Chem. Rev.* **2012**, *112*, 5780-5817.
- [244] Gonzalez-Elipe, A. R., Munuera, G. & Espinos, J. P. XPS intensities and binding energy shifts as metal dispersion parameters in Ni/SiO₂ catalysts. *Surf. Interface Anal.* **1990**, *16*, 375-379.
- [245] Wang, Z.-L., Yan, J.-M., Ping, Y., Wang, H.-L., Zheng, W.-T. & Jiang, Q. An efficient CoAuPd/C catalyst for hydrogen generation from formic acid at room temperature. *Angew. Chem. Int. Ed.* **2013**, *52*, 4406-4409.
- [246] Davis, J. B. A., Baletto, F. & Johnston, R. L. The effect of dispersion correction on the adsorption of CO on metallic nanoparticles. *J. Phys. Chem. A* **2015**, *119*, 9703-9709.
- [247] A. A. Khassin, T. M. Yurieva, V. V. Kaichev, V. L. Bukhtiyarov, A. A. Budneva, E. A. Paukshtis, V. N. Parmon, *J. Mol. Catal. A: Chem.* **2001**, *175*, 189-204.
- [248] Heilen, G., Mercker, H. J., Frank, D., Reck, R. A. & Jäck, R. *Ullmanns Encyclopedia of Industrial Chemistry*. fifth ed., VCH, Weinheim, **1985**, *2A*, 1-18.
- [249] Müller, T. E., Hultsch, K. C., Yus, M., Foubelo, F. & Tada, M. Hydroamination: direct addition of amines to alkenes and alkynes. *Chem. Rev.* **2008**, *108*, 3795-3892.
- [250] Leung, A. Y. K., Hellgardt, K. & Hii, K. K. Catalysis in flow: nickel-catalyzed synthesis of primary amines from alcohols and NH₃. *ACS Sustainable Chem. Eng.* **2018**, *6*, 5479-5484.
- [251] Niu, F., Xie, S. H., Bahri, M., Ersen, O., Yan, Z., Kusuma, B. T., Pera-Titus, M., Khodakov, A. Y. & Ordonsky, V. V. Catalyst Deactivation for Enhancement of Selectivity in Alcohols Amination to Primary Amines. *ACS Catal.* **2019**, *9*, 5986-5997.
- [252] Cherkasov, N., Ibhaden, A. O., McCue, A. J., Anderson, J. A. & Johnston, S. K. Palladium-bismuth intermetallic and surface-poisoned catalysts for the semi-hydrogenation of 2-methyl-3-butyn-2-ol. *Appl. Catal. A* **2015**, *497*, 22-30.
- [253] Anderson, J. A., Mellor, J. & Wells, R. P. K. Pd catalysed hexyne hydrogenation modified by Bi and by Pb. *J. Catal.* **2009**, *261*, 208-216.
- [254] Pino, N., Sitthisa, S., Tan, Q. H., Souza, T., López, D. & Resasco, D. E. Structure, activity, and selectivity of bimetallic Pd-Fe/SiO₂ and Pd-Fe/ γ -Al₂O₃ catalysts for the conversion of furfural. *J. Catal.* **2017**, *350*, 30-40.
- [255] Fulajtárova, K., Soták, T., Hronec, M., Vávra, I., Dobročka, E. & Omastová, M. Aqueous phase hydrogenation of furfural to furfuryl alcohol over Pd-Cu catalysts. *Appl. Catal. A* **2015**, *502*, 78-85.

- [256] Ordonsky, V. V., Luo, Y., Gu, B., Carvalho, A., Chernavskii, P. A., Cheng, K. & Khodakov, A. Y. Soldering of iron catalysts for direct synthesis of light olefins from syngas under mild reaction conditions. *ACS Catal.* **2017**, *7*, 6445-6452.
- [257] Shi, R. J., Wang, F., Tana, Li, Y., Huang X. M. & Shen, W. J. A highly efficient Cu/La₂O₃ catalyst for transfer dehydrogenation of primary aliphatic alcohols. *Green Chem.*, **2010**, *12*, 108-113.
- [258] Smith, M. B. & March, J. *Advanced Organic Chemistry*. (5th edition., Wiley, New York, **2001**).
- [259] Prades, A., Corberán, R., Poyatos, M. & Peris, E. [IrCl₂Cp*(NHC)] Complexes as highly versatile efficient catalysts for the cross-coupling of alcohols and amines. *Chem. Eur. J.* **2008**, *14*, 11474-11479.
- [260] Kondo, T., Yang, S., Huh, K.-T., Kobayashi, M., Kotachi, S. & Watanabe, Y. Ruthenium complex-catalyzed facile synthesis of 2-substituted benzo-azoles. *Chem. Lett.* **1991**, *20*, 1275-1278.
- [261] Watanabe, Y., Tsuji, Y. & Ohsugi, Y. The ruthenium catalyzed *N*-alkylation and *N*-heterocyclization of aniline using alcohols and aldehydes. *Tetrahedron Lett.* **1981**, *22*, 2667-2670.
- [262] Sreedhar, B., Reddy, P. S., Reddy, M. A., Neelima, B. & Arundhathi, R. AgOTf catalyzed direct amination of benzyl alcohols with sulfonamides. *Tetrahedron Lett.* **2007**, *48*, 8174-8177.
- [263] Zhang, G. Q., Yin, Z. W. & Zheng, S. P. Cobalt-catalyzed *N*-alkylation of amines with alcohols. *Org. Lett.* **2016**, *18*, 300-303.
- [264] He, L., Lou, X. B., Ni, J., Liu, Y. M., Cao, Y., He, H. Y. & Fan, K. N. Efficient and clean gold-catalyzed one-pot selective *N*-alkylation of amines with alcohols. *Chem. Eur. J.* **2010**, *16*, 13965-13969.
- [265] Akkarasamiyo, S., Sawadjoon, S., Orthaber, A. & Samec, J. S. M. Tsuji-Trost reaction of non-derivatized allylic alcohols. *Chem. Eur. J.* **2018**, *24*, 3488-3498.
- [266] Bricout, H. Carpentier, J.-F. & Mortreux, A. Synthetic and kinetic aspects of nickel-catalysed amination of allylic alcohol derivatives. *Tetrahedron* **1998**, *54*, 1073-1084.
- [267] Emer, E., Sinisi, R., Capdevila, M. G., Petruzzello, D., Vincentiis, F. D. & Cozzi, P. G. Direct nucleophilic S_N1-type reactions of alcohols. *Eur. J. Org. Chem.* **2011**, *2011*, 647-666.
- [268] Baeza, A. & Nájera, C. Recent advances in the direct nucleophilic substitution of allylic alcohols through S_N1-type reactions. *Synthesis* **2014**, *46*, 0025-0034.
- [269] Marakatti, V. S., Manjunathan, P., Halgeri, A. B. & Shanbhag, G. V. Superior performance of mesoporous tin oxide over nano and bulk forms in the activation of a

carbonyl group: conversion of bio-renewable feedstock. *Catal. Sci. Technol.* **2016**, *6*, 2268-2279.

[270] Mahshid, S., Askari, M. & Ghamsari, M. S. Synthesis of TiO₂ nanoparticles by hydrolysis and peptization of titanium isopropoxide solution. *J. Mater. Process. Tech.* **2007**, *189*, 296-300.

[271] Yates, D. J. C. Infrared studies of the surface hydroxyl groups on titanium dioxide, and of the chemisorption of carbon monoxide and carbon dioxide. *J. Phys. Chem.* **1961**, *65*, 746-753.

[272] Watanabe, S., Ma, X. L. & Song, C. Characterization of structural and surface properties of nanocrystalline TiO₂-CeO₂ mixed oxides by XRD, XPS, TPR, and TPD. *J. Phys. Chem. C* **2009**, *113*, 14249-14257.

[273] Parfitt, G. D. The surface of titanium dioxide. *Prog. Surf. Membrane Sci.* **1976**, *11*, 181-226.

[274] Benkoula, S., Sublemontier, O., Patanen, M., Nicolas, C., Sirotti, F., Naitabdi, A., Gaie-Levrel, F., Antonsson, E., Aureau, D., Ouf, F.-X., Wada, S.-I., Etcheberry, A., Ueda, K. & Miron, C. Water adsorption on TiO₂ surfaces probed by soft X-ray spectroscopies: bulk materials vs. isolated nanoparticles. *Sci. Rep.* **2015**, *5*, 15088.

[275] Wang, T., Ibañez, J., Wang, K., Fang, L., Sabbe, M., Michel, C., Paul, S., Pera-Titus, M. & Sautet, P. Rational design of selective metal catalysts for alcohol amination with ammonia. *Nat. Catal.* **2019**, *2*.

[276] Dume, C. & Hödderich, W. F. Amination of 1-octanol. *Appl. Catal. A: Gen.* **1999**, *183*, 167-176.

[277] Deng, D., Kita, Y., Kamata, K. & Hara, M. Low-temperature reductive amination of carbonyl compounds over Ru deposited on Nb₂O₅·nH₂O. *ACS Sustainable Chem. Eng.* **2019**, *75*, 4692-4698.

[278] Timsina, Y. N., Gupton, B. F. & Ellis, K. C. Palladium-catalyzed C-H amination of C(sp²) and C(sp³)-H bonds: mechanism and scope for N-based molecule synthesis. *ACS Catal.* **2018**, *87*, 5732-5776.

[279] Jain, J. R. & Pillai, C. N. Catalytic dehydration of alcohols over alumina: mechanism of ether formation. *J. Catal.* **1967**, *9*, 322-330.

[280] Kostestkyy, P., Yu, J. Y., Gorte, R. J. & Mpourmpakis, G. Structure-activity relationships on metal-oxides: alcohol dehydration. *Catal. Sci. Technol.* **2014**, *4*, 3861-3869.

[281] Shi, B. C. & Davis, B. H. Alcohol dehydration: mechanism of ether formation using an alumina catalyst. *J. Catal.* **1995**, *157*, 359-367.

[282] Li, Z., Assary, R. S., Atesin, A. C., Curtiss, L. A. & Marks, T. J. Rapid ether and alcohol C-O bond hydrogenolysis catalyzed by tandem high-valent metal triflate + supported Pd catalysts. *J. Am. Chem. Soc.* **2014**, *136*, 104-107.

- [283] Assary, R. S., Atesin, A. C., Li, Z., Curtiss, L. A. & Marks, T. J. Reaction pathways and energetics of etheric C-O bond cleavage catalyzed by lanthanide triflates. *ACS Catal.* **2013**, *3*, 1908-1914.
- [284] Mukhopadhyay, I. & Billingham, B. E. High resolution synchrotron radiation Fourier transform infrared spectrum of the COH-bending mode in methanol-D1 (CH₂DOH). *Infrared Phys. Technol.* **2017**, *85*, 184-210.
- [285] Ajjan, F. N., Jafari, M. J., Rebiś, T., Ederth, T. & Inganäs, O. Spectroelectrochemical investigation of redox states in a polypyrrole/lignin composite electrode material. *J. Mater. Chem. A* **2015**, *3*, 12927-12937.
- [286] Smith, B. C. The C-O bond III: ethers by a knockout. *Spectroscopy.* **2017**, *32*, 22-26.
- [287] Heiba, E.-A. I. & Landis, P. S. Alumina-catalyzed cleavage of ethers and thermal decomposition of aluminum alkoxides. *J. Catal.* **1964**, *3*, 471-476.
- [288] Velasco, M. J., Rubio, F., Rubio, J. & Oteo, J. L. Hydrolysis of Titanium Tetrabutoxide. Study by FT-IR Spectroscopy. *Spectrosc. Lett.* **1999**, *32*, 289-304.